Modelling the Effects of Topography on Ice Sheet Erosion, Scotland

Neil F. Glasser

Doctor of Philosophy

University of Edinburgh

1991

BEST COPY

AVAILABLE

"Irrationally held truths may be more harmful than reasoned errors."

THOMAS HENRY HUXLEY

Text cut off in original

ACKNOWLEDGEMENTS

The work presented in this thesis was funded by a N.E.R.C. Research Studentship. I would like to express my gratitude to my supervisor, David Sugden, for his endless ideas and advice. Special thanks are also due to my parents and family for all their support and encouragement over the last three years. Fellow postgraduates Diederick Kohnhorst, Andy Kerr, Jane Boygle and Alan Gilchrist all read draft chapters of the thesis and their comments were much appreciated.

Various people provided field assistance including Cameron Smart and Matthew Bennett. Nick Hulton, Richard Hindmarsh and Bruce Gittings all helped in solving numerous computing problems. I would also like to thank all those who gave up valuable time to discuss research problems, namely Martin Kirkbride, Vanessa Brazier, Adrian Hall, Geoffrey Boulton, Charles Warren, Mark Boyle, Eddie Brown and Loretta Lees. The staff, postgraduates and undergraduates of Edinburgh University Geography Department deserve a special mention for their help, in particular Sheena, Susan and Margaret, and Ray Harris, Nicola Exley, Anona Lyons and Norma Henderson of Drummond Street Reprographics Unit. The Scottish Office Air Photograph Library gave access to aerial photographs and Balmoral Estate granted access to their land.

I would also like to thank Mary, who provided the Pritt Stick which proved so valuable in the production of the thesis.

DECLARATION

This thesis has been composed solely by myself. The work presented is my own unless otherwise acknowledged.

Neil Glasser

Neil F. Glasser

CONTENTS AT A GLANCE

		PAGES
Chapter 1 -	Introduction	1-19
Chapter 2 -	Modelling basal ice temperatures with uniform ice flow	20-76
Chapter 3 -	Modelling basal ice temperatures including convergence and divergence of flow	77-127
Chapter 4 -	Preglacial and glacial landscapes: Criteria used for mapping	128-155
Chapter 5 -	The pattern and depth of ice sheet erosion in the study area	156-240
Chapter 6 -	The correlation between basal thermal regime and ice erosion	241-263
Chapter 7 -	Conclusions and further work	264-279
Appendix		280
List of references		281-298

FULL LIST OF CONTENTS

Abstract i
Acknowledgements ii
Contents at a glance iii
Full list of contents iv

PAGE NUMBER

Chapter 1 - Introduction

1.1 Aim 1
1.2 Specific objectives 1
1.3 Scientific background 2
1.3.1 The study of glacial erosion 2
1.3.2 Basal thermal regime and glacial erosion 6
1.4 Methodology and approach 11
1.4.2 Approach 11
1.4.2 Method 12
1.4.3 Study area 16

Chapter 2 - Modelling basal ice temperatures with uniform ice flow

2.1 Aim 20
2.2 Method 20
2.2.1 The Budd fixed column model 20
2.2.2 Model assumptions 21
2.2.3 Derivation of input parameters 25
2.2.3.1 Ice Sheet profile 25
2.2.3.2 The geographical extent of the ice sheet 31
2.2.3.3 The ice age temperature regime 33
2.2.3.4 Altitudinal lapse rate 38
2.2.3.5 Accumulation rate 38
2.2.3.6 Geothermal heat flux 40
2.3 Basic calculations 40
2.3.1 Ice thickness 42
2.3.2 Ice surface gradient 42
2.3.3 Basal temperature gradient 43
2.3.4 Surface temperature gradient 45
2.3.5 Dimensionless thermal parameter 46
2.4 Model output: Basal thermal regime 47
2.4.1 Standard model run 53
2.5 Sensitivity tests 65
2.5.1 Changing the ice sheet profile 66
2.5.2 Changing the accumulation rate 68
2.5.3 Changing the ice surface temperature 70
2.5.4 Changing the basal topography 71
2.6 Conclusions 73
2.7 Limitations 75

Chapter 3 - Modelling basal ice temperatures including convergence and divergence of flow

3.1 Aim 71
3.2 Rationale 77
3.3 Previous work 80
3.4 Calculating basal temperatures 83
3.4.1 Ice thickness 84
3.4.2 Topographic geometry 90
3.4.3 Illustration of method 98
3.5 Results 102
3.5.1 Basal thermal regime in the field study areas 102
3.5.2 Basal thermal regime in the flowband 110
3.6 Sensitivity tests 119
3.6.1 Sensitivity tests in the five field study areas 120
3.6.2 Sensitivity tests at the flowband scale 123
3.7 Conclusions 124
3.8 Limitations 126

Chapter 4 - Preglacial and glacial landscapes: Criteria used for mapping

4.1 Aim 128
4.2 Preglacial landscapes 128
4.2.1 Plateau surfaces 129
4.2.2 Fluvial valleys 131
4.2.3 Topographic sheeting 134
4.2.4 Saprolites 138
4.2.5 Tors 145
4.2.6 Overall significance 149
4.3 Glacial landscapes 150
4.4 Conclusion 151

Chapter 5 - The pattern and depth of ice sheet erosion in the study area

5.1 Aim 156
5.2 Approach 156
5.3 The regional pattern of ice sheet erosion 157
5.3.1 Method 157
5.3.2 Reliability of aerial photograph interpretation 158
5.3.3 The regional pattern of ice sheet erosion 166
5.3.4 The regional pattern of aerial scouring 168
5.3.5 Landscape classification 170
5.3.6 The distribution of the landscape classes 172
5.4 Ice sheet erosion in the field study areas 173
5.4.1 Method 173
5.4.2 Cairngorm study area 178
5.4.2.1 Site location and description 178
5.4.2.2 The preglacial landscape 179

5.4.2.3 The glacial landscape 192
5.4.2.4 Reconstruction of the preglacial landscape 196
5.4.2.5 The depth of ice sheet erosion 200
5.4.3 Glen Feshie study area 202
5.4.3.1 Site location and description 202
5.4.3.2 The preglacial landscape 202
5.4.3.3 The glacial landscape 207
5.4.3.4 The depth of ice sheet erosion 207
5.4.4 Balmoral study area 208
5.4.4.1 Site location and description 208
5.4.4.2 The preglacial landscape 209
5.4.4.3 The glacial landscape 209
5.4.4.4 The depth of ice sheet erosion 211
5.4.5 Speyside study area 218
5.4.5.1 Site location and description 218
5.4.5.2 The preglacial landscape 218
5.4.5.3 The glacial landscape 221
5.4.5.4 The depth of ice sheet erosion 225
5.4.6 Aberdeen study area 227
5.4.6.1 Site location and description 227
5.4.6.2 The preglacial landscape 228
5.4.6.3 The glacial landscape 230
5.4.6.4 The depth of ice sheet erosion 233
5.5 The depth of ice sheet erosion in the regional transect 234
5.6 Conclusions 239

Chapter 6 - The correlation between basal thermal regime and ice sheet erosion

6.1 Aim 241
6.2 The comparison between basal thermal regime and ice sheet erosion 243
6.3 Comparisons at the regional scale 243
6.3.1 Standard model run 243
6.3.2 Convergence and divergence of flow 246
6.4 Comparisons at the local scale 249
6.4.1 Speyside field study area 254
6.4.2 Glen Feshie field study area 254
6.4.3 Cairngorm field study area 254
6.4.4 Balmoral field study area 255
6.4.6 Synthesis of comparisons at the local scale 256
6.5 Confidence level of results 256
6.5.1 Model reliability 257
6.5.2 Field evidence 261

Chapter 7 - Discussion and conclusions

7.1 Alternative explanations 264
7.1.1 Glaciological factors 264
7.1.2 Geological factors 266
7.2 Implications of results 268

7.2.1 Basal thermal regime, topography, and ice sheet erosion 268
7.2.2 The importance of the ice sheet maximum 269
7.2.3 Depth and rate of ice sheet erosion 272
7.2.4 Meltwater production under the former ice sheet 276
7.2.5 The problem of the mismatch in the Aberdeen field study area 277
7.3 Further work 278
7.4 Conclusions 279

Appendix - Mathematical Nomenclature 280
List of references 281

CHAPTER ONE

INTRODUCTION

1.1 Aim

The aim of this thesis is to consider the spatial variation in ice sheet erosion under former Scottish ice sheets. The emphasis of the research is on the pattern of ice sheet erosion at the regional scale, intermediate between that of individual landforms and an ice sheet as a whole. The basal thermal regime of the former ice sheet is calculated and the predicted pattern of basal temperatures compared to the observed pattern of ice sheet erosion derived from fieldwork. This approach is used to test the hypothesis that basal thermal regime is the crucial factor determining the ability of an ice sheet to erode its bed.

1.2 Specific objectives

There are 5 specific objectives:

(1) To calculate the basal thermal regime of a former Scottish ice sheet at its maximum assuming uniform sheet flow over the basal topography.

(2) To calculate the basal thermal regime of a former Scottish ice sheet at its maximum taking into account the convergence and divergence of ice flow as it moves over the irregular topography.

(3) To map the distribution of landforms of glacial erosion from the centre to the periphery of the ice sheet to establish the regional pattern of erosion and the intensity of modification of the landscape by ice sheet erosion.

(4) To map the distribution of glacial and preglacial landforms at detailed field study sites and make estimates of minimum and maximum depths of ice sheet erosion in representative areas.

(5) To compare the pattern of ice sheet erosion in the field with the modelled pattern of basal thermal regime in order to study the processes by which ice sheets modify landscapes.

1.3 Scientific background

1.3.1 The study of glacial erosion

Ice sheets are agents of net erosion since they move outward from a central source, removing and transporting debris in the process (Boulton 1979). The ability to produce stratigraphic sequences from sedimentary deposits and the recent progress made in dating techniques has meant that much of the recent research in glacial geomorphology has concentrated on the depositional effects of former ice sheet expansion. This emphasis on glacial deposition is especially apparent in the Scottish context (for example Sissons 1981; Sutherland 1984). However, the study of glacial erosion is important for

several reasons:

(1) Glacial erosion plays an important geomorphological role in shaping the earth's surface. It is one of the prime agents of continental erosion, currently affecting 14.9 x 10^6 km^2 or 10 per cent of the land surface of the planet (Sugden and John 1976). During the Quaternary, ice is estimated to have covered up to 30 per cent of the land surface of the planet (Embleton and King 1975). Rates of erosion beneath ice sheets, both observed (Boulton 1979; Budd et al. 1979; Iverson 1990) and theoretical (Andrews 1972), greatly exceed the rates of other erosional processes such as periglacial and fluvial erosion (Braun 1989). From the quantity of glacially derived ocean sediment in the North Atlantic it has been estimated that former ice sheets were capable of erosion that was an order of magnitude greater than any contemporary processes (Braun 1989).

(2) Glacial erosion plays an important role within the ice sheet system. Oerlemans (1984) recognises that over the time scale of glacial cycles erosion by ice sheets can, through bedrock lowering, be as important as changes in sea level in altering mass balance. An uninvestigated feedback loop may exist between the high basal ice velocities found in subglacial valleys and ice sheet erosion. McIntyre (1985) suggests that glacial erosion due to high basal sliding velocities has substantially smoothed the bedrock and contributed to its lowering under Antarctic ice streams, ensuring the continued existence of the ice streams. Where ice flow is channelled down

pre-existing depressions the increase in glacial erosion may be sufficient to carve deep troughs and thus ensure continued preferential flow (Oerlemans 1984). Interactions between glacial erosion and bed morphology have also been noted by Mazo (1987) and Sharp et al. (1989). For example, under the present day Antarctic ice sheet the removal of deformable sediment through glacial erosion by ice streams influences ice stream velocities (Alley 1989). The removal of the deformable strata by glacial erosion may help to stabilise an otherwise potentially unstable ice sheet.

(3) The depositional products of glacial erosion are widely used as tests in the reconstruction of former ice sheets (Andrews 1982). Many ice sheet models use the glacial geological evidence as tests of former ice conditions and flow directions (eg Boulton et al. 1978; Boulton et al. 1985; Boulton and Clark 1990; Andrews et al. 1985; Payne et al. 1989). Erratic dispersal is frequently used to reconstruct former ice flow lines (eg Boulton et al. 1978; Boulton et al. 1985; Andrews and Miller 1979) yet there is insufficient information concerning the entrainment and transport of these erratics. Without detailed consideration of the spatial and temporal variations in glacial erosion these tests may rest upon an insecure basis.

(4) There has been much debate over the magnitude of erosion attributable to former ice sheets. White (1972, 1988) has argued that ice sheets may account for erosion hundreds of metres deep in North America, over the area

covered by the Laurentide ice sheet. Gravenor (1975) and Sugden (1976) advocate minimal glacial erosion beneath the Laurentide ice sheet on the basis of terrestrial evidence, with depths of erosion limited to a maximum of a few tens of metres. Attempts to correlate depths of glacial erosion with sediment depths in the offshore record have also proved controversial. Estimates of erosion again vary from hundreds of metres in depth (Laine 1980; Laine and Bell 1982; Bell and Laine 1980, 1985; Grosswald and Glazovsky 1984) to less than twenty metres in depth (Kaszycki and Shilts 1979, 1980, 1987).

(5) There is evidence that ice sheets can be both erosive and protective. In Scotland there are localities where the preglacial landscape has survived significant modification by ice sheets (Hall and Sugden 1987). The preservation of other non-glacial deposits is known to be a result of protection under glacial conditions. Jonsson (1983) notes the appearance of undisturbed beach ridges under the retreating cold-based Svalbard ice caps. Marchant and Denton (1990) note the survival of Antarctic desert pavements under overriding ice, and Marchant (1990) describes in situ ash deposits preserved beneath repeated advances of the Taylor Glacier, Antarctica. Furthermore, the preservation of periglacial boulder fields, known to have formed during the last interglacial, is noted in the mountains of west central Sweden (Kleman and Borgstrom 1990). Other fossil periglacial features belonging to a previous interglacial are known in northern Scandinavia

(Lagerback 1988a). The preservation of former glacial deposits is also possible under ice sheets, for example the deglaciation features known to have formed prior to the last deglaciation in Scandinavia. The survival of cross-cutting glacial drainage channels (Rodhe 1988) and the existence of several generations of ice-marginal meltwater channels (Kleman et al. 1991) is strong evidence that such features were preserved beneath ice sheets. The preservation of other glacial deposits, such as linear till ridges (Kleman 1988), and of the glacial sedimentary stratigraphy (Lagerback 1988b; Lagerback and Robertsson 1988) in Scandinavia is further evidence of glacial protection. In Antarctica, unconsolidated glacial sediments and moraine morphology are also known to have survived glacial overriding (Marchant et al. 1991). Ice sheet erosion is a highly selective process, yet the reasons for this selectivity are poorly understood. The location of areas of glacial erosion and protection under former Scottish ice sheets have not been fully identified. The basal thermal regime of the ice sheet is unknown, and the influence of topography and basal thermal regime on the processes of ice sheet erosion requires evaluation.

1.3.2 Basal thermal regime and glacial erosion

Many factors are important in glacial erosion. Variables previously stressed include bedrock structure (Harland 1957; Addison 1981; Rastas and Seppala 1981), lithology (Zumberge 1955), pressure release (Lewis 1954), preglacial relief (Klimaszewski 1964), preglacial weathering (Boye 1968; Lindstrom

1988), periglacial weathering (Bakker 1965; Feininger 1971), ice velocity (Andrews 1972), ice flow patterns (Nye and Martin 1968; Sharp et al. 1989a), effective pressure at the glacier/bed interface (Boulton 1974), meltwater production (Robin 1976; Rothlisberger and Iken 1981), scale (Rudberg 1973; Glasser and Warren 1990), and duration of glaciation (Porter 1989). Although these variables are important, the crux of the problem is thought to be the operation of the processes of glacial erosion at the ice/rock interface. A fundamental constraint on glacial erosion is the thermal regime of the ice sheet; in particular the necessity for basal ice at the pressure melting point in order that basal meltwater be released is recognised.

The importance of basal thermal regime is illustrated by the two main glacial erosional processes of abrasion and plucking. Abrasion, the wearing down of bedrock by debris in basal ice, is especially important on the upstream side of bedrock obstacles where ice is in complete contact with the bed (Carol 1947; Weertman 1957). Fundamental requirements for abrasion are basal debris, sliding of basal ice, and supply of debris to the bedrock surface (Table 1.1). Ice thickness, basal water pressure, relative hardness of rock particles and bedrock, particle characteristics and efficient removal of rock flour by meltwater are also important (Sugden and John 1976). The importance of basal meltwater for the process of glacial abrasion is threefold:

(1) Basal meltwater acts as a lubricating layer between the ice sheet and its bed, and thus enables basal sliding (Hallet 1979). Without this lubricating film of meltwater, basal sliding past even the smallest elements of the bed roughness does not occur, and glacial abrasion is inhibited. In addition, the sliding velocity of the basal ice is important because it determines the amount of abrasive material in the basal ice which can pass a given area of bedrock per unit time. The faster the sliding velocity, the more abrasive material is dragged over the glacier bed.

(2) Basal meltwater flushes out the fine rock particles and rock flour produced by glacial erosion (Sharp et al. 1989b). Without the removal of these finer particles, subsequent glacier sliding is hindered by lodgement at the rock/ice interface. Vivian (1970) notes that under the Alpine Glacier d'Argentiere the layer of basal meltwater is sufficiently thick to evacuate rock flour with a grain size of less than 0.25 mm in diameter, and that this allows the larger particles to actively abrade the bedrock.

(3) Melting in the lower layers of an ice sheet ensures a continued supply of debris to the ice/rock interface. Thus fresh tools are brought to the base of the ice sheet to replenish those used in the process of glacial abrasion. The renewal of the abrasive material by basal melting can only occur beneath warm based ice.

Basal melting and the release of subglacial meltwater are therefore crucial for the operation of glacial abrasion. Given that the basal ice initially contains sufficient debris, subglacial meltwater is necessary to fulfill the other fundamental requirements for glacial abrasion (Table 1.1).

Glacial plucking, the removal of blocks along joint planes, is most effective in the lee of bedrock obstacles, where confining pressures are lower and cavitation may occur (Lliboutry 1968; Brepson 1979). Although the effectiveness of glacial plucking is controlled to a certain extent by bedrock structure and lithology (Lewis 1954; Harland 1957; Addison 1981), the need for basal melting is fundamental. Without sufficient subglacial meltwater to enable basal sliding, cavitation is unlikely to occur (Sharp et al. 1989a), no meltwater is available to freeze blocks into the basal ice, and hydraulic fracturing cannot occur (Rothlisberger and Iken 1981). Basal meltwater is also important because of the role attributed to fluctuations in basal water pressure in enabling rock fracture to occur beneath glaciers (Iverson 1991). The characteristics of basal meltwater flow, water pressure, and shape and connectivity of conduits are also important (Hooke 1989, Hooke et al. 1990). Without basal ice at the pressure melting point block removal due to glacial plucking is limited.

In situations where basal ice is frozen to bedrock and no meltwater is

Fundamental requirements for abrasion	(1) Basal debris (2) Sliding of basal ice (3) Transport of debris down towards bedrock
Other factors affecting rate and type of abrasion	(4) Ice thickness (5) Basal water pressure (6) Relative hardness of rock particles and bedrock (7) Particle characteristics (8) Efficient removal of rock flour

Table 1.1 Tentative list of variables affecting the process of glacial abrasion.
Source: Sugden and John (1976) p.153.

available for glacier sliding and regelation (cold based ice), the processes of abrasion and plucking cannot operate at the ice/rock interface. In this situation, it is expected that no erosion will take place and that the preglacial landscape will be preserved. Although Shreve (1984) has suggested that extremely slow glacier sliding is possible at sub-freezing basal temperatures freezing basal temperatures, there is no evidence that cold based ice is capable of erosion.

Areas of an ice sheet where basal ice is at the pressure melting point are therefore important in glacial geomorphology. In these areas, meltwater is released at the base and ice sheet movement, dominated by basal sliding, allows the operation of both glacial abrasion and plucking at the ice sheet sole. Other factors within the ice sheet system which control the location of areas of basal melting, such as ice depth and velocity, are important but are not expected to individually explain the link between glaciological processes and glacial erosion. A comparison between calculated basal thermal regime and field evidence of ice sheet erosion therefore provides a strong test for the hypothesis that the requirement for basal melting is the fundamental control on ice sheet erosion. This thesis makes this comparison for a former Scottish ice sheet.

1.4 Methodology and approach

1.4.1 Approach

The crux of the thesis is the comparison between the predicted basal thermal regime at ice sheet maximum and the observed pattern of ice sheet erosion. Zones of basal ice at the pressure melting point should be associated with areas of ice sheet erosion whereas zones of basal ice below the pressure melting point are thought to be associated with areas of glacial protection.

If zones of basal melting and freezing at ice sheet maximum correlate with areas of ice sheet erosion and protection respectively, then it may be concluded that basal thermal regime is the fundamental constraint on ice sheet erosion. It also follows that much of the erosion took place at ice sheet maximum. If there is no correlation it may be concluded that other factors are more important than basal thermal regime in the processes of ice sheet erosion; it could also be that the erosion did not take place at ice sheet maximum.

1.4.2 Method

To make the comparison, two methods are adopted; numerical modelling of the basal thermal regime at ice sheet maximum, and field mapping of landforms of ice sheet erosion. The focus of the modelling is on the regional scale. The advantages of this are twofold:

(1) The regional scale is large enough to cover an area from the postulated ice sheet centre to its margin, and allows various sequences of thermal

regimes to be recognised within this transect (Boulton 1972).

(2) Studies at the regional scale have the advantage that it is possible to include the role of topography in models of basal thermal regime. Topography is known to be an important variable within the ice sheet system because of its influence on patterns of ice discharge (Thorp 1987; Payne and Sugden 1990). There are three main reasons why a detailed consideration of subglacial topography is required in the calculation of ice sheet basal thermal regime:

(i) Like any sediment or rock in the earth's crust, temperatures in an ice sheet increase with depth. Ice is a relatively poor conductor of heat and the geothermal heat produced deep in the earth cannot escape through thick ice. The result of this is to create large differences between surface and basal temperatures in thick ice masses (Hooke 1977). Everything else being equal, the temperature in an ice mass will increase linearly by approximately 1°C for every 44 metres in depth. Basal temperatures in an ice sheet will therefore be relatively high over topographic depressions such as valleys or basins where ice is thick, and relatively low over high mountain summits or plateaux where ice is thin.

(ii) Rothlisberger (1968) has considered the relationship between the geothermal heat flux under ice sheets and topography, suggesting that

terrestrial heat flow is influenced by basal topography. The geothermal heat flux is more intense near depressions than rises due to the convergence of heat flow into depressions. Thus basal melting is more likely under bedrock hollows than rises (Rothlisberger 1968).

(iii) Subglacial topography influences the flow regime of an ice sheet. In particular it exercises a strong control on patterns of convergence and divergence of flow (McIntyre 1985). The effect of convergent flow is generally to increase velocities within ice sheets whilst divergent flow decreases ice velocities. Thus in areas where the subglacial topography favours convergent ice flow, relatively high basal ice velocities are encountered. Ice sheet velocity is directly linked to basal ice temperature through frictional heat production and the process of basal sliding. Relatively high basal ice temperatures are therefore expected in areas where the subglacial topography gives rise to convergence of ice flow, and relatively low basal ice temperatures in areas where the subglacial topography gives rise to divergence of ice flow. A basal ice velocity of only 20 ma^{-1} produces the same amount of frictional heat as the average geothermal heat flux (Paterson 1981).

Previous attempts to calculate basal ice temperatures for former ice sheets in Scotland (Gordon 1979) and North America (Sugden 1977), suggest a relationship exists between areas formerly covered by basal ice at the

pressure melting point and areas of ice sheet erosion. The limitation of these comparisons between basal ice conditions and ice sheet erosion is that neither study includes a detailed representation of the subglacial topography in the calculation of basal thermal regime. The model of Gordon (1979) is two dimensional, whilst that of Sugden (1977) is based on calculations of basal temperature using grid squares of 100 kilometres. In the models presented in this thesis, basal topography is considered in three dimensional terms and a relatively high resolution grid is used in the calculation of basal thermal regime.

The calculation of the basal thermal regime of a regional flowband of a former Scottish ice sheet at its maximum is considered in Chapters 2 and 3. In Chapter 2 the calculations of basal thermal regime assume that ice flow remains uniform as it flows over an irregular topography. Variations in thermal regime are therefore due to location within the ice sheet and changes in ice thickness caused by the basal topography. In Chapter 3 the influence of the basal topography on ice flow is taken into consideration, and basal temperatures are calculated allowing for the convergence and divergence of ice flow. Although there is no existing theory of three dimensional ice flow within ice sheets (Hooke 1989), the problem is solved by allowing basal ice velocities to vary in accordance with the subglacial topography. Variations in thermal regime are due not only to changes in ice thickness, but also to changes in velocity brought about by the convergence and divergence of ice

flow.

1.4.3 Study area

The study area (Figure 1.1) represents a transect from the centre to the margin of a former Scottish ice sheet, and measures approximately 140 by 22 kilometres. The most powerful means of comparing basal thermal regime to field evidence of glacial erosion would be to cover the entire area of the former ice sheet but this is not possible within the scope of one thesis. Instead, it was decided to concentrate on a transect study area in order to cover a small area in detail rather than a large area in lesser detail.

There are three major advantages with this choice of study area:

(1) It represents a transect from the centre to the margin of the former ice sheet and can therefore be considered a flowband of that ice sheet. This allows the variation in basal thermal regime to be calculated for a complete sector of the former ice sheet and simplifies the necessary calculations.

(2) The transect encompasses a variety of landscape types, including the coastal lowlands surrounding the North Sea in the east, the high level plateau of the Cairngorm Mountains and the two major river valleys of the

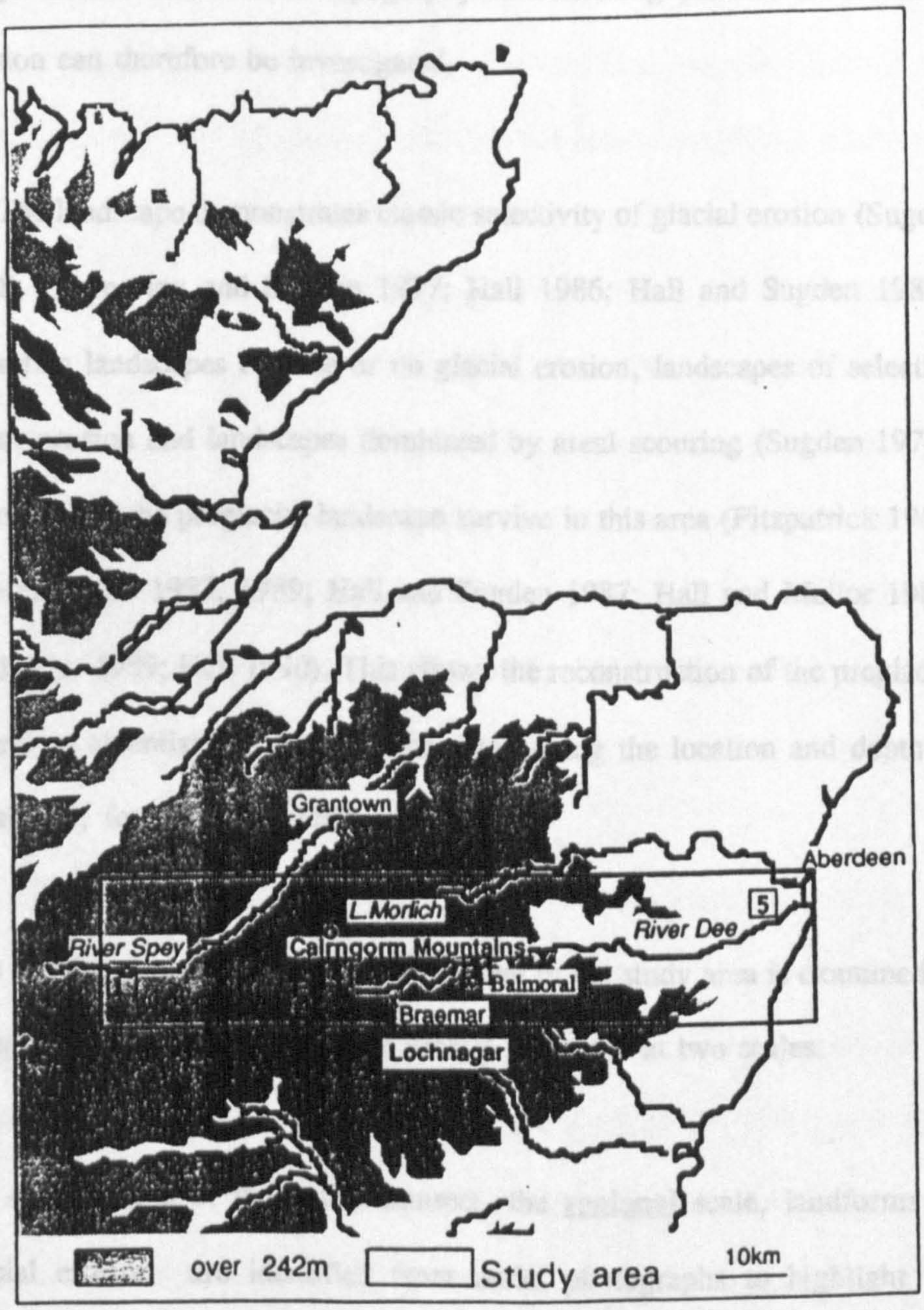

Figure 1.1 The regional transect study area and location of the five detailed study areas. (1) Speyside (2) Glen Feshie (3) Cairngorms (4) Balmoral (5) Aberdeen.

Dee and the Spey (Figure 1.1). This variable topography allows detailed consideration to be made of the ice sheet bed in the calculation of basal ice temperatures. The role of topography in determing patterns of ice sheet erosion can therefore be investigated.

(3) The landscape demonstrates classic selectivity of glacial erosion (Sugden 1968; Clapperton and Sugden 1977; Hall 1986; Hall and Sugden 1987), including landscapes of little or no glacial erosion, landscapes of selective linear erosion and landscapes dominated by areal scouring (Sugden 1974). Remnants of the preglacial landscape survive in this area (Fitzpatrick 1963; Sugden 1968, 1987, 1989; Hall and Sugden 1987; Hall and Mellor 1988; Hall et al. 1989; Hall 1990). This allows the reconstruction of the preglacial relief, an essential pre-requisite for determining the location and depth of erosion by former ice sheets.

The location and depth of ice sheet erosion in the study area is examined in Chapter 5. Mapping of the study area is presented at two scales:

(1) At the scale of the entire transect, the regional scale, landforms of glacial erosion are identified from aerial photographs to highlight the pattern of ice sheet erosion. From this the intensity of modification of the landscape by ice sheet erosion is determined and a landscape classification of the transect made.

(2) Five detailed study sites are examined within the regional transect, one located in each of the landscape classes identified from aerial photography (Figure 1.1). At this **local** scale, detailed field mapping allows the recognition not only of glacial landforms but also of preglacial landforms; an exercise not possible at the larger regional scale. This provides a check on the accuracy of the aerial photograph interpretation and allows areas of glacial erosion and protection to be identified. The preservation of the preglacial landscape allows estimates of the minimum and maximum depth of ice sheet erosion to be made for each area. On the assumption that each of the detailed study sites is representative of its landscape classification, minimum and maximum estimates of the depth of erosion are calculated for the entire transect.

In Chapter 6, the calculations of basal thermal regime are compared to the observed pattern of erosion under the former ice sheet. Comparison is made between the predicted pattern of basal temperatures assuming uniform ice flow, the pattern of basal temperatures including convergence and divergence of ice flow, and the pattern of ice sheet erosion identified in the study area. Comparison is made between the predicted basal thermal regime of the five detailed study areas and the distribution of glacial and preglacial landforms in these areas. Chapter 7 concludes the thesis by summarising the main findings of the study.

CHAPTER TWO

MODELLING BASAL ICE TEMPERATURES WITH UNIFORM ICE FLOW

2.1 Aim

The aim of this chapter is to model basal ice temperatures for a former Scottish ice sheet at its maximum. The calculations assume that ice flow is uniform as the ice sheet moves over its bed.

2.2 Method

2.2.1 The Budd fixed column model

The model used is based on that of Budd et al. (1971a), in which the temperature at the base of an ice sheet is calculated by solving a heat conduction equation through a series of vertical columns along a flow line. The model has been used previously by Sugden (1977) and Gordon (1979) to calculate basal temperatures beneath former ice sheets, and calculations of temperatures in ice sheets using the model have been observed to fit closely those observed in reality (Budd et al. 1971b; Zotikov 1986).

The model solves the heat conduction equation through a vertical column of ice in relation to the heat gained and lost in that column. Temperatures in

an ice sheet are related to heat from four sources; (1) the geothermal heat flux (2) heat produced by internal deformation (3) heat produced by basal sliding (4) accumulation of fresh snow. Of these four heat sources the first three all have warming effects on basal ice temperatures, whilst the latter (accumulation of fresh snow) has a net cooling effect. It is therefore possible to calculate the basal temperature of an ice sheet if we have knowledge of the boundary conditions which determine its temperature distribution. There are 5 such boundary conditions; (1) ice thickness (2) accumulation rate (3) ice sheet surface temperature (4) basal heat gradient (5) surface warming rate.

2.2.2 Model assumptions

The main assumption required when using the Budd column model is that the ice sheet is in steady state. This assumption simplifies the equations used in calculations of basal temperatures. Without the assumption of steady state equilibrium, complex time-dependent temperature calculations must be made to take account of changes in the temperature distribution which arise from the redistribution of mass (Philberth and Federer 1971; Jenssen 1977; Hindmarsh et al. 1989). This problem arises because ice deformation rates and ice temperature are mutually interactive (Paterson 1981). A simple model is employed in this case since the above models cannot cope with a three-dimensional basal topography.

A further series of simplifications are made in calculating the basal temperatures. Conduction is assumed to occur in a vertical sense only; the advection rate through the column is assumed to be constant and equal to the surface warming rate; all frictional heat is applied at the base of the glacier; the strain rate is constant; the thermal diffusivity of ice is constant; and basal melting does not occur. The rationale behind these assumptions and the full derivation of the fixed column model are discussed by Budd et al. (1971a). The model used to calculate basal ice temperatures for the former Scottish ice sheet is presented in Budd et al. (1971a), and was formulated and originally tested against the present-day Antarctic ice sheet.

There are several areas which might lead to the suggestion that the Budd column model is not applicable to a former Scottish ice sheet. These are:

- The different scales involved
- The different topographic and climatic settings
- The assumption of steady state.

Different scales

At the scale of an ice sheet the dynamics of an ice mass can be regarded as a system. Thus there are certain laws governing, for example, ice sheet motion, which are universally applicable to all ice sheets. The present-day Antarctic ice sheet and the former Scottish ice sheet are both three-

dimensional ice domes spreading outwards towards their boundaries; both behave according to the physical laws determining equations of motion and ice physics. The dynamics of any given ice mass can be obtained by establishing the equations of motion in terms of stresses, introducing the stress-strain relationship (flow law) and solving the equations of motion to obtain the velocity distribution. This velocity distribution in turn greatly influences basal ice temperatures. Different ice masses of different scales will inevitably have unique velocity and temperature distributions and therefore the velocity and temperature distributions of the present-day Antarctic and former Scottish ice sheets will differ. However, since there is no evidence to suggest that the different scales involved will introduce any numerical error to the Budd column model it is applied to a former Scottish ice sheet in this case.

Different topographic and climatic settings

Since the present-day Antarctic and former Scottish ice sheets will inevitably possess unique topographic and climatic settings, it might be suggested that the Budd column model can not be legitimately transferred from the Antarctic to the Scottish case. However, because the temperature distribution in an ice sheet is a function of a set of interrelated factors in the ice sheet system (eg accumulation rate, surface temperature, velocity) and the mathematical relationships between these factors are well established, there

is no reason why the model should not be applicable to any ice sheet.

The only foreseeable difference is that unique topographic and climatic settings will produce unique temperature distributions. Indeed, changes in the formulation of the column model (which we might consider analogous to inherent differences between the two ice sheets) produce surprisingly little change in the results obtained (Budd et al. 1971a). Individual flowline calculations were carried out by Budd et al. (1971a) for a number of different cases to examine the effects of the different models on calculated basal temperatures. The main result was that refinements to the basic fixed column model produced variations which were small compared to those due to changes in the input data. Furthermore, the power of the column model is illustrated by the fact that it enabled Budd et al. (1971a) to fit the observed Camp Century (Greenland) temperature profile with an error standard deviation of 0.03 °C and the Byrd profile to 0.4 °C. This demonstrates that column model can be applied to ice sheets other than the Antarctic without the introduction of numerical error.

The assumption of steady state

Another possible reason which might prevent the Budd column model from being applicable to the Scottish case is the assumption that the ice sheet is in steady state. The Antarctic ice sheet is a permanent Quaternary feature; the Scottish ice sheet is an ephemeral feature over this time period. The

greater size and age of the Antarctic ice sheet means it is more likely to have attained steady state than the Scottish ice sheets; although it may be the case that neither ever reached a true steady state. A full discussion of the effects of non-steady state conditions on ice sheet temperature distribution is given in Chapter 6. Although the assumption of a steady state is a limitation of the model, it does not negate the applicability of the Budd column model to the Scottish case.

2.2.3 Derivation of input parameters

2.2.3.1 Ice sheet profile

In this model, the surface profile of the ice sheet affects the values of ice thickness, ice surface elevation, ice surface temperature, ice velocity and ice surface gradient. Our present knowledge of the surface configuration of the last Scottish ice sheet is limited, as is our knowledge of its geographical extent (Sissons 1981). The surface form of the ice sheet can be derived in one of two ways; either by comparison with existing ice sheet profiles or from reconstructions based on glaciological theory.

The use of existing ice sheets as an analogue for a former Scottish ice sheet is difficult, not least because there are no ice sheets currently in existence which approximate the dimensions of the last Scottish ice sheet (half width of approximately 220 km). The vast ice sheets of Greenland and Antarctica are too large to be of much use, whilst ice caps such as those of Svalbard

and Vatnajokull are smaller than the last Scottish ice sheet. In addition, there is evidence that the last Scottish ice sheet may have been a very complex shape, consisting of several coalescent ice domes (Thorp 1987).

The second method of reconstructing the surface morphology of the ice sheet is to use theoretical ice sheet profiles to represent the former ice surface. Comparisons of theoretical ice sheet profiles with modern ice sheets (e.g. Dowdeswell 1986) suggest that most modern ice sheet profiles can be approximated by mathematical solutions such as those resembling parabolic or elliptical forms. This is because, at the scale of an ice sheet, the most important factor in determining the surface profile from a glaciological point of view is the flow of ice. The rate of flow, in turn, is dependent on the plastic properties of ice (Paterson 1981). It is therefore possible to construct theoretical ice sheet profiles using certain assumptions about the plastic properties of ice.

In addition to the plastic properties of ice, surface profiles are a function of accumulation and ablation rates. Paterson (1981) suggests that when reconstructing former ice surface profiles where values of accumulation and ablation are unknown it is best to start with the simplest model. In this case the simplest model is that of Nye (1952), in which the ice surface is treated as parabolic. Parabolic solutions are based on the formula

$$h = K_1 (s - x)^{1/2} \qquad (2.1)$$

(Paterson 1981)

where h is a point on the ice sheet surface, s is the half width of the ice sheet, x is the distance from the ice divide and K_1 is a constant dependent on the basal shear stress.

Changes in the value of K_1 affect the surface profile of the ice sheet, although the solution remains essentially parabolic. This is because the value chosen to represent the basal shear stress will determine the flow of ice, which in turn determines the surface profile. Assuming a basal shear stress of 100 kPa, the term K_1 is equal to 4.7; if a basal shear stress of 50 kPa is assumed this value falls to 3.4. Given the likely errors involved in estimating values for basal shear stress under former ice sheets, surface profiles were calculated for both 50 and 100 kPa basal shear stresses (Figure 2.1). Vialov (1958) suggests an alternative theoretical ice sheet profile, of a more elliptical surface form, based on the formula

$$\left(\frac{s}{x}\right)^{1/2} + \left(\frac{H}{h}\right)^{1/2} = 1 \qquad (2.2)$$

Vialov (1958)

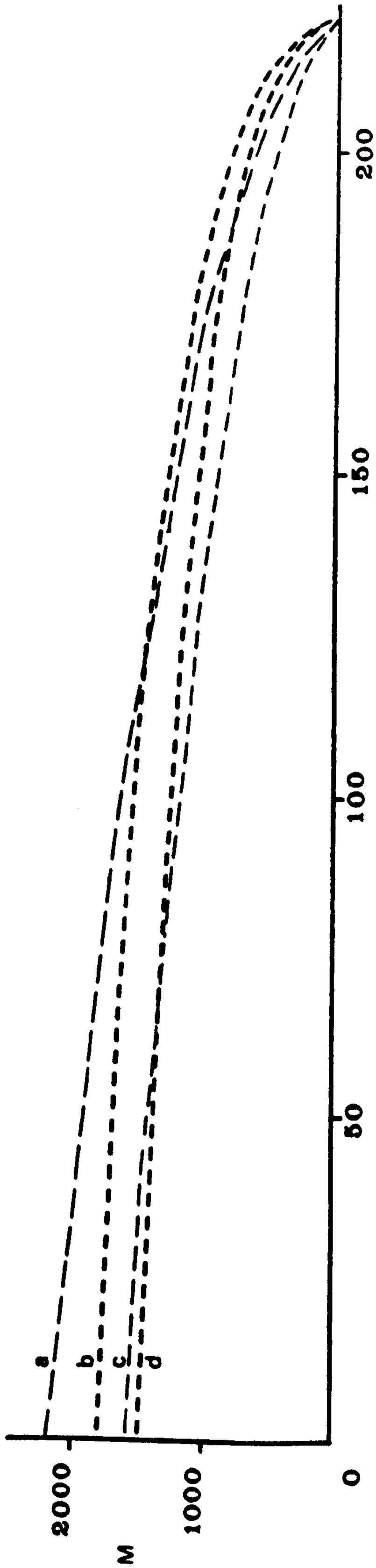

Figure 2.1 Theoretical ice sheet profiles:
(a) Nye parabola, basal shear stress = 100 kPa
(b) Vialov's analysis, H = 1800 metres
(c) Nye parabola, basal shear stress = 50 kPa
(d) Vialov's analysis, H = 1500 metres.

where s is the half width of the ice sheet, x is the distance from the ice divide, H is the height at the ice divide and h is a point on the ice sheet surface. For comparison, ice sheet profiles constructed using Vialov's analysis with H = 1500 metres and H = 1800 metres are also shown in Figure 2.1.

Figure 2.2 shows how these theoretical profiles compare to the modern day ice sheets of Greenland, West Antarctica and Vatnajokull. The Vatnajokull profile is approximated well by a Nye parabola with a basal shear stress of 50 kPa. However, the Greenland and Antarctic profiles show steeper profiles than are predicted by the theoretical solutions due to the mountainous terrain close to the ice sheet margins.

In this study a parabolic ice sheet profile is used to represent the ice surface of the former ice sheet. There are several advantages of such a choice. There is a strong similarity between a simple parabola and the Vatnajokull ice cap profile, which is the closest analogy to a former Scottish ice sheet in terms of size and climate. The parabolic profile is also widely used in other ice sheet reconstructions (eg Boulton et al. 1978). Furthermore, the parabolic profile agrees with qualitative field evidence of the vertical extent of the ice sheet. A 50 kPa parabolic profile predicts an ice surface altitude 100 to 200 metres above the highest summits in the Cairngorm Mountains.

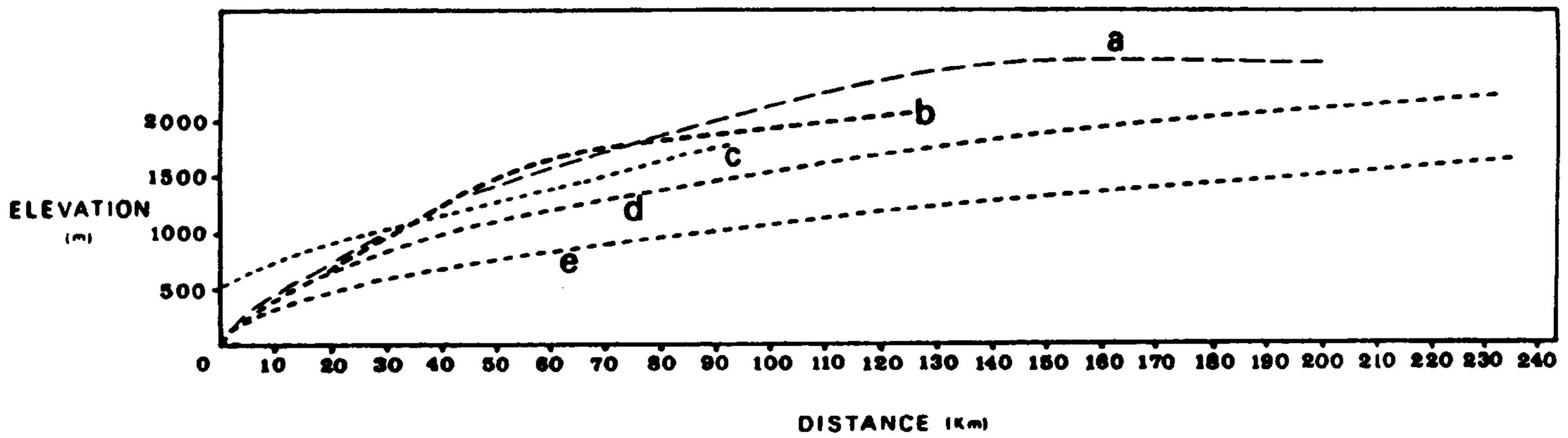

Figure 2.2 Ice sheet profiles: theoretical and observed.
(a) S.W. Greenland
(b) Palmer Land, Antarctica
(c) Vatnajoküll, Iceland
(d) Nye parabola, basal shear stress = 100 kPa
(e) Nye parabola, basal shear stress = 50 kPa.

This is in agreement with the work of Sugden (1968) who postulated ice thicknesses sufficiently thick to submerge the underlying topography, yet thin enough to allow topography to control patterns of ice discharge in the mountains. The elliptical solution of Vialov (1958) is not used as there is less agreement between the theoretical profile produced and the observed ice sheet profiles.

2.2.3.2 The geographical extent of the ice sheet

The method used to calculate the ice surface profile involves reconstructing a parabolic ice sheet profile up-glacier from the ice sheet margin and superimposing this over the basal topography (Figure 2.3). It is necessary to establish the areal extent of the ice sheet in order to calculate its surface profile, and thus the position of the former ice margin in the east of Scotland and the former ice divide must be located.

The maximum extent of the last Scottish ice sheet in the North East of Scotland is recorded by the glaciomarine and marine deposits of the Wee Bankie Formation (Holmes 1977; Thomson and Eden 1977; Stoker et al. 1985) and the Swatchway Formation (Stoker and Bent 1985). If this formation is of late Devensian age then the maximum extent of the last Scottish ice sheet was some 30 to 70 km east of the present day coastline. Stewart (1991) has suggested that the Wee Bankie moraine is of late Devensian age on the basis of seismic facies analysis of its sediment

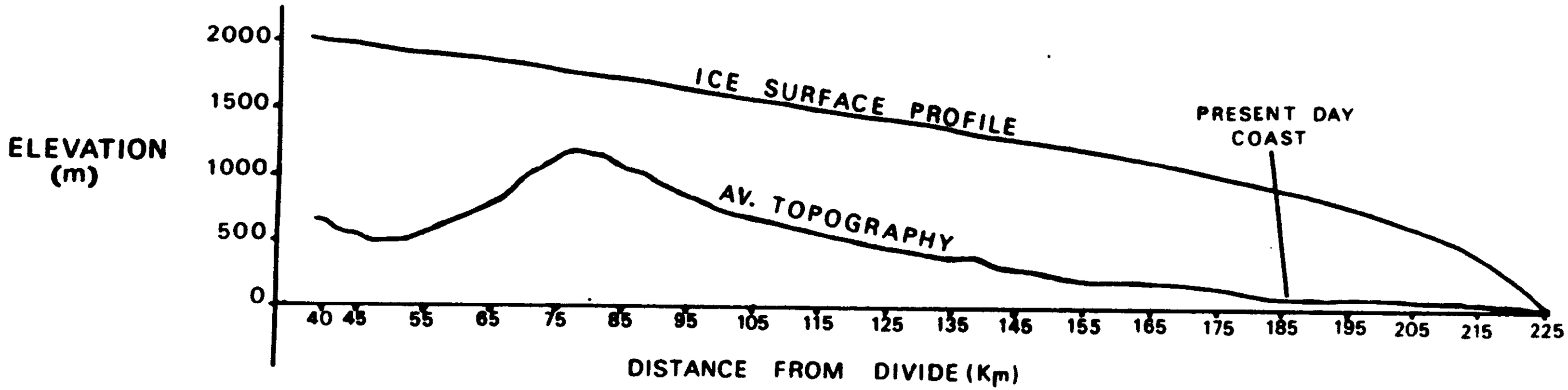

Figure 2.3 Reconstructed ice sheet profile superimposed on averaged topography to illustrate method used in calculations.

succession and detailed sedimentological analysis of morainic material. It therefore follows that the Scottish and Scandinavian ice sheets were separate bodies and did not coalesce in the North Sea basin (Stoker et al. 1985; Nesje and Sejrup 1988). For the purpose of this reconstruction the Wee Bankie moraine is taken as representing the late Devensian maximum of the Scottish ice sheet in the North Sea.

It is a long held view that the late Devensian ice divide was located over the Western Highlands of Scotland, in particular in the area surrounding the collecting grounds of the Rannoch basin. This has been suggested on topographic, climatological and glaciological grounds. Mapping of ice flow indicators such as friction cracks, striae, roches moutonnees and evidence from the transportation of erratics in the Rannnoch Moor, Fannich and Rosshire areas suggests the former ice divide was located along a line roughly north - south between Rannoch Moor and Fannich (Thorp 1987; Reed 1988). For the purpose of this reconstruction it is assumed that the ice divide of the last Scottish ice sheet was situated in the area postulated by these authors. The location of the former ice divide, the Eastern margin, and the major flowlines of the ice sheet are shown in Figure 2.4.

2.2.3.3 The ice age temperature regime

One of the upper boundary conditions in the model is the ice sheet surface

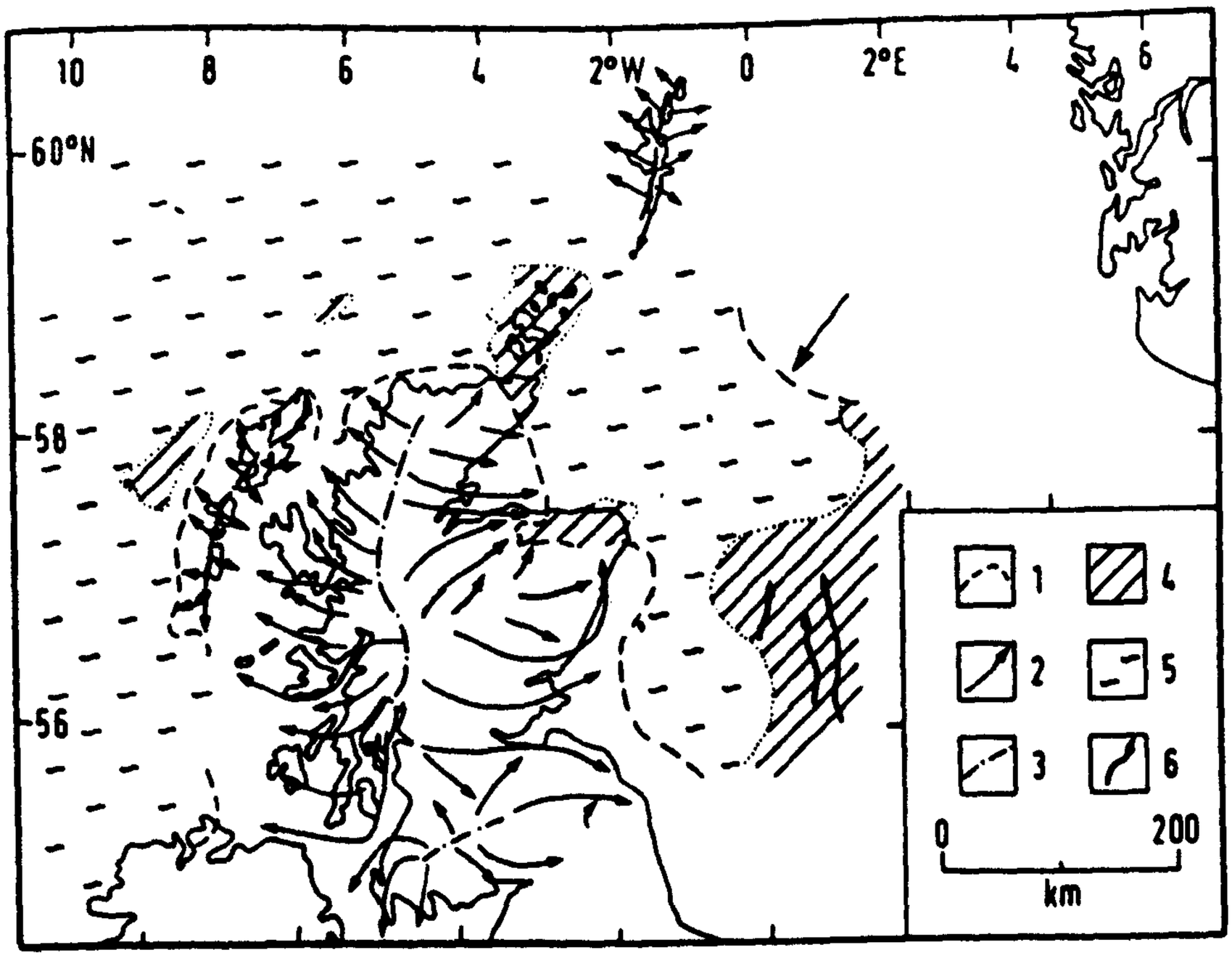

Figure 2.4

Palaeogeographic reconstruction of the Late Devensian ice sheet maximum. 1. Ice sheet margin; 2. Ice flow direction; 3. Ice divides; 4. Unglacierized land areas; 5. Sea; 6. Channels. Source: Sutherland (1984) p.232.

temperature. It is therefore necessary to derive ice surface temperatures for the last Scottish ice sheet. The most precise method is to estimate the average annual temperature at the ice sheet margin and to calculate ice sheet surface temperatures up-glacier for a given ice sheet profile using an altitudinal lapse rate. Values are required for the average annual temperature at the ice margin and the rate of temperature decline with altitude.

Values for the depression in air temperatures during the late Devensian in Scotland vary widely (Table 2.1). The estimates vary according to the nature of the evidence on which they are based; those based on former periglacial phenomena (Frenzel 1967; Williams 1975; Watson 1977) suggest that mean annual temperatures in Britain were between -4°C and -10°C. The existence of former ice wedge casts and involutions in periglacial areas surrounding the former ice sheet leads to a consensus that mean annual temperatures were around -9°C. This represents a cooling of some 17°C from the present day mean annual temperature of +8°C in this area of Scotland.

Another method of establishing temperatures during the late Devensian is that based on studies of Coleopteran fossil assemblages. Beetles display a marked preference for very restricted environmental conditions, and individual species are easily identifiable in fossil remains (Lowe and Walker 1984). The identification of beetles currently existing only in Arctic environments in Quaternary sediments in Britain has been used to make

EVIDENCE	CLIMATIC INFERENCE	SUGGESTED TEMPERATURE	SOURCE
Fossil frost wedges	Mean annual temperature	Mean annual temp. -1°C at sea level	Sissons (1983)
Periglacial phenomena	Mean annual temperature	Mean annual temp. -8°C to -10°C	Williams (1975)
Existence of former pingoes	Mean annual temperature	Mean annual temp. -4°C	Frenzel (1967)
Periglacial evidence	Mean annual temperature	Mean annual temp. -8°C to -9°C	Watson (1977)
Coleopteran assemblages	Mean annual temperature	Mean annual temp. -8°C to -12°C	Coope (1977)
Literature review	Mean annual temperature	Mean annual temp. -2°C to -4°C	Lamb (1977)

Table 2.1 Suggested mean annual temperature depression for Scotland in the late Devensian.

inferences about the climate at that time (Coope 1975). These studies suggest that mean annual temperatures were between -8°C and -12°C (Coope 1977). This temperature depression represents a reduction in air temperatures of some 16°C to 20°C below present day values, slightly more extreme than suggested by the periglacial phenomena. This is explained by an increase in the continentality of the British climate, with a mean annual temperature range of around 30°C. Temperatures may have been as high as +10°C in the summer months, dropping as low as -20°C in the winter. This continentality is attributed to ice sheet conditions.

Finally, studies of the climatic record in ice cores suggest that temperature depressions of this order of magnitude are reasonable. Studies of oxygen isotopes, chemical trace elements, acidity and continental dust in ice cores suggest ice age temperature depressions of around 6°C in Antarctica (Lorius et al. 1990) and more than 7°C in Greenland (Dansgaard et al. 1989) during Quaternary glaciations. These radical changes in the polar environments can be used as a minimum estimate of the temperature depression for the more sensitive mid-latitudes, where ice sheets built up on currently unglaciated land.

In this reconstruction, mean annual air temperature at sea level was set at -9°C in eastern Scotland. This is equivalent to a reduction in mean annual

temperature of 17°C from the present day value. Since this is considerably more extreme than the value adopted by Gordon (1979) in his calculations of basal temperatures beneath the ice sheet in Northern Scotland, sensitivity tests using a mean annual temperature of -6°C and -3°C were also undertaken.

2.2.3.4 Altitudinal lapse rate

To calculate ice sheet surface temperatures from the given temperature depression at the margin it is necessary to know the decrease in surface temperature with altitude and continentality. An altitudinal lapse rate is used to relate the annual average temperature at the margin to ice surface temperatures up-glacier. Diamond (1960) found that an altitudinal lapse rate of 0.7°C per 100 metres in altitude fitted ice surface temperatures over the Greenland ice sheet. A more extreme lapse rate of 1.0°C per 100 metres is suggested by Budd et al. (1971a) for the Antarctic ice sheet. This latter lapse rate is more appropriate to continental ice sheets whilst that of Diamond (1960) describes more maritime ice sheets. In this study the lower lapse rate of 0.7°C per 100 metres is therefore adopted.

2.2.3.5 Accumulation rate

The value chosen to represent the accumulation rate is vital because it determines important variables such as the ice sheet velocity (and thus frictional heating), and the rate at which cold snow and firn is brought down

into the ice sheet (the surface warming rate). Both of these variables have a profound effect on basal temperatures within ice sheets.

There are many uncertainties involved in determining the accumulation rate of a former Scottish ice sheet. Some of these uncertainties are those surrounding the status of the surrounding ocean bodies and their role in supplying moisture to the Scottish ice sheet. For example, the southward penetration of the North Atlantic polar front reduces temperatures and simultaneously introduces moisture starvation over Scotland (Kerr, submitted). Precipitation values also depend on whether the North Sea was arid (Devoy 1987) or only partially reduced in size (Nesje and Sejrup 1988). There is also the problem of establishing the role of the ice sheet in determining regional climate through albedo-temperature feedback and orographic precipitation changes.

Bearing in mind these uncertainties it was decided to select a mean accumulation value for the region, and not to attempt to simulate variations in precipitation with elevation and distance from the coast. Payne (1988) has derived precipitation values for Scotland during glacial periods using a numerical model to simulate the growth and movement of precipitation tracks from the North Atlantic. The movement of moisture bearing depressions is related to sea surface temperatures over the Atlantic, and the model has been used to successfully simulate present day precipitation

(Payne 1988). The model predicts a mean precipitation rate of 0.75 ma^{-1} over North East Scotland; equivalent to a 50 per cent reduction in mean present day precipitation over the flowband. An identical value was used by Boulton et al. (1978) in their British ice sheet model.

Calculations using the effectiveness formulae of Payne (1988) suggest that at the given temperature depression, 100 per cent of any precipitation would fall as snow. It is therefore legitimate to assume that the accumulation rate is equal to the precipitation rate of 0.75 ma^{-1} and this value is used in the standard model run. As a test of the sensitivity of the model to changes in the accumulation rate, further calculations are made using an accumulation rate of 0.375 ma^{-1}; one quarter of present day mean precipitation.

2.2.3.6 Geothermal heat flux

In addition to frictional heat generated by ice movement, a substantial quantity of geothermal heat enters the base of an ice sheet from the earth's crust. This is termed the geothermal heat flux. Values for geothermal heat flux are given by Lee and Uyeda (1965, Figure 44). The value for northern Scotland corresponds to a geothermal heat flux of 0.05 W/m^2/second and this value is used in the calculation of basal ice temperatures.

2.3 Basic calculations

The calculation of the basal thermal regime is made in the following way. A parabolic ice surface profile is established using the method outlined in section 2.2.3.1. The eastern margin of the ice sheet is positioned at the Wee Bankie moraine and the profile is reconstructed inland as far as the former ice divide. The upper boundary conditions are set by this profile since it determines conditions on the ice sheet surface, along with the assumed temperature depression, altitudinal lapse rate and accumulation rate.

The formula used by Budd et al. (1971a) to calculate the basal ice temperature is

$$\theta_b = \theta_s - Z\left[Y_b \frac{erf\, y}{y} - Y_s 2E_{(y)}\right] \qquad (2.3)$$

(Budd et al. 1971a)

where θ_b = basal temperature

θ_s = mean ice surface temperature

Z = ice thickness

Y_b = basal temperature gradient

Y_s = ice surface temperature gradient

(y) = a dimensionless thermal parameter

The ice surface temperature is already known and the other terms in the equation are determined as follows.

2.3.1 Ice thickness

The ice thickness at any point along the flowband is given by subtracting the present day topography from the calculated ice sheet profile. In calculating this figure an allowance is made for the effect of isostatic depression caused by the weight of the overlying ice. To take account of this crustal depression the ice thickness is multiplied by 0.267 the height of the overlying ice load (Brotchie and Silvester 1969). Crustal depression occurs on a regional scale and to allow for this, steady state average ice thicknesses are used in its calculation. Isostatic depression is determined at 5 kilometre intervals along the flowband by calculating a mean of ice thickness at 12 points along a line normal to ice flow. A regional estimate of crustal depression is therefore given in each area. This has the desired effect of increasing isostatic depression under thick ice and reducing it under thin ice. Calculated depths of isostatic depression under the ice sheet vary from 150 to 300 metres, depending on the overlying ice thickness. These depths are consistent with estimates of 250 to 300 metres of glacio-isostatic uplift since the end of the last ice age based on the altitude of raised beaches in Scotland (Gray and Lowe 1977).

2.3.2 Ice surface gradient

The ice surface gradient is determined by the ice sheet profile because, at the scale of an ice sheet, surface gradient is largely independent of subglacial relief. The surface gradient is calculated at 5 kilometre intervals along the ice surface profile by averaging the slope angle between the two surrounding points. This gives the average slope over 10 kilometres. Surface gradients are generally small, increasing from 3.6×10^{-3} at the ice divide to 5.6×10^{-3} near the equilibrium line altitude.

2.3.3 Basal temperature gradient

The basal temperature gradient (Y_b) is a measure of the amount of heat supplied to the sole of an ice sheet through glacier movement and geothermal heat. It is given by;

$$Y_b = Y_g + \frac{\tau V}{JK} \qquad (2.4)$$

(Budd et al. 1971a)

where Y_g = geothermal heat gradient (0.05 W/m^2/sec)

τ = basal shear stress

V = ice velocity

J = mechanical equivalent of heat, unity in S.I. terms

K = the thermal conductivity of ice, taken to be 22.6×10^{-6} W/m/sec.

Basal shear stress (τ_b) is determined by

$$\tau_b = \rho g h \sin \alpha \qquad (2.5)$$

(Paterson 1981)

where ρ = the density of ice

g = the gravitational constant

h = ice thickness

$\sin \alpha$ = ice surface slope

The ice velocity (V) is determined by the velocity necessary to maintain ice sheet balance. Assuming the ice sheet is in steady state equilibrium, then all mass accumulated above any point on the ice sheet must be evacuated through that point. Balance velocities have the advantage of being less complex than velocity calculations based on the physical properties of ice where, for example, the relative proportion of velocity accounted for by internal deformation and basal sliding is unknown. Budd et al. (1971a) suggest that balance velocity calculations are likely to be as accurate as any

more complex mathematical solutions. The mean velocity of a column of ice is given by

$$V = \frac{\overline{A}_s x}{Z} \qquad (2.6)$$

(Budd et al 1971a)

where x = distance from ice divide

$\overline{A}_s$ = mean accumulation over that distance

Z = ice thickness

2.3.4 Surface temperature gradient

Ice surface temperatures decrease up glacier, resulting in a corresponding decrease in the temperature of accumulating firn on the glacier surface. The rate of surface warming is expressed as

$$V \alpha \lambda \qquad (2.7)$$

(Budd et al 1971a)

where V = balance velocity

α = ice surface slope

λ = altitudinal lapse rate

The negative surface temperature gradient is given by

$$Y_s = \frac{V \alpha \lambda}{A} \qquad (2.8)$$

(Budd et al. 1971a)

This term accounts for the advection of cold firn into the ice sheet from its surface layers.

2.3.5 Dimensionless thermal parameter

The dimensionless thermal parameter (y) is given by

$$y = \left(\frac{AZ}{2k}\right)^{1/2} \qquad (2.9)$$

(Budd et al. 1971a)

where is the temperature-dependent thermal diffusivity of ice, taken to be 1.2×10^{-6} W/m/sec. The error function ($erf\ y$) is defined as

$$erf\, y = \int_0^y \exp\left(-x^2\right) dx \qquad (2.10)$$

(Budd et 1971a)

The function $E_{(y)}$ is the integral

$$E_{(v)} = \int_0^v F(x)\, dx \qquad (2.11)$$

(Budd et al 1971a)

in which $F(x)$ is the Dawson integral

$$F_{(x)} = \exp\left(-x^2\right) \int_0^x \exp\left(t^2\right) dt \qquad (2.12)$$

(Budd et al 1971a)

Budd (1969) has graphed values of these functions and they are tabulated by Abramowitz and Stegun (1965).

2.4 Model ouput: Basal thermal regime

The equations were solved using the inputs of ice sheet profile, ice surface temperature pattern, accumulation rate and basal topography. In the initial calculations, a series of runs were made based on the values thought to best represent the late Devensian ice age environment in Scotland. In this **standard model run** the ice sheet profile is based on a basal shear stress of 50 kPa, the accumulation rate is set at 0.75 ma^{-1} and surface temperatures are determined assuming a mean annual temperature of $-9^{0}C$ at the margin and an altitudinal lapse rate of 0.7°C/100m (Table 2.2). In order to represent the basal topography accurately, present day topography was sampled on 1:50,000 maps at a regular spacing of 2 x 5 kilometres, providing a grid of 444 data points under the ice sheet. This sampling strategy provides a good representation of the existing topography (Figure 2.5). Basal ice temperatures were then calculated at each of the 444 data points, enabling contoured maps of basal ice temperatures to be produced. The topographic elevation at each of the 444 calculation points is taken from Ordnance Survey 1:50,000 maps and is therefore a true representation of elevation at those points. However, this does not necessarily mean that it is a true representation of the topography since the spread of sampling points may be too coarse to reflect the true topographic features of the landscape. The purpose of Figure 2.5 is to present a visual match between the sampled topography and the actual topography. In the absence of any statistical tests, the sampled topography can be said to provide a good representation of the actual topography if the following criteria are satisfied:

VARIABLE	VALUE	SOURCE
Ice sheet profile	50 kPa parabola	Nye (1952)
Ice sheet margin	40 km east of present day coast	Stoker et al. (1985)
Temperature at ice sheet margin	Annual average -9°C	Dansgaard (1986) Coope (1977) Williams (1975)
Altitudinal lapse rate	0.7°C/100 metres	Diamond (1960)
Accumulation rate	0.75 ma^{-1}	Payne (1988) Boulton et al. (1977)
Geothermal heat flux	0.05 $W/m^2/sec$	Lee and Uyeda (1965)

Table 2.2 Input values used in standard model run.

CONTAINS
PULLOUTS

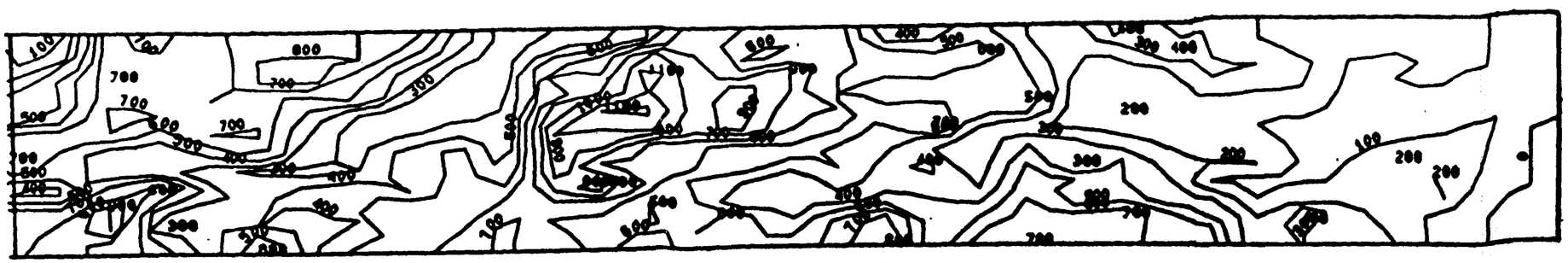

Figure 2.5 The basal topography in the regional flowband:
(a) Basal topography used in the model as determined from the grid of 444 sample points. Contour interval 100 metres.
(b) Actual topography digitised from O.S. 1:50,000 map sheets. Contour interval 100 metres.

Note that the sample topography provides a good representation of the actual topography.

- All major topographic features of the landscape are represented

- These topographic features are in the correct geographical location, both individually and relative to one another.

Figure 2.5 shows this to be the case; the high altitude area of the Cairngorm Mountains, the major drainage routes such as the Dee and Spey River valleys and the North Sea coastline are all easily picked out on the sampled topography. In addition, these major topographic features all occur in the correct geographic location relative to the Ordnance Survey maps. Thus the Dee and Spey River valleys are separated by the Cairngorm Mountains, the Dee forms one continuous topographic depression running west to east across the area with areas of relatively high land to the north and south, and its valley widens and shallows towards the coast. In conclusion, the sampled topography satisfies the criteria for providing a good match with the actual topography.

The sensitivity of the model to changes in these input values is examined using sensitivity analysis. In total, 14 model runs were made using different combinations of input values (Table 2.3). These included changes in the ice sheet profile, the accumulation rate, the surface temperature at the margin and the basal topography.

Model run 7 (Table 2.3) is the standard model run against which the

Run	Accumulation rate (ma^{-1})	Profile	Temp. at ice sheet margin	Lapse rate
1	0.75	100 kPa	-9°C	0.7°C/100m
2	0.75	100 kPa	-6°C	0.7°C/100m
3	0.75	100 kPa	-3°C	0.7°C/100m
4	0.375	100 kPa	-9°C	0.7°C/100m
5	0.375	100 kPa	-6°C	0.7°C/100m
6	0.375	100 kPa	-3°C	0.7°C/100m
*7	0.75	50 kPa	-9°C	0.7°C/100m
8	0.75	50 kPa	-6°C	0.7°C/100m
9	0.75	50 kPa	-3°C	0.7°C/100m
10	0.375	50 kPa	-9°C	0.7°C/100m
11	0.375	50 kPa	-6°C	0.7°C/100m
12	0.375	50 kPa	-3°C	0.7°C/100m
13	Averaged topography			
14	Flat topography			

* Run 7 is the standard model run.

Table 2.3 Input parameter values used in the model runs.

sensitivity tests are compared. In the discussion of the model runs, 2 outputs are shown:

(1) The calculated pattern of basal ice temperatures contoured at 2°C intervals. In these outputs temperatures greater than 0°C are notional as any excess heat is used to melt a thin layer of ice at the base of the ice sheet.

(2) The pattern of basal thermal regime, in which the the output is divided into three distinct zones: zones of basal melting, zones where the basal ice is between 0°C and -8°C (and localised pressure melting may occur), and zones where the basal ice is below -8°C (and pressure melting does not occur).

The contoured basal ice temperatures for each run, and maps of the corresponding basal thermal regime are shown in Figures 2.6 to 2.15. Of the 14 model runs made, runs 1 to 12 (Figures 2.6 to 2.13) are those using the detailed bed sampling strategy, whilst runs 13 and 14 (Figures 2.14 and 2.15) are those using less accurate representations of the ice sheet bed (Table 2.3).

2.4.1 Standard model run

In the standard model run, the majority of the ice sheet is characterised by basal ice below the pressure melting point. Basal temperatures increase from

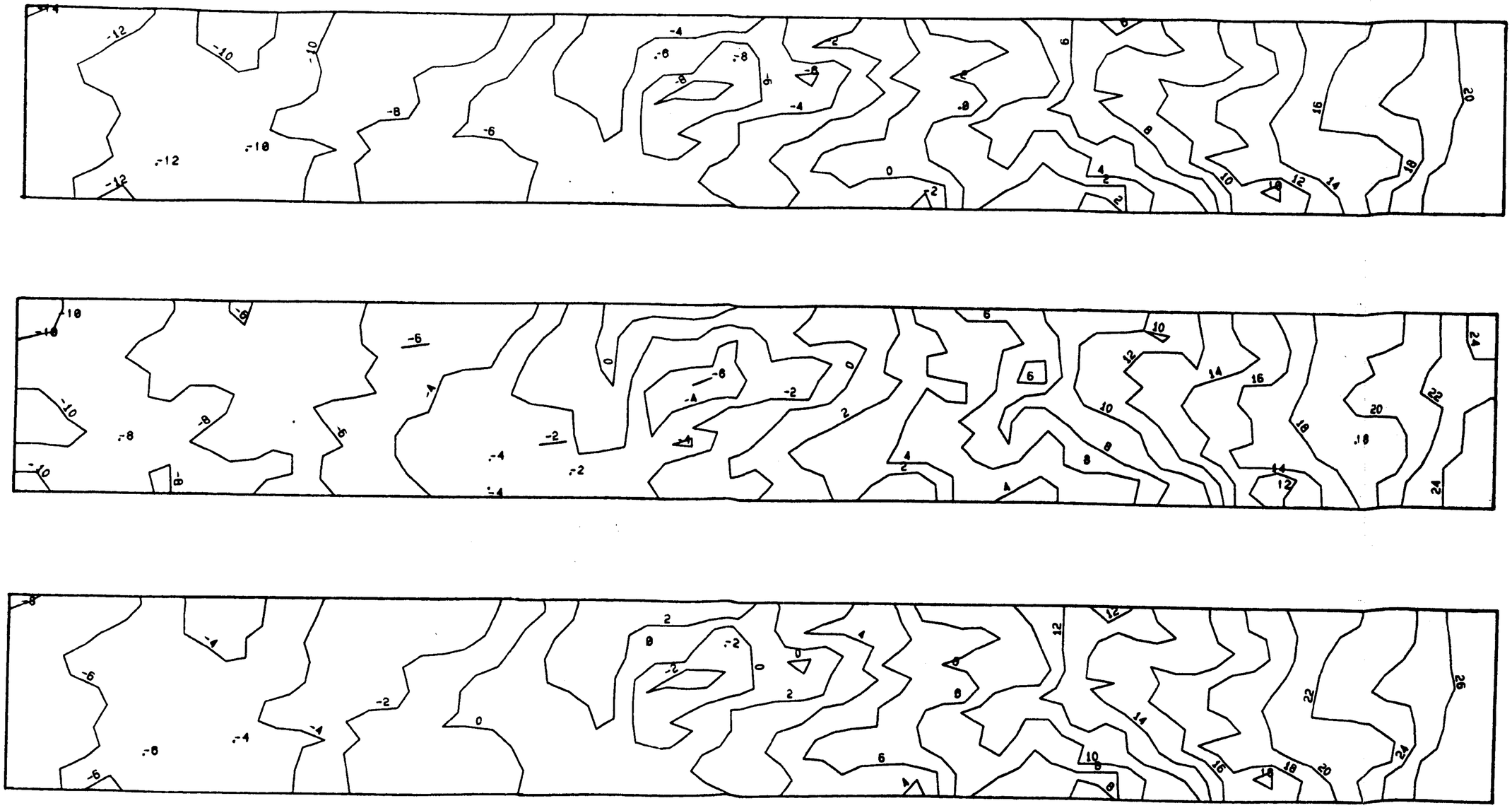

Figure 2.6 Contoured basal ice temperatures for the regional flowband:
(a) Run 1
(b) Run 2
(c) Run 3.

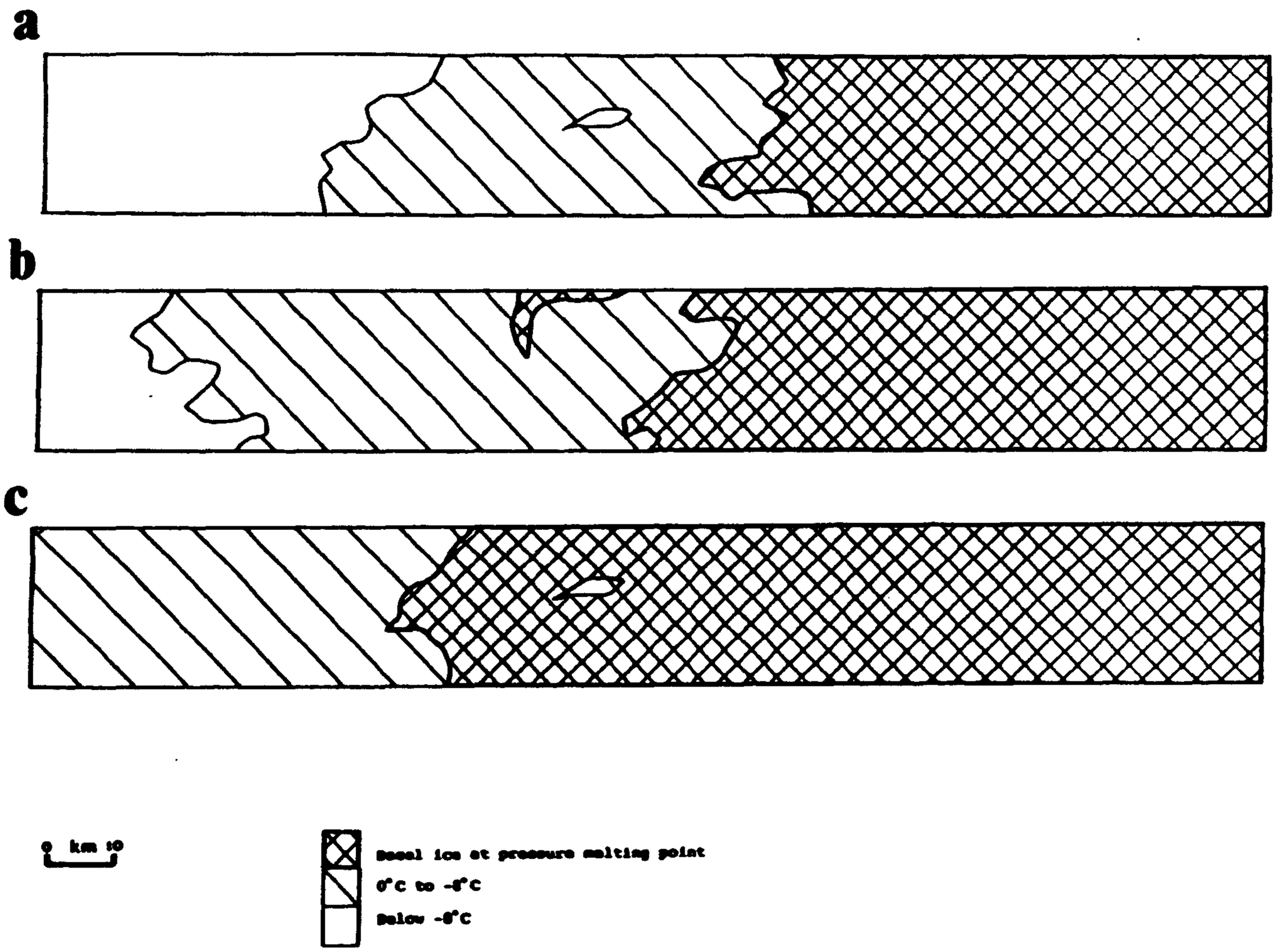

Figure 2.7 Basal thermal regime in the regional flowband:
(a) Run 1
(b) Run 2
(c) Run 3.

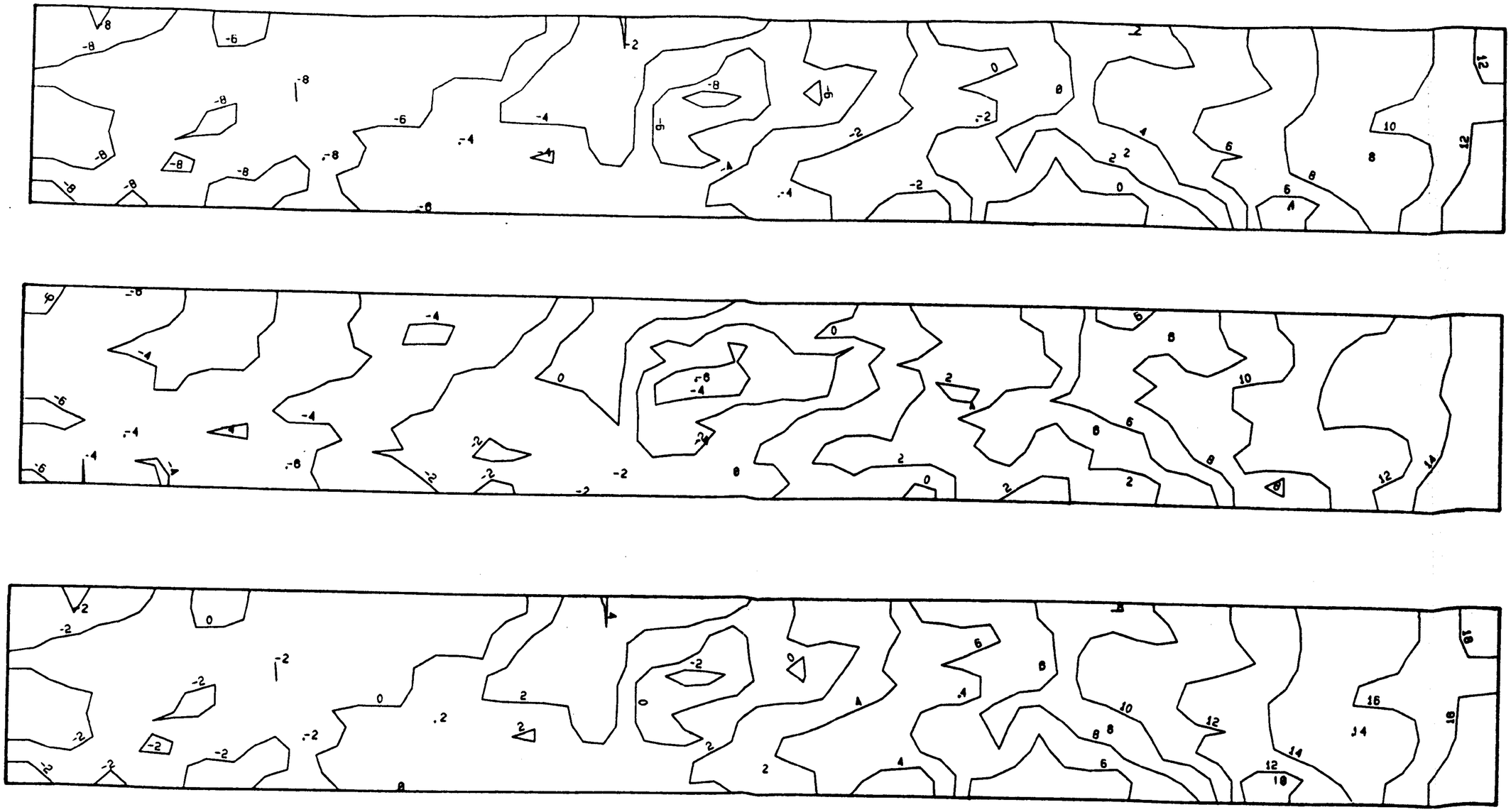

Figure 2.8 Contoured basal ice temperatures for the regional flowband:
(a) Run 4
(b) Run 5
(c) Run 6.

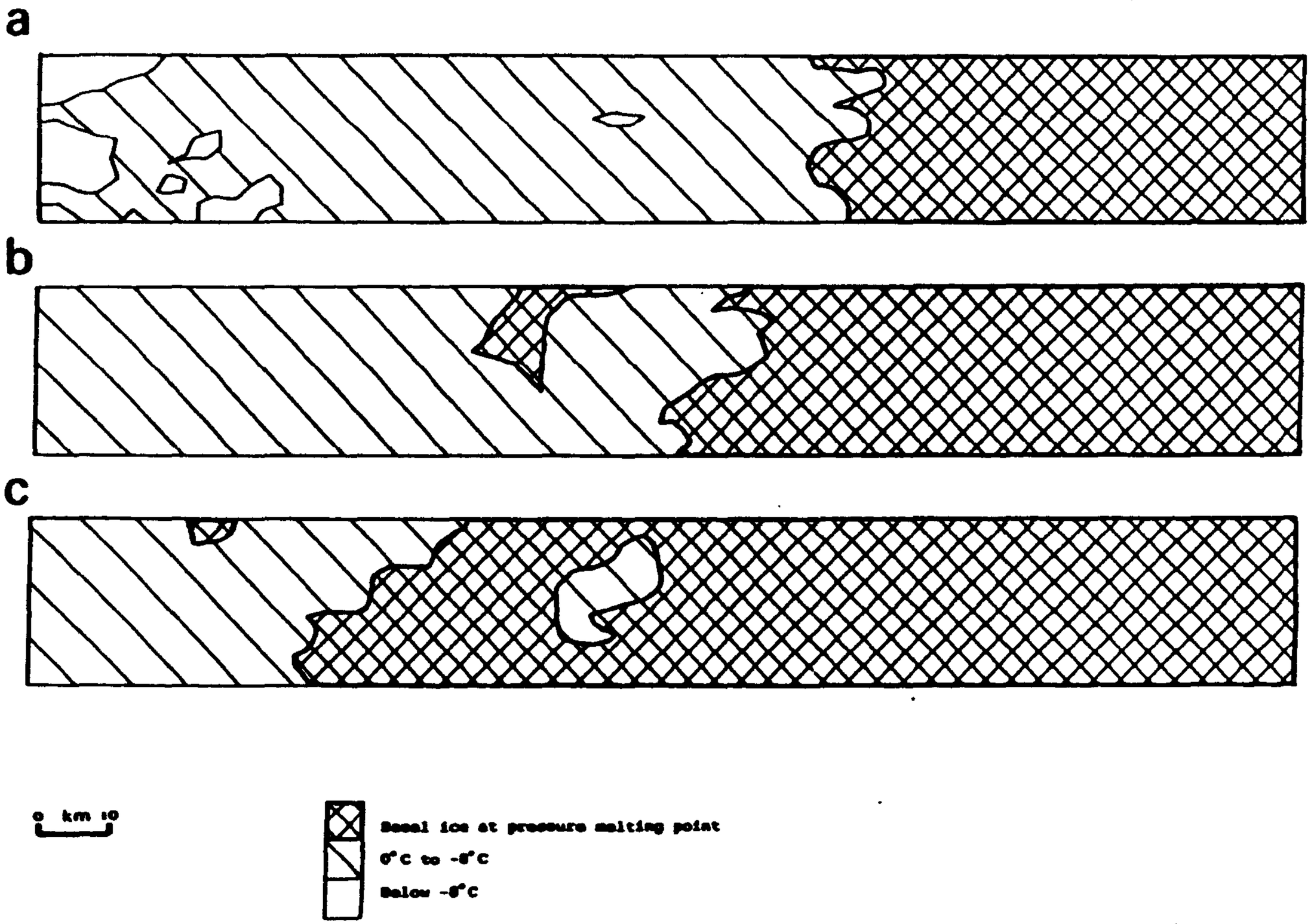

Figure 2.9 Basal thermal regime in the regional flowband:
(a) Run 4
(b) Run 5
(c) Run 6.

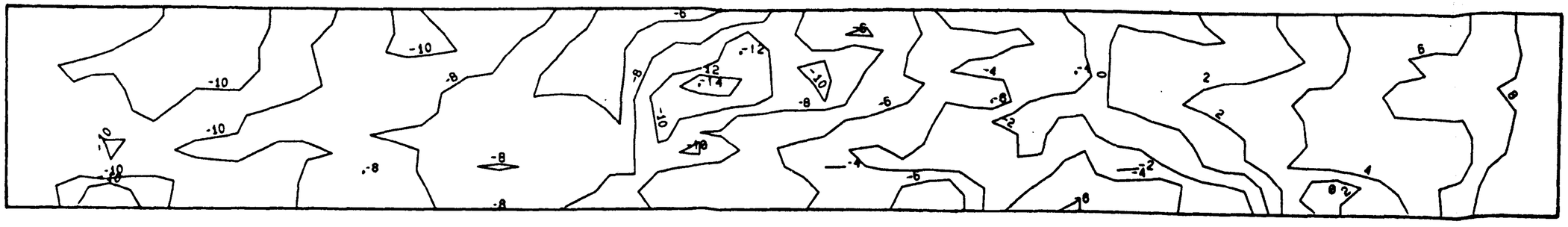

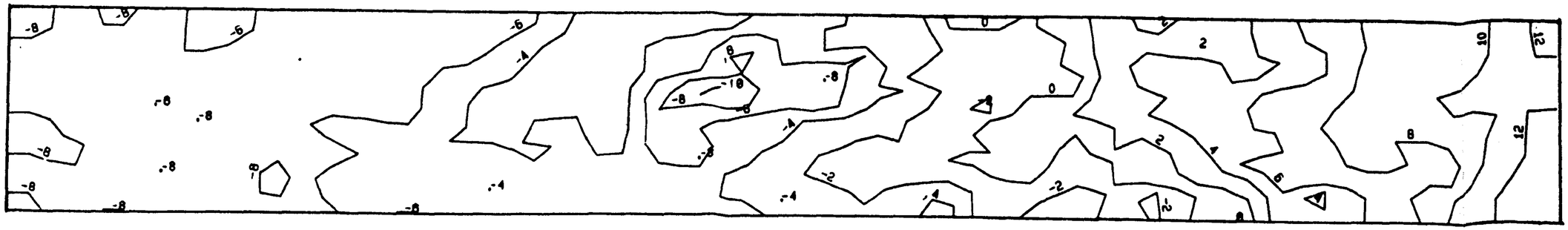

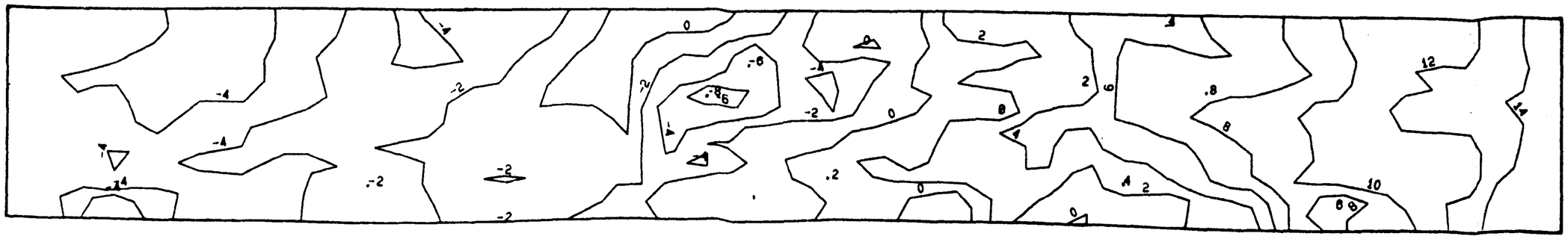

0 km 10

Figure 2.10 Contoured basal ice temperatures for the regional flowband:
(a) Run 7 (Standard model run)
(b) Run 8
(c) Run 9.

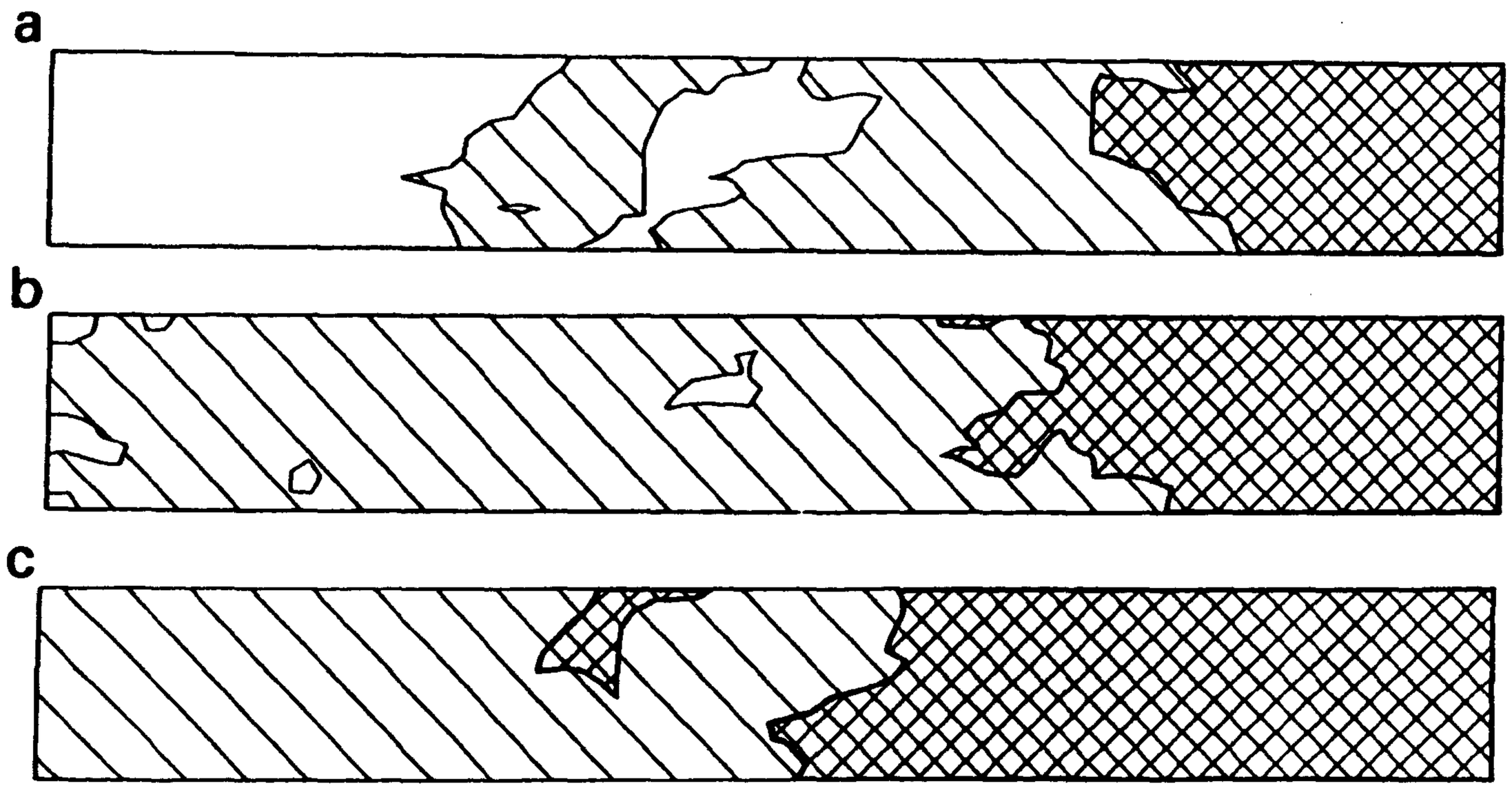

Figure 2.11 Basal thermal regime in the regional flowband:
(a) Run 7 (Standard model run)
(b) Run 8
(c) Run 9.

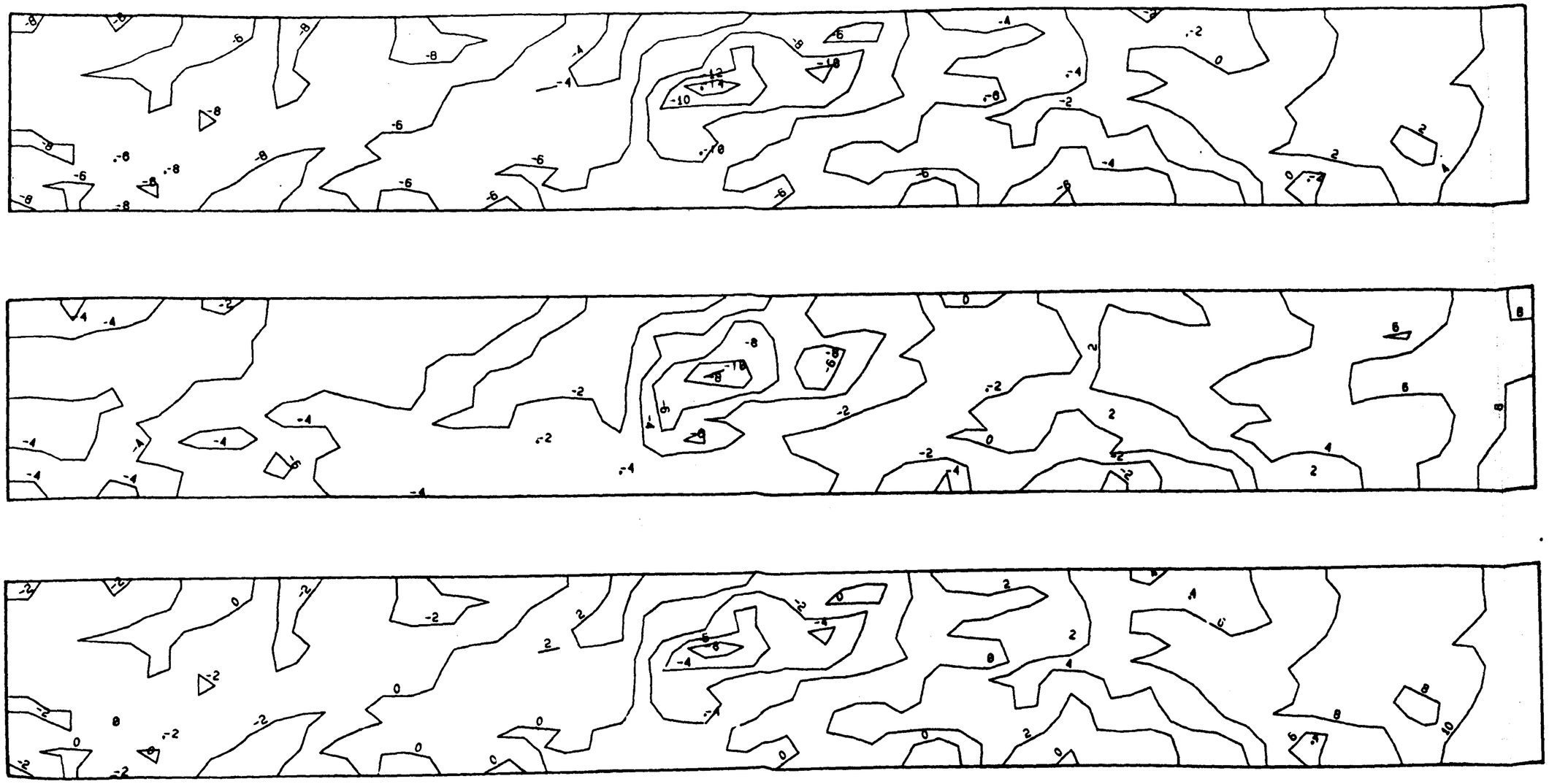

Figure 2.12 Contoured basal ice temperatures for the regional flowband:
(a) Run 10
(b) Run 11
(c) Run 12.

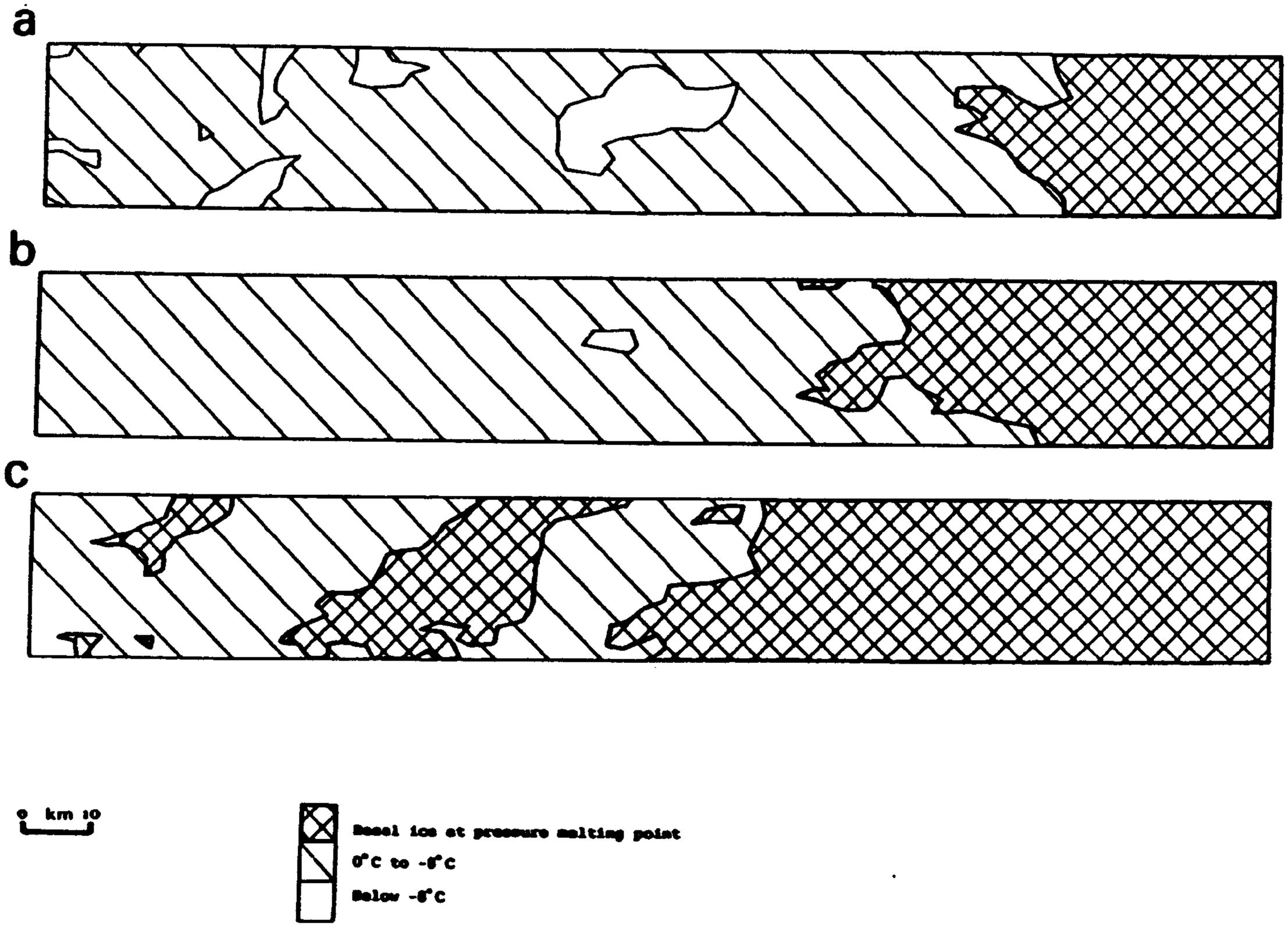

Figure 2.13 Basal thermal regime in the regional flowband:
(a) Run 10
(b) Run 11
(c) Run 12.

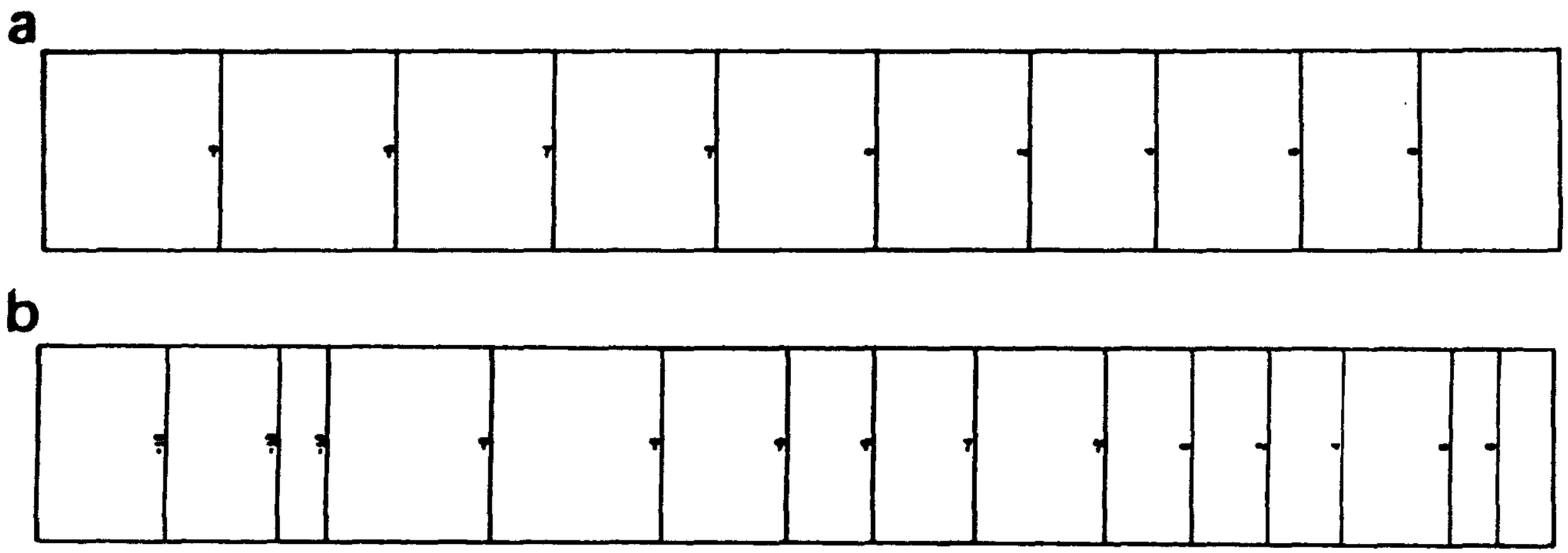

Figure 2.14 Contoured basal ice temperatures for the regional flowband:
(a) Flat bed
(b) Averaged topography.

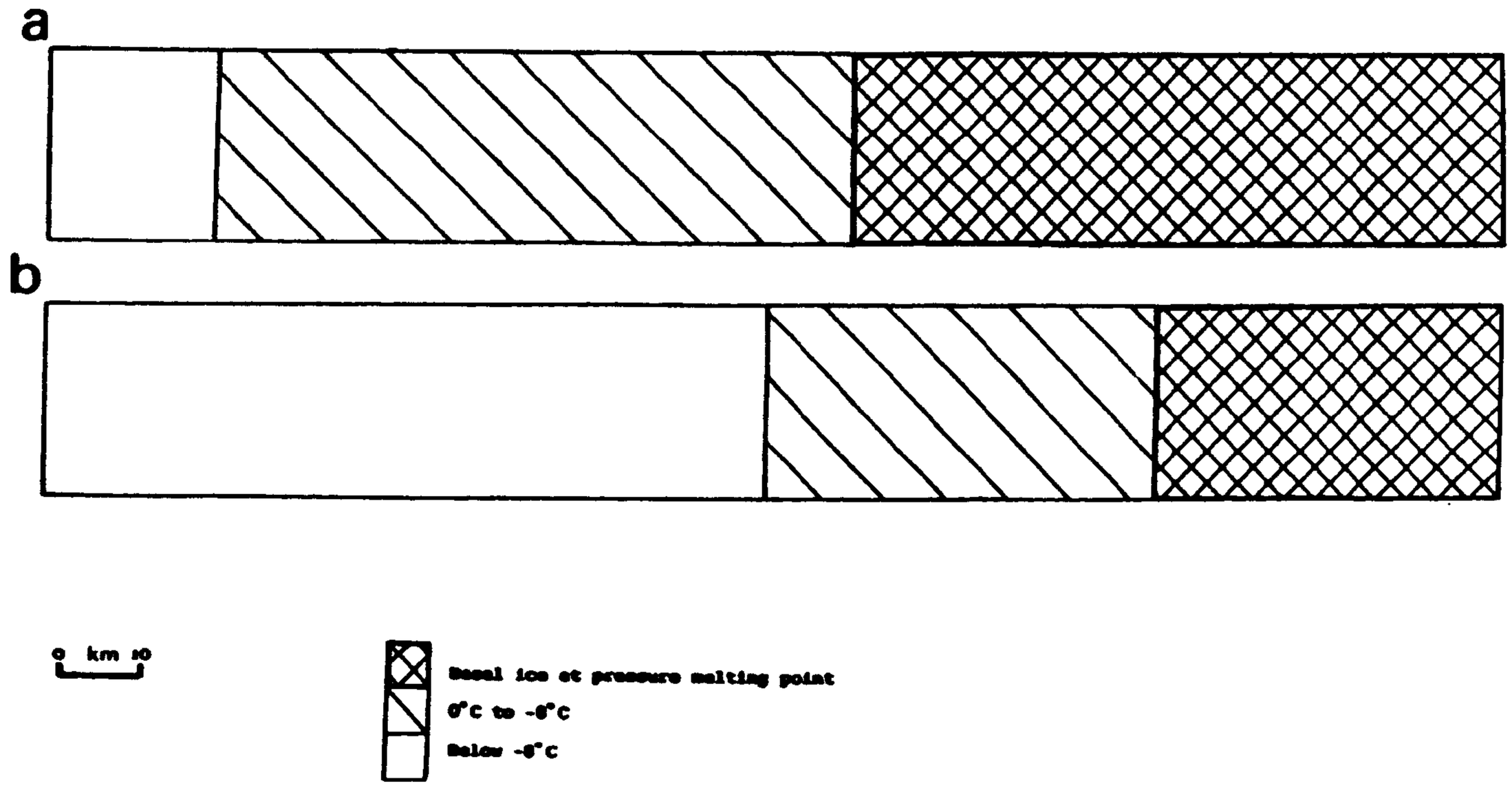

Figure 2.15 Basal thermal regime in the regional flowband:
(a) Flat bed
(b) Averaged topography.

-10°C near the ice divide to +8°C at the eastern margin (Figure 2.10a). The 0°C isotherm occurs near to the ice sheet margin. In general, the pattern of basal thermal regime is one of a cold based zone surrounding the ice divide (below -8°C), with a zone of ice at the pressure melting point only near the ice sheet margin (Figure 2.11a). Separating these zones is an area where the ice is cold based but localised pressure melting may occur (between 0°C and -8°C).

An area of cold based ice exists in the centre of the flowband, where basal ice temperatures fall as low as -14°C (Figure 2.10a). This cold zone coincides with an area of relatively thin ice caused by the high topographic elevation (Figure 2.5). The cold zone is flanked by two areas of relatively warm ice where temperatures rise as high as -6°C (Figure 2.10a). These warm zones coincide with areas of relatively thick ice over topographic depressions, in this case the valleys of the Spey and Dee (Figure 2.5).

In summary, the pattern of basal thermal regime in the standard model run is one of a predominantly cold based ice sheet with a zone of basal melting only near the margin. Large areas of the centre of the ice sheet are below -8°C. Within these zones, topography influences basal ice temperatures; relatively warm basal temperatures are associated with thick ice and relatively cold basal temperatures are associated with thin ice.

2.5 Sensitivity tests

In view of the assumptions involved in estimating the input parameter values used in the model, it is useful to assess the sensitivity of the model to changes in these parameters. Basal temperatures were calculated using a variety of input parameter values to determine the effect that changes have on the pattern of basal thermal regime calculated in the standard model run. These sensitivity tests are useful because they isolate the role of each of the input parameters in the model. The full list of model runs and input parameter values are shown in Table 2.3. It is important to ascertain if the model output (basal ice temperature) is sensitive to changes in the model input parameters. Only once the model sensitivity has been established can conclusions about the reliability of the model be made. The use of multiple model runs created during the sensitivity tests gives a range of possible thermal conditions under the former ice sheet. This allows a comparison to be made between results produced for different climatic scenarios. The sensitivity tests also show the changes in ice sheet thermal regime due to the predominance of certain factors in the model runs. This gives insight into the relationships between the various factors (topographic, climatological and glaciological) used in the model.

The structure of the sensitivity tests used is to vary systematically all the values of the major input parameters. This produced a series of 14 different model runs, each created with a unique set of input parameter values (see

Table 2.3.). The variations in basal thermal regime can then be compared to the basal thermal regime produced by the standard model run. These 14 model runs cover the entire range of climatological, glaciological and topographic values which might reasonably be encountered in the Scottish ice age environment. Unfortunately, the nature of these sensitivity tests does not lend itself to statistical testing; we are concerned with changes in basal thermal regime and movements of their geographical boundaries, not with changes in absolute temperature values. Since this does not warrant any statistical testing, comparisons are visual (see Figures 2.6 - 2.15).

2.5.1 Changing the ice sheet profile

Model runs were made with 50 and 100 kPa ice sheet profiles. Changing the ice sheet profile strongly affects ice thicknesses; the steeper 100 kPa profile resulting in greater ice thicknesses and steeper surface gradients than the 50 kPa profile. Surface gradient is an important term in the calculation of basal shear stress; an increase in basal shear stress raises the basal temperature due to greater frictional heat production.

This is reflected in the basal temperatures calculated using the two different ice sheet profiles. Basal temperatures in the model runs using the 100 kPa profiles (Figures 2.6 to 2.9) are consistently higher than those in the model runs using the 50 kPa profiles (Figures 2.10 to 2.13). The effect of changing the ice sheet profile is clearly seen by comparing model run 1 (Figures 2.6a

and 2.7a) to the standard model run (Figures 2.10a and 2.11a). Although the pattern of basal temperature is similar, the absolute values change and basal temperatures are higher under the thicker 100 kPa ice sheet profile. Basal temperatures over the Cairngorm Mountains reach -8°C under the 100 kPa profile (Figure 2.6a) compared to -14°C under the 50 kPa profile in the standard model run (Figure 2.10a). In conjunction with the greater ice thicknesses, the 0°C isotherm is located nearer the ice divide under the 100 kPa profiles than under the 50 kPa profiles. The extent of basal melting is therefore larger in those runs using the 100 kPa ice sheet profile (Figures 2.6 to 2.9).

The increase in basal melting with the adoption of a 100 kPa ice sheet profile is a function not only of the greater overall ice thicknesses, but also of the extra frictional heating under the steeper profile. This is especially important near the ice sheet margin. With the 50 kPa profiles (Figure 2.12), basal freezing dominates and the 0°C isotherm is located near the ice sheet margin. Relatively low temperatures are found in areas of thin ice such as the Cairngorms where the combination of thin ice and low velocities produce basal freezing. With the 100 kPa ice sheet profiles ice thicknesses increase and the zone of basal melting extends further west (Figure 2.8).

In summary, the model was found to be sensitive to the profile chosen to represent the ice surface. Basal ice temperatures are higher and areas of basal melting larger using 100 kPa ice sheet profiles than with 50 kPa

profiles. However, in none of the sensitivity tests is the change in ice sheet profile sufficient to do anything other than alter the boundaries of the thermal regimes. For example, changing the ice sheet profile does not alter the basal thermal regime of the entire flowband; it only allows the replacement of basal freezing with basal melting in specific areas of the flowband, notably nearest the ice margin.

2.5.2 Changing the accumulation rate

Model runs were made with the accumulation rate set at 0.75 ma^{-1} and 0.375 ma^{-1}. Changes in the accumulation rate are important because they affect the negative surface warming rate (advection of cold ice) and determine the velocity of the ice column (and hence frictional heat production). Theoretically, where accumulation rates are very low the advection of cold ice will be relatively more important than frictional heat production, and basal temperatures will be relatively cold. At the other extreme, where accumulation rates are high, large ice velocities produce greater amounts of frictional heat and basal ice temperatures will tend to be relatively warm.

The relationship between accumulation rate and basal ice temperature is demonstrated in Figures 2.6 (a) and 2.8 (a). The accumulation rate in the first case is 0.75 ma^{-1}, and 0.375 ma^{-1} in the second. In both cases velocity is low at the divide, increasing towards the margin. The effect of decreasing accumulation to 0.375 ma^{-1} is to increase basal temperatures slightly at the

divide due to a reduction in the advection of cold ice, but to decrease temperatures near the margin because the lower balance velocity creates less frictional heat. This pattern is relatively stable, and altering the accumulation rate does not radically change the pattern of cold ice sheet centre and warmer ice sheet margin.

However, the relationship between accumulation rates and basal ice temperature is complex because of the two-fold effect of increasing accumulation rates; (1) an increase in frictional heat production and therefore an increase in basal temperatures and (2) an increase in the advection of cold surface ice and therefore a decrease in basal temperatures. Near the ice divide, where velocities are low, decreasing accumulation from 0.75 to 0.375 ma^{-1} has little effect on frictional heat production but affects the negative surface warming term. With the higher accumulation rate of 0.75 ma^{-1}, the advection of cold ice is important near the ice divide. However, near the equilibrium line where velocities are higher, the higher accumulation rate of 0.75 ma^{-1} creates more frictional heat and basal temperatures are relatively high. Changes in the accumulation rate therefore have different effects depending on location within the ice sheet. High accumulation at the ice sheet centre leads to lower basal temperatures; high accumulation at the ice sheet margin leads to higher basal temperatures.

This can be summarised as follows:

Low accumulation, low velocity = warm basal temperatures

Low accumulation, high velocity = cold basal temperatures

High accumulation, low velocity = cold basal temperatures

High accumulation, high velocity = warm basal temperatures

2.5.3 Changing the ice surface temperature

Model runs with the ice surface temperature varying between -9°C and -3°C show that there is a direct relationship between ice surface temperature and basal temperature in the model. The colder the ice surface temperature the colder the basal temperature, and vice versa (Figures 2.6a to c). If all inputs except the mean annual temperature at the ice sheet margin are held constant, the basal temperatures under the ice sheet become progressively warmer as the climatic regime becomes warmer (Figures 2.6a to c).

Increases in surface temperature can therefore produce basal melting over most of the flowband. In Figure 2.9 (a), where the mean annual temperature at the ice sheet margin is -9°C, basal melting is limited. However, in Figure 2.9 (c), where the mean annual temperature at the margin is -3°C, calculated basal temperatures are at the pressure melting point over almost the entire ice sheet bed. The only remaining areas of basal freezing are those over the Cairngorm Mountains where there is a patch of relatively thin ice, and near the ice divide where velocities are low. In summary, the model is sensitive

to the mean annual temperature imposed at the ice sheet margin. The warmer the imposed ice marginal temperature, the greater the extent of basal melting.

2.5.4 Changing the basal topography

A final set of sensitivity tests involves changing the method by which the ice sheet bed is represented in the model. This is achieved by modelling basal temperatures with the ice sheet resting on; (1) an averaged topography of the type used in many other ice sheet models and; (2) a flat bed.

In order to generate an averaged topography of the flowband, the ice sheet bed was represented by the mean topographic elevation at 5 kilometre intervals along the flowband. This mean was determined from 12 evenly spaced sample points along a line transverse to ice flow at the 5 kilometre intervals. Figure 2.14 (b) shows the variation in basal temperatures from the ice divide to the eastern margin using the averaged topography. The isotherms are straight because the calculations are based solely on mean topographic elevation and there are no topographic irregularities to influence the pattern of temperatures. Basal temperatures increase from -10°C at the ice divide to the pressure melting point near the ice sheet margin. The gradual increase in basal temperatures outward from the ice divide is only influenced by topography at a regional scale. Over the Cairngorm Plateau

the eastward warming trend is interrupted by an area of relatively low basal ice temperatures (Figure 2.14b). This relatively cold zone occurs because the high mean topographic elevation creates an area of relatively thin ice. The overall increase in basal temperatures from ice sheet centre to margin is a function of increasing ice velocity and surface gradient with distance from the ice divide.

The disadvantage of using averaged topography to represent the ice sheet bed is that no account is taken of large scale bed undulations such as valleys and mountain plateaux. Calculations of basal thermal regime using averaged topography to represent the ice sheet bed are only valid on a broad spatial scale. This effect is shown by comparing the standard model run to Figure 2.14 (b), because the input parameters are identical in both cases except for the representation of the basal topography. In both runs basal freezing exists under much of the ice sheet, and the ice sheet only attains its pressure melting point near the ice sheet margin. Using an averaged topography, the pattern of basal temperatures is relatively simple, with an increase in basal temperatures outward from the ice divide. In the standard model run the temperature field is more complex due to variations in ice thickness caused by topography. This topographic effect is masked by using an averaged topography to represent the ice sheet bed.

In order to isolate fully the role of topography a model run was made with the ice sheet resting on a flat bed (Figures 2.14a and 2.15a). Because the ice sheet bed is uniformly flat, the overall ice thicknesses are great and the 0°C isotherm is located closer to the ice divide than in the standard model run. There is a linear increase in basal temperature with distance from the ice divide because there are no topographic hollows or high points in the bed. In the absence of topographic irregularities, we may conclude that basal temperatures under the Scottish ice sheets at their maximum increase towards the margins. This is because; (1) surface temperatures are higher near the margin and a direct relationship exists between surface temperature and basal temperature; (2) velocities increase outward from the ice divide to the margin, reaching a maximum near the equilibrium line altitude of the ice sheet. This outward increase in velocity is accompanied by an increase in frictional heat production and; (3) the term representing the negative surface warming rate decreases in importance towards the margin as ice accumulates at progressively warmer temperatures. There is therefore less advection of cold ice downwards from the ice surface near the ice sheet margin.

2.6 Conclusions

The sensitivity tests show that the conditions most likely to produce basal melting under a former Scottish ice sheet are those of a high surface temperature at the margin, a steep ice sheet profile and a relatively low accumulation rate (Figure 2.8c). The conditions most likely to produce basal freezing under the ice sheet are those where the surface temperature is relatively cold and the ice sheet profile is relatively shallow (Figures 2.10a and 2.12a). The accumulation rate does not appear to be particularly important in this context, as basal freezing is widespread for runs made with both accumulation rates of 0.75 and 0.375 ma^{-1}.

The main conclusions which can be drawn from the calculations of basal ice temperatures are as follows:

(1) Basal freezing is the dominant thermal regime in the standard model run, primarily because of the low imposed marginal temperature. Basal melting occurs only near the ice sheet margin.

(2) The zone of basal freezing is fairly stable for the 50 kPa parabolic profile, where reasonable changes in the input parameters of ice surface temperature and accumulation rate are not sufficient to raise basal temperatures to the pressure melting point.

(3) Basal melting becomes the dominant thermal regime if the 100 kPa

parabolic profile is adopted. This steeper profile produces greater ice thicknesses, and basal melting occurs where identical runs with a 50 kPa profile produce basal freezing.

(4) The zone of relatively cold based ice over the Cairngorm mountains, an area of low ice thicknesses, is a stable feature. It persists in the model even when the combination of input parameters most likely to produce basal melting is adopted.

(5) Topography is an important variable affecting the basal temperature of an ice sheet. This is because the basal topography affects the pattern of ice thickness, which is important in controlling basal ice temperatures. Temperatures in ice sheets are relatively high where ice is thick and relatively low where ice is thin. The sensitivity tests suggest that topography may be a crucial factor in determining areas in which an ice sheet reaches its pressure melting point.

(6) Using an averaged topography to represent the ice sheet bed hides many significant local variations in basal thermal regime. This is especially important at the scale under consideration, where subglacial relief is highly variable.

2.7 Limitations

The model of Budd et al. (1971a) provides an effective method of analysing the variations in basal thermal regime under ice sheets, and how this varies with subglacial topography. One major limitation, however, is that no account can be made for the effect of differential velocity under ice sheets in response to the basal topography; it is only able to consider the effects of ice thickness alone. In order to refine the model to take account of this convergence and diverence of flow due to the subglacial topography, explicit calculations of ice sheet velocity are required. These calculations form the basis of the following chapter.

CHAPTER THREE

MODELLING BASAL ICE TEMPERATURES INCLUDING CONVERGENCE AND DIVERGENCE OF FLOW

3.1 Aim

The aim of this chapter is to calculate basal temperatures for a former Scottish ice sheet at its maximum allowing for convergence and divergence of ice flow. Calculations of basal thermal regime are made for topographic cross-sections in the five field study areas, and the pattern of basal temperatures is calculated for the entire flowband. The calculations for the cross-sections are used for comparison with the mapped distribution of preglacial and glacial landscapes in the sample areas, and the calculated basal thermal regime for the flowband is compared to the regional pattern of ice sheet erosion identified from aerial photograph interpretation.

3.2 Rationale

The results of the model runs presented in Chapter 2 suggest that ice in a predominantly cold based ice sheet may be relatively warm over topographic depressions such as valleys, whilst remaining relatively cold over topographic highs. The implications of this are as follows:

(1) Warmer ice in valleys is more likely to experience basal melting and therefore basal sliding (Budd and Young 1979).

(2) Even where basal melting does not occur, relatively warm ice in topographic depressions will deform faster than surrounding cold ice leading to faster rates of flow (Paterson 1981).

(3) Ice deformation may be increased in valleys if there is sufficient longitudinal stress to concentrate ice flow through topographic constrictions. The direction and magnitude of this effect is uncertain as an unknown amount of additional resistance to flow is introduced by frictional drag on the valley sides (Nye 1965; Whillans 1981).

To understand the mechanisms by which ice flow becomes channelled into ice streams it is necessary to look at large scale ice sheet dynamics (Figure 3.1). Where the subglacial terrain is relatively homogeneous there is little propensity for flow lines to converge and no streaming of flow takes place. Ice flow is therefore uniform (Figures 3.1 c and d). In reality, however, the ice sheet bed will contain topographic irregularities which exercise a control on flow, causing flowlines to converge and streaming of flow to take place along topographically suitable routes (Figures 3.1 a and b).

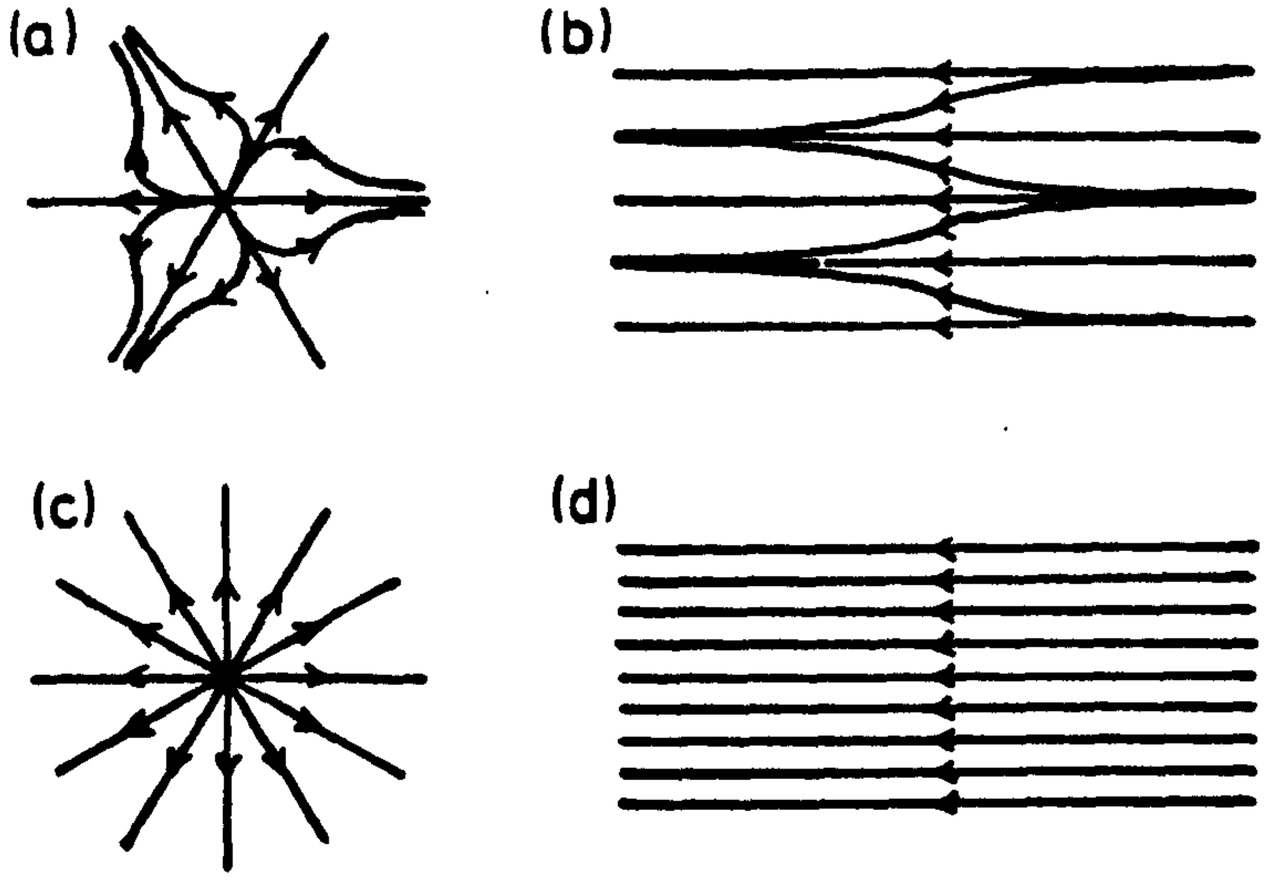

Figure 3.1 Schematic modes of ice sheet flow:
(a) and (b) streamlines for case of ice streams
(c) and (d) uniform flow without ice streams.
Source: Mazo (1987) p.146.

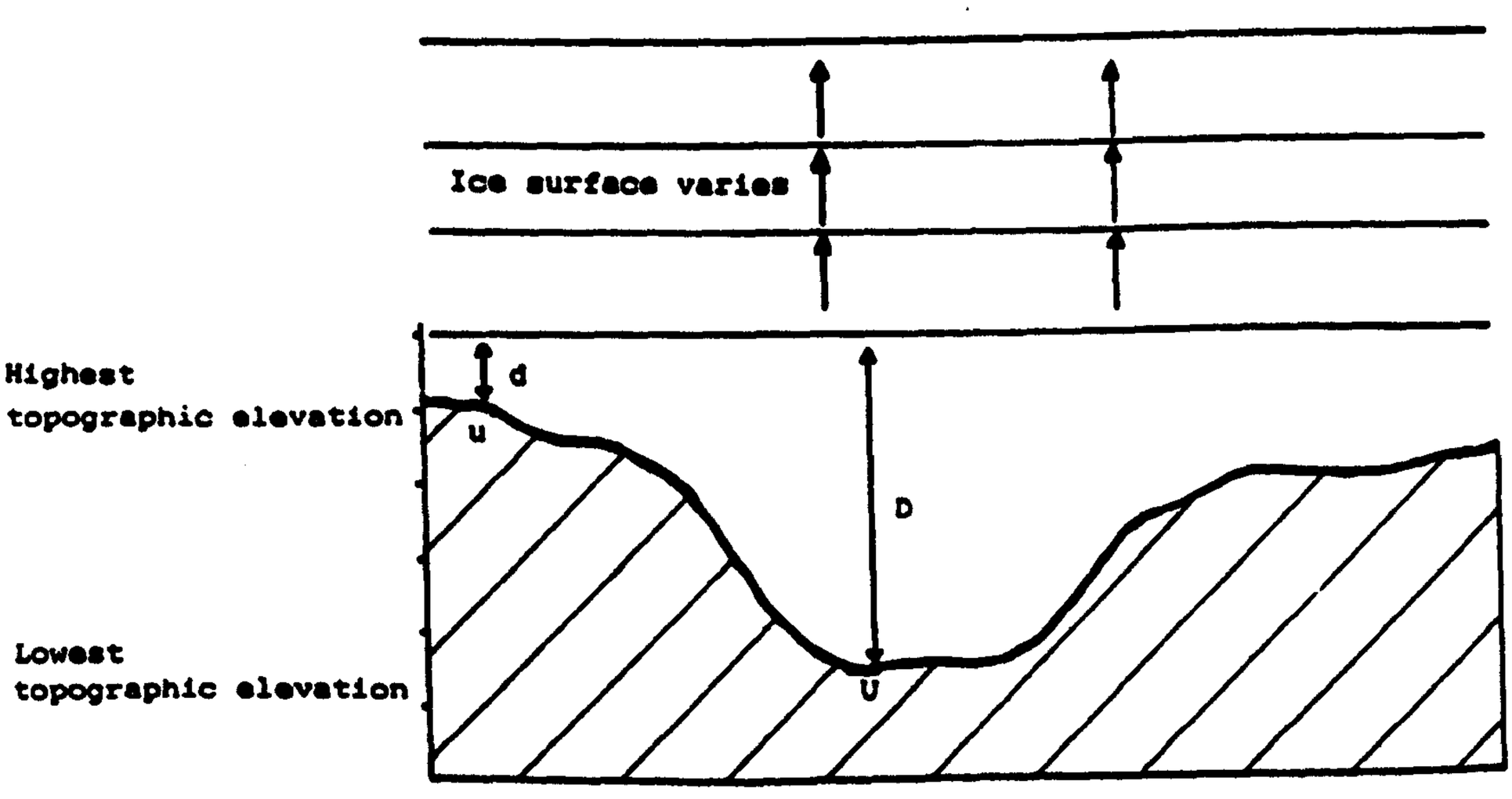

Figure 3.2 Schematic topographic cross section used in calculation of deformation velocities. Ice surface varies in altitude over the basal topography, causing ice thickness d over an interfluve and ice thickness D over a valley to vary. Corresponding variations in ice velocities u and U can then be calculated.

It is therefore possible to distinguish between two types of ice flow; convergent and divergent flow. Convergent flow occurs where the underlying topography channels flow lines into ice streams and divergent flow occurs where flow lines are spreading. The implication of this is that velocities within ice sheets will increase where flow lines converge and decrease where flow lines diverge. In order to calculate the consequent changes in basal thermal regime it is necessary to quantify the differences in velocity between valleys and interfluves as a result of convergence and divergence of flow.

3.3 Previous work

Previous work in this area is limited, with a tendency to concentrate on within-valley variations in ice velocity rather than the differences between valleys and interfluves. Nye (1965) calculated variations in ice velocity and shear stresses within valley cross-sections of different geometric shapes. Velocity and shear stress were calculated for channels of rectangular, elliptical and parabolic cross-sections in order to assign multiplier terms to the flow law for ice. Maximum shear stress does not occur precisely at the edge of channels but at a certain distance in from the edge. The calculations assume that all movement is due to internal deformation and it is suggested that the pattern of frictional drag in the channels is not changed drastically by the inclusion of basal sliding. However, the calculations do not give any

indication of how ice sheet velocities vary between the channels considered and the surrounding areas.

Harbor et al. (1988) consider the problem of erosion under warm based valley glaciers. A coupled ice dynamics and glacial erosion model is used to simulate the development of U-shaped glacial valleys from an original V-shaped cross-section. Their glacial erosion model computes within-valley variations in erosion rates using the glaciological parameters which control erosion such as sliding velocity, basal shear stress and rate of energy dissipation.

Mazo (1987, 1989) models the genesis of ice streams and large scale longitudinal bed channels under ice sheets by considering the coupling between the eroding ice sheet and its eroded bed. The critical feature is the dependence of the rate of bed erosion on the physical characteristics of the eroding ice mass. This leads to a coupling between perturbations in ice flow and perturbations in the bed topography. The major limitation is that no account is taken of other mechanisms that may generate instabilities in ice flow such as strain heating and ice anistropy.

Reeh (1982) attempts to include the effects of topography on flow patterns within an ice sheet by modelling a three dimensional steady state ice sheet. The effect of topography on surface elevation contours and flow patterns is

highlighted by modelling the ice sheet firstly on a horizontal base with an arbitrary edge curve, and secondly on a plane sloping base with a rectilinear ice margin. However, the resolution of the model is too coarse to include valleys of the dimensions under consideration here.

The only model to consider the variation in velocity between valleys and interfluves under an ice sheet is that of Oerlemans (1984). Glacial erosion is modelled under a polar ice sheet which is cold based except in pre-existing valleys, where it may be warm based. Oerlemans' glacial erosion law provides an explanation for the development of glacial troughs from pre-existing river valleys due to preferential erosion by faster flowing, warm based ice. However, no detail is given of how relative velocities vary between valleys and interfluves. Suffice to say, ice will always be warmer in troughs ensuring faster flow. In this manner, small valleys may develop into trough-like features with large ice discharge. Troughs may have a discharge of hundreds of metres per annum, whilst surrounded by cold based stagnant ice on higher bedrock where velocities are only a few metres per annum.

The models of Harbor et al. (1988), Oerlemans (1984), Mazo (1987), and Reeh (1982) are not applicable to the present problem because:

(1) The model of Harbor et al. (1988) is only applicable to variations in

intensity of glacial erosion under a temperate valley glacier, and is restricted to a single valley.

(2) The model of Oerlemans (1984) ignores the convergence and divergence of ice flow due to topography.

(3) The model of Mazo (1987) deals with dimensionless bed perturbations and does not consider the role of basal temperatures in glacial erosion. Other mechanisms that may cause instabilities in ice flow, such as strain heating, are ignored. If velocities within ice sheets vary greatly then changes in strain heating may cause great variations in erosion.

(4) The model of Reeh (1982) is not applicable as it does not directly account for the influence of topography on the ice flux and flow pattern of the ice sheet.

3.4 Calculating basal temperatures

To include the role of topography in calculations of basal ice temperatures a method is required which directly links topography and ice sheet velocity. In particular the method is concerned with; (1) the effect of ice thickness on velocity and; (2) the effect of convergence and divergence of flow on velocity.

3.4.1 Ice thickness

For a given ice surface, ice thickness is high over valleys and low over interfluves (Figure 3.2). Changes in the ice surface elevation cause the ice thickness (D) over a valley and the ice thickness (d) over an interfluve to vary. The differential in altitude between the valley and interfluve in this example is 400 metres, causing D to exceed d by 400 metres in each case. Corresponding calculations of ice velocities U and u, allowing the ice surface to vary from 100 to 1900 metres above the highest point of the topography at 1100 metres, were made to determine how changes in ice thickness cause variations in ice velocity between valleys and surrounding interfluves.

Assuming all movement is due to shear deformation, ice discharge can be calculated using the formula

$$q = \frac{2A}{n+2}(\rho g)^n h^{n+2}\left(\frac{dh}{dx}\right)^n \qquad (3.1)$$

(Drewry 1986)

where A = flow law parameter, taken to be 8.75×10^{-13} $Pa^{-3}s^{-1}$

n = flow law multiplier, taken to be 3

h = ice thickness

$\left(\frac{dh}{dx}\right)$ = surface slope, taken to be a typical gradient of 2.7×10^{-3}

The aim of this section of the thesis is to investigate the effect of varying ice thickness on calculated ice sheet velocity. The flow of large ice masses is, at a general level, the result of the gravity forces which induce spreading of the ice by deformation under its own weight (creep). Thus, although ice velocity is also a function of surface slope, ice temperature, and accumulation and ablation rates, these complexities can be simplified by using equations which relate ice movement to shear deformation alone.

The use of a shear deformation equation assumes that ice movement by basal sliding is negligible. This assumption is made because the relative proportions of total ice velocity in an ice sheet due to deformation and sliding are highly variable (these proportions are largely temperature-dependent with sliding velocity high under warm-based ice sheets and low under cold-based ice sheets). Although an equation based on deformation will tend to underestimate overall velocities, it does allow conclusions to be drawn concerning the variation in ice sheet velocity with changing ice thickness.

The equation used to do this is from Drewry (1986) and relates ice velocity to basal shear stress (the so-called driving stress which depends on surface

slope, ice density, ice thickness and gravity). These four terms used to calculate velocity are expressed in the creep relationship termed the "Glen Flow Law", which uses a flow law parameter (A) and a flow law multiplier (n) to determine how changes in ice thickness and ice surface slope affect ice velocity. The equation is obviously very sensitive to the values chosen for the flow law parameter and the flow law multiplier since they are power functions in the equation.

The flow law parameter (A) varies with temperature according to the Arrhenius relation (Paterson 1981). Since the value of A depends on many variables (for example the ice temperature, the size, shape and orientation of the ice crystals, the purity of the ice) it is notoriously difficult to quote "typical" values for A (Paterson 1981). In discussing the values obtained for A through experimental studies, Paterson (1981) found that calculated values may vary by up to one order of magnitude. The values calculated for A at different ice temperatures are given by Paterson (1981; Table 3.3). He recommends that a mean value of A of 5.2×10^{-13} s^{-1} Pa^{-3} at -10 °C be used in the calculation of the flow of glaciers and ice sheets. This recommendation is based on experiments measuring the natural deformation of ice through borehole tilting and ice shelf spreading. The value of 5.2×10^{-13} suggested by Paterson is very close to that of 8.75×10^{-13} given by Drewry (1986), used in this study. The value of A for ice at -10 °C is used in this case since this represents best the range of temperatures calculated for

a former Scottish ice sheet in Chapter 2.

Values for the flow law multiplier (n) have been found to vary between 1.9 and 4.5, with a mean of 3 (Drewry 1986). This has been established from laboratory experiments with ice, from the measurement of borehole and tunnel closures beneath ice sheets, and from studies of creep rates on ice shelves (Paterson 1981). In a review of these methods of measurement Paterson also suggests a value of n=3 should be used over the stress range 40 to 100 kPa, and concludes that "For the range of stresses normally encountered in glaciers, a flow law...with n=3 seems to be a valid approximation and is usually adopted" (Paterson 1981, p.27). A value of n=3 is therefore adopted in this study.

One criticism which can be made of the equation in general is that since it deals with large-scale ice dynamics it is only applicable to large ice sheets, and not to valley glaciers. However this limitation does not apply since any former Scottish ice sheet must have been considerably larger than of valley glacier proportions.

Following equation 3.1, the average velocity of a column U is then given by

$$\overline{U} = q/h \qquad (3.2)$$

(Drewry 1986)

The calculated velocities U and u are shown in Table 3.1, along with ice depths D and d. These calculations show that ice sheet velocities are low (under 40 ma^{-1}) at ice thicknesses of less than 1800 metres. These depths are encountered at few points under a former Scottish ice sheet. For example, to produce ice depths of this magnitude even in a mountainous region such as the Cairngorms would require an ice surface altitude of 2900 metres. This is unrealistic, bearing in mind that a 50 kPa ice sheet profile predicts an ice surface elevation of 1400 metres in this region (Chapter 2). With an ice sheet surface only 100 metres above the Cairngorm summits ice velocities are reduced to under 1 ma^{-1} (Table 3.1).

Table 3.1 also displays the calculations D/d and U/u. Where ice thicknesses are high the ratio D/d is low (1.21) and where ice thicknesses are low D/d is high (5). Where ice thicknesses are high the ratio U/u is low (2.1) and where ice thicknesses are low U/u is high (617). As the ice surface altitude increases, the values of D/d and U/u decrease. Differences in ice velocity between valleys and interfluves are therefore likely to be greater where ice thicknesses are small, as D/d is relatively high. Under thick ice there there will be little difference between ice velocity in valleys and interfluves, as

Ice Surface (m)	D(m)	d(m)	U(ma^{-1})	u(ma^{-1})	D/d	U/u
1200	500	100	0.247	0.0004	5	617
1300	600	200	0.51	0.006	3	85
1400	700	300	0.95	0.03	2.33	32
1500	800	400	1.62	0.1	2	16
1600	900	500	2.6	0.247	1.8	11
1700	1000	600	4	0.51	1.67	8
1800	1100	700	5.79	0.95	1.57	6
1900	1200	800	8.2	1.62	1.5	5
2000	1300	900	11.3	2.6	1.44	4.3
2100	1400	1000	15.2	4	1.4	3.8
2200	1500	1100	20	5.79	1.36	3.45
2300	1600	1200	26	8.2	1.33	3.17
2400	1700	1300	33	11.3	1.3	2.9
2500	1800	1400	41	15.2	1.29	2.7
2600	1900	1500	52	20	1.27	2.6
2700	2000	1600	63	26	1.25	2.4
2800	2100	1700	77	33	1.23	2.3
2900	2200	1800	93	41	1.22	2.26
3000	2300	1900	110	52	1.21	2.1

Table 3.1 Calculation of ice sheet velocity with variable ice thickness.

D/d is relatively low. These calculations suggest that ice velocities will increase in depressions at the expense of interfluves, and that this effect will be most pronounced where the ice surface is little above the underlying terrain.

3.4.2 Topographic geometry

The second stage is to allow for the spatial geometry of the land over which the ice is flowing. Figure 3.3 is a schematic representation of the effects of basal topography on ice flow. Four situations are depicted; Figures 3.3 (a) and (b) show the effects of relief amplitude relative to ice thickness and Figures (c) and (d) show the effect of topographic geometry. The calculations shown in Table 3.1 suggest that the velocity differential between valleys and interfluves will be high where relief amplitude is great, as this creates the largest differences in ice thickness (Figure 3.3 a). With greater ice thicknesses, the difference in velocity is much smaller as the thickness damps the effect of topography on ice flow. The opposite situation exists under thin ice where the effect of topography is exaggerated.

Figures 3.3 (c) and (d) show the effect of topographic geometry on ice flow. In Figure 3.3 (c), a sinusoidal valley, flowlines converge in the valley due to; (1) the existence of a valley likely to channel flow and; (2) the capture of flow from uplands. In Figure 3.3 (d), a broad and shallow concave valley, little convergence of flow is likely due to the topography, and no

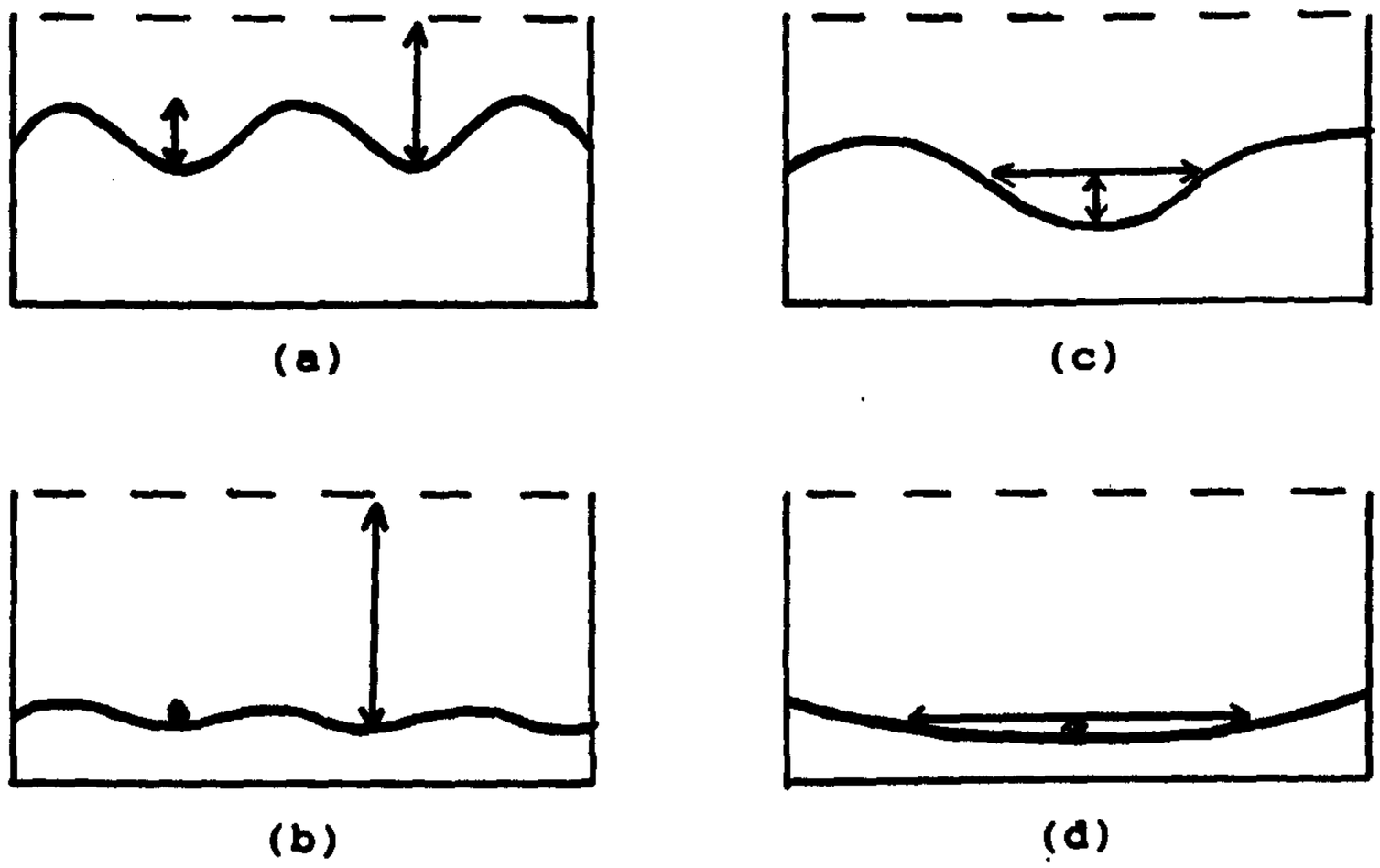

Figure 3.3 Schematic of effects of basal topography on ice flow:
(a) Relief amplitude high relative to ice thickness
(b) Relief amplitude low relative to ice thickness
(c) Valley depth high relative to valley width
(d) valley depth low relative to valley width.

acceleration of flow is expected.

The situations in Figures 3.3 (a) to (d) can be viewed as a continuum if the combined effects on ice flow of relief amplitude relative to ice thickness and topographic geometry are considered. The maximum influence of topography on patterns of ice flow will be in a situation where relief amplitude is high relative to ice thickness and the topographic geometry favours convergent flow (Figure 3.3 a). The minimum influence on flow will be exercised in a situation where relief amplitude is low relative to ice thickness and the topographic geometry does not favour convergent flow (Figure 3.3 d). The two extremes of this continuum would be an ice sheet barely thick enough to cover a highly varied topography (great effect on flow) and a relatively thick ice sheet resting on a uniform bed (no effect on flow).

The differential in velocity due to changes in shear deformation between valleys and interfluves gives an indication of the importance of topography in determining ice velocities, but the major limitation of the method is that the calculations depend solely on movement due to internal deformation, and no account is taken of velocity due to basal sliding. This is because sliding laws are not yet fully understood, especially in areas of undulating bed topography where calculations are very complex. In the absence of quantitative information on the proportion of ice sheet velocities due to basal sliding, calculations of velocity differences by deformation alone probably

underestimate overall velocities, especially in deep valleys where basal sliding may be a large component of the total velocity.

To gain a perspective on the influence of topography on ice flow, a method was devised to include the effect of variations in ice flow on basal temperatures. There are several assumptions which are implicit within this framework:

(1) The ice surface over valleys and interfluves is assumed to remain constant and the effects of any surface lowering of the ice sheet over valleys is ignored. This assumption is legitimate under thick ice, but surface lowering may be more important under thin ice.

(2) Ice flow is assumed to be parallel to the upper surface slope. There is therefore a greater propensity for ice to flow round large obstacles in the direction of flow rather than to deform upwards over such obstacles.

(3) Ice is assumed to move faster in topographic depressions than on surrounding interfluves due to; (i) greater ice deformation and; (ii) convergence of flow. The negative effect of the additional frictional drag produced on valley walls is ignored.

(4) Convergence of ice flow is assumed to affect the lower half of any slope

of a valley and to be compensated for by divergence on the upper half.

(5) The increase in ice velocity is assumed to be proportional to the relief amplitude of the topography relative to ice thickness, and to topographic geometry. As a starting point this relationship is assumed to be linear. Increased flow of ice in valleys is compensated for by a reduction in ice velocities over interfluves. Ice sheet velocities are therefore linked to the ability (or otherwise) of the basal topography to accommodate ice flow.

The method of calculation is as follows. A cross- section of the basal topography is drawn transverse to the direction of overall ice flow at 5 kilometre intervals along the regional flowband. The ice surface elevation is determined by the 50 kPa ice sheet profile so that average ice thicknesses, surface temperatures and isostatic depression are identical to the standard model run. The balance velocity at each cross-section is distributed according to; (1) the relief amplitude of the topopgraphy relative to the ice thickness, the topographic relief factor (r), and; (2) the topographic geometry of the cross-section, the topographic geometry factor (g). Thus velocities vary over the cross-section as a result of the basal topography, although the overall velocity at each cross-section remains equal to the balance velocity. The methods used to assign ice sheet velocity to topographic cross-sections are as follows:

(1) It is necessary to determine whether the relief amplitude of the topography is sufficiently large relative to ice thickness to exercise control over velocities. The most direct method of ascertaining this is to measure the relief amplitude of the topography (i.e. the difference in altitude between the highest and lowest points in the cross-section) and compare this to the maximum ice thickness (i.e. the difference in height between ice surface elevation and the lowest point in the cross-section). Figures 3.4 (a) and (b) illustrate these concepts. In Figure 3.4 (a) the maximum ice thickness of 6 units compares with a relief amplitude of 1 unit, whilst in Figure 3.4 (b) the maximum ice thickness of 3 units compares with a relief amplitude of 1 unit.

If relief amplitude is exactly equal to maximum ice thickness then total control on flow is exercised and the ratio is 1. In situation (a) the relief amplitude to ice thickness ratio is 0.16 implying that relief amplitude is low relative to ice thickness, whilst in situation (b) it is 0.33, implying that relief amplitude is high relative to ice thickness. In this study convergent flow is only considered to occur in cross-sections where the relief amplitude divided by maximum ice thickness is greater than 0.2. This introduces a threshold below which convergent flow does not occur, and above which it may occur. In the absence of any previous work on this subject this threshold was chosen since preliminary calculations of topographic cross sections show that that valleys where relief amplitude divided by maximum ice thickness is below 0.2 tend to be broad and shallow. In contrast, those with values

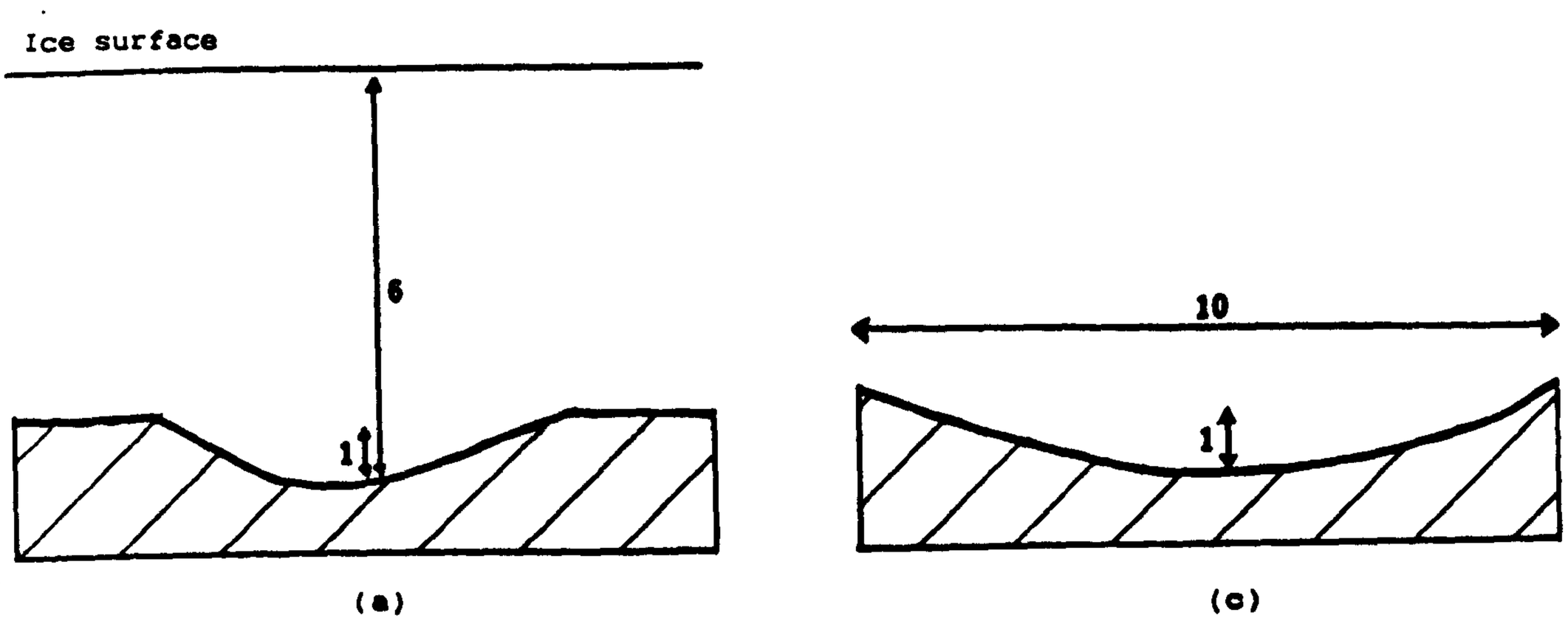

Figure 3.4 Calculation of the two topographic factors used to assign values to the convergence and divergence of ice flow:
(a) and (b) Relief amplitude relative to ice thickness, the topographic factor r.
(c) and (d) Topographic geometry, the topographic factor g.

greater than 0.2 tend to be more parabolic in cross section with steeper sides and narrower valley floors. Although Nye (1965) used valley cross sectional form to assign multiplier terms to the ice flow law his work does not extend to convergent flow. Since valley cross-sectional geometry in reality is a continuum from broad and shallow to narrow and deep, the distinction between valleys likely or unlikely to instigate convergence of ice flow is placed at 0.2 as a starting point. This boundary is not claimed to be definitive and it is recognised that other workers may argue for other values to be chosen. It is, however, a starting point in locating the topographic areas under ice sheets which are likely to produce convergence of flow.

(2) The effects of topographic geometry on ice flow are assessed by the propensity of the topography to initiate channelling or streaming of ice flow. The method used is to consider the shape of the basal topography in terms of the number, depth and width of valleys present. The ability of a valley to channel ice flow is assumed to be related to its depth to width ratio (Figures 3.4 c and d). The valley depth is measured vertically at the centre line of the valley and the width is measured across the highest point of the valley in the cross-section. In Figure 3.4 (c) the topography is unlikely to channel ice flow, and the valley depth to width ratio is 1/10 or 0.1. In Figure 3.4 (d) the topography is more likely to cause channelling of flow, and the valley depth to width ratio is 2/5 or 0.4. A value close to 1 implies that channelling of flow is likely and a value close to 0 implies little

channelling of flow is likely.

In combination, these two measures of topographic relief and topographic geometry determine the changes in ice sheet velocity due to the irregular basal topography. At each of 36 cross-sections the balance velocity of the ice sheet was multiplied by the derived values of (g) and (r) to increase ice sheet velocities in areas of convergent flow. In order to maintain the overall balance of the ice sheet at each cross-section, velocities in areas of divergent flow (i.e. interfluves and rises in the topography) are reduced. Thus the original balance velocity is redistributed over the cross-section in order to allow for the convergence and divergence of ice flow.

3.4.3 Illustration of method

The method is best illustrated by using one of the cross-sections as an example. Figure 3.5 is the basal topography in the central area of the Dee valley, near Balmoral (for location see Figure 1.1). The maximum relief amplitude in the cross-section is 210 metres, and the maximum ice thickness is 999 metres. The topographic relief factor (r) is therefore 210/999 = 0.21. Two major valleys exist. The topographic geometry factor (g) in the northern valley is 1/2 = 0.5. In the southern valley it is 1.7/5 = 0.34. The increase in velocity due to convergence of flow (V_c) in these areas is therefore:

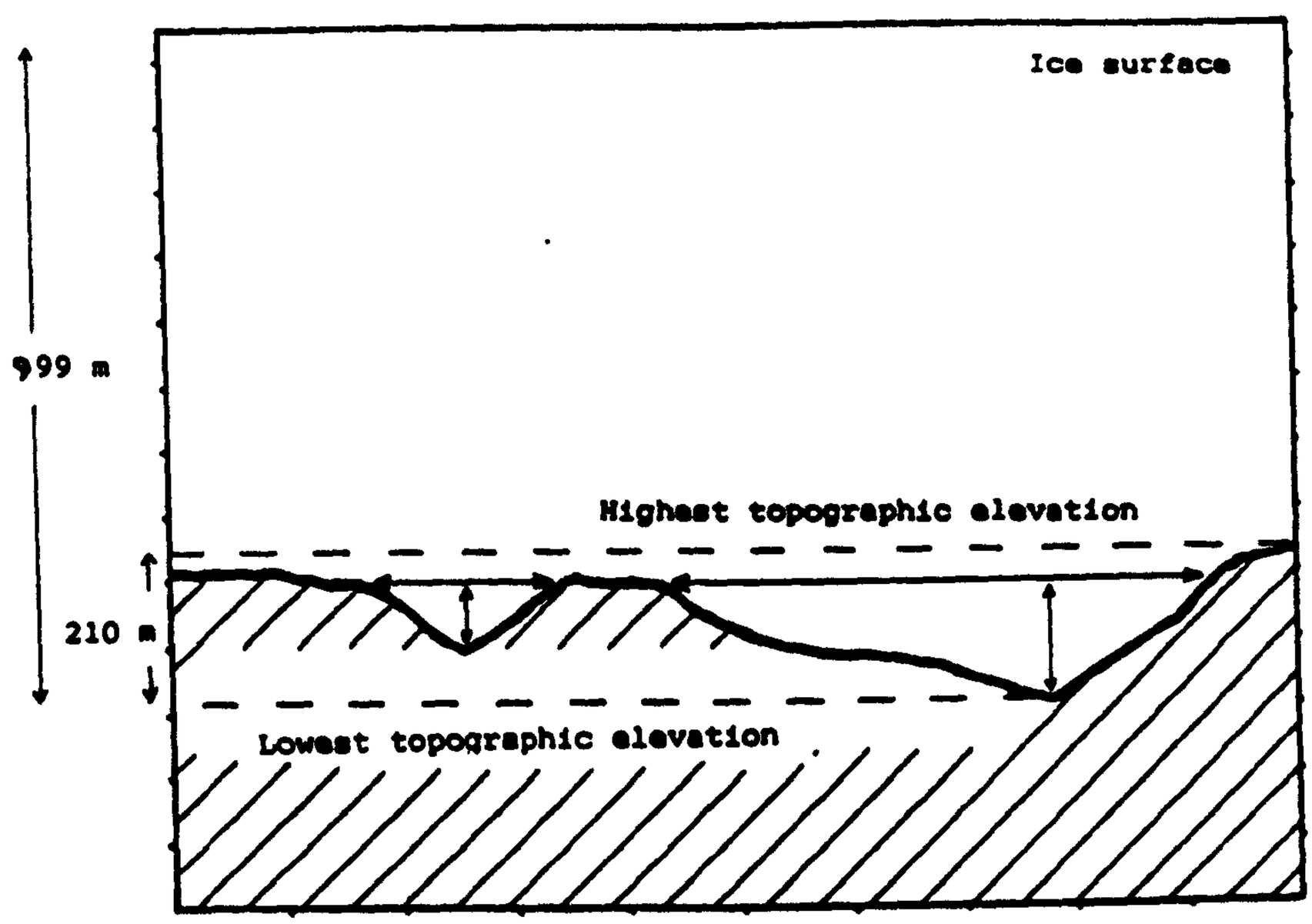

Figure 3.5 Example of method used to assign values to the convergence and divergence of ice flow: A topographic cross section through the Dee Valley.

$$V_c = v + rv + gv \qquad (3.3)$$

Where v is the balance velocity of the ice sheet and r and v are the topographic relief factor and topographic geometry factor respectively.

The *construction* of this numerical relationship is based on the assumption that convergence of flow introduces an increase in ice velocity and that this increase is linear. If this is the case, then the velocity including convergence of flow is equal to the original balance velocity multiplied by topographic relief and topographic geometry added to the original balance velocity. It is this mathematical relationship which is expressed above in equation 3.3. Further extension to this work would involve the case where a non-linear relationship exists between topographic relief, topographic geometry, and velocity. In the absence of any such studies the simple case of a linear relationship is used here. Any attempt to use anything other than the simple linear case cannot be justified given the infancy of such studies.

Substituting the values of r and g gives:

Northern valley: v + 0.21v + 0.5v

Southern valley: v + 0.21v + 0.34v

The balance velocity at this point is 111 ma^{-1} and substituting this value gives:

Northern valley: 111 + 23.3 + 55.5 = 189.8 ma^{-1}

Southern valley: 111 + 23.3 + 38 = 172.3 ma^{-1}

Velocities are therefore increased to these values in the two areas of convergent flow in this cross-section. In order to maintain balance, velocities are reduced in the remaining areas of the cross-section from 111 ma^{-1} to 65 ma^{-1}. The method produces a sudden break between areas of fast and slow ice velocities. For example, ice flowing at 189 ma^{-1} in the valley is surrounded by an interfluve where ice velocity is only 65 ma^{-1}. This rapid transition is an artifact of the method but is a reasonable approximation because it is typical of many ice sheet outlets, where fast moving ice streams drain otherwise slow moving ice sheets (Alley et al. 1989).

This method was used to calculate ice sheet velocities at 12 points in all the cross-sections of the basal topography. Thus velocities are derived for the same 444 points used in Chapter 2. The Budd column solution is still applicable as the necessity for overall balance of the ice sheet is satisfied at each cross-section along the flow band. The other boundary conditions used in the calculation of basal temperatures are the same as in the standard model run, allowing direct comparison to be made; 50 kPa ice sheet profile,

surface temperatures based on a mean annual temperature of -9°C at the ice sheet margin with an altitudinal lapse rate of 0.7°C per 100 metres, and accumulation rate of 0.75 ma^{-1}.

3.5 Results

The results are presented in two sections. First, the results of calculations of velocities and basal temperatures at the valley scale are given for the five cross-sections which contain the detailed field study sites. Second, basal ice velocities are calculated for the regional flowband.

3.5.1 Basal thermal regime in the field study areas

The topographic cross-sections are shown in Figures 3.6 to 3.10. In each case basal temperatures are shown for situation (a) where ice flow is assumed to be uniform and basal temperatures vary only with thickness, and for situation (b) where basal temperatures include the effect of convergence and divergence of flow. Basal temperatures are indicated along the cross-sections and areas of basal melting are heavily shaded. Comparison between situation (a) and (b) at each study area shows the influence of convergence and divergence of flow on basal thermal regime. In each case the upper boundary of the box marks the ice surface derived from a 50 kPa parabolic ice sheet profile, and the lower boundary of the box represents present day sea level (0 metres o.d.). Full details of the calculations are given in Table 3.2. Where more than one area of convergent flow exists

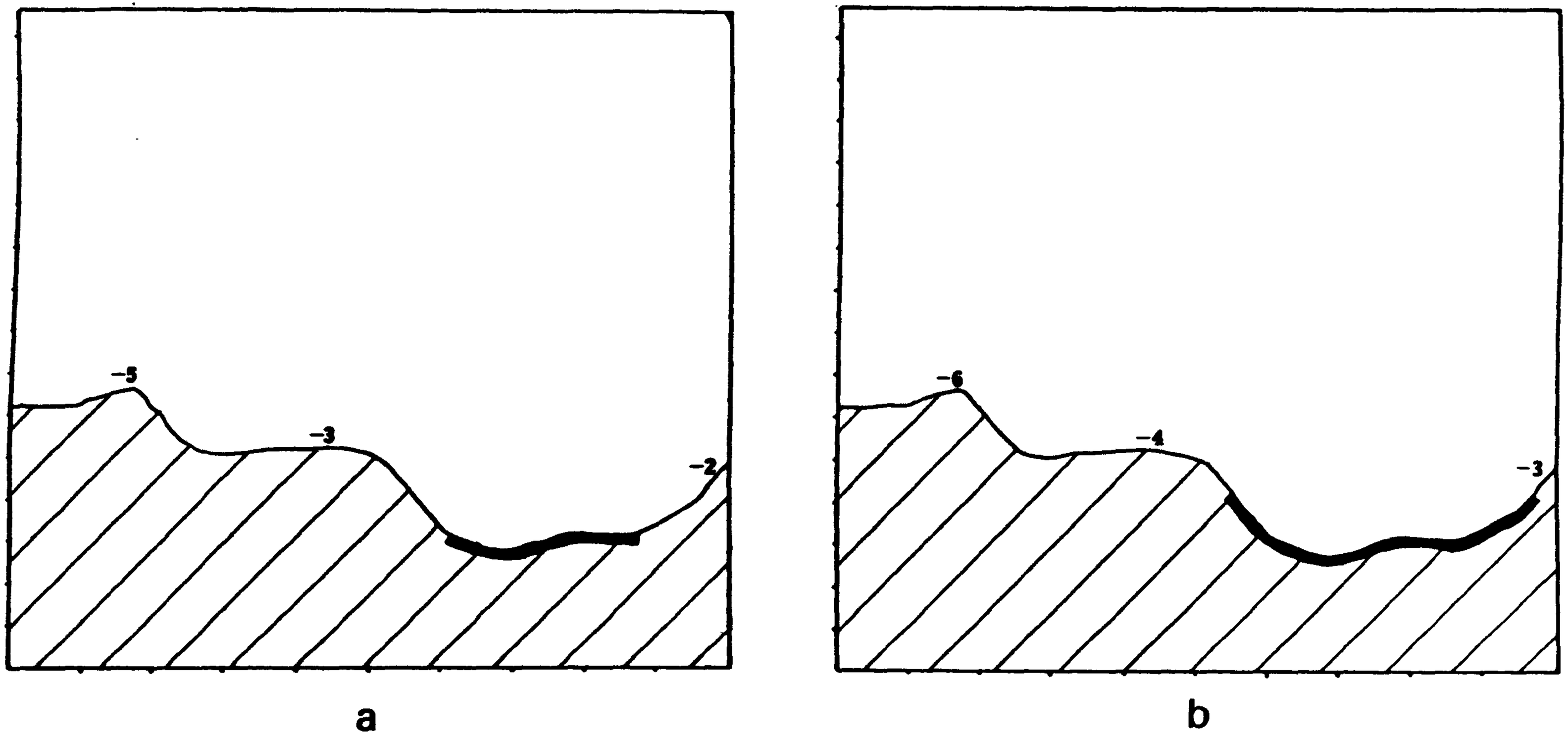

Figure 3.6 Calculated basal ice temperatures for Speyside field study area:
(a) Uniform ice flow
(b) Convergence and divergence of ice flow.

Areas of basal melting indicated by heavy shading

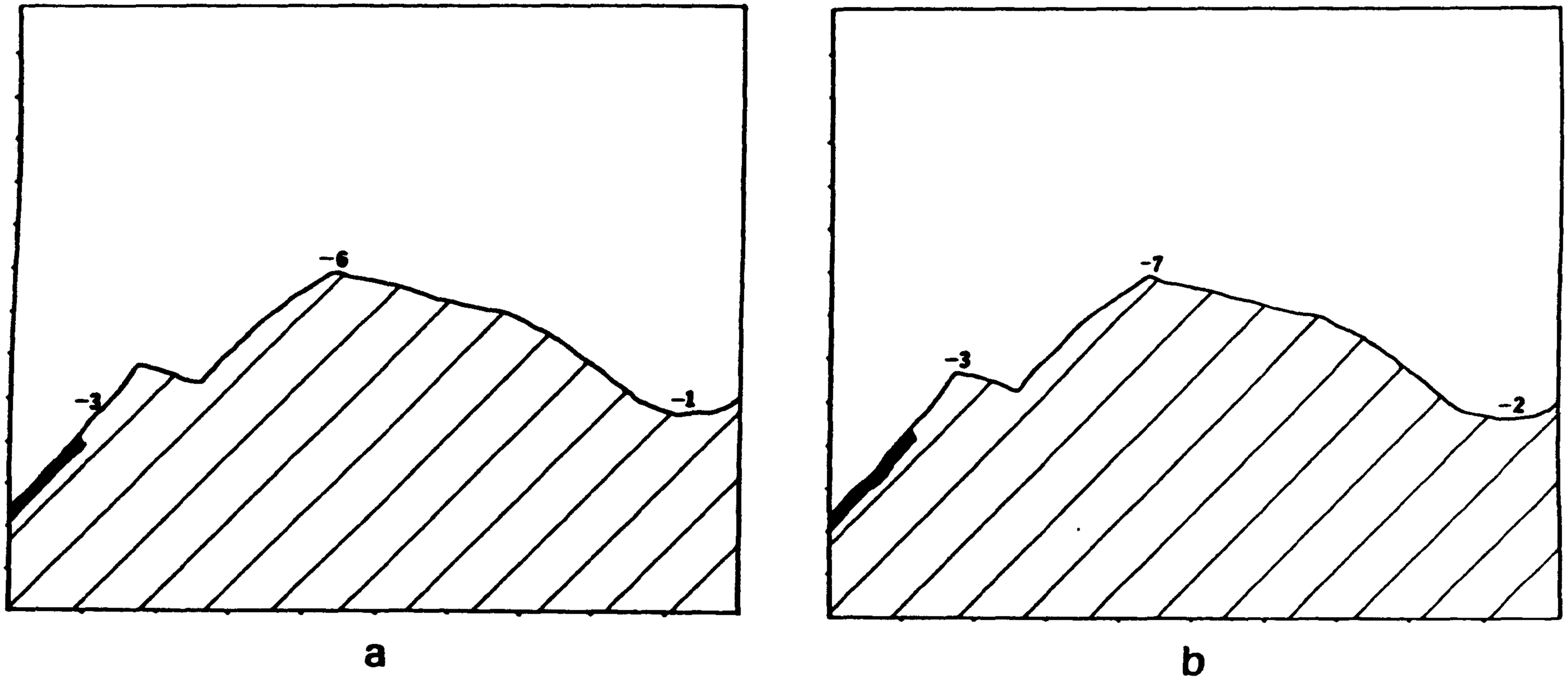

Figure 3.7 Calculated basal ice temperatures for Glen Feshie field study area:
(a) Uniform ice flow
(b) Convergence and divergence of ice flow.

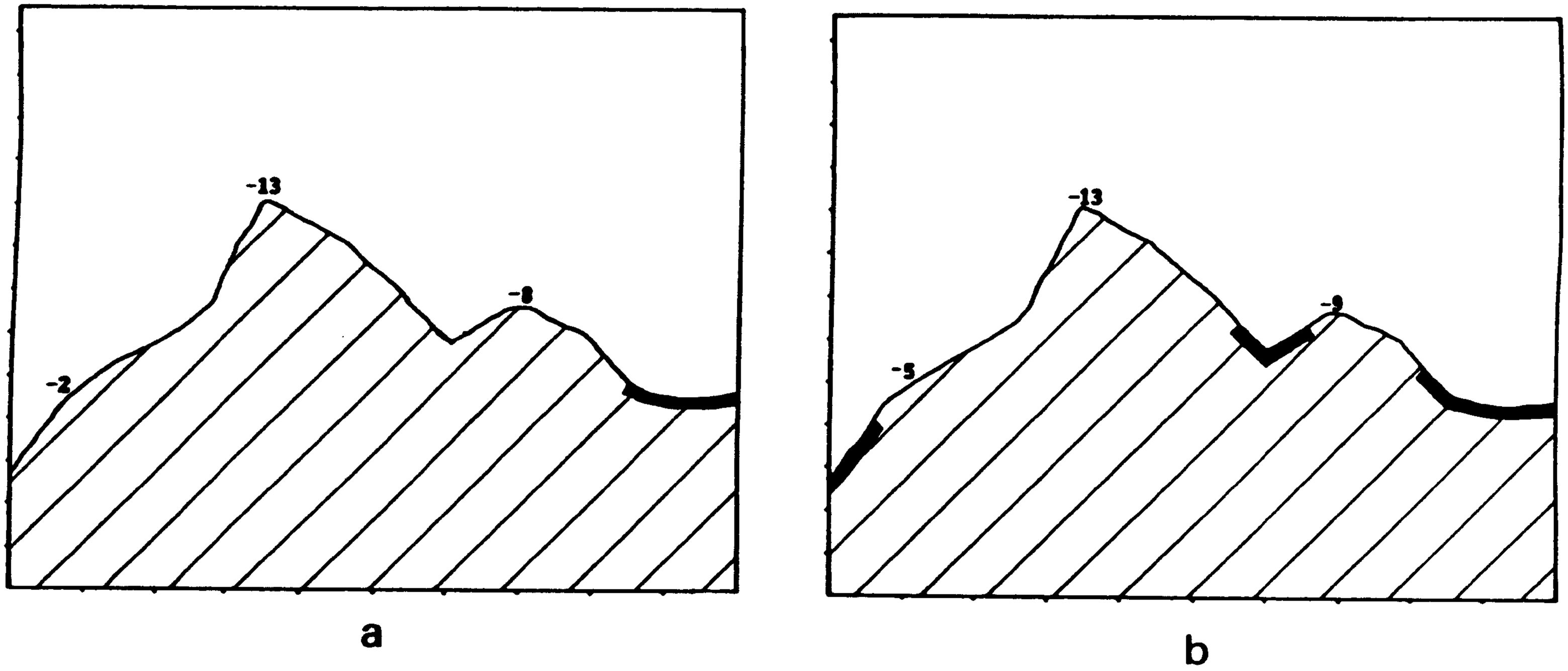

Figure 3.8 Calculated basal ice temperatures for Cairngorms field study area:
(a) Uniform ice flow
(b) Convergence and divergence of ice flow.

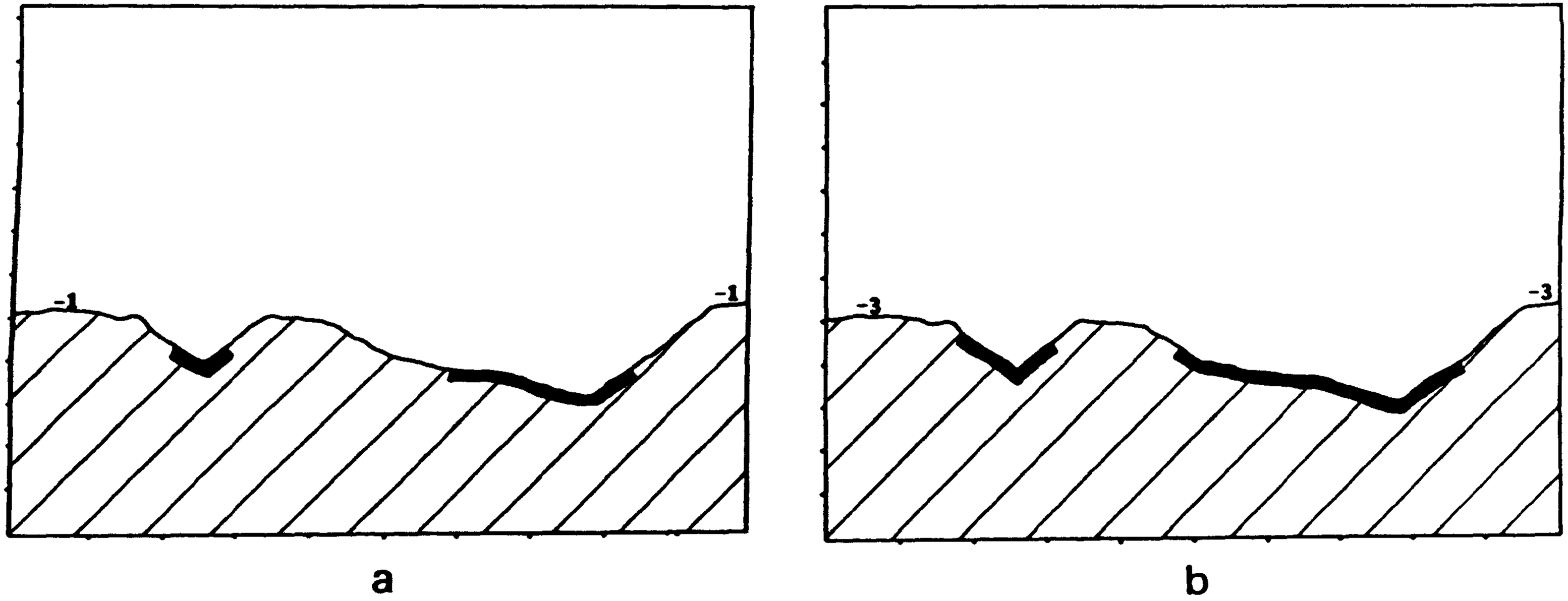

Figure 3.9 Calculated basal ice temperatures for Balmoral field study area:
(a) Uniform ice flow
(b) Convergence and divergence of ice flow.

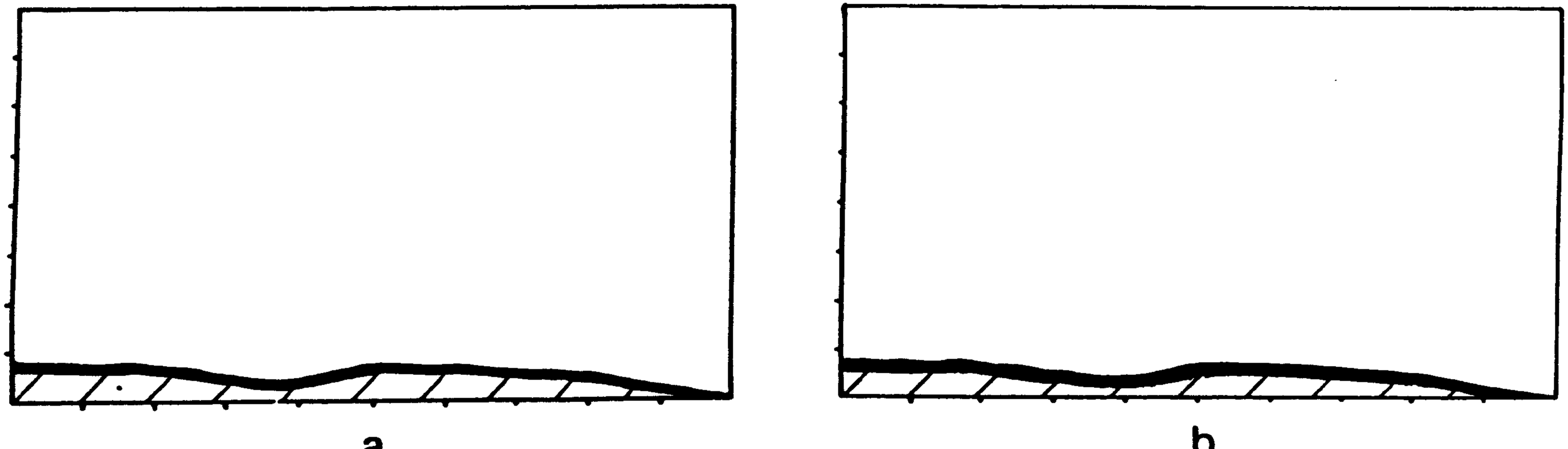

Figure 3.10 Calculated basal ice temperatures for Aberdeen field study area:
(a) Uniform ice flow
(b) Convergence and divergence of ice flow.

Study area	Balance velocity (ma^{-1})	g	r	Convergent velocity (ma^{-1})	Divergent velocity (ma^{-1})
Spey	36	0.2	0.31	54	27
Feshie	84	0.75	0.46	185	50
Cairngorms					
(i)	98	0.7	0.56	221	19
(ii)	98	0.66	0.56	218	19
(iii)	98	0.375	0.56	190	19
Balmoral					
(i)	111	0.5	0.21	190	65
(ii)	111	0.34	0.21	172	65
Aberdeen	163	<0.1	0.09	163	163

Table 3.2 Data used in calculation of velocity in the field study areas

within a cross-section this is denoted by (i), (ii), (iii) after the field study area name. Differences in velocity calculated for these areas are due to differences in the values derived for the topographic geometry factor, g (Table 3.2).

In the Speyside field study area no new areas of basal melting are initiated by including convergence of flow; the effect is to increase the size of the existing area of basal melting. Basal temperatures on the interfluves, which are below the pressure melting point in both situations (a) and (b), are reduced by including convergence and divergence of flow in the calculations (Figure 3.6). In the Glen Feshie field study area, the increase in velocity in the Spey valley only slightly increases the area of basal melting because the large ice thickness means this depression is initially an area of basal melting (Figure 3.7a). The increase in ice velocity in the valley is compensated for by a reduction in velocity on the interfluves, and this causes a reduction in basal temperatures. In the Cairngorm field study area the effect of including convergence of flow in the calculations is to increase the extent of the existing area of basal melting, and to initiate two new areas of basal melting in depressions (Figure 3.8 a and b). Commensurate with this is a reduction in the calculated basal temperatures on the interfluves. In the Balmoral field study area the effect of including convergence of flow in the calculations is to increase the extent of the existing areas of basal melting, but it is not sufficient to produce new areas of basal melting. The decrease in velocity

on the interfluves causes basal ice temperatures to drop from -1°C to -3°C (Figure 3.9 a and b). In the Aberdeen field study area no convergence of flow occurs due to the low-lying gentle topography and consequently there is no variation in basal ice velocity. Basal temperatures in this cross section vary only in relation to changes in ice thickness due to the basal altitude. The entire cross section is characterised by basal melting in both situations (a) and (b) (Figure 3.10). No convergence and divergence of flow is included and the calculations are made using the original balance velocity of 163 ma^{-1} in both situations.

The comparison between the basal ice temperatures in the five cross-sections with; (a) uniform ice flow and; (b) convergence and divergence of flow, show that including variable ice flow in the calculations emphasises the difference in basal temperatures between valleys and interfluves. The method leads to an increase in the area of basal melting in valleys and a compensating decrease in basal ice temperatures on interfluves. The increase in basal ice temperatures in the valley areas will also lead to an increase in basal melt rates.

3.5.2 Basal thermal regime in the flowband

The calculations for the 36 cross-sections illustrate the regional pattern of ice velocity due to convergence and divergence of flow (Table 3.3). Basal ice velocites for the flowband contoured at intervals of 25 ma^{-1} are shown in

Profile number	(1)	(2)	(3)	(4)	(5)	(6)
1	1945	450	100	350	1845	0.19
2	1902	430	30	400	1827	0.21
3	1879	550	100	450	1779	0.25
4	1861	380	100	280	1761	0.16
5	1808	550	40	510	1768	0.29
6	1776	590	50	540	1726	0.31
7	1695	650	330	320	1365	0.23
8	1698	570	280	290	1418	0.2
9	1687	550	280	270	1407	0.19
10	1642	670	280	390	1362	0.29
11	1642	670	230	440	1412	0.31
12	1616	630	200	430	1416	0.3
13	1600	610	190	420	1410	0.3
14	1578	540	180	360	1398	0.26
15	1557	550	190	360	1367	0.26
16	1445	800	250	550	1195	0.46
17	1412	920	280	640	1132	0.56
18	1375	830	400	430	975	0.44
19	1367	680	360	320	1007	0.32
20	1350	790	270	520	1080	0.48
21	1338	670	270	400	1068	0.37
22	1309	520	310	210	999	0.21
23	1297	630	250	380	1047	0.36
24	1275	490	280	210	995	0.21
25	1252	510	210	300	1042	0.29
26	1200	550	200	350	1000	0.35
27	1204	500	130	370	1074	0.34
28	1161	530	110	420	1051	0.4
29	1150	400	100	300	1050	0.29
30	1109	430	90	340	1019	0.33
31	1093	230	80	150	1013	0.15
32	1050	280	60	220	990	0.22
33	1023	200	50	150	973	0.15
34	976	140	40	100	936	0.1
35	930	140	40	100	890	0.11
36	895	80	0	80	895	0.09

Column Legend

(1) Ice surface altitude, including isostatic depression
(2) Highest topographic elevation
(3) Lowest topographic elevation
(4) Topographic relief (2)-(3)
(5) Maximum ice thickness (1)-(3)
(6) Topographic relief divided by maximum ice thickness

Table 3.3 Data used in calculation of basal ice temperatures at the 36 cross sections.

Figure 3.11 (a). Velocities in the western half of the flowband are under 50 ma^{-1}, increasing to 150 ma^{-1} near the eastern margin. The proposed pattern of velocities is determined by the basal topography and a large lobe of fast flowing ice develops down the route of the Dee Valley. Here ice velocities may have been up to 3 times greater than on the adjacent interfluves, with velocities in the valley reaching 225 ma^{-1}. A similar ice stream may have developed in the Spey Valley, allowing the 50 ma^{-1} contour to reach westward up-valley into an area of otherwise slow moving ice. Basal velocities are low over the Cairngorm Mountains, except in the valleys. Here velocities of over 200 ma^{-1} are found in an area where average velocities are around 50 ma^{-1}.

The calculated pattern of basal ice temperatures including convergence and divergence of flow is shown in Figures 3.12 and 3.13. Figure 3.12 shows the contoured basal ice temperatures at 2°C intervals for the regional flowband. All positive temperatures are notional since any excess heat at the base is used in the production of meltwater. Figure 3.13 shows the same data but with the basal ice temperatures divided into three temperature regimes; basal melting, 0°C to -8°C, and below -8°C. Areas of basal melting are cross-hatched, basal ice between 0°C and -8°C is shaded diagonally, and ice below -8°C is unshaded.

Basal melting is the dominant thermal regime in the flowband, accounting

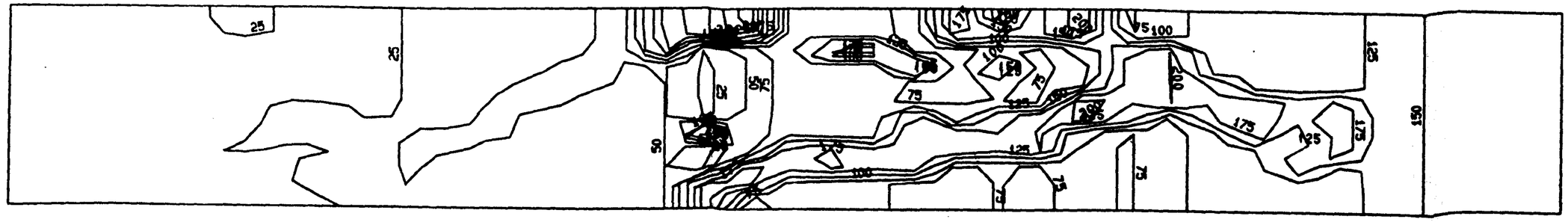

Figure 3.11 Basal ice velocities in the flowband contoured at 25 ma^{-1}:
(a) Full convergence of ice flow
(b) 0.75 times full convergence of ice flow.

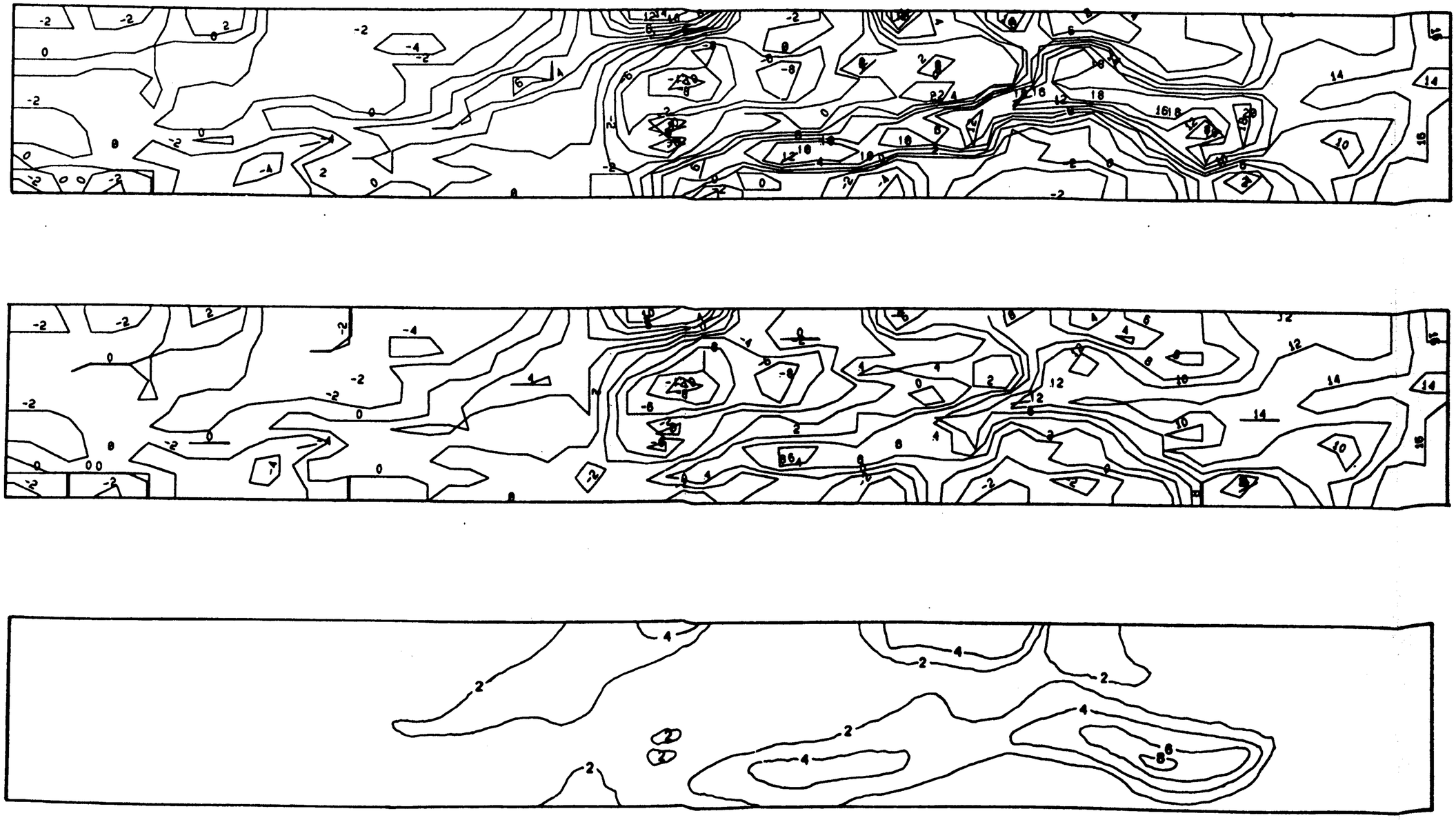

0 km 10

Figure 3.12 Basal ice temperatures in the flowband contoured at 2° C intervals:
(a) Full convergence of ice flow
(b) 0.75 times full convergence of ice flow
(c) Difference between the two methods in °C.

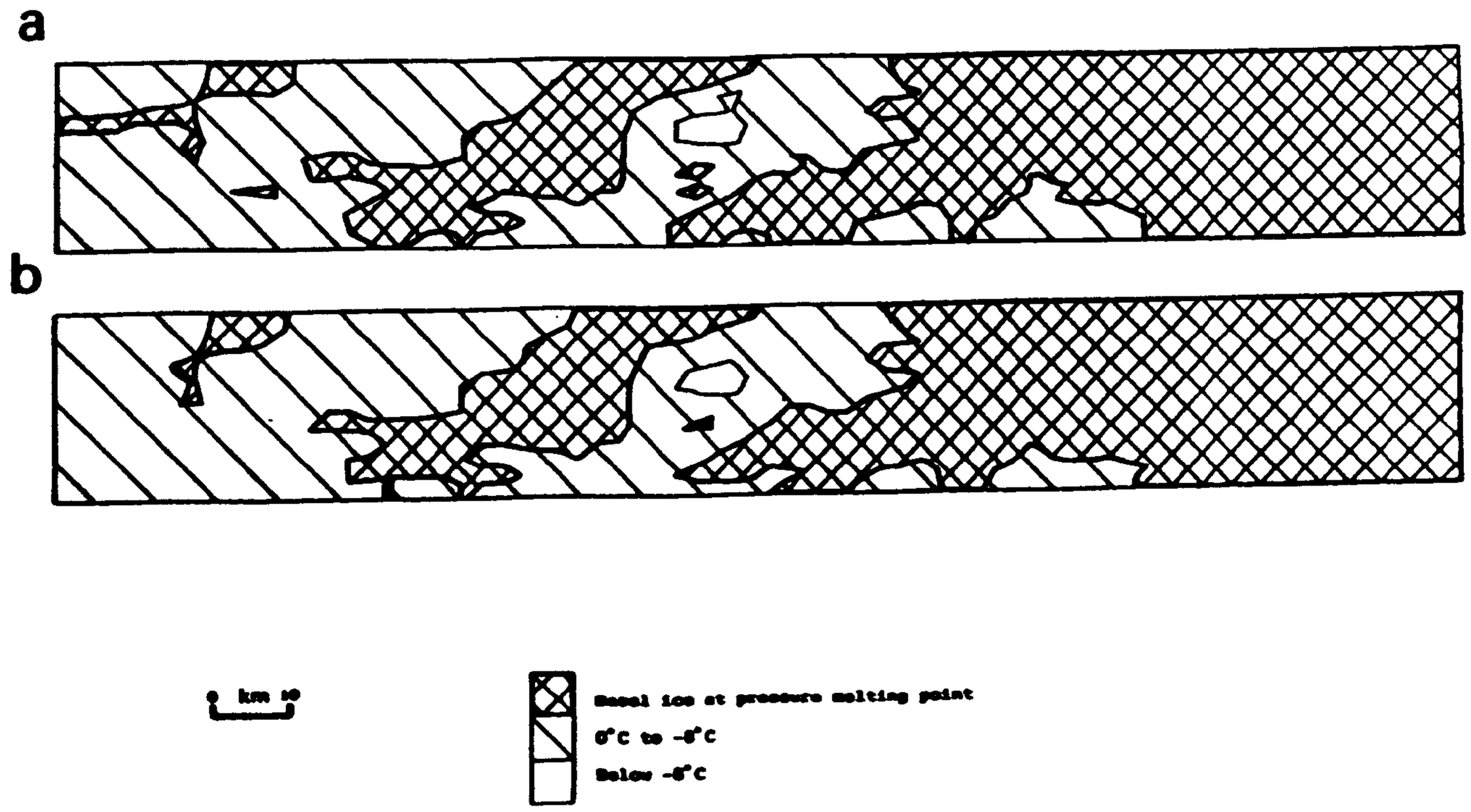

Figure 3.13 **Basal thermal regime in the flowband**
(a) Full convergence of ice flow
(b) 0.75 times full convergence of ice flow.

for more than 70 per cent of the area. The zone of basal melting is continuous in the east, but occurs also to a lesser extent in the west (Figure 3.13). An area of basal freezing exists in the centre of the flowband, covering an area of relatively high topography (Figure 3.14). This zone of basal freezing occurs over the Cairngorm Mountains and Glen Feshie plateau, where basal temperatures drop as low as -12°C. This mountainous region is characterised by basal freezing, and the cold based zone separates large areas of basal melting. However, even within this cold based zone relatively warm based areas exist at a local scale. For example, in the southern Cairngorms the isotherms indicate that basal ice is at the pressure melting point at one point within the wider cold based zone (Figure 3.12). This area of basal melting is located over a deep trough where a combination of thick ice and convergent flow enables localised basal melting.

In the Dee valley not only is the basal ice at the pressure melting point, but the predicted temperatures are up to 24°C higher than in the cold zone over the Cairngorm Mountains. The same situation occurs to the south and west of the Cairngorm Mountains, where basal temperatures are up to 18°C higher than in the mountains themselves. The relatively high velocities in the valleys of the Dee and Spey allows basal melting to occur within an area which is generally cold based (Figure 3.13).

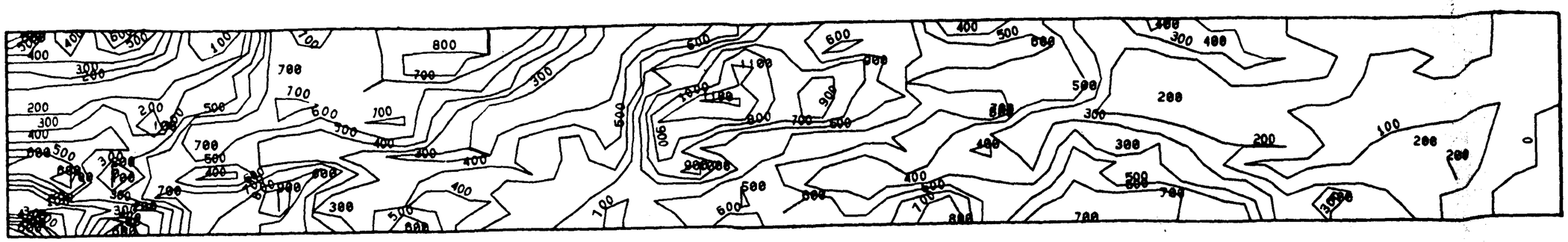

Figure 3.14 The basal topography of the regional flowband contoured at 100 metre intervals.

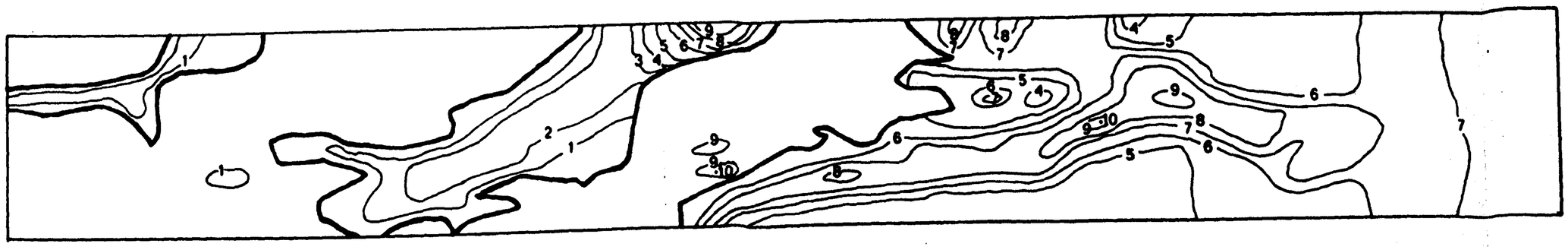

Figure 3.15 Rate of meltwater production in the flowband contoured in mma^{-1}.

0 km 10

The areas of basal melting in topographic depressions are a function of the greater ice thicknesses and the increase in basal ice velocities associated with convergence of flow. Conversely, where flow is divergent the basal ice is relatively cold and remains frozen at the base. Thus ice streams develop down the routes of the Dee and the Spey. These ice streams are characterised by high velocity and high basal ice temperatures. Increases in basal ice temperatures are halted where the channelling effect of the valleys decreases, for example in the lower Dee (Figure 3.12). Although basal ice temperatures are still above the pressure melting point here, they are up to 10°C lower where the channelling effect of the Dee decreases (Figure 3.12).

In areas of basal melting the rate of meltwater production can be calculated from the difference between the calculated base gradient (Y_c) and the geothermal heat gradient (Y_g) such that;

$$m = (Y_c - Y_g)\, K/L \qquad (3.4)$$

(Sugden 1977)

Where K is the conductivity of ice and L is the latent heat of fusion of ice.

A map of basal melt rates shows that meltwater production rises from 1 mma^{-1} in the extreme west of the flowband to 7 mma^{-1} near the equilibrium line (Figure 3.15). The rate of meltwater production is controlled to a great

extent by basal ice velocity. High melt rates, up to 10 mma^{-1}, are found in areas of high velocity where ice converges down the Spey and Dee Valleys. Melt rates increase with distance down the Spey Valley, but decline slightly near the mouth of the Dee Valley as its channelling effect decreases (Figure 3.15).

3.6 Sensitivity tests

The calculations of basal thermal regime rely heavily on the velocity term, because, together with geothermal heat this determines the heat flux at the base of the ice sheet. Two sensitivity tests were carried out:

(1) At the valley scale, tests were carried out to determine the percentage increase in velocity necessary to produce basal melting in valleys.

(2) At the flowband scale, a test was carried out to determine how sensitive the model is to changes in velocity due to convergence of flow. This is achieved by recalculating basal temperatures with velocities increased not by the full increment suggested by the method, but by a reduced increment related to shear deformation alone.

These sensitivity tests are concerned with "fine tuning" of the model to determine the magnitude of changes required to create basal melting and basal freezing in the field area. Since this can be quantified in absolute

values, the results of the sensitivity tests are presented in terms of percentage change in ice velocity required to alter the basal thermal regimes.

3.6.1 Sensitivity tests in the five field study areas

Calculations of basal temperatures were made allowing velocity to vary, to determine the magnitude of changes necessary to produce areas of basal melting and freezing in each cross-section. The percentage change necessary to alter the thermal regime of the basal ice is compared to the percentage change suggested by the method for convergence and divergence of flow (Table 3.4). The amount of influence which topography must exert on velocity in order to produce basal melting and/or freezing can then be calculated.

The sensitivity tests in the Speyside field study area show that an increase in velocity of 40 per cent will produce basal melting in areas previously characterised by basal freezing. The area of basal melting in the Spey Valley itself persists even with a 33 per cent reduction in ice velocity. In the Glen Feshie field study area the replacement of basal freezing on the interfluves with basal melting requires an increase of over 500 per cent in the balance velocity. In comparison, the method of calculating convergent velocities suggested an increase in velocity of 120 per cent of the balance velocity in the valley. Large increases in velocity are required to remove the area of basal freezing on the interfluves, and basal melting persists in the valley

Study area	(1)	(2)	(3)	(4)
Spey	+50	+40	-25	-33
Feshie	+120	+500	-40.5	-24
Cairngorms				
(i)	+125.5	+5	-80.6	-13
(ii)	+122.4	+27	-80.6	-13
(iii)	+93.9	+18	-80.6	-13
Balmoral				
(i)	+71.2	+44	-41.4	-62
(ii)	+55	+36	-41.4	-62
Aberdeen	0	No basal freezing	0	-68.7

Column Legend

(1) Increase in velocity in areas of convergent flow expressed as a percentage of original balance velocity
(2) Minimum increase in velocity required to produce basal melting in areas of convergent flow expressed as a percentage of original balance velocity
(3) Reduction in velocity in areas of divergent flow expressed as a percentage of original balance velocity
(4) Minimum reduction in velocity required to eliminate basal melting in areas of divergent flow expressed as a percentage of original balance velocity

Table 3.4 Sensitivity tests in the field study areas.

even with a reduction in velocity of 24 per cent. In the Cairngorm field study area new areas of basal melting were initiated by adopting the convergence and divergence method. Although the method suggested velocity increases of around 100 per cent, increases of only 5 per cent are required to produce basal melting in the major valleys (Table 3.4). In this area, even a small increase in velocity due to topography is sufficient to produce basal melting in the major depressions. In the Balmoral field study area the zones of basal melting in the Dee valley and basal freezing on the interfluve appear to be stable features (Table 3.4). In the Aberdeen field study area no convergent flow occurred and ice flow was considered to be uniform. A reduction in ice velocity of 68.7 per cent of the balance velocity is required to replace the zone of basal melting with basal freezing. The large change required suggests the zone of basal melting is a stable feature.

The significance of these sensitivity tests is that in situations where thick ice exists over topographic depressions, only a small increment in velocity due to convergence of flow is required to produce basal melting. In the Cairngorm field study area this increment is as little as 5 per cent of the original balance velocity. Basal melting still persists in some valley areas under thick ice even if velocity is reduced. Conversely, large increases in velocity are needed to remove basal freezing on interfluves under thin ice. Thus the basic pattern of basal temperatures is stable; large increases in velocity are required to eliminate basal freezing on interfluves whilst

relatively small increases are required to achieve this in topographic depressions.

3.6.2 Sensitivity tests at the flowband scale

The second sensitivity test involves the calculation of basal temperatures in the flowband with a reduced increment attached to convergence of flow. The test is useful because the velocities calculated in areas of convergent flow may be overestimates, and this therefore provides a check on the sensitivity of the pattern of basal temperatures to changes in velocity. The method is to increase balance velocities by 0.75 times the suggested increment, equivalent to a 25 per cent reduction in the velocities predicted by the original method. Velocities in the divergent areas of the cross-sections are again adjusted in order to maintain overall ice sheet balance.

The main effect of this reduction is to create smaller differences in velocity between valleys and interfluves than in the original calculations. This can be seen in Figure 3.11 which shows contoured basal ice velocities for; (a) full convergence of flow and; (b) 0.75 convergence of flow. Velocities are high in major valleys such as the Dee and Spey with the full increment (Figure 3.11 a), but decrease slightly with the reduced convergence increment (Figure 3.11 b). However, even with the reduced increment, velocities of between 125 and 150 ma^{-1} in the Dee Valley compare to 100 ma^{-1} on the interfluves. Local differences in velocity also occur in the Cairngorm

Mountains, where ice sheet velocities of 150 ma^{-1} occur in valleys adjacent to interfluves where velocities are only 75 ma^{-1}.

Reducing the increment attached to convergence of flow by 25 per cent decreases the temperature difference between areas of convergent and divergent flow (Figure 3.12). The difference in basal ice temperatures between the two methods becomes clear when it is expressed as the temperature increase in °C between the 0.75 convergence increment method and the full convergence method (Figure 3.12c). Over most of the flowband the temperature difference is less than 2°C. The main difference between the two methods is that basal temperatures are generally 4 to 6°C warmer in the Dee convergence zone if the full convergence increment is used. Attaching a smaller increment to convergence reduces the importance of the ice stream in the Dee Valley. However, the overall pattern of basal thermal regime remains stable and the main patterns shown in Figure 3.13 (a) are preserved in Figure 3.13 (b). The central zone of basal freezing still separates two areas of basal melting, and in the west of the flowband basal freezing and melting alternate. The pattern of basal temperatures is not critically sensitive to the changes in the increment attached to convergent flow. Basal melting occurs in valleys even if a reduced increment is attached to convergence of flow.

3.7 Conclusions

The main conclusions which can be drawn from the modelled basal ice temperatures including convergence and divergence of flow are as follows:

(1) A simple model of the variation in velocity due to the differing flow regimes within the ice sheet can be constructed on the assumption that ice velocity is related to relief amplitude and topographic geometry.

(2) Calculations of ice velocity allowing ice thickness to vary suggest that the greatest ice velocities will be found in deep subglacial valleys where overlying ice thicknesses are greatest. Lowest velocities occur where the ice sheet is relatively thin over the underlying topography.

(3) The increases in ice velocity due to the channelling of flow enhance basal melting in valleys, whilst interfluves and higher ridges remain frozen at the base. Subglacial valleys such as the Dee and Spey become the sites of ice streams and are characterised by fast ice velocities and basal melting.

(4) Where the ice sheet is thick over topographic depressions, small increases in ice velocity (as little as 5 per cent of the balance velocity) are required to produce basal melting in areas characterised by basal freezing in the standard model run.

(5) In areas where the subglacial topography is suitable for ice flow

(uniform, low relief amplitude) little channelling of flow occurs. This landscape type is found near the eastern margin of the former Scottish ice sheet, where calculated basal temperatures suggest the ice was warm based. Ice velocities must be reduced to one third of the balance velocity to remove this area of basal melting.

3.9 Limitations

The method outlined in this chapter allows ice sheet velocities to be assigned to topographic cross- sections, but two limitations must be noted:

(1) It is assumed that the increase in velocity due to topography is linear. It is likely, however, that the relationship is more complex than this and the two may be related in a non-linear manner.

(2) The model ignores some of the effects of continuity of flow. For example, the Dee valley is a significant topographic depression which shows up sequentially in over 10 of the cross-sections (a distance of 50 kilometres), yet at each cross-section the balance velocity is used to determine ice velocities. It is likely that if convergent flow occurs upstream of a point, then the effects of increased flow will be transmitted to the next cross-section downstream.

Thus the model does not take account of the additional velocities which may

result from any channelling of flow further upstream. This would serve to increase velocities even further in valley areas. Both these limitations suggests that the calculated basal ice temperatures in areas of convergent flow are minimum values.

CHAPTER FOUR

PREGLACIAL AND GLACIAL LANDSCAPES:

CRITERIA USED FOR MAPPING

4.1 Aim

The aim of this chapter is to outline the criteria used to identify preglacial and glacial landscapes in the five field study areas. A review of the literature and previous work on the subject is combined with descriptions of typical landform types, in order that the means of identifying these landscapes are made clear.

4.2 Preglacial landscapes

It has long been recognised that preglacial landscapes still survive today in formerly glaciated areas, not only in Scotland (Godard 1962; Hall 1983), but in formerly glaciated parts of continental Europe (Aseyen and Makkaveyen 1977; Lidmar-Bergstrom 1982) and North America (Bouchard and Godard 1984; Feininger 1971). The existence of such preglacial landscapes has been used in the reconstruction of preglacial landsurfaces (Sugden 1968) and in the calculation of depths of Pleistocene glacial erosion (Jahns 1943; Hall and Sugden 1987).

The preglacial landsurface remnants surviving in Scotland today can be

divided into two groups:

(1) Those large scale remnants which survive due to limited ice sheet erosion. In this category we may include large scale features such as old plateau surfaces and associated fluvial valleys.

(2) The small scale preglacial structures which are often found in association with the above features. These include bedrock features such as topographic sheeting, saprolites and tors.

4.2.1 Plateau surfaces

In a recent paper Hall (1991) outlines the main stages in the pre-Quaternary evolution of the Scottish Highlands. Offshore sediment volumes suggest that rates of erosion over the last 135 million years have been relatively low compared to the present interglacial. Watson (1985) and Hall (1991) present evidence to suggest that rates of terrestrial erosion in Scotland over the last 400 million years have been relatively modest compared to the high rates of 500 - 410 million years ago. However, offshore sediment volumes can only be used to support this argument through the Cretaceous and Cenozoic (the last 135 million years) since the North Atlantic has only been in existence since this time. Further offshore sedimentary evidence comes from the North Sea basin, where sediment volumes suggest that early Tertiary denudation was on a modest scale (Hall 1991, p.6).

The discussion of erosion rates over geological timescales is included by way of an introduction to the concepts of long-term landscape evolution discussed later in this chapter. The wider geological setting is intended to broaden the scope of the chapter, since many discussions of glacial erosion tend to neglect the geological context. The pre-Quaternary morphogenesis is vital since it provides the basis for the mapping of the location and depth of glacial erosion in subsequent chapters of the thesis. The pre-Quaternary discussion is intended to illustrate the sequence of events affecting the Scottish landscape prior to the onset of the Quaternary glaciations.

The calculation of Tertiary erosion rates suggests that the summit surface of the Scottish Highlands at 900 - 1000 metres lies only a few hundred metres below its erosional level at the end of the Cretaceous as noted by Watson (1985). Mountain ranges such as the Cairngorms are high-level preglacial plateau remnants. In the Cairngorms, the existence of torfields and of scattered shallow pockets of sandy regolith implies the former existence of a deep weathering cover and indicates that etching of this ancient surface continued throughout the Tertiary until Pleistocene glaciation (Hall 1991).

High level plateaux such as the Cairngorms, with their rolling relief, are a good example of a pre-Tertiary landsurface. Since most Highland areas were positioned hundreds of metres above base level during the Tertiary, the terrain has undergone a prolonged subaerial evolution, with etching giving

progressive differentiation of relief (Hall 1991). The Cairngorm plateau is therefore preserved as a surface characterised by gentle rolling slopes and hill summits which are rounded and convex in profile. The plateau surface has been preserved throughout the glacial era with glacial forms often cut into the older rolling relief (Sugden 1968).

4.2.2 Fluvial valleys

A feature which may be considered diagnostic of preglacial landscapes is the existence of valleys which have retained their intrinsic river - worn shape, and remain unmodified by glacial and/or major fluvioglacial erosion. Such fluvial valleys may be identified on three grounds; (1) the shape of the long profile; (2) the cross-sectional shape of the valley in which they flow and; (3) the drainage network which they occupy. These are discussed below.

(1) Figure 4.1 is a generalised profile of the longitudinal profile of most rivers. The profile is generally smooth, and displays a marked concavity. The concave profile of rivers in humid temperate regions is explained with reference to increasing stream discharge with distance from source. Rivers increase in size downstream as tributaries increase the contributing drainage area and thus the discharge. Concomitant with the downstream increases in the channel's width and depth and the general tendency for bed particle size to decrease, the gradient generally flattens (Leopold et al. 1964). This smooth, concave profile has been established by Wheeler (1979) in a study

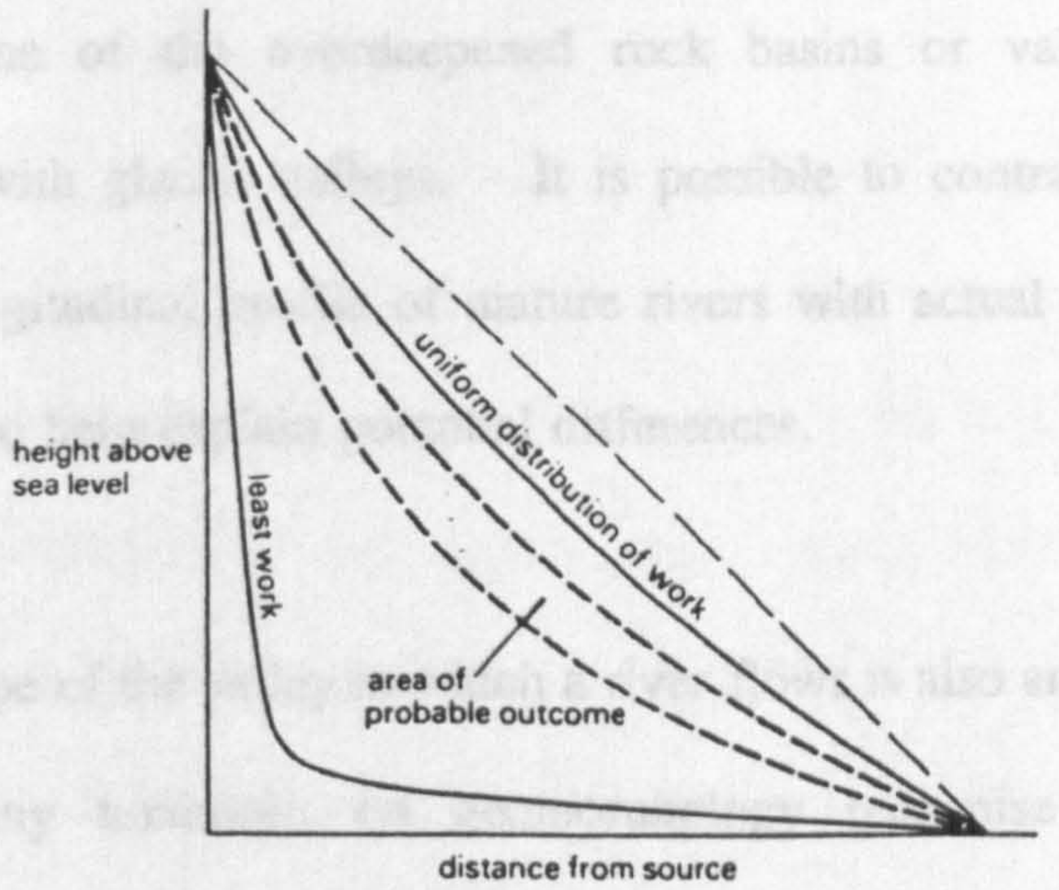

Figure 4.1 Generalized long profile of a river, showing characteristic concave long profile.
Source: Clowes and Comfort (1982) p.121.

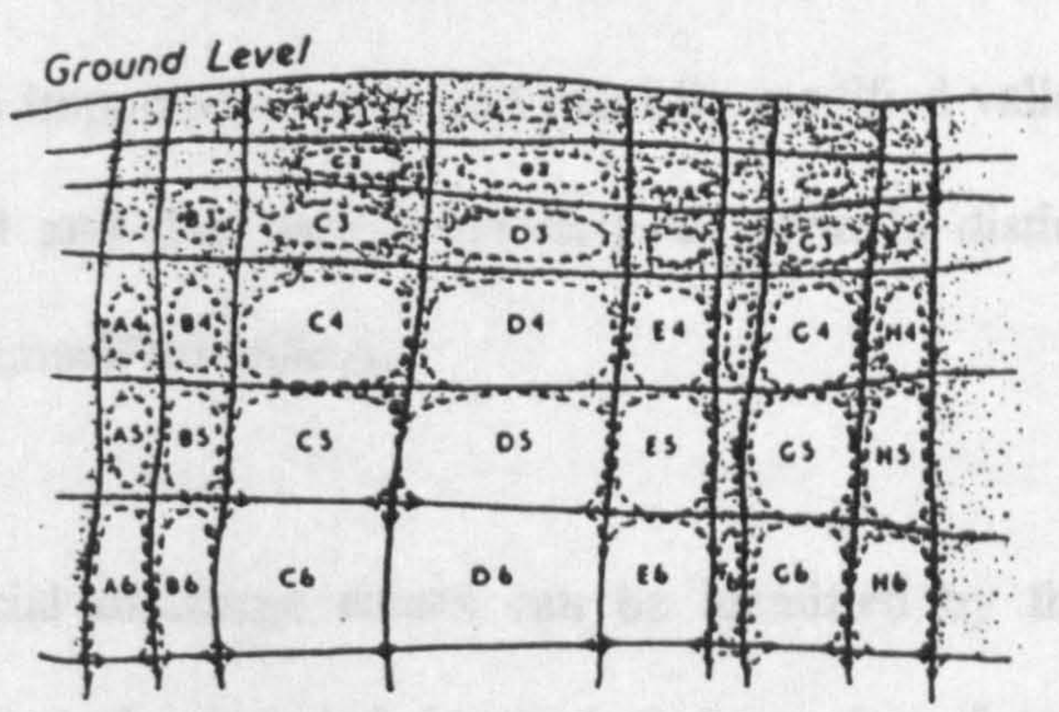

Figure 4.2 (a) and (b) Stages in the evolution of a tor by sub-surface rock rotting.
Source: Linton (1955) p. 473.

of some 115 British rivers. The smooth longitudinal profile of river valleys exhibits none of the overdeepened rock basins or valley steps often associated with glacial valleys. It is possible to contrast the generally concave longitudinal profile of mature rivers with actual river profiles to highlight and help explain potential differences.

(2) The shape of the valley in which a river flows is also an indication of its origin. Many textbooks on geomorphology recognise that rivers in mountainous areas tend to occupy channels characterised by V shaped profiles, but that the cross-profile of a glacial trough, for example, is usually significantly different (Summerfield 1991). The difference is usually described as the difference between a U shaped valley and a V shaped valley. It is important to note that glacially modified valleys exist in parts of Scotland and that their cross-sectional form is distinct from that of glacially unmodified valleys.

(3) Preglacial discharge routes can be identified by the form of their drainage network. A full discussion of the various forms these drainage networks may take is given in Summerfield (1991). Preglacial drainage patterns are characterised by dendritic systems with irregular branching of tributary streams in many directions, usually at angles considerably less than 90°. This is quite different to the deranged drainage which is often found in recently glaciated areas. Here the preglacial drainage has been effaced, and

the new drainage has not had time to develop any significant degree of integration.

Hall (1991) discusses the evolution of the drainage system in Scotland and suggests that many valley drainage routes, such as the Don, the Dee, and the Spey were established as such in the early Tertiary. These drainage routes were maintained during the late Tertiary prior to significant capture and diversion of drainage during the Quaternary (Hall 1990; Linton 1959). Major preglacial valley segments may be recognised by the presence of high level basins (e.g. Moine Mhor), open valley reaches (e.g. upper Glen Geldie), and valley benches (e.g. Geldie/Dee).

4.2.3 Topographic sheeting

Topographic sheeting is a feature found in many rock masses, but particularly common amongst granitic rocks (Gerrard 1988). Characteristics of sheet structures are; (1) division of rock into individual planes parallel to topographic surfaces; (2) an increase in thickness of sheeting with depth and; (3) the existence of near-surface fractures (termed flagstones or fretting) between individual sheets (Plate 4.1)

Sheeting joints in granite have been described from every conventionally defined climatic region of the earth (Twidale 1982). There is a general agreement that sheet structures in granite are not primary structural features

Plate 4.1 Topographic sheeting above Glen Geusachan, Cairngorm Mountains.

(Sparks 1971; Spencer 1977), but that they postdate the consolidation of the granite rocks as they cut through other structures such as orthogonal joints, cleavage, rift and grain, and flow structures (Twidale 1982). Sheeting is also observed parallel to fluvial topographic surfaces and valley patterns, further evidence that it is not a primary structural feature.

It is generally accepted that such sheeting is the result of dilation upon the removal of a primary confining pressure (to which the rock has become adjusted) through removal of a superincumbent load (Spencer 1977; Ollier 1984; Gerrard 1988). Rock masses that have been deeply buried or been subjected to tectonic stresses acquire a considerable amount of 'locked - in' strain energy. Some of this strain will be released when confining pressures are released. This process is named rebound and is defined as the expansive recovery of crustal material, either instantaneously, time - dependently or both, initiated by the removal or relaxation of superincumbent loads (Nichols 1980). Further evidence for this rebound is given from various reports of rock expansion associated with quarrying (Jahns 1943; Nichols 1980).

Normally the release of strain energy in rock is time-dependent (Gerrard 1988) and the mechanism by which pressure release occurs is almost certainly the erosion of the earth's surface, which constitutes the confining load. Assigning an age to the formation of sheeting is not always easy. Matthes (1930), Jahns (1943), Chapman and Rioux (1958) and Selby (1977)

have all shown that sheeting in granites lies parallel to preglacial land surfaces. These authors are of the opinion that the formation of sheeting is a slow process and that such sheeting is preglacial in origin. Richey (1964) and Sugden (1968) note that topographic sheeting predates glaciation as the sheet structures have been eroded by ice. Jahns (1943) demonstrates that granite sheeting in New England is preglacial in origin through its relationship to glacial facets.

Other workers, however, have suggested that the erosion responsible for pressure release may be a glacial event. Lewis (1954) and Battey (1960) have noted the formation of sheets parallel to glacial surfaces. A similar result is given by Matthes (1937), although he also recognised that the formation of sheets is extremely slow.

Sparks (1971) suggests this disagreement about the relation of sheets to glaciated surfaces may be a measure of the amount of glacial erosion required to produce pressure release joints in different areas. The pressure exerted by about 180 metres thickness of granite is approximately equal to the tensile strength of the rock at the earth's surface, so that the denudation of approximately this thickness of rock might be expected to produce sheet structures parallel to the surface (Sparks 1971). There is little doubt that sheets may develop parallel to classic forms such as troughs, and this is further evidence of stress release leading to sheet formation. However, the

two sets are easily distinguished by their character and association with preglacial and glacial surfaces. Thus the formation of narrowly spaced sheeting with large thickness and depth lying parallel to gentle plateau land surfaces represents preglacial sheeting. On the other hand, sheeting parallel to 'new' glacial facets in troughs is distinguished from the preglacial sheeting on the grounds of its limited thickness, steep surface dip and parallelism to glacial land surfaces.

4.2.4 Saprolites

Saprolite is the product of the deep chemical weathering of rocks and minerals. Typically, the original minerals have been converted to clay, there is no change in volume and the weathered rock retains the structures of the original parent rock (Ollier 1984). Saprolites are currently forming under tropical, subtropical and warm temperate environments where rates of chemical weathering are high (Summerfield 1991). It should be noted that the term "saprolite" is usually applied only to weathering mantles where original bedrock structures are preserved and weathering has been accomplished without any change in volume (Summerfield 1991). Strictly speaking, therefore, the term "saprolite" should be reserved for weathering mantles which reflect the operation of isovolumetric weathering with the retention of original bedrock structures. "Saprolite" is therefore a distinct category of weathering mantle and should be distinguished from the generic terms "weathering mantle" and "regolith".

In the following discussion, there are several instances where occurrences of regolith in Scotland are referred to as "saprolite". Although the term "saprolite" should only be used in reference to isovolumetric weathering, the complicating factor is that since much of the weathering mantle formerly covering Scotland has been removed isovolumetric weathering cannot be demonstrated. Such exposures should always be referred to as a "weathering mantle" unless isovolumetric weathering can be proved.

However, the distinction between "weathering mantle" and "saprolite" is often blurred, such that references to "saprolite" in this chapter reflect the views of other authors. For example, Hall (1991, p.14) refers to weathering mantles in the western Cairngorms as "thin saprolites", suggesting that some of the weathering profiles found in Scotland are indeed the product of isovolumetric weathering. Some of the Scottish weathering mantles may therefore represent true "saprolite". In this chapter, the term "saprolite" is used sensu lato to refer to deep weathering mantles in Scotland.

There is a large literature surrounding the development of saprolite in these environments (see for example Thomas 1974; Twidale 1982; Faniran and Jeje 1983; Gerrard 1988; Ollier 1984), and it is generally accepted that chemical weathering rates are influenced by temperature, precipitation and drainage. In conjunction with bedrock mineralogy, the above factors determine the mineralogical composition of resultant weathering mantles

(Summerfield 1991; Ollier 1984).

Although the formation of saprolite is currently confined to humid tropical and subtropical areas, remnants of such weathering mantles are known to exist in areas where they are no longer forming under present day climatic conditions. Occurrences are reported from areas far removed from such temperate climatic zones such as Norway (Sorensen 1988), Finland (Kejonen 1985; Lahti 1985), Sweden (Hillefors 1985; Lundqvist 1985, 1988; Lidmar-Bergstrom 1988a), the United States (Feininger 1971), and Canada (Watts 1981; Bouchard 1985).

In Scotland, too, the existence of saprolite weathering covers has long been recognised (Barrow et al. 1913; Phemister and Simpson 1949; Linton 1955; Fitzpatrick 1963; Godard 1963; Hall 1983). However, it is only recently that their origin and significance has been documented. Data on granulometry and clay mineralogy, backed by geochemistry, indicate that two main weathering types exist (Hall 1985). The most widespread is the gruss weathering type in which a relatively low degree of alteration has caused disintegration into a granular sand (Plate 4.2). The second weathering type, clayey gruss, is confined mainly to the central Buchan area. It represents advanced alteration, and parent rocks have been reduced to a sticky, clayey silty sand. Detrital primary mineralogy is dominated by quartz, fines contents are relatively high and clay mineral assemblages consist of mature

Plate 4.2 Saprolite at Coire Raibert, Cairngorm Mountains. The intensity of weathering decreases from a sandy saprolite at the surface to bedrock at the base of the exposure.

Kaolinite-illite suites (Hall 1985).

The relative ages of these two weathering types have been established using evidence from correlative deposits in the North Sea, saprolite mineralogy and geomorphology. The gruss weathering profiles are thought to be of middle Pleistocene age or older on two grounds. First, the presence of weathered biotite and feldspar and inherited clays throughout a middle to late Pleistocene sequence of glacial, glaciofluvial and periglacial deposits at Kirkhill, Buchan, attaches a minimum age to the weathering. Second, there is the presence of hydromorphic iron and manganese minerals in weathering profiles now occupying free-draining sites (Hall 1985). Suggestions that the deep weathering is wholly of interglacial age are rejected in view of the disparity between rates of rock alteration during the present interglacial, the relatively short durations of previous interglacials, and the observed depths of weathering (Hall 1985). A period or periods of deep weathering before the glacial Pleistocene is indicated.

Analysis of the clay mineralogy of these saprolites indicates that the gruss weathering type was formed under temperate environments. The more intense alteration shown by the clayey grusses, however, requires warmer, probably subtropical environments (Hall 1985). Such climates have not prevailed in Scotland since the middle Miocene, around 10 million years ago, (Buchardt 1978). Hall (1985, p393) concludes that "...the clayey gruss

weathering type predates the late Miocene and that the gruss weathering type developed continuously through the Pliocene and early Pleistocene".

Rainbird et al. (1990) have compared the clay mineralogy of a sub-Huronian saprolith (lithified saprolite) in Quebec, Canada, with a modern weathering profile developed on the Devonian Toorongo granodiorite in eastern Australia. This work suggests that although there are inherent differences (bulk-composition, age, structure, post-depositional history, and perhaps climate) the basic mineralogical and geochemical trends observed are essentially the same and can be attributed to the effects of primary weathering reactions, such as those between rain-water and parent protolith (Rainbird et al. 1990, p820). A direct mineralogical comparison is possible between these ancient and modern weathering profiles.

Weathering profiles in Scotland may show a marked spatial variation in depth. Up to 20 metres of weathering has been reported from parts of central Buchan (Hall 1986), although depths of weathering around 10 metres are more common. This depth is comparable to that found in the humid tropics today, where weathering occurs to depths of up to 100 metres (Ollier 1984). The Scottish weathering profiles often display no 'weathering front' (Mabbutt 1961) between the weathered and non-weathered bedrock. Instead, there is a gradual downward decrease in the degree of disaggregation in the profiles (Hall and Mellor 1988). Weathered rock grades into fresh rock,

although incipient alteration may reduce the mechanical strength of rock below the surficial disaggregated zones (Hall 1986). This gradual downward change in degree of alteration fits with the generalised sequence of weathering zones in saprolites given by Ollier (1984, p181), who recognises the following sequence:

(1) Soil (horizons possibly overlapping lower zones)

(2) Structureless regolith

(3) Saprolite retaining structure

(4) Structured regolith with rounded corestones

(5) Structured regolith with angular, locked corestones

(6) Unweathered rock

The significance of the saprolite is its age. The Scottish saprolites must be preglacial because Quaternary environments, even in the present interglacial, were cold. A Pliocene and early Pleistocene age is attributed to the period of deep weathering on the basis of clay mineralogy (Hall et al. 1989). Deep weathering products which owe their formation to hydrothermal alteration are also preglacial in age, and can be distinguished from the products of temperate deep weathering by their high chlorite content.

Much of the preglacial regolith covering Scotland has been removed by subsequent erosion. The surviving pockets of the preglacially weathered rock

are all that is left of the thick regolith which existed at the beginning of the Pleistocene glaciations. This weathering would certainly have penetrated deeper into parent rocks in existing valleys and in fracture zones, but it is likely that the rest of the land surface was deeply weathered as well (Lundqvist 1985). The distribution of saprolites in Scotland has been used as evidence of the selectivity of glacial erosion (Hall and Mellor 1988), and in reconstructions of the depth of ice sheet erosion (Hall and Sugden 1987). The latter suggest that ice sheet erosion has removed a layer of saprolite between 10 and 50 metres in depth from north east Scotland (Hall and Sugden 1987).

4.2.5 Tors

Tors are another feature which owe their formation to deep weathering processes. Tors are defined as "...small hills or heaps of boulders, usually about 4 to 20 metres high, rising abruptly from the surrounding gentle ground surface" (Ollier 1984, p191). A two-cycle process of deep weathering followed by exhumation is thought to account for their formation (Linton 1955). Figure 4.2 is the model proposed by Linton for the formation of tors on Dartmoor. A period of sub-surface deep weathering, guided by joint systems in the original rock, is followed by a phase of mechanical stripping of the incoherent products of the chemical weathering.

The two-phase model rests on the asumption that highly selective chemical

weathering in warm and moist climatic conditions prepares the uppermost layer of the bedrock mass. This weathering allows the development of a saprolite cover upon corestones and the basal weathering front. Then, perhaps after some change in climatic conditions, the thick waste mantle is carried away by external agents, stripping bare the underlying and uneven bedrock surface (Kaitanen 1985). In the case of tors found in formerly glaciated regions, glacial erosion may be one process responsible for the removal of the deep weathering products which previously surrounded the central core stone or tor.

Ollier (1984) compares the formation of tors to that of inselbergs, whilst Twidale (1982) in a discussion of the tors of south west England, notes that similar features occur in different and various climates in other parts of the world and are known as inselbergs. The term Castle Koppies is suggested for such deep weathering remnants (Twidale 1982). The deep weathering required for the formation of tors is currently found only in tropical, subtropical and warm temperate environments (Thomas 1965; Ollier 1965). It is necessary to ascribe a date to the period of deep weathering which formed the tors in areas where such climates no longer prevail, although the gap between weathering and exhumation may have been very long. McCraw (1965) describes the tors of Otago, New Zealand, and notes how they are overlain by Tertiary deposits. The period of deep weathering in this case is probably pre-Tertiary in age. Similarly, the Cretaceous oysters observed by

Lidmar-Bergstrom (1988b) in weathering pits in Scandinavian tors suggests this as a minimum age for the deep weathering.

In a similar way, the tors found in Scotland may have their origin in the Miocene to early Pleistocene age bracket (or earlier), as this is the last period of profound deep weathering in the area. The present day tors represent the basal surface of the weathering during these periods, stripped of their saprolite weathering cover. They may therefore be regarded as remnants of the preglacial landsurface.

Tors are found in several locations in upland Britain, etched into a variety of rock types (Linton 1952, 1955), including both glaciated areas such as the Cairngorm Mountains (Sugden 1968, 1975 and Plate 4.3), and in unglaciated areas such as Dartmoor (Waters 1954). In addition, tors are reported from other localities around the world, including Arctic Canada (Watts 1981; Sugden and Watts 1977), Australia (Caine 1967) and Portugal (Linton 1955). In the Scottish context, tors are mainly developed in granite bedrock. The occurrence of tors in Scotland is further evidence supporting the deep weathering hypothesis of Hall (1985). In this case, the tors represent the former weathering front and the removal of all former saprolite cover is indicated.

It is important to note, however, that an alternative explanation for the

Plate 4.3 A large tor on the summit of Bennachie, North East Scotland. The morphology of the tor is determined by the master joints. Note the topographic sheeting and laminar fretting in the rock.

formation of tors exists. Many authors have considered tors to be periglacial in origin. The main line of argument is that the present day tors were stripped by periglacial processes, most notably solifluction (Palmer 1956). Further evidence for the periglacial evolution of tors is the existence of extensive blockfields on mountain summits containing tors. Although periglacial processes may account for the exposure of some smaller tors, the deep weathering process is more likely as an overall process of formation for several reasons. First, there is a close association between tors and preglacial rolling relief, often with occurrences of deeply weathered rock. Second, Sugden (1965) notes that the Scottish tors show no association with altiplanation terraces or other major periglacial features. Third, some tors can be proved to have been over-ridden by ice (Sugden 1968) and therefore pre-date at least one glacial period. Although periglacial processes may affect the detailed form of tors, the deep weathering hypothesis seems to explain more fully their gross morphology.

4.2.6 Overall significance

This review suggests that there are certain landscape features which can readily be identified as having their origins in preglacial times. The undulating plateau surfaces of the Cairngorm Mountains have survived since the Tertiary, and are associated with other preglacial forms such as dendritic drainage networks and concave river profiles. The episode of deep chemical weathering responsible for the formation of saprolites in Scotland has been

dated to the Pliocene and early Pleistocene on the basis of clay mineralogy (Hall 1985). Pockets of saprolite are remnants of this weathering mantle and represent the preglacial weathering cover. Tors and tor-like features are found where preglacially weathered bedrock has been completely removed to leave the less-weathered central core intact. The widespread formation of granite sheets parallel to land surfaces is another association typical of preglacial surfaces.

The existence of such features indicates that the survival of elements of the preglacial landscape may be possible even in an area such as Scotland where erosion by glaciers and ice sheets has been locally very important. The recognition and identification of these preglacial remnants is crucial as it allows the intensity and spatial variation in ice sheet erosion to be reconstructed. Furthermore, knowledge of the preglacial relief enables quantitative estimates of the depth and volume of ice sheet erosion to be made.

4.3 Glacial landscapes

It is assumed that there is a certain set of identifiable landforms whose formation can be linked to glacial erosional processes. The morphology and characteristics of such landforms, as well as the processes responsible for their formation, have been described in many textbooks on glacial geomorphology (Embleton and King 1975; Sugden and John 1976; Eyles

1983; Drewry 1986). The morphology of many glacial landforms suggests that links may exist between preglacial and glacial forms, for example that between the shape of preglacial tors and glacial roches moutonnees (Lindstrom 1988).

The mapping of the landforms produced by the former ice sheet involves the use of aerial photograph interpretation and field survey to identify the location and distribution of ice moulded and glacially scoured bedrock, glacial troughs, roches moutonnees, and other glacial erosional features. Such landforms are readily identifiable in the field due to their freshness of form and the presence of fresh bedrock at the surface, often with distinct morphological characteristics such as stoss and lee formations, striae, or glacially abraded and plucked surfaces.

4.4 Conclusion

The evidence presented in this chapter suggests that there are distinctive landforms and structures which are associated with both glacial and preglacial landscapes. Preglacial landforms which exist in formerly glaciated regions must have withstood innundation by one or more ice sheets. A set of landforms can also be related to the processes of glacial erosion where all traces of the preglacial landscape may have been removed. A continuum exists between the total preservation and total destruction of these preglacial landscapes by erosion, including the possibility that many glacial landforms

are inherited directly from preglacial structures.

Figure 4.3 is an attempt to explain the relationship between this preglacial landscape evolution and glacial erosion. During Time I, after the intrusion of the main Tertiary igneous centres, gradual surface lowering takes place through dynamic etching (Hall 1990). The gradual removal of the surface load allows expansion of the granite batholith and sheet structures form parallel to topographic surfaces.

At some later time period (Time II), deep weathering of the Tertiary rocks takes place under tropical, humid conditions. This weathering may have penetrated to great depths and allowed formation of the highly-altered clayey gruss saprolite (Hall 1985). A secondary, less intense, phase of deep weathering under temperate, humid conditions allowed formation of the gruss weathering type. Core stones form below where the chemical weathering allows complete disaggregation of the bedrock. Below the weathering front the bedrock remains unaltered. Sheet structures may continue to form as weathering proceeds.

Following some climatic deterioration a glacial cycle begins (Time III). There may be a brief period of periglacial conditions before the land becomes submerged beneath an ice sheet. Where ice flow is sufficiently vigorous or prolonged, and basal conditions allow erosion to proceed, the

TIME	EVENT	EFFECT
I	Gradual surface lowering of Tertiary igneous centres	Major sheet structures in granites developed
II	Deep weathering under tropical and/or temperate, humid conditions	Formation of chemically weathered regolith; clayey gruss, gruss saprolites and core stones. Continued development of sheet structures
III	Glacial period	Stripping and/or protection of preglacial regolith. Tors and core stones may emerge
IV	Interglacial period. Equilibrium change; possible limited weathering under temperate, humid conditions	Possible minor chemical weathering of rock and mass wasting
V	Glacial period	Stripping and/or protection of preglacial regolith continues (and interglacial weathering products if present). Sculpting of glacial forms in former weathering front following complete saprolite removal

Time stages IV and V cycle through Pleistocene...

Figure 4.3 The relationship between preglacial landscape evolution and glacial erosion in Scotland.

preglacial weathering mantle is stripped by glacial erosion. After removal of the saprolite the less intensely weathered core stones may emerge to form the present day tors. The preglacial regolith may survive intact where glacial erosion is ineffective.

After the recession of the ice sheet, climatic amelioration during an interglacial (Time IV) may allow further weathering to occur under temperate, humid conditions. There may also be active mass wasting during periglacial periods at the beginning and close of glacial periods, such as today. Such periods may be geomorphologically very important as they represent a period of transition from one equilibrium to another. These periods of weathering may enable the formation of slightly weathered gravels, but are probably not severe enough or sufficiently long-lived to allow the formation of saprolite. During the next glacial stadial (Time V) there is continued stripping of the preglacial regolith and the removal of any weathering cover which may have formed during the interglacial. After the removal of all the preglacial saprolites, the weathering front appears at the earth's surface and the sculpting of glacial forms in solid bedrock takes place.

It is important to note that more than two glacial cycles are probably required to produce this end result, and that even then scattered patches of preglacially weathered bedrock may remain where ice sheet erosion is

ineffective. However, if erosion by the ice sheet is particularly effective or prolonged then the stripping of the preglacial cover **and** sculpting of glacial forms in bedrock may occur in favourable locations during the first stadial.

The recognition of glacial and preglacial landforms in formerly glaciated regions is therefore a fundamental starting point in reconstructing patterns of ice sheet erosion. The spatial distribution of these landforms provides a record of the effectiveness or ineffectiveness of the processes of ice sheet erosion in a region.

CHAPTER FIVE

THE PATTERN AND DEPTH OF ICE SHEET EROSION IN THE STUDY AREA

5.1 Aim

The aim of this chapter is to determine the location and depth of ice sheet erosion in a transect from the centre to the margin of a former Scottish ice sheet. This is achieved by mapping at; (a) the regional scale of the entire flowband and; (b) the local study areas within the flowband. The spatial variation in depth and intensity of erosion provides a test for the predicted pattern of basal ice temperatures calculated in Chapters 2 and 3.

5.2 Approach

(1) A map of features of ice sheet erosion in the transect was compiled from aerial photograph interpretation, and a landscape classification produced for the area.

(2) A representative site 5 by 5 km in size was examined in the field for each of the landscape classes. This provides an independent check on the accuracy of the aerial photograph interpretation and allows detailed mapping of glacial and preglacial landforms. On the basis of the field evidence, estimates of the minimum and maximum depth of ice sheet erosion are made for each study area.

(3) On the assumption that the field study areas are representative of the broader landscape classification, estimates of the minimum and maximum depth of ice sheet erosion are calculated for the entire transect.

5.3 The regional pattern of ice sheet erosion

5.3.1 Method

The study area was examined on 3250 panchromatic stereo aerial photographs at a scale of 1:10,000. Land-forms of ice sheet erosion were mapped on to 1:50,000 base maps of the area using the aerial photographs. The criteria outlined in Chapter 4 were used in the mapping of landforms from the aerial photographs. Such mapping from aerial photographs has previously been used by Sugden (1974, 1978) to classify landscapes in North America and Greenland. A full description of the technique and classifications used is given in these papers. The landforms of ice sheet erosion stand out because they are carved in bedrock and easily distinguished from vegetation and soils. Sharp breaks of slope associated with cliffs and troughs are visible, as are areas of exposed bedrock exhibiting areal scouring and roches moutonnees. Features related to local valley glaciation, such as corries, were mapped but are not included in the discussion of the overall pattern of ice sheet erosion.

5.3.2 Reliability of aerial photograph interpretation

The map derived from the aerial photograph interpretation (Figure 5.1) was checked by comparison with the five sample field areas (Figures 5.2 to 5.6). A key for use with the geomorphological maps is presented in Figure 5.7. In the Cairngorm study area, the field map and the features mapped from aerial photography are similar, but the map compiled from the aerial photograph interpretation underestimates the coverage of areal scouring by about 5 per cent (Figure 5.2). This is because there is a critical size, around 5 x 5 metres in size, below which patches of bedrock exhibiting areal scouring are not visible on aerial photographs. In the Glen Feshie study area, no landforms of ice sheet erosion occur and this result is obtained by mapping using both aerial photography and fieldwork (Figure 5.3). The large roches moutonnees and areal scouring in the Balmoral study area show a similar distribution using the two methods because the size of the features is sufficiently large for recognition on aerial photography (Figure 5.4). In the Speyside study area the extent of areal scouring is only slightly underestimated on the map compiled using aerial photography, again by about 5 per cent (Figures 5.1 and 5.5). There is agreement between the two methods in the Aberdeen study area since the isolated patches of areal scouring are identified on both maps (Figures 5.1 and 5.6). The streamlined hills in this area were not mapped from aerial photography because their low relief over horizontal distances of hundreds of metres makes their identification difficult.

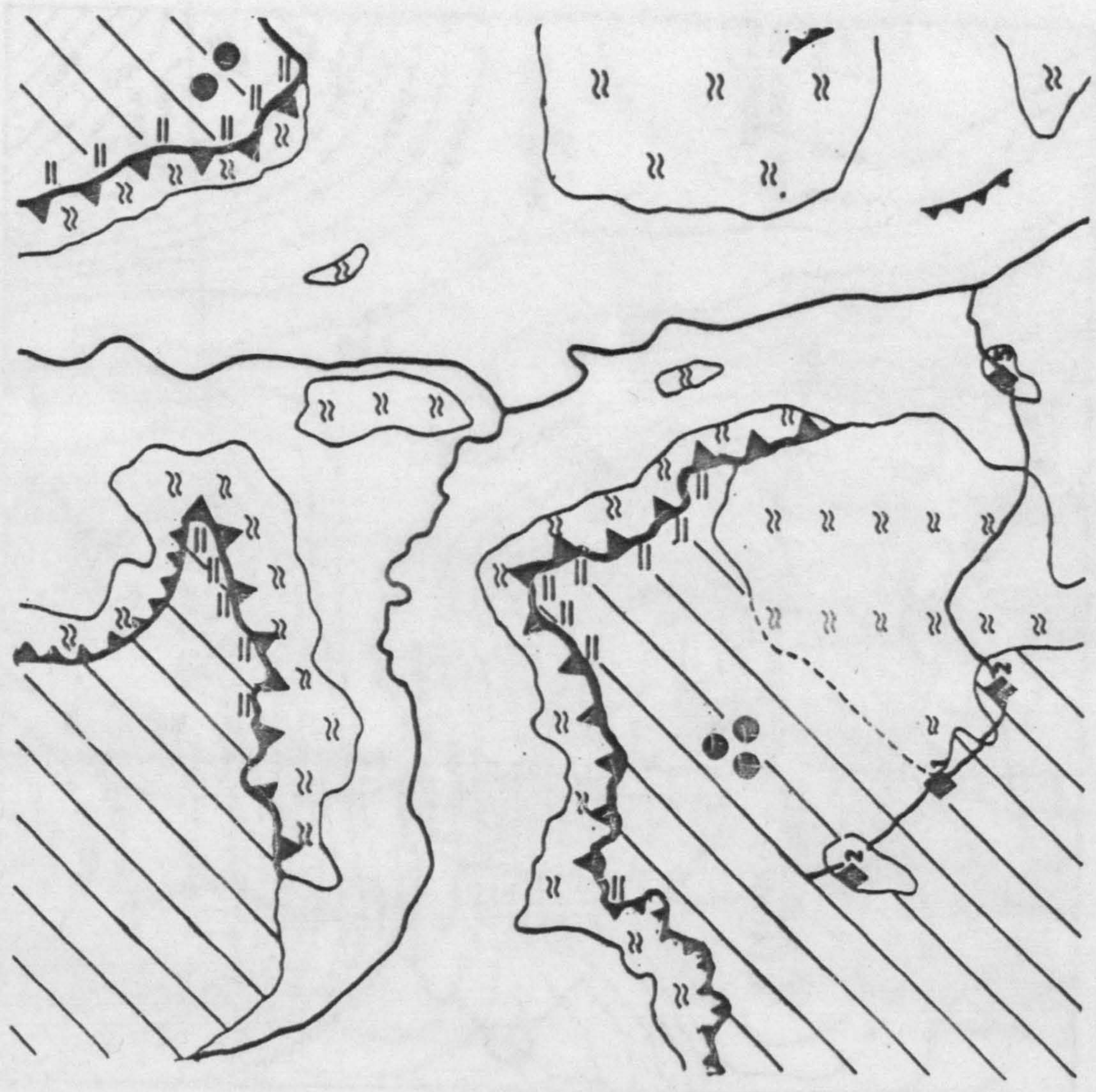

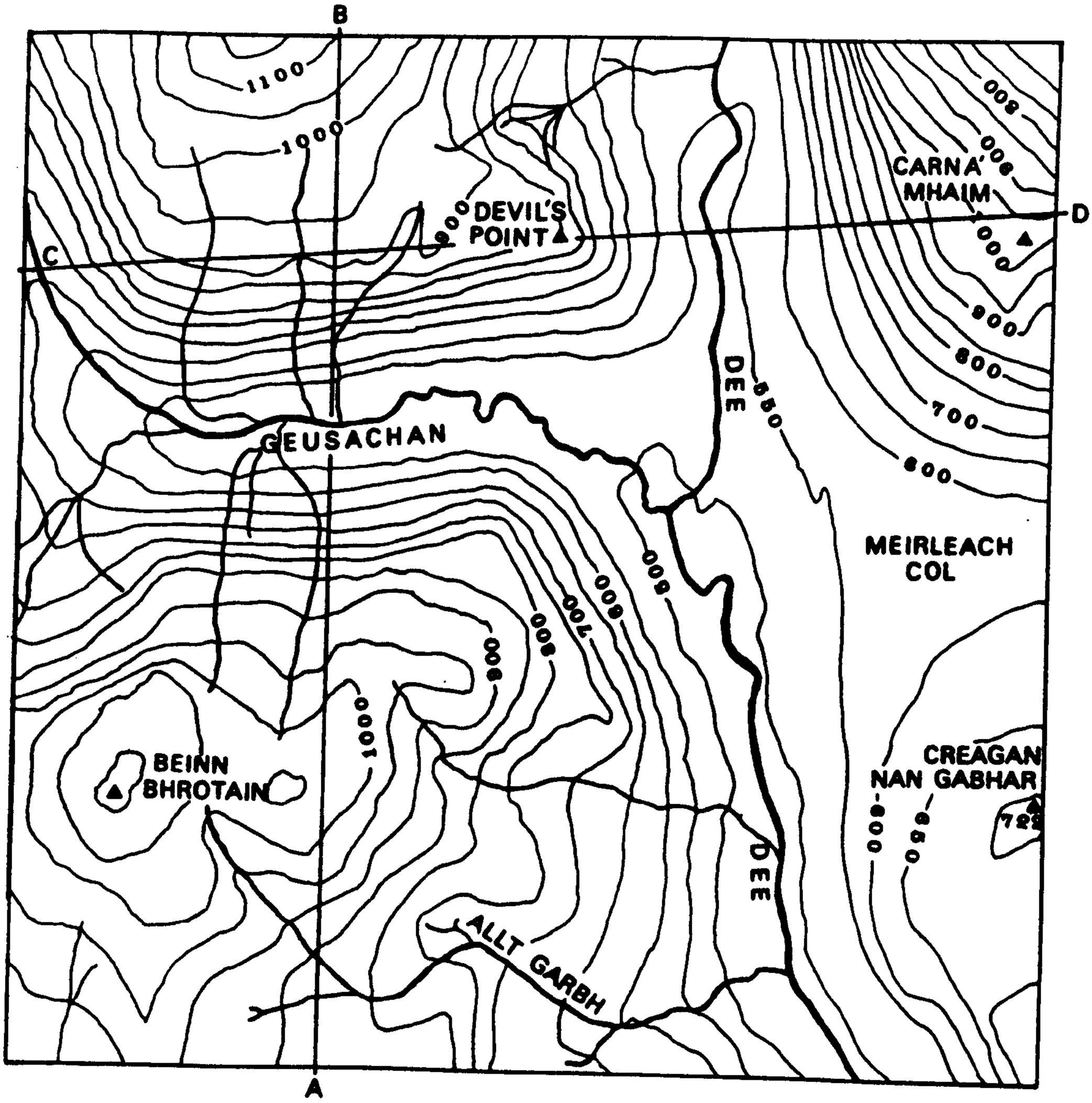

Figure 5.2 Geomorphological map of Cairngorm field study area. Lines A-B and C-D refer to topographic profiles drawn in Figure 5.10. For key see Figure 5.7.

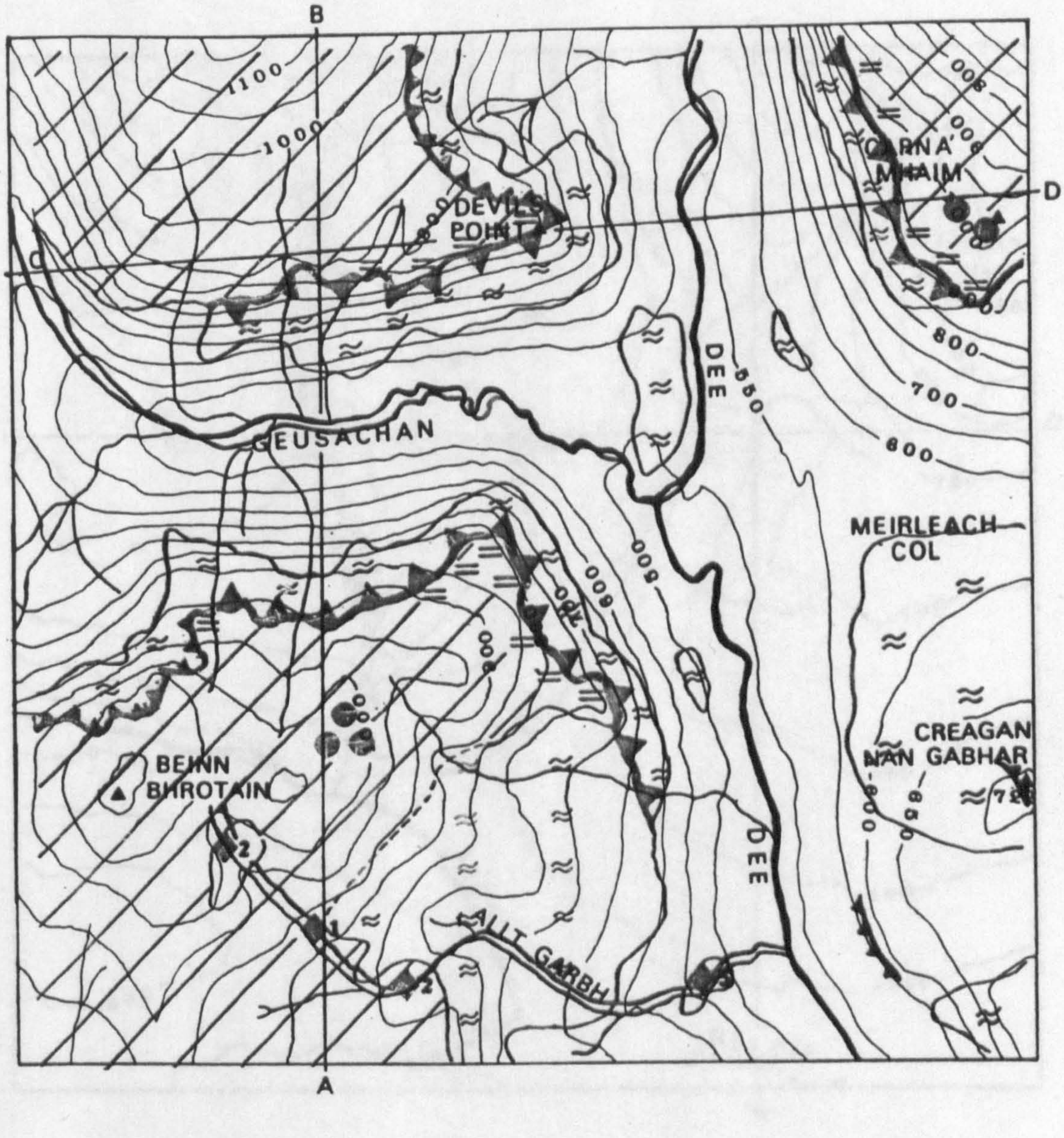

Figure 5.2 Geomorphological map of Cairngorm field study area. Lines A-B and C-D refer to topographic profiles drawn in Figure 5.10. For key see Figure 5.7.

13
15
1

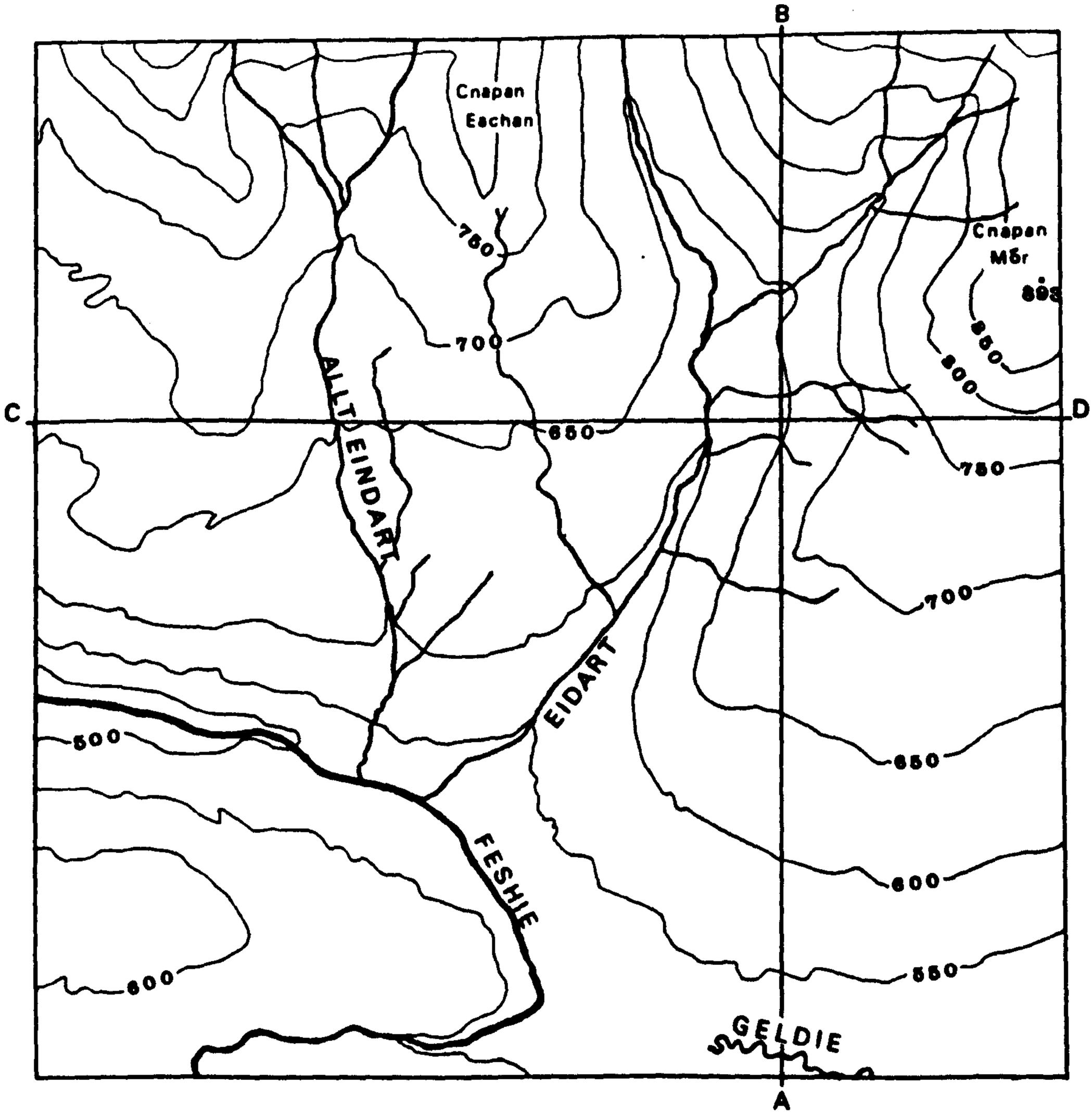

Figure 5.3 Geomorphological map of Glen Feshie field study area. Lines A-B and C-D refer to topographic profiles drawn in Figure 5.20. For key see Figure 5.7.

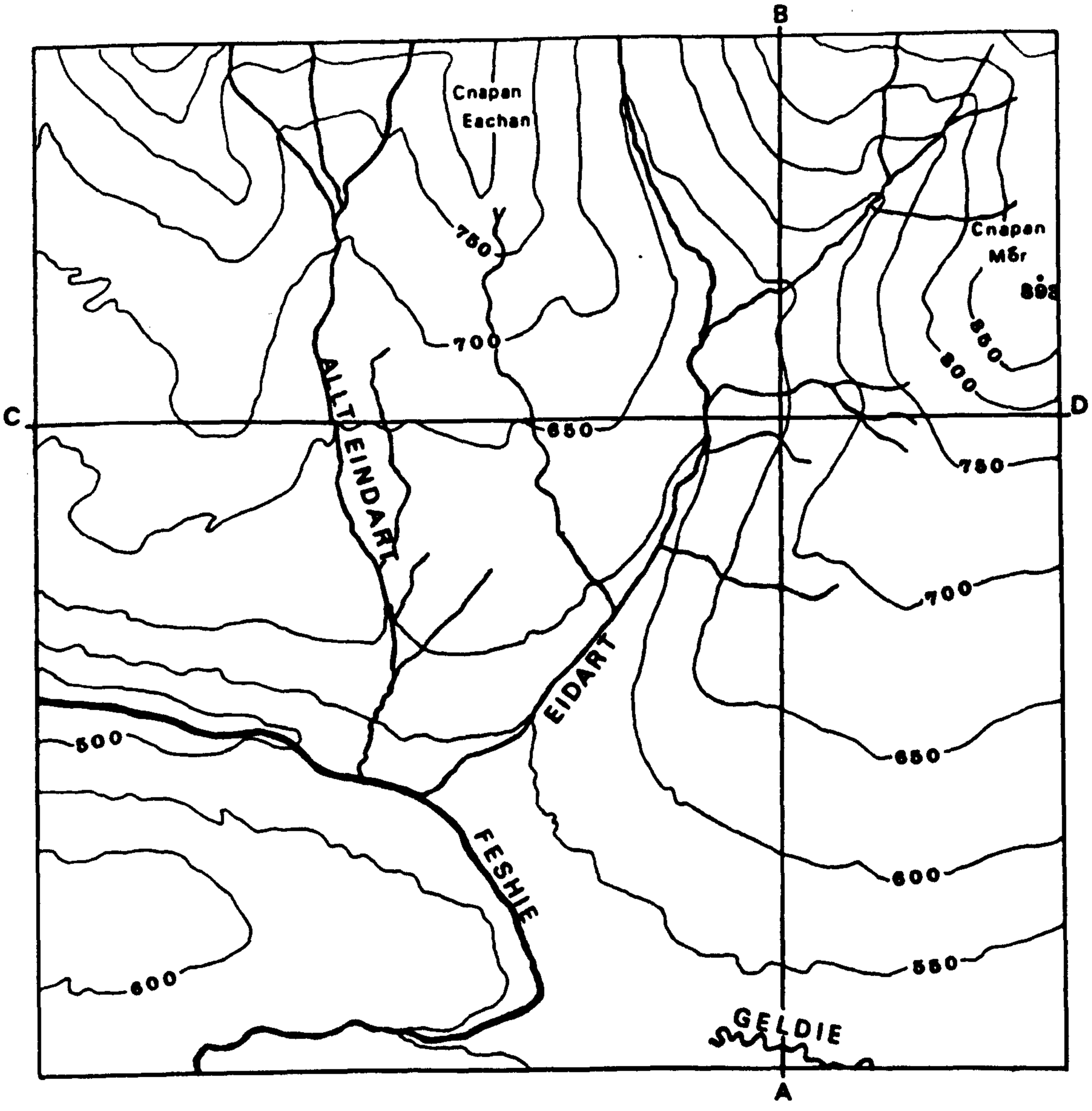

Figure 5.3 Geomorphological map of Glen Feshie field study area. Lines A-B and C-D refer to topographic profiles drawn in Figure 5.20. For key see Figure 5.7.

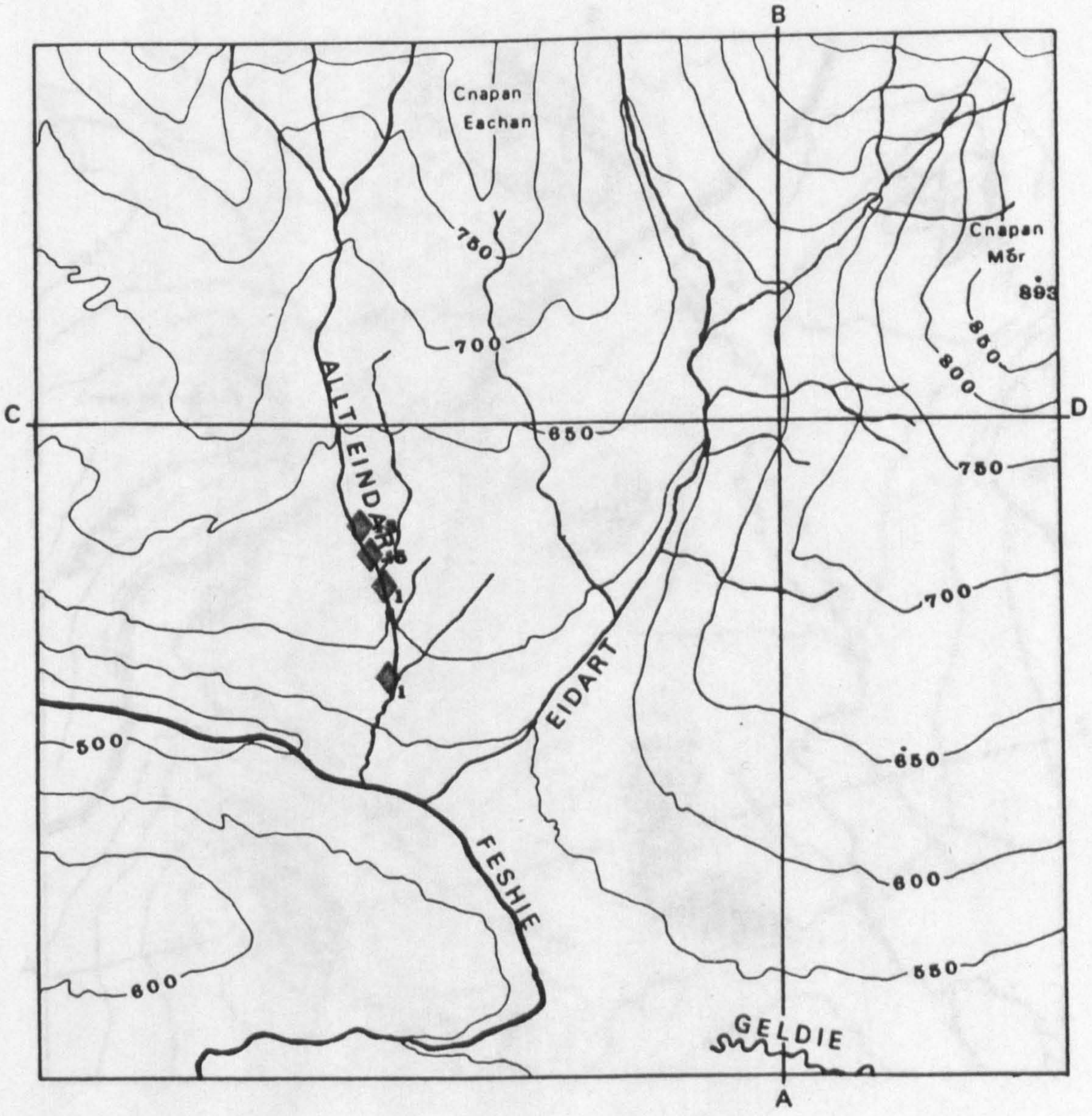

Figure 5.3 Geomorphological map of Glen Feshie field study area. Lines A-B and C-D refer to topographic profiles drawn in Figure 5.20. For key see Figure 5.7.

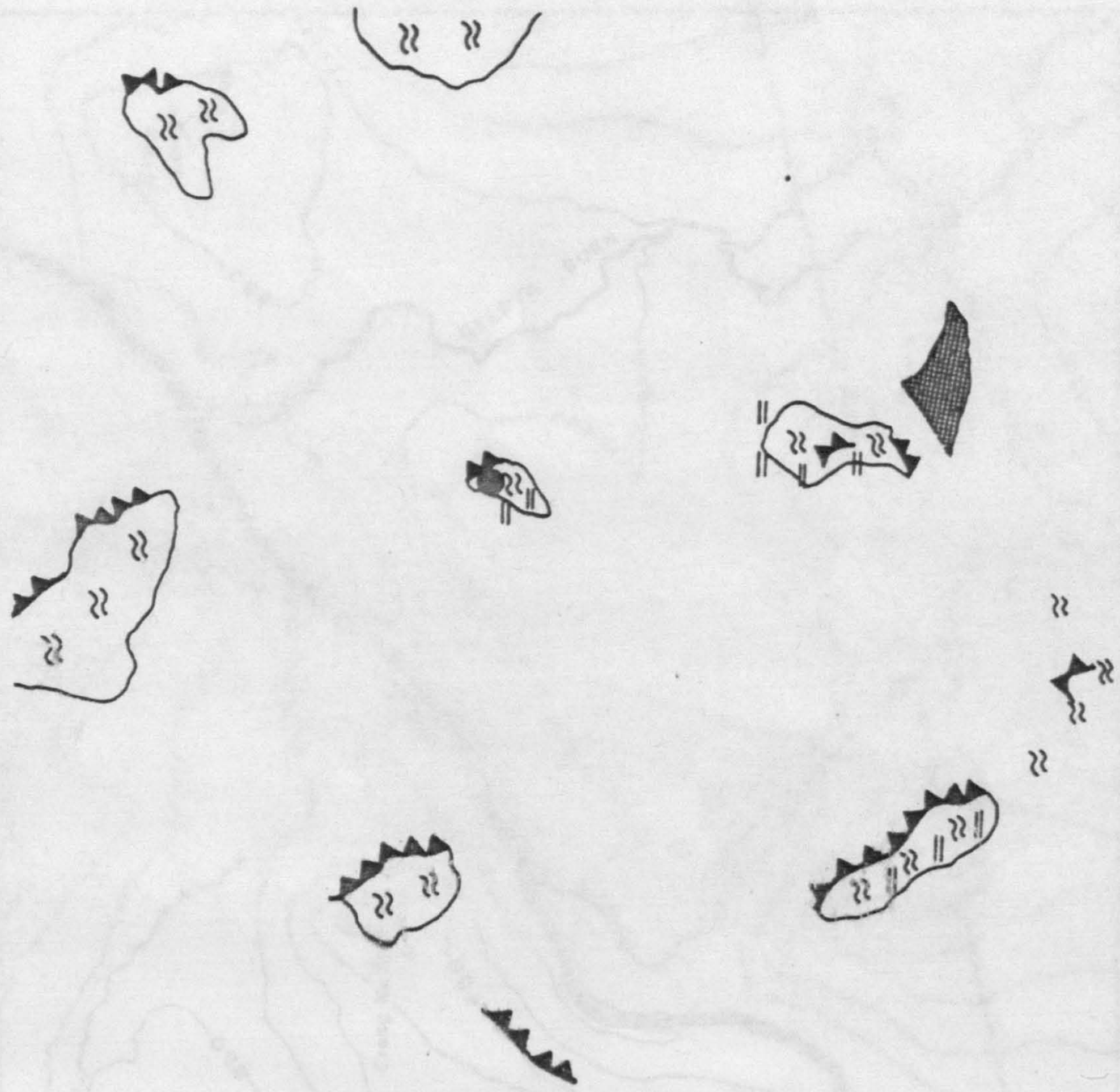

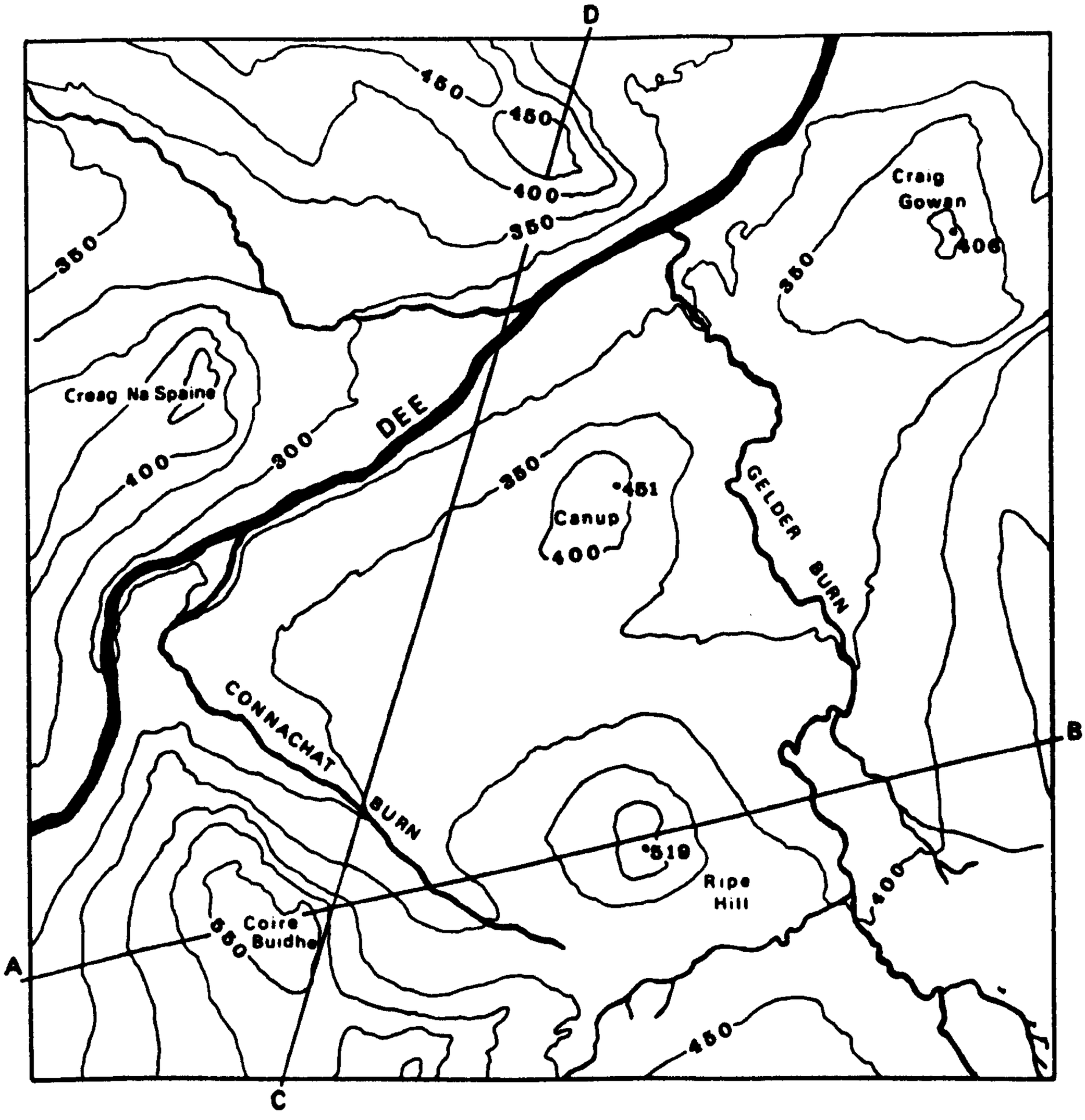

Figure 5.4 Geomorphological map of Balmoral field study area. Lines A-B and C-D refer to topographic profiles drawn in Figure 5.23. For key see Figure 5.7.

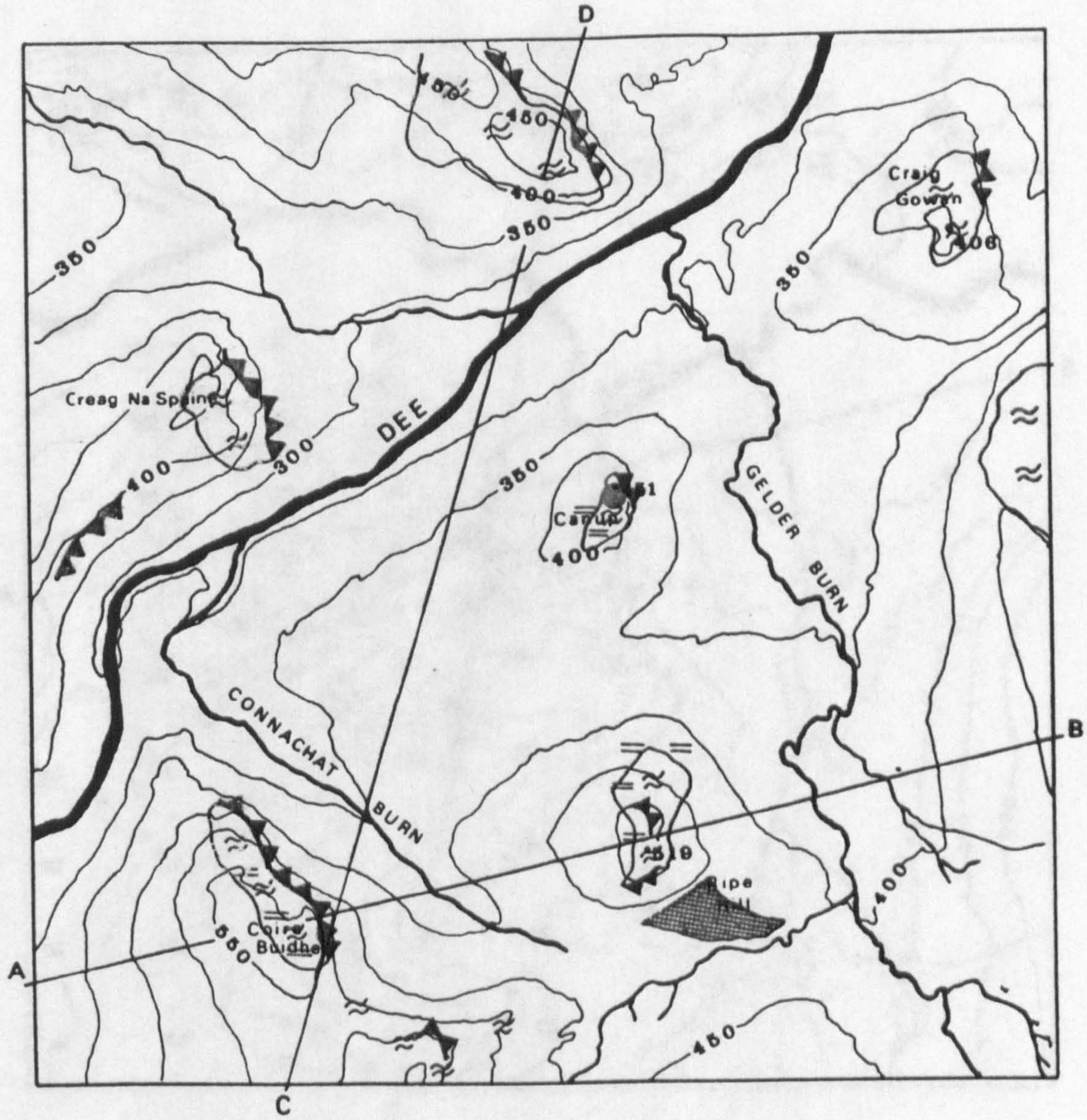

Figure 5.4 Geomorphological map of Balmoral field study area. Lines A-B and C-D refer to topographic profiles drawn in Figure 5.23. For key see Figure 5.7.

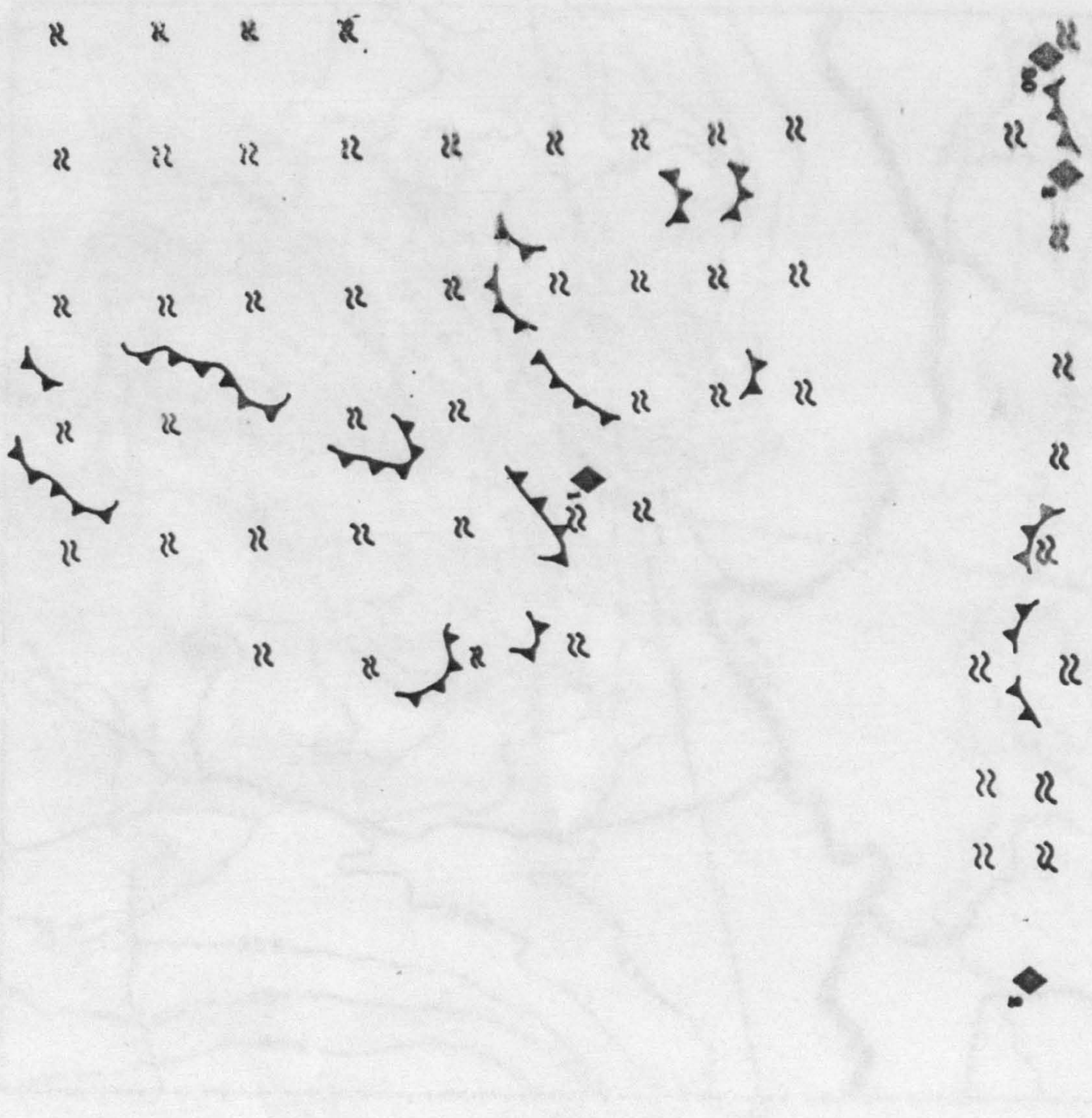

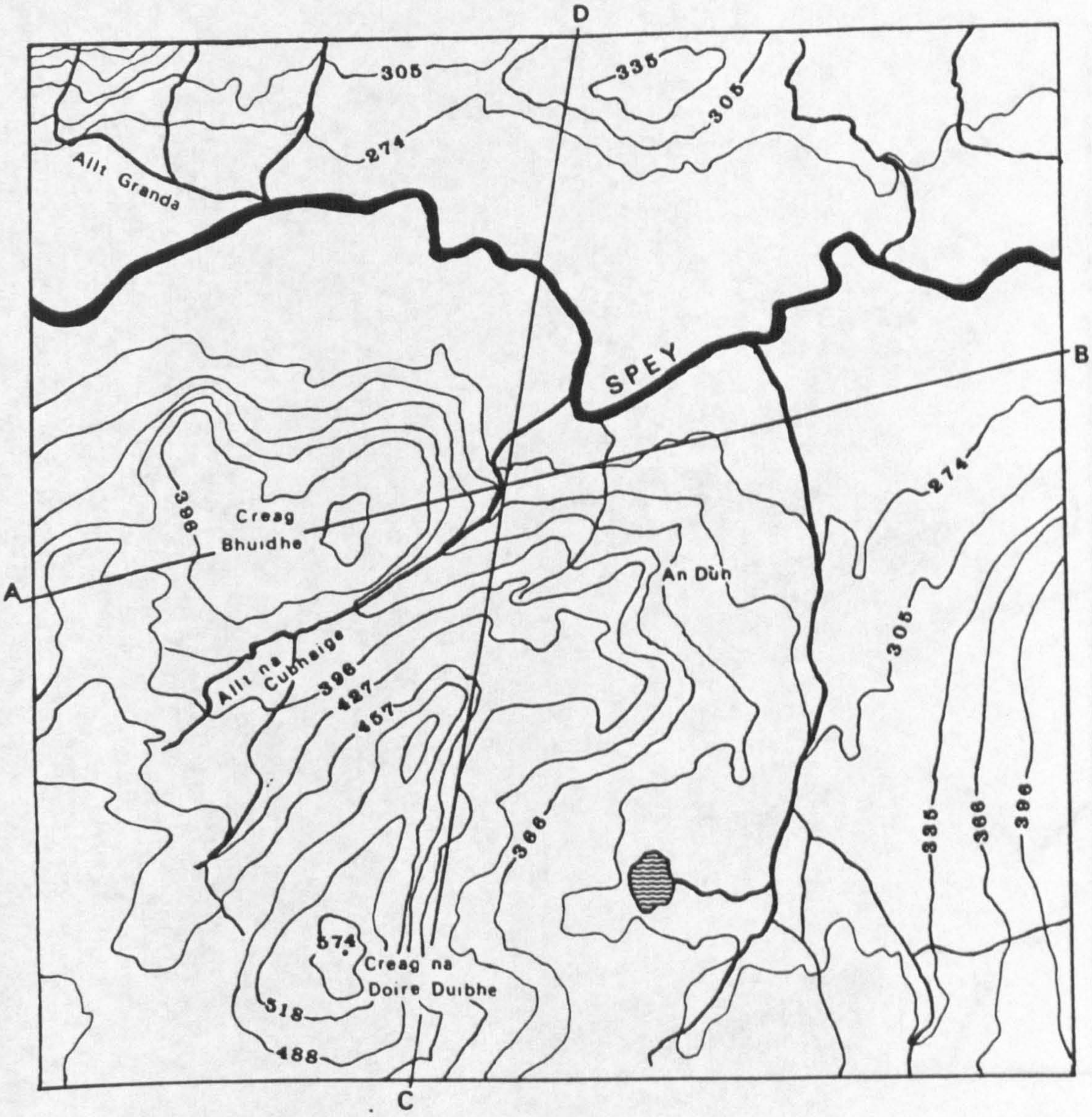

Figure 5.5 Geomorphological map of Speyside field study area. Lines A-B and C-D refer to topographic profiles drawn in Figure 5.28. For key see Figure 5.7.

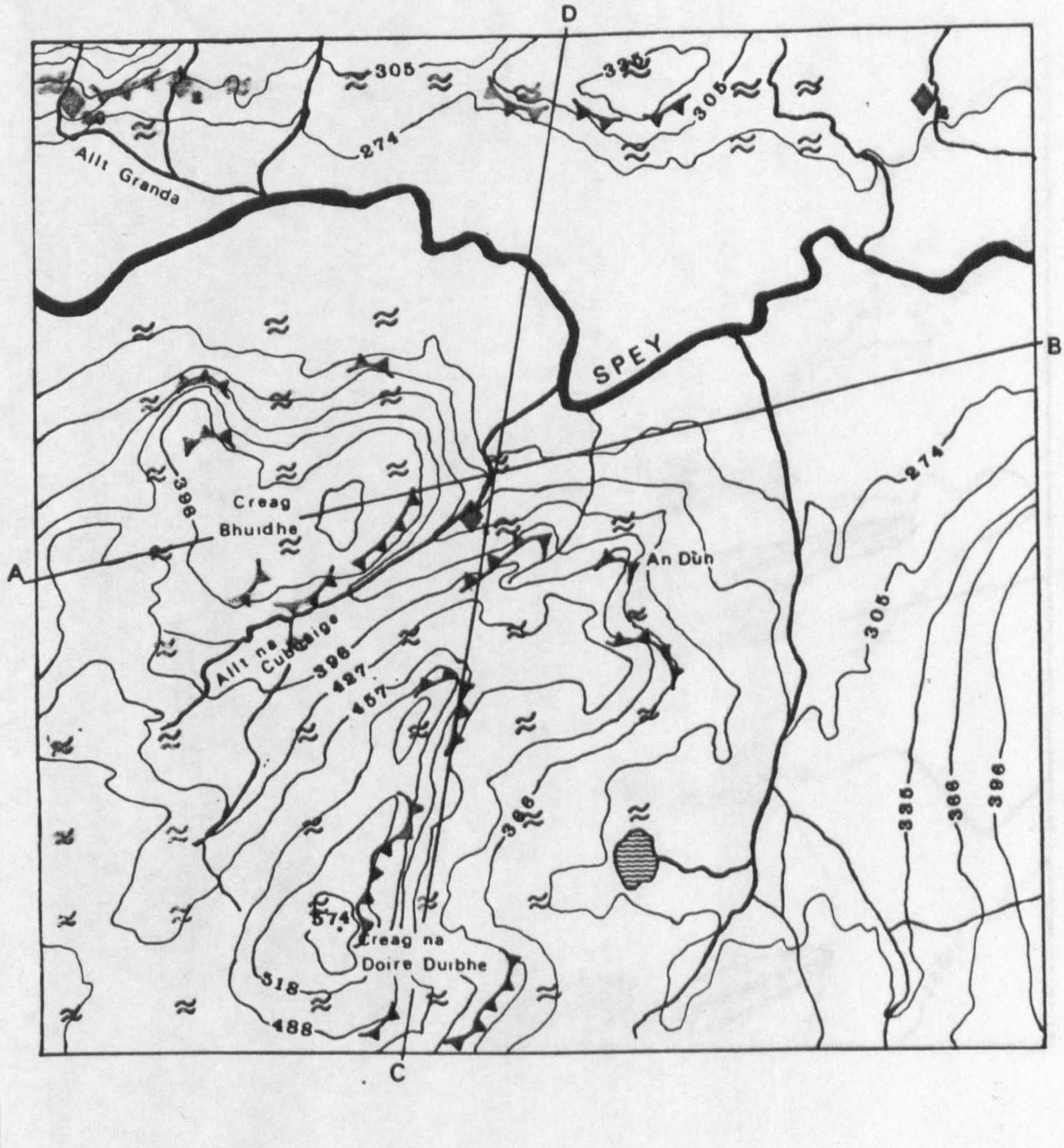

Figure 5.5 Geomorphological map of Speyside field study area. Lines A-B and C-D refer to topographic profiles drawn in Figure 5.28. For key see Figure 5.7.

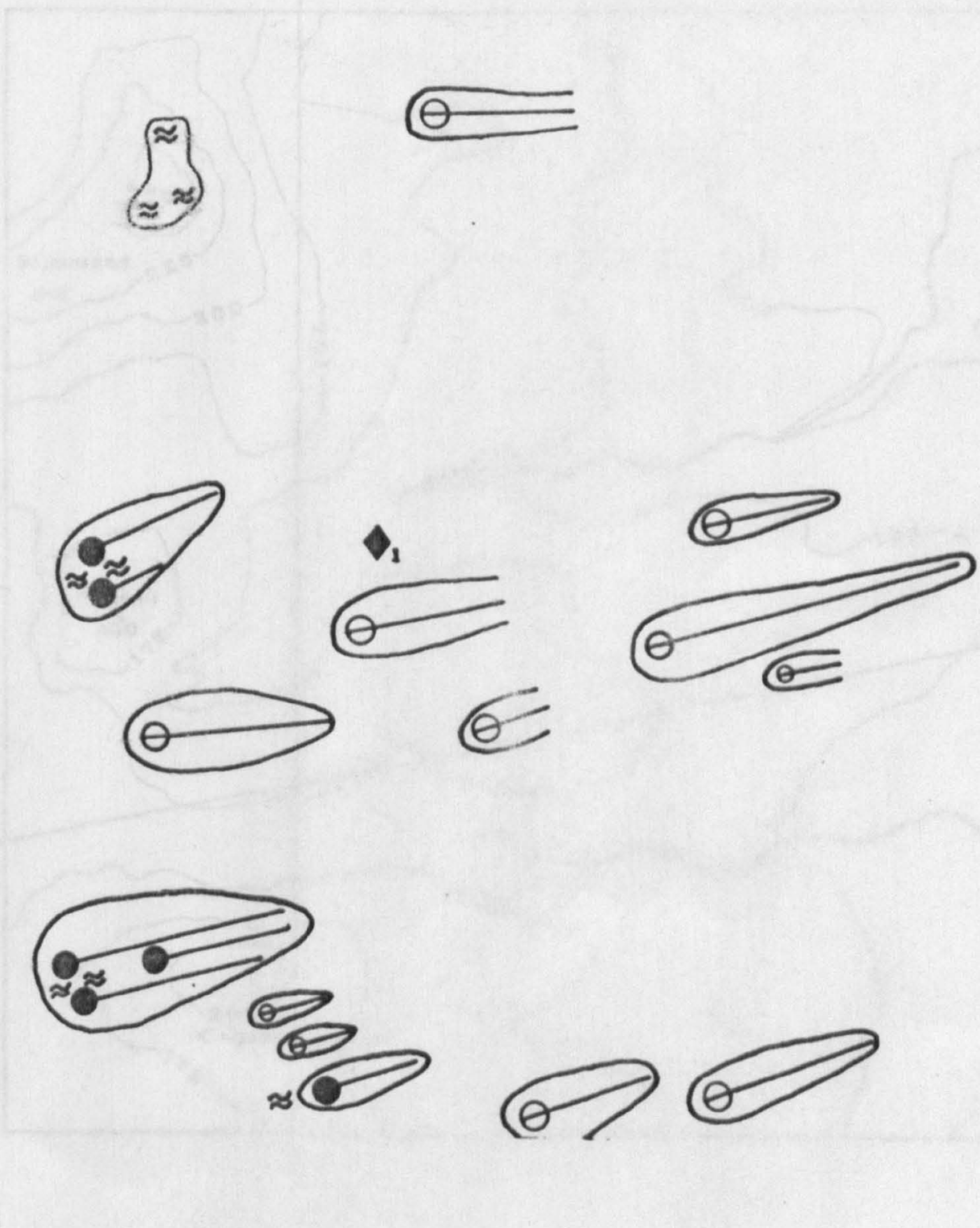

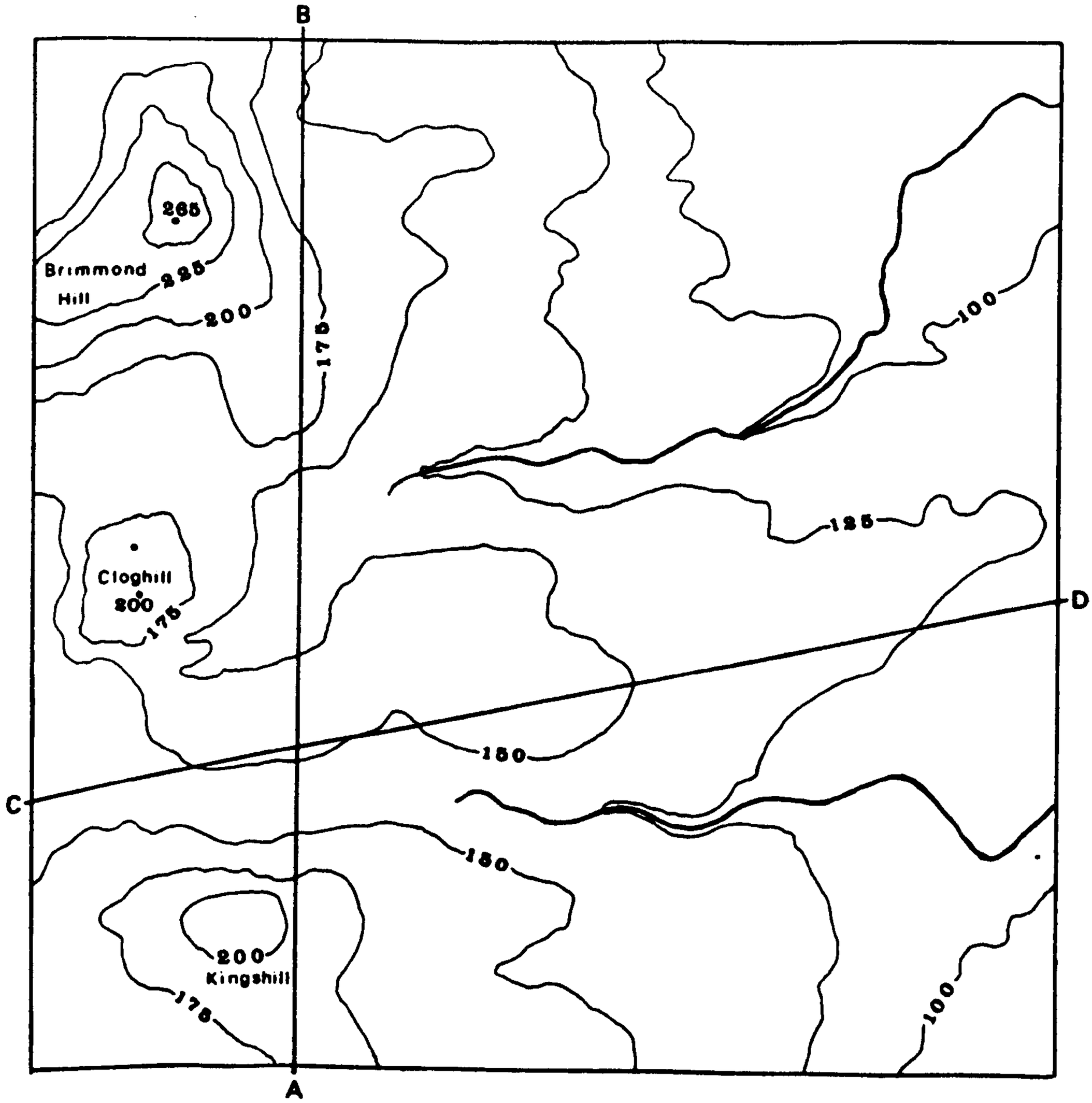

Figure 5.6 Geomorphological map of Aberdeen field study area. Lines A-B and C-D refer to topographic profiles drawn in Figure 5.29. For key see Figure 5.7.

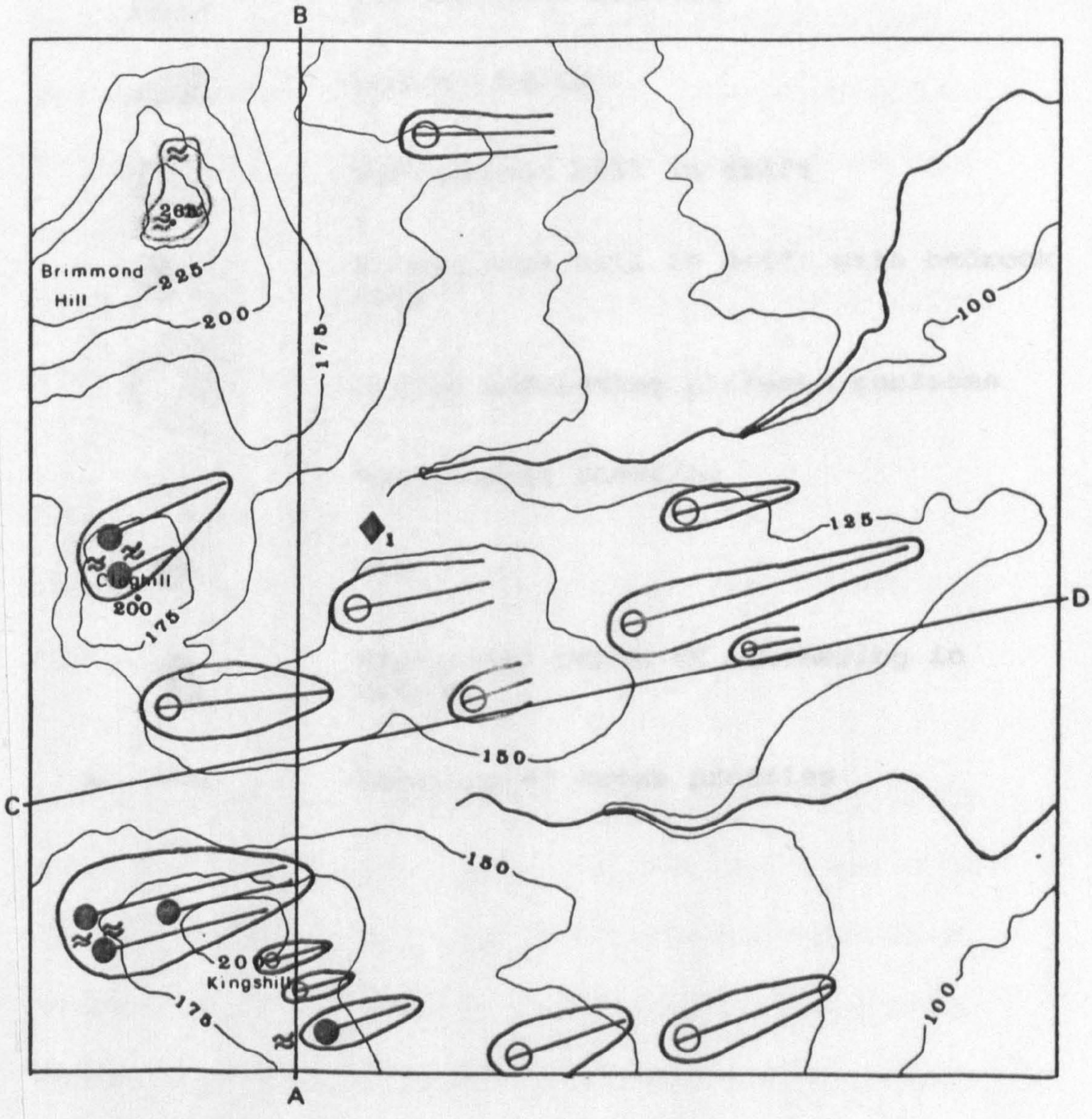

Figure 5.6 Geomorphological map of Aberdeen field study area. Lines A-B and C-D refer to topographic profiles drawn in Figure 5.29. For key see Figure 5.7.

Glacial trough

Cliff and other sharp breaks of slope

Ice smoothed bedrock

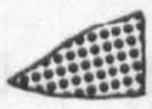

Boulder train

Streamlined hill in drift

Streamlined hill in drift with bedrock knob

Gently undulating plateaux surfaces

Topographic sheeting

Tor

Saprolite: Depth of weathering in metres

A———B Location of cross profiles

Figure 5.7 Key for geomorphological maps shown in Figures 5.2 to 5.6.

Independent fieldwork checking of the map presented in Figure 5.1 is important because it determines the level of confidence which can be placed in the aerial photograph interpretation. Since there is a good agreement between the extent of areal scouring in each of the study areas mapped in the field and the extent of areal scouring identified using aerial photography, the pattern of ice sheet erosion can be identified reliably in the entire transect using aerial photography. The pattern of ice sheet erosion shown in Figure 5.1 is considered to be an accurate picture of the pattern of erosion on the ground.

5.3.3 The regional pattern of ice sheet erosion

The regional pattern of ice sheet erosion is shown in Figure 5.1. The main features are:

(1) Glacial troughs occur only in the central area of the transect, in the area within and around the Cairngorm Mountains. The large troughs of the Geusachan, Dee, Derry, Avon. Einich and Lairig Ghru are incised into the western Cairngorms, whilst the troughs of Slochd Mor and Builg dissect the eastern Cairngorms. Trough formation is restricted to areas where relative relief is above 600 metres. Elsewhere in the study area, where the topography is relatively low lying or gently undulating, large glacial troughs do not exist.

(2) Cliffs occur either on valley sides or hill summits throughout the entire transect, although they are most common in western and central areas and rare in the east (Figure 5.1). There are three types of cliffs. Firstly, there are those which occur in conjunction with patches of areal scouring. These are particularly common in the western and central parts of the transect, especially along the Dee and Spey Valleys. These cliffs may be oriented in any direction, although on the valley floors and on hill summits they tend to be oriented transverse to the longitudinal valley axis (Figure 5.1). Secondly, there are those which occur along the edges of the Spey and Dee Valleys and are carved into the valley walls. These cliffs are oriented parallel to the longitudinal valley axis and are particularly common where valley spurs or promontories project outwards into the main valley, for example in the upper reaches of the Dee Valley near the Cairngorm Mountains (Figure 5.1). Thirdly, there are those cliffs which form the corries found in mountainous areas. These are the product of local valley glaciation and are given no further consideration here.

(3) Areal scouring occurs throughout the study area and is easily recognised by the predominance of bare bedrock and the lack of vegetative cover. Areal scouring may occur both as individual outcrops of bedrock or in association with lee side cliff faces (Figure 5.1). There is a marked contrast between the density of areal scouring in the east and west of the transect. In the west the

occurrences of scoured bedrock are found at all altitudes, while in the east the occurrences of scoured bedrock are rare and are restricted to isolated hill summits over 200 metres (Figure 5.1). Zones of areal scouring are found along the routes of the two main valleys of the Dee and Spey (Figure 5.1). Areal scouring dominates the valley floors, and the density of these features decreases with distance from the valley centre line. Zones of areal scouring associated with major cliff faces show a tendency to cluster along valley routes, especially in the east. In the central Dee Valley is an area of large roches moutonnees.

5.3.4 The regional pattern of areal scouring

The regional pattern of areal scouring was identified by analysing the number of individual occurrences of areal scouring in grid cells measuring 5 by 5 km. The number of individual occurrences in a 5 by 5 km grid was used in preference to the percentage area of the grid containing landforms of areal scouring due to the difficulties involved in calculating the latter for small exposures. Areal scouring is developed along the Dee and Spey valleys where 10 to 14 individual ocurrences of scouring are found within a 5 x 5 km grid (Figure 5.8). Areas of intense scouring (> 15 occurrences per grid) are restricted to the central area of the Dee Valley. Areas where scouring is poorly developed (5 to 9 occurrences) occur throughout the western and central parts of the study area. Areal scouring is rare in the east of the transect and on the highland between the Cairngorm Mountains and

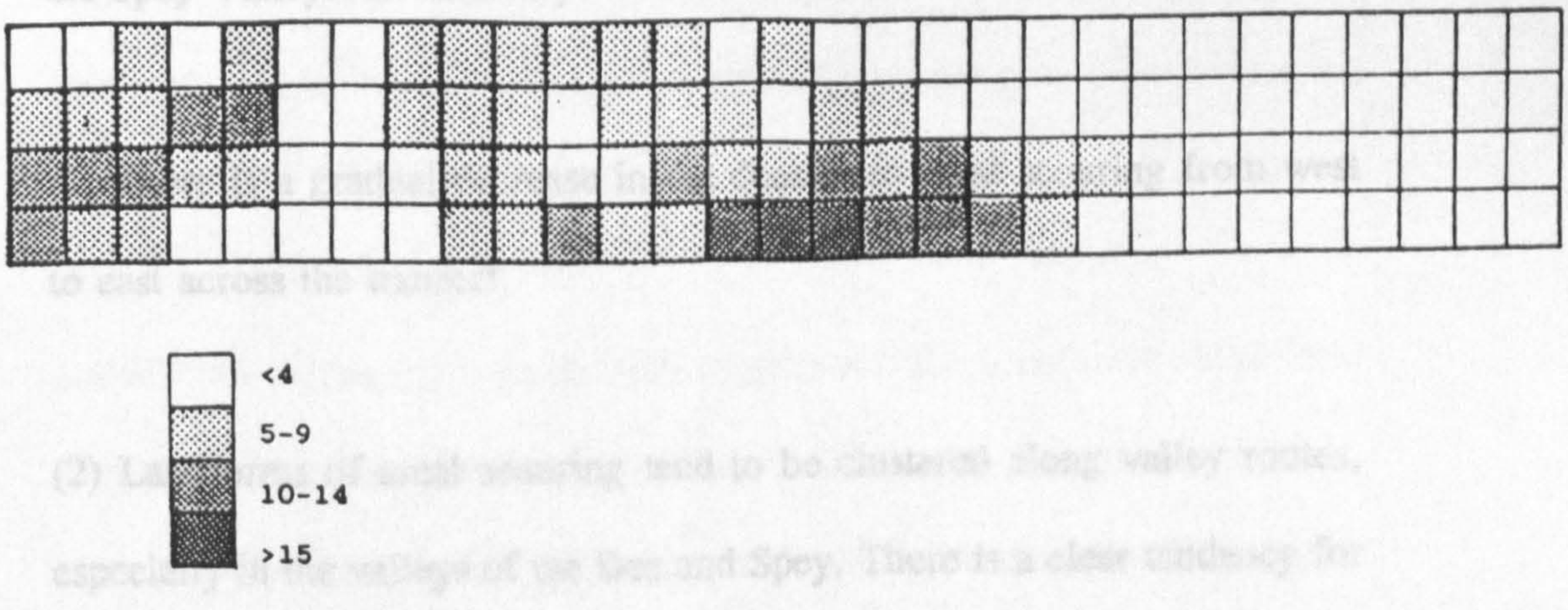

Figure 5.8 The frequency of landforms of areal scouring in the regional transect study area. Shading refers to number of features occurring in 5 x 5 km grid squares.

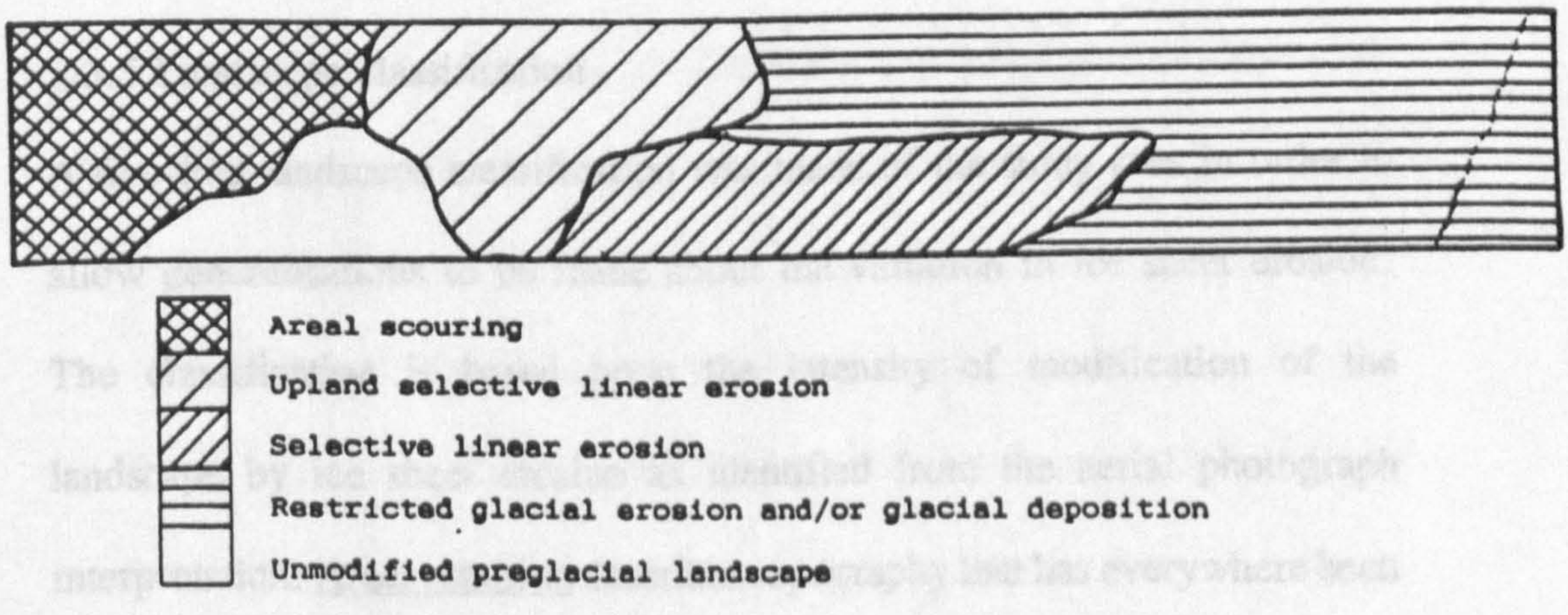

Figure 5.9 Landscape classification of the regional transect study area.

the Spey Valley. In summary:

(1) There is a gradual decrease in the density of areal scouring from west to east across the transect.

(2) Landforms of areal scouring tend to be clustered along valley routes, especially in the valleys of the Dee and Spey. There is a clear tendency for erosional features to be in topographic depressions rather than on interfluves and higher ground.

(3) Little areal scouring occurs in the east of the area, which borders the plain of Buchan, and on the highland to the south west of the Cairngorm Mountains.

5.3.5 Landscape classification

A five-fold landscape classification was made of the study area in order to allow generalisations to be made about the variation in ice sheet erosion. The classification is based upon the intensity of modification of the landscape by ice sheet erosion as identified from the aerial photograph interpretation. Areal scouring describes topography that has everywhere been affected by glacial erosion by an ice sheet (Sugden 1974). Landscapes of areal scouring are characterised by frequent exposures of bare bedrock, rock basins and sparse vegetative cover. Eminences between depressions are often

smooth on all sides, although they may also be shaped into roches moutonnees with plucked lee sides. Generally, landscapes of areal scouring have a limited relief amplitude of less than 100 metres.

Landscapes of upland selective linear erosion are characterised by high level plateau surfaces which are dissected by glacial troughs. The plateau surfaces may retain some, or all, of their preglacial form and regolith, whilst intervening valleys display abundant forms of glacial erosion. A distinction is made between selective linear erosion in uplands, and selective linear erosion in lower lying topography. Both landscape types represent areas where the intensity of modification of the landscape by ice sheets is locally high, yet selective.

Restricted glacial erosion and/or glacial deposition is characterised by gently undulating topography with smooth slopes where forms of glacial erosion are poorly developed. The landscape is generally covered by glacial till, although isolated outcrops of bedrock may appear at the surface. The survival of the main outline of the preglacial landscape and the scarcity of landforms of ice sheet erosion indicate that the intensity of modification by ice sheets is low.

Unmodified preglacial landscapes include areas known to have been covered by ice sheets or ice caps but which show no obvious sign of the event

(Sugden and John 1976). They display no exposed bedrock slabs and the landscape is essentially fluvial in character with smooth slopes, associated with networks of stream valleys.

5.3.6. The distribution of the landscape classes

Figure 5.9 shows the distribution of the five landscape classes. Landscapes dominated by areal scouring cover approximately 525 km^2 of the transect and occur in the west of the area. Upland selective linear erosion is restricted to the centre of the transect in the Cairngorm Mountains and occupies approximately 475 km^2, whilst lower-lying areas of selective linear erosion stretch eastward totalling approximately 500 km^2. The unmodified preglacial landscape, comprising an area of approximately 250 km^2, survives on the highland surfaces especially in the south and east. The eastern section of the study area is an area of restricted glacial erosion and/or glacial deposition, accounting for approximately 1025 km^2.

In summary, the western section of the transect appears to have been most heavily affected by ice sheet erosion and there is a decreasing modification eastwards. This overall trend is interrupted by the existence of unmodified preglacial landscapes over the high ground near the former ice divide (Figure 5.9).

5.4 Ice sheet erosion in the field study areas

5.4.1 Method

A map of the distribution of glacial and preglacial landforms was produced for each of the five study areas (Figures 5.2 to 5.6). These landforms were recognised on the basis of the criteria outlined in Chapter 4, and a key intended for use with the five geomorphological maps is shown in Figure 5.7. Although geomorphological field evidence is the basis for each map, additional evidence and data are taken from geological maps, river profiles and Ordnance Survey maps. North/south and east/west topographic profiles are drawn for each of the field study areas, and the locations of these profiles are indicated on the contour maps.

At each field site an estimate of the minimum and maximum depth and volume of ice sheet erosion is made. Patterns and depths of erosion in any landscape can only be identified when there is full knowledge of the landscape before and after the erosive event. Calculating depths of erosion in a formerly glaciated land is therefore a formidable task since the exercise cannot be attempted unless there is a knowledge of the preglacial landscape. In most cases, the form of the post glacial topography is clear but little detail remains of the preglacial landscape. There are two options open to the researcher;

(a) not attempting the exercise at all

(b) making assumptions as to the form of the preglacial topography and being aware of these limitations.

The second approach has been taken in this study, and estimates of depths of glacial erosion are order of magnitude estimates. The exercise of estimating depths of glacial erosion has never been attempted for such a large area of Scotland before, and the work presented in this thesis marks a starting point in such studies.

As with all first attempts, the methods and assumptions used are open to criticism. In this case since the form of the preglacial topography must be assumed, it is this assumption which must be questioned most fully. Inevitably there is an element of circularity in this argument since the preglacial topography must be assumed in order to estimate the depth of glacial erosion. However, this is also a logical step in a landscape such as Scotland where the preglacial topography is not fully known. Assumptions concerning the depth of preglacial weathering based on analogy and current scientific knowledge are made, and from the surviving remnants of the preglacial landscape it is possible to build a picture of the location and depths of glacial erosion. Without these assumptions concerning the form of the preglacial landscape the exercise of estimating depths of glacial erosion is impossible.

In this study the depth of regolith prior to the onset of the Quaternary glaciations is assumed to lie in the range of 10 to 50 metres (Hall and Sugden 1987). However, since this probably represents a considerable simplification of the likely topographic configurations at the onset of the glacial periods, it is useful to consider alternative topographic scenarios. This presents a problem since the rates of present-day erosional processes are not well established, let alone those which may have operated in the past. However, it is a useful exercise to consider the erosional processes which may have been active prior to glaciation and to begin to prioritise them. In addition, the erosional processes which were active during the period of deep weathering before glaciation must also be considered. If this period were prolonged and/or characterised by fast rates of erosion then the depth of regolith surviving at the onset of glaciation would be less than the 10 to 50 metres suggested by Hall and Sugden (1987).

Erosional processes which may have been active prior to the onset of glaciation include;

- fluvial
- periglacial
- aeolian
- coastal

Rates of **fluvial erosion** vary greatly over time and space and are dependent on a variety of factors such as climate, tectonic setting and relief. Thus rates of fluvial denudation are notoriously difficult to calculate (Summerfield 1991). Since Scotland has been tectonically stable (i.e. no major uplift or orogenic events immediately preceding the Quaternary) over the relatively short timescale under consideration, rates of fluvial erosion may be considered similar to those of 0.03 to 0.07 mma^{-1} quoted by Summerfield (1991) for temperate regions. If this were the case then we expect some removal of the products of Tertiary deep weathering, both during the period of deep weathering and immediately prior to the onset of the Quaternary glaciations. The depth of weathering present prior to glaciation would therefore be reduced, although it is difficult to say by how much since neither the rates of fluvial erosion or duration are established.

Rates of **periglacial erosion** are likely to be relatively low since these areas are typically a low energy environment. Although catastrophic events such as flooding and annual snowmelt may bring about localised erosion, periglacial environments are characterised by slow processes such as freeze/thaw, frost heave and solifluction. Low rates of transport of material through processes such as soil creep are also common. In such climatic periods there is normally a surplus supply of material to rivers since precipitation is low, and these are periods of river aggradation and not of river down-cutting. Although it is difficult to estimate the volume of

periglacial erosion throughout glacial periods since the rates and duration are unknown, it is likely to be low. Indeed, periglacial weathering is often cited as a factor preparing the ground surface for subsequent glacial erosion (Bakker 1965, Feininger 1971). The conclusion is that since rates of periglacial erosion are low and that a periglacial climate did not prevail over Scotland for any great length of time, that the volume of erosion attributable to periglacial processes is probably small.

Erosion by **aeolian** processes could be a significant factor adding to preglacial erosion of the weathering mantle. However, there are no known loess-type deposits reported anywhere in Scotland and the loess deposits found in southern England lie exclusively outside the limits of the Quaternary glaciations. This loess is probably of glacial origin and represents a period(s) of deposition under an arid, periglacial climate of material derived form the ice sheet further north. The conclusion is that rates of aeolian denudation prior to glaciation were probably low.

Coastal erosion, by definition, only affects a thin strip of the landscape around the coastline. Without the ability to erode over wide areas of the country, coastal erosion would not contribute greatly to the preglacial erosion of any weathering mantle. The conclusion is that the total volume of coastal erosion prior to glaciation was probably low.

The estimates of depths of glacial erosion are based on the assumption that the study area was covered in a weathering mantle 10-50 metres deep in preglacial times (Hall and Sugden 1987). If landscapes affected by ice sheet erosion are dominant, fresh bedrock is widespread and saprolite does not exist, then it is assumed that all of the former weathering regolith has been removed and the depth of erosion is at least 50 metres. If saprolite remains at the surface then the depth of erosion is assumed to be less than 50 metres, and an approximate value estimated from the depth and distribution of the saprolite remaining. If the preglacial surface is intact and includes tors, topographic sheeting and saprolite, then it is assumed that minimal ice sheet erosion of less than 10 metres has occurred. These estimates are used to calculate a minimum and maximum figure for the depth of ice sheet erosion within each field study area. Since each sample area has been selected to represent a particular landscape type, it is then possible to extrapolate from the sample areas to the transect as a whole in order to calculate regional erosion depths.

5.4.2 Cairngorm field study area

5.4.2.1 Site location and description

The Cairngorm Mountains constitute the largest single area of land over 900 metres above sea level in the British Isles. The massif itself consists of a large granite pluton, referred to by Barrow et al. (1912) as the 'older granite' of this area of Scotland. It is comprised of at least two main units;

(1) the main granite, which is a more or less equigranular microcline-oligoclase-biotite granite and; (2) porphyritic granite generally distinguished by conspicuous feldspar phenocrysts (Harry 1965). The contacts between these two units are steep, as are the external boundaries of the entire intruded granite mass. The field site is located in the south of the Cairngorms, centred on the large valleys of Glen Geusachan and Glen Dee (Figure 5.2).

5.4.2.2 The preglacial landscape

Large areas of the preglacial landscape are represented by the Cairngorm Mountain summits and the gently rolling slopes which surround them. These slopes are found only above the 900 metre contour line (Figure 5.2), and are characterised by hill summits which are rounded and convex in their upper portions, with slope gradients of only 40 metres in 2 kilometres common (Figure 5.10). These gently undulating slopes comprise approximately 25 per cent of the total area. Valley patterns on the gentle slopes are dendritic and characteristically fluvial; stream valleys such as Allt Garbh retain their preglacial fluvial form and contrast with the deranged drainage pattern of the Geusachan trough (Figure 5.2).

Exposures of saprolite are found in association with the gentle slopes on the eastern flank of Beinn Bhrotain, where deeply weathered rock comprises the eastern and south eastern flanks of the hill (Figure 5.2). The exposure is

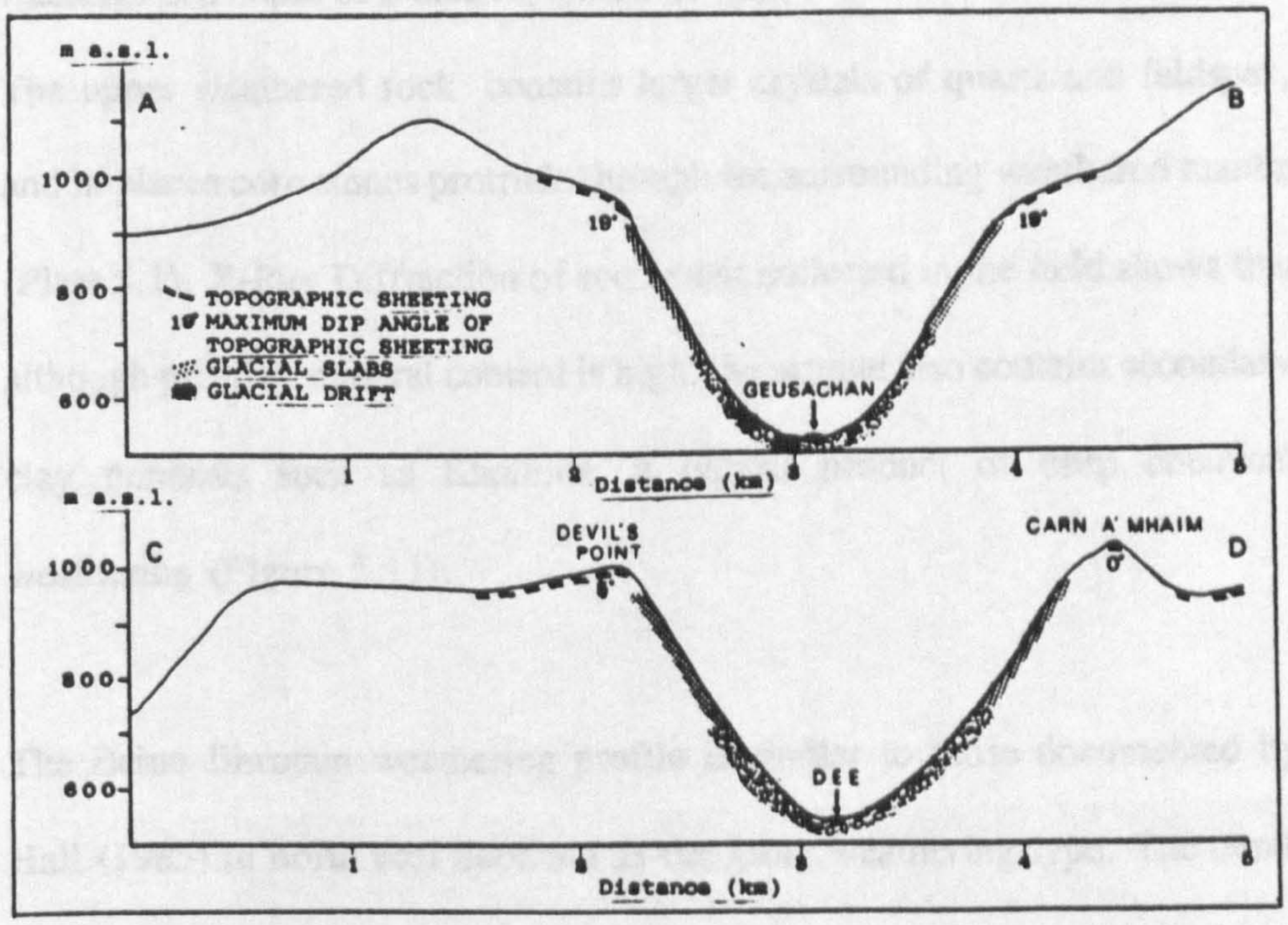

Figure 5.10 Topographic profiles of Cairngorm field study area. For location of profiles see Figure 5.2.

continuous for 300 metres, forming a band up to 20 metres wide across the south east face of Beinn Bhrotain. The depth of weathering at this site is between 1 and 2 metres. The saprolite is deep red and consists of coarse gravel. Particle size increases downwards through the weathering profile. Sections reveal a transition from highly weathered material at the surface, through more consolidated saprolite, to rock which is only weathered along fractures at a depth of 2 metres, where unweathered bedrock is encountered. The upper weathered rock contains larger crystals of quartz and feldspar, and in places core stones protrude through the surrounding weathered mantle (Plate 5.1). X-Ray Diffraction of specimens collected in the field shows that although primary mineral content is high, the sample also contains secondary clay minerals such as Kaolinite, a typical product of deep chemical weathering (Figure 5.11).

The Beinn Bhrotain weathering profile is similar to those documented by Hall (1985) in north east Scotland as the gruss weathering type. The depth and vertical variation in the degree of alteration, and the chemical and mineralogical composition are similar to gruss of early Pleistocene age (A. Hall, pers. comm.). The saprolite is similar to the weathering cover known to exist in the Cairngorms in areas such as Coire Raibert (002 034), the summit of Cairn Gorm (Margaret's Coffin) and Loch Avon (997 022) (Linton 1955; Sugden 1968). The survival of saprolites is also known in other areas of Scotland (Fitzpatrick 1963; Hall and Mellor 1989).

Plate 5.1 Saprolite exposure at Beinn Bhrotain, Cairngorm Mountains. Core stones are emerging from the surrounding weathered mantle.

← Plate 5.2 Large hydrothermal vein at Allt Garbh, Cairngorm Mountains.

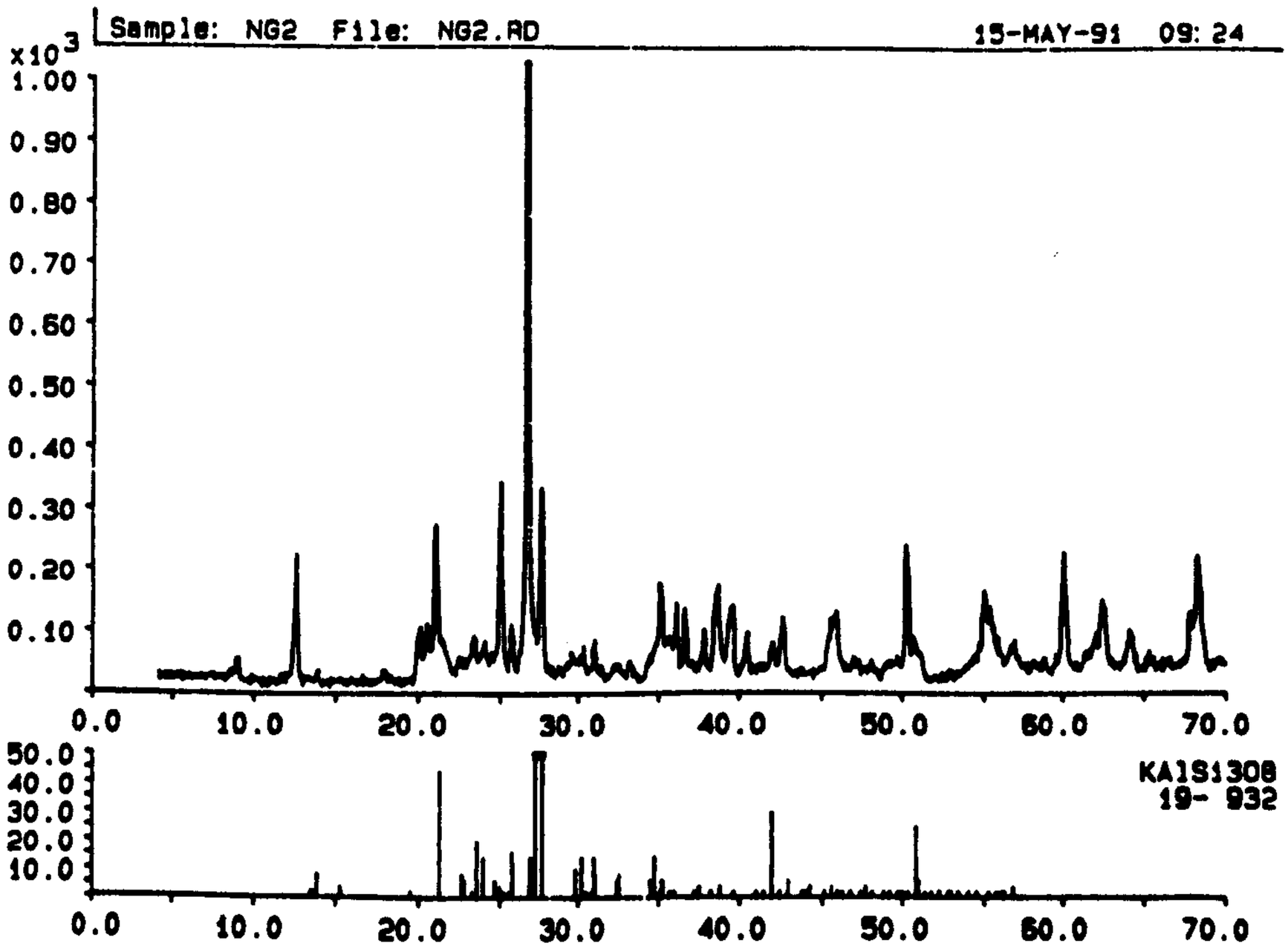

NO.	MATCH SCORE	REF PATTERN	PHASE FORMULA/NAME
1	7.9	19- 932	MICROCLINE, INTER
2	7.0	19- 479	MICROCLINE, INTER
3	6.9	6- 221	KAOLINITE 1MD
4	6.1	22- 687	MICROCLINE, MAX
5	4.2	33-1161	QUARTZ, LOW
6	3.8	12- 703	MICROCLINE
7	3.7	29-1488	KAOLINITE 1MD

Figure 5.11 X-Ray diffraction results obtained from analysis of weathered rock on Beinn Bhrotain. See text for full explanation.

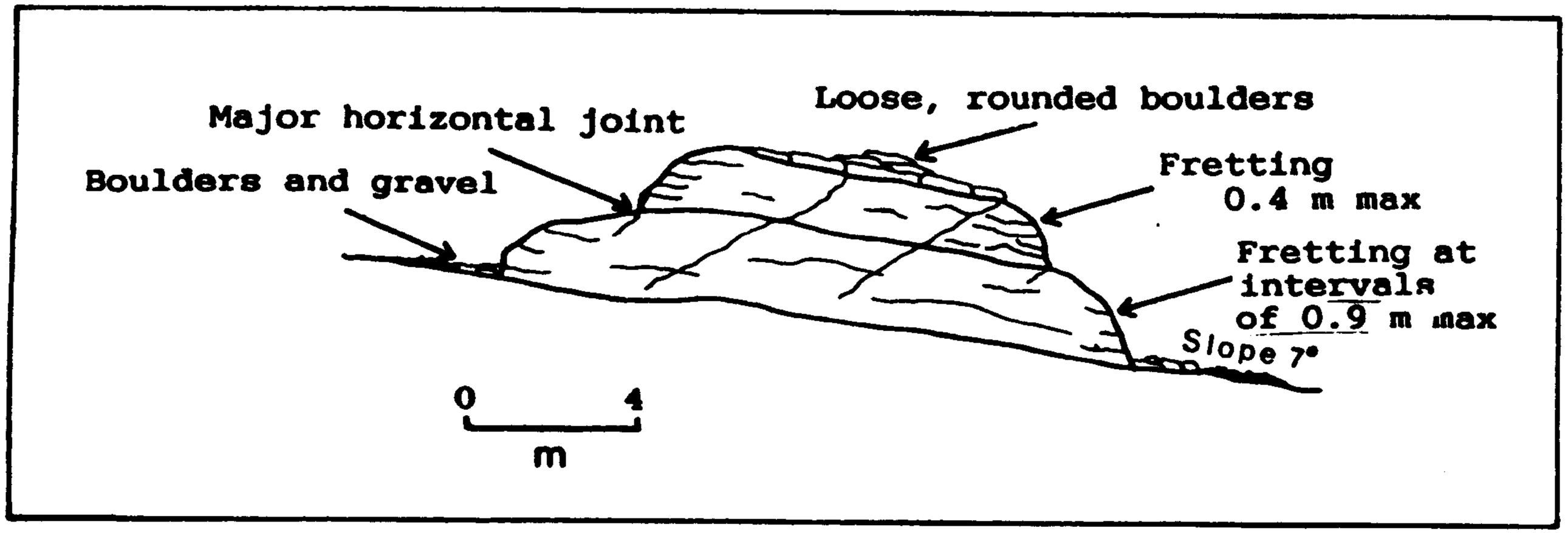

Figure 5.12 Field sketch of tor on unnamed summit at 1020 metres, Cairngorm Mountains. Fretting interval increases with depth, and major horizontal joints parallel the plateau surface.

A second area of weathered bedrock occurs in the stream banks of Allt Garbh (Figure 5.2). Although visually similar to the Beinn Bhrotain exposure, the depth of weathering at Allt Garbh is greater, attaining depths of 5 metres, and is covered by a 5 to 10 centimetre thick veneer of glacial till. The exposure is the same deep red colour and has decomposed to a coarse granite gravel (Plate 5.2). However, the weathering at this site may be due to deep hydrothermal alteration. There are three lines of evidence to support this; (1) weathering is restricted to within the stream walls and not widespread over the adjacent area; (2) there is no base to the weathering and; (3) the occurrence of chlorite in hand specimens examined in the field, a characteristic product of hydrothermal alteration. Since hydrothermal alteration can penetrate to great depths, the original depth of weathering is unknown and this exposure cannot be reliably used to estimate the depth of ice sheet erosion.

Tors occur on the unnamed summit at 1020 metres above the mouth of Glen Geusachan (Figure 5.2). There are 4 separate tor stumps, protruding to a maximum height of 4 metres. The largest tor is 20 by 20 metres, and displays numerous parallel joints and frets spaced between 0.4 and 1.5 metres apart (Figure 5.12). The tors are crossed by two sets of vertical joints striking at right angles to each other at 30° and 120°. The major horizontal joints parallel the slope of the surrounding ground at 7° (Figure

5.12). Tors also occur on the summit of Carn a' Mhaim, with a maximum height of approximately 1.5 metres and a width of approximately 1.6 metres. These tors are surrounded by a thick mantle of debris and display sub-horizontal joints parallel to surface slopes (Plate 5.3).

Outcrops of stacked boulders are common in the area to the north west of Beinn Bhrotain. Individual outcrops may rise to several metres above the surrounding ground and are bounded along three main axes, each represented by a joint system in the bedrock (Plate 5.4). The first are a set of sub-horizontal joints which define the upper surfaces and are consistently parallel or sub-parallel to the surface slope. Laminar fretting is often developed parallel to these surfaces. The second and third joint sets cross the surface of the exposures at right angles to each other and delimit the size of the outcrops, which is usually of the order of 20 metres across. The ubiquity of the sub-horizontal joints gives the outcrops the appearance of having been 'stacked', with the uppermost layers containing loose, rounded individual boulders. The boulder stacks are least consolidated where joints are closely spaced and most consolidated where joints are furthest apart. The depth of the boulder layers increases from 10 to 20 centimetres at the surface to approximately 2 metres at the base. These outcrops may be the remnants of heavily disintegrated tors.

Areas of granite sheeting cover several zones of the Cairngorm plateau and

Plate 5.3 Two large tors on the summit of Carn a' Mhaim, Cairngorm Mountains.

Plate 5.4 Boulder outcrop on the plateau north west of Beinn Bhrotain, Cairngorm Mountains. Compare size and shape of boulders to those in Plate 5.1.

its adjacent slopes (Figure 5.2). Sheeting is restricted to small outcrops rising up to 1 metre above the surrounding plateau surface in patches 1 to 2 metres in diameter. This sheeting is found extensively to the south and west of the Devil's Point. Measurements of the sheeting on the plateau above Glen Geusachan show that the surface dip of the joints is nearly horizontal (1° to 5°), and is parallel to the surrounding plateau surface (Figure 5.13). The dip direction is between 350° and 070°, slightly dipping towards north. A set of vertical joints dissect the sheeting at dip angles of between 79° and 90°, striking at around 140°. A second set of vertical joints dissect the first at a similar angle, but strike at around 050°. The granite is characterised by numerous thin sheets and closely spaced laminar fretting (Plate 5.5).

Below the 900 metre contour line the dip of the sheeting increases to a maximum of 19°. This gently dipping sheeting is truncated by a second family of steeply dipping sheeting associated with the Glen Geusachan trough where angles of up to 49° are recorded (Figure 5.14 a and b). This contrast can be seen by comparing strike and dip data displayed on a stereonet for the sheeting on the plateau above Glen Geusachan with that for the steeply dipping slabs on the trough side below (Figures 5.13 a and 5.14 a). A similar relationship exists north of Carn a' Mhaim, where sheets dipping at angles of between 2° and 16° towards the west are dissected by the same two sets of vertical joints (Figure 5.13 b). In all of the plateau

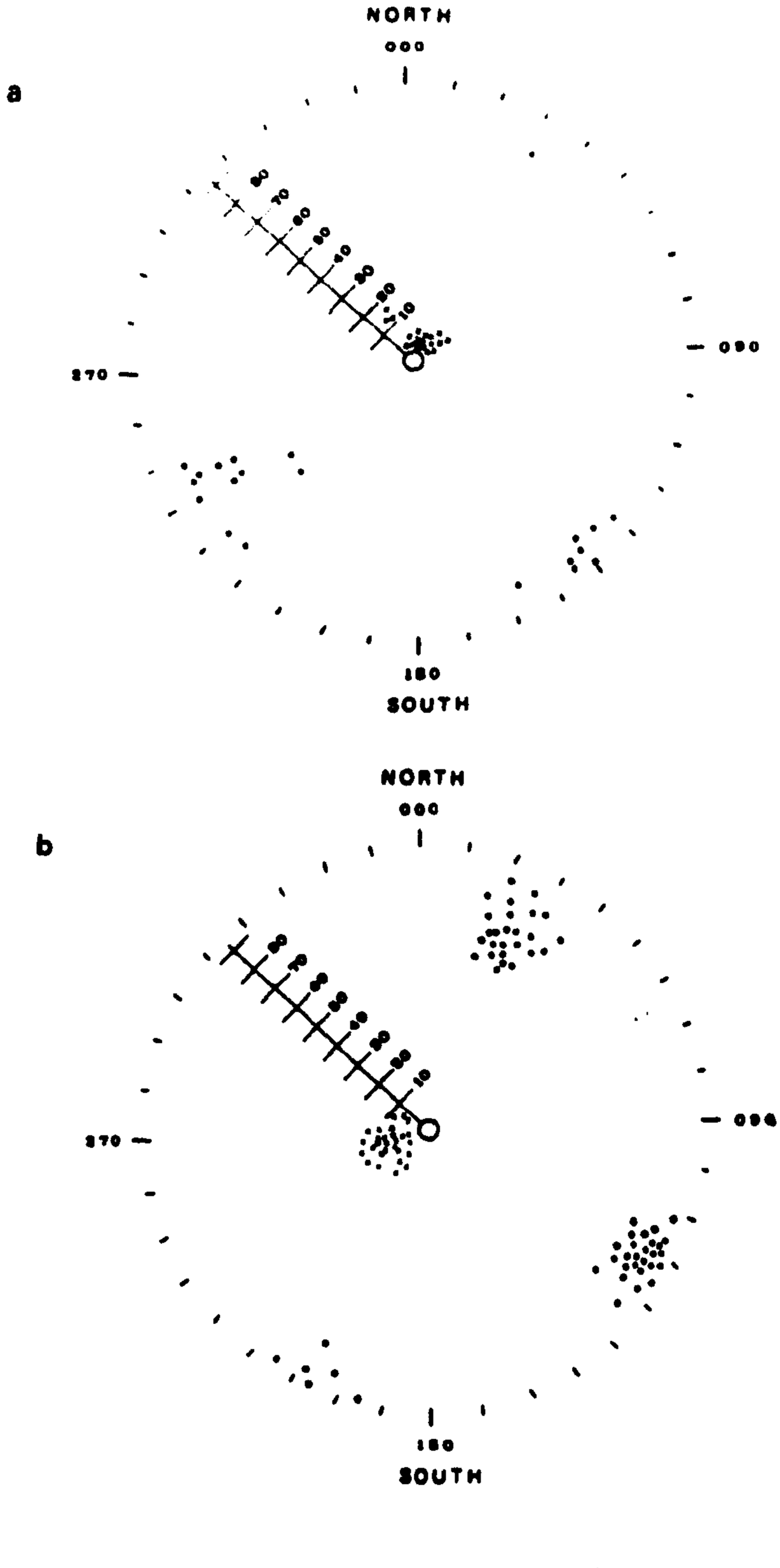

Figure 5.13 Stereonet plot of topographic sheeting on the Cairngorm plateau:
(a) Devil's Point, above Glen Geuscahan
(b) Carn a' Mhaim, above Glen Dee
Dots refer to strike and dip of major joint sets and crosses refer to strike and dip of topographic sheeting.

Plate 5.5 Topographic sheeting above Glen Geusachan, Cairngorm Mountains. Individual sheets parallel the surface slope and are separated by laminar fretting.

Plate 5.6 Glacial slabs, Glen Geusachan, Cairngorm Mountains. The large ice-smoothed slabs contrast with the preglacial topographic sheeting (Plate 5.5).

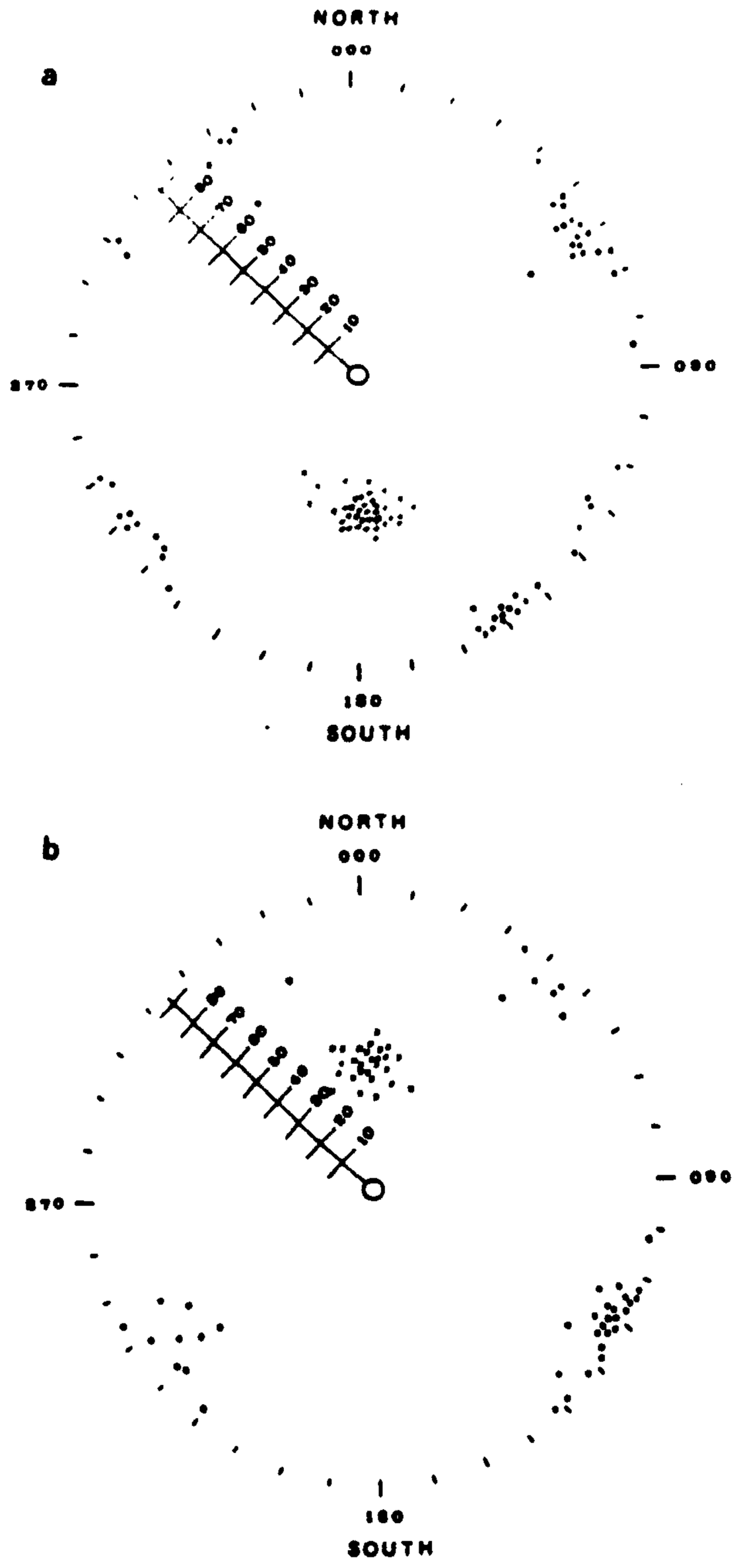

Figure 5.14 Stereonet plot of sheeting on glacial slabs:
(a) North wall, Glen Geusachan
(b) South wall, Glen Geusachan
Dots refer to strike and dip of major joint sets and crosses refer to strike and dip of sheets.

locations the dip of the granite sheets is approximately parallel to the upper topographic surfaces. The parallelism of the sheeting with the underlying topography, the closely spaced sub-horizontal jointing, and the predominance of the laminar fretting between joints suggests that this is the preglacial topographic sheeting often developed in granites by slow pressure release.

In summary, there is widespread evidence that much of the preglacial landscape survives in this area. The gentle slopes of the Cairngorm plateau, with their convex summits and fluvial drainage networks, retain their preglacial form. The period of deep weathering responsible for the saprolite and tors is thought to be an early Pleistocene event (Hall 1985), as is the formation of topographic sheeting (Jahns 1943). The suite of preglacial forms identified in this area of the Cairngorm Mountains agrees with wider views of landscape evolution in Scotland (Hall 1990).

5.4.2.3 The glacial landscape

The most striking features of ice sheet erosion are the two glacial troughs of Glen Geusachan and Glen Dee. The bedrock walls of the troughs have been smoothed into giant slabs, which are particularly well developed in Glen Geusachan (Plate 5.6). Here the slabs constitute the walls of the trough from c. 700 metres to c. 950 metres in altitude. The slabs are also well developed in the Dee Valley although they are only visible in patches due to the presence of a sporadic drift cover. Joint studies on the glacial slabs

of Glen Geusachan (Figure 5.14) and Glen Dee (Figure 5.15) show the two perpendicular vertical joint sets known to characterise the Cairngorm granite. These joints strike at roughly 030° and 120°, and commonly dip at angles of between 70° and 90°. Individual slabs dip at angles of between 23° and 49° (Figures 5.14 and 5.15).

An interesting relationship is that between the slope angle and slab dip angle in the trough walls. The dip of the sheeting in the glacial troughs is consistently parallel to the slope angle of the trough wall, increasing from 23° at the base of Glen Geusachan to 49° at the top. At the upper limit of the glacial slabs, there is an area of confused jointing where glacial slabs are mixed with topographic sheeting (Plate 5.7). The joint studies allow a distinction to be made between the bedrock in the glacial troughs and that of the gentle slopes above. Although both are characterised by near vertical joints and sheeting parallel to surface slopes, the steepness of the sheeting in the troughs is distinctive. In addition, the sheeting on the trough walls does not display the laminar fretting between individual sheets found on the plateau surfaces.

There are abundant fresh bedrock forms in the area. Ice scoured bedrock is found on the slopes high above the western side of the Dee Valley and on the floor of the Dee Valley at its confluence with the Geusachan (Plate 5.8). Individual bedrock exposures on the floor of Meirleach col, 8 to 10 metres

Plate 5.7 The transition between glacial slabs and topographic sheeting in Glen Geusachan, Cairngorm Mountains. A large outcrop of topographic sheeting rests on the ice-smoothed valley wall.

Plate 5.8 Ice scoured bedrock in Glen Dee, Cairngorm Mountains.

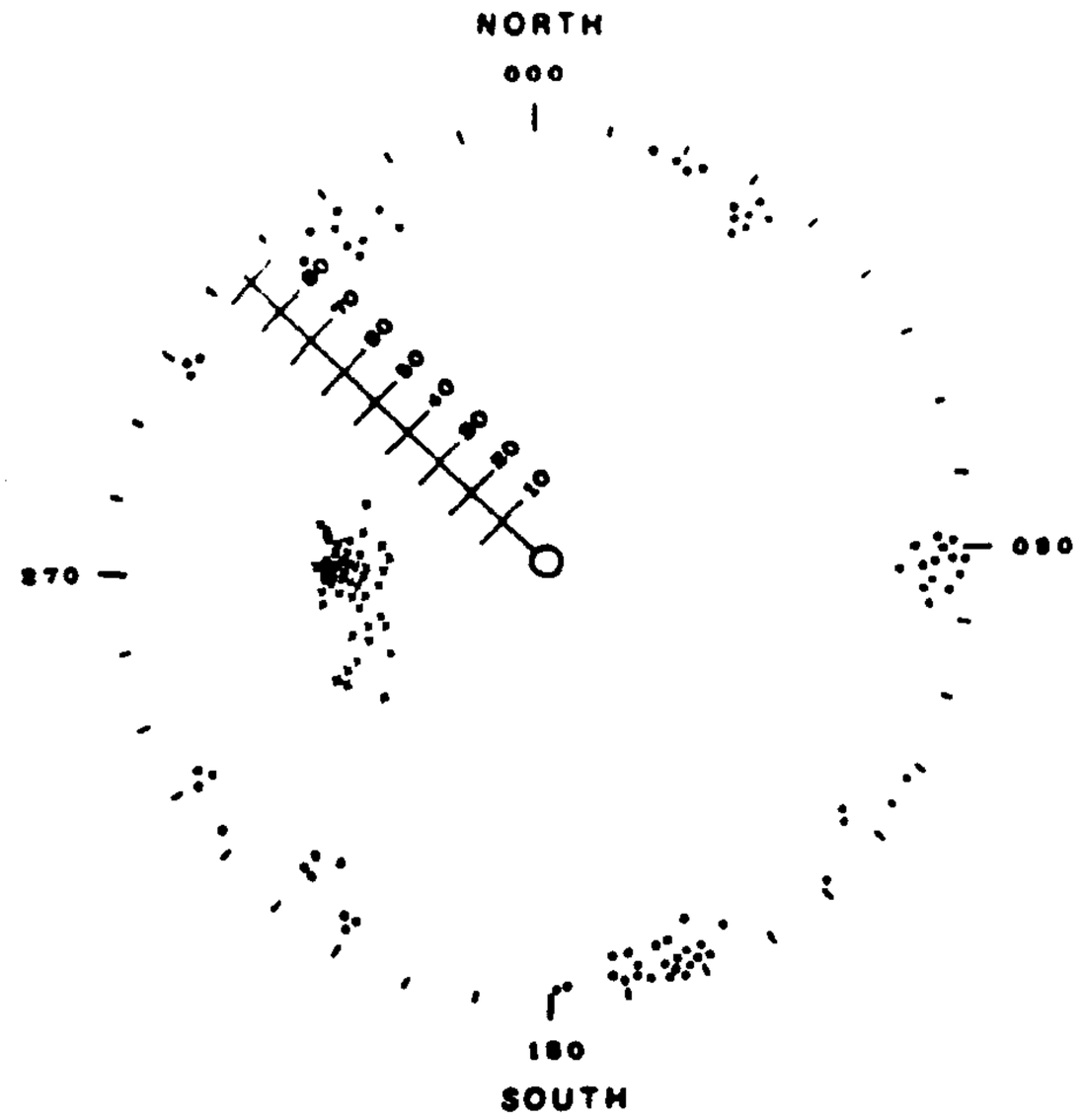

Figure 5.15 Stereonet plot of sheeting on glacial slabs: East wall, Glen Dee.
Dots refer to strike and dip of major joint sets and crosses refer to strike and dip of sheets.

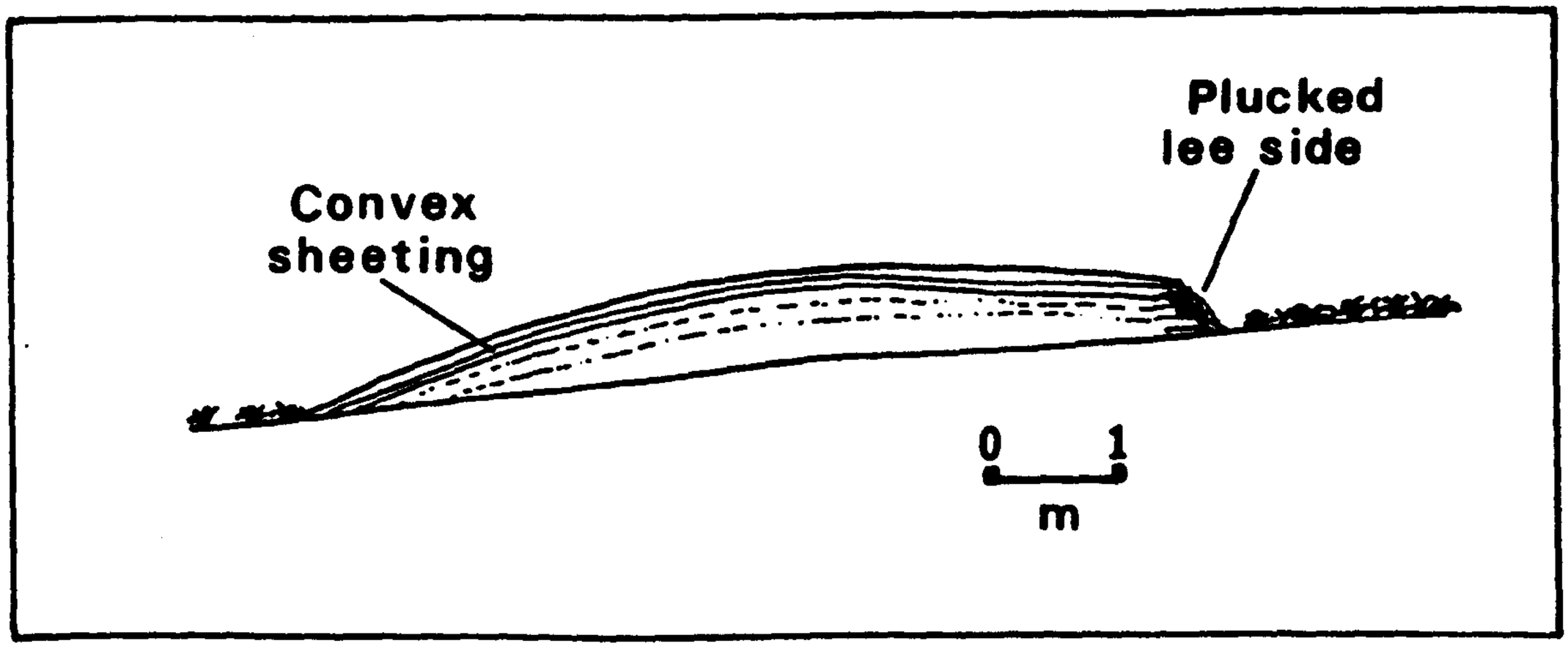

Figure 5.16 Incipient roche moutonnée formed in topographic sheeting, Meirleach Col, Cairngorm Mountains.

in diameter, are separated by areas of shallow peat formation. The slabs are convex and topographic sheeting is observed on upper surfaces and truncated east faces (Figure 5.16). These outcrops are preglacial topographic sheeting with incipient roches moutonnees (Figure 5.16). Similar exposures are found widely over the northern and western flank of Creagan nan Gabhar. The summit of the hill itself is moulded in bedrock and presents a classic stoss and lee profile, with a smooth western side and cliffed eastern face.

5.4.2.4 Reconstruction of the preglacial landscape

It is possible to reconstruct the preglacial relief of the area (Figure 5.17). By definition, areas where the preglacial landscape survives are close to their preglacial level and depths of erosion are minimal. Thus the gentle plateau slopes with tors and saprolite are within 10 to 50 metres of their preglacial surface level.

Reconstructing the preglacial form of the glacial troughs is more difficult, although the parallelism of the granite sheets with the preglacial topography enables former valley profiles to be reconstructed. In the absence of knowledge of the preglacial valley morphology, the reconstructions are based on the assumption that the preglacial valleys were v-shaped in cross-profile. This is a legitimate assumption for fluvial valleys (Morisawa 1985). The assumption of a V-shaped cross-profile yields the minimum depth of the preglacial valley because no allowance is made for any basal

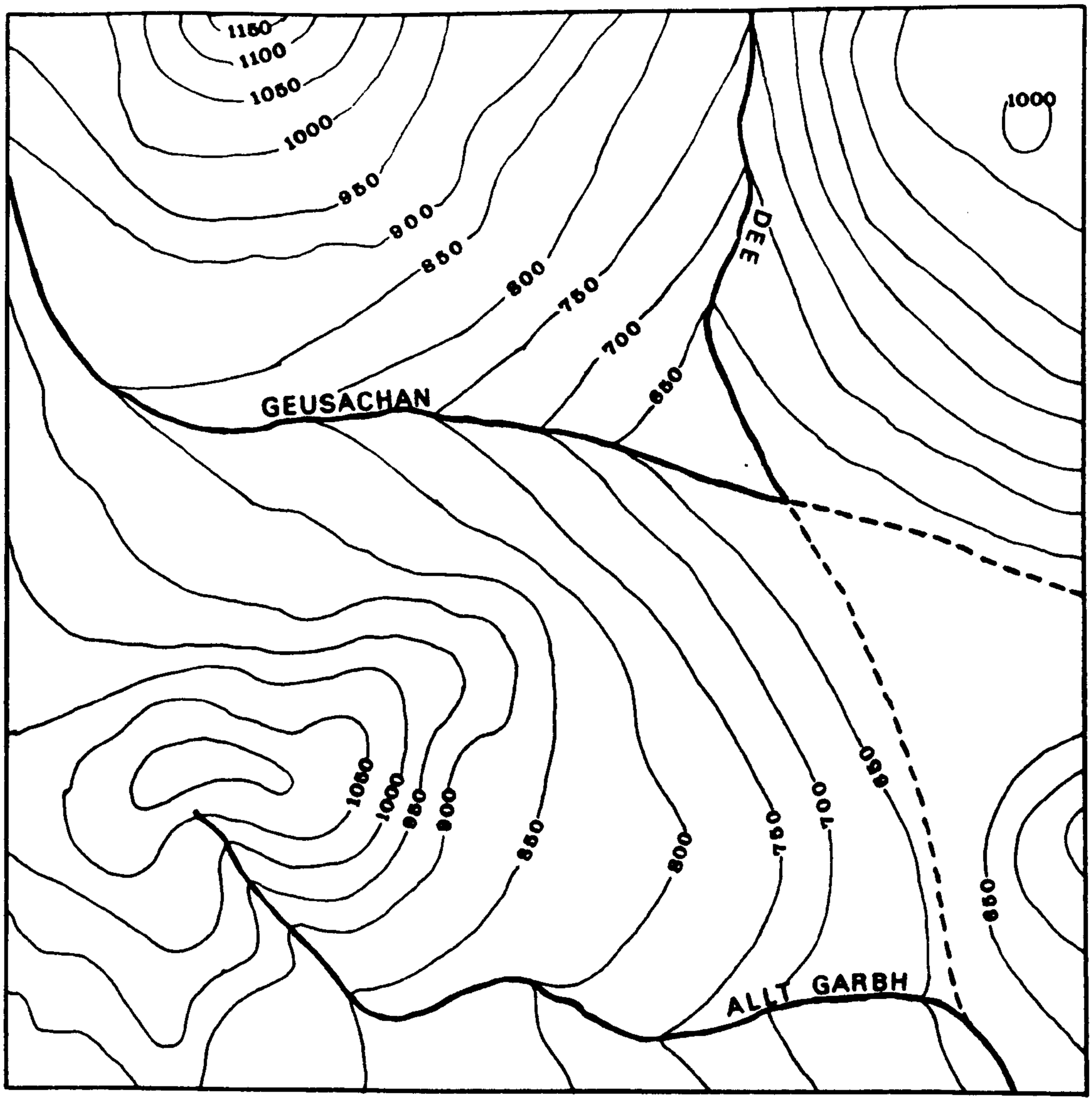

Figure 5.17 Reconstruction of the preglacial landscape in the Cairngorm field study area. Broken lines refer to uncertain path of preglacial rivers.

convexity of the former valley sides. Above the present day valleys, the sheeting on the plateau shoulders dips out of the cliffs at a maximum angle of 19°. Extrapolation of this angle across the present day valleys therefore gives a minimum estimate of the depth of the preglacial valley. Two profiles across Glen Geusachan are illustrated in Figure 5.18. The maximum angle of the sheeting is marked, and the reconstructed preglacial valley profiles are shown by the dashed lines. The three profiles suggest that the preglacial valley floors were some 150-250 metres above the present valley floor. Topographic sheeting on Mearleach col suggests this was in place preglacially and thus the Geusachan Burn may have joined the Dee to flow over this col in preglacial times.

Further evidence of the nature of the preglacial land surface is provided by the river profile of Allt Clais an t-Sabhail shown in Figure 5.19. In its upper 150 metres, the stream flows on the gentle slopes of the plateau and possesses an exponential gradient and concave longitudinal profile. Extrapolation of the upper section of the stream profile into Glen Geusachan using a characteristic concave river profile (Morisawa 1985) suggests a glacial overdeepening of between 150 and 175 metres. This method gives a minimum estimate of the depth of the preglacial valley because the preglacial river may have been incised into its valley.

Together, these remnants of the preglacial landscape allow the preglacial

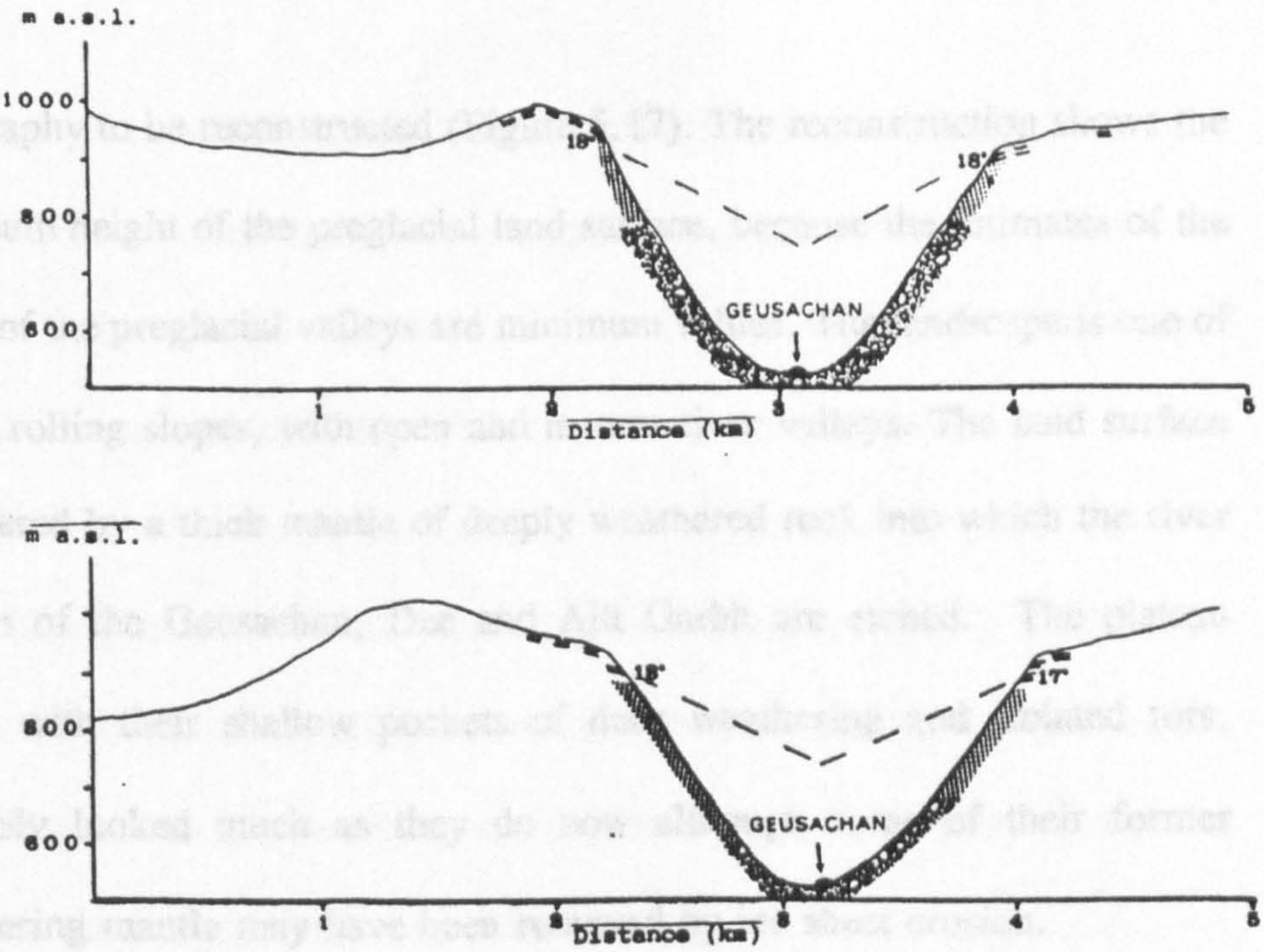

Figure 5.18 Topographic profiles across Glen Geusachan. Maximum dip angle of topographic sheeting is indicated and the reconstructed preglacial valleys are shown by broken lines. Key as Figure 5.10.

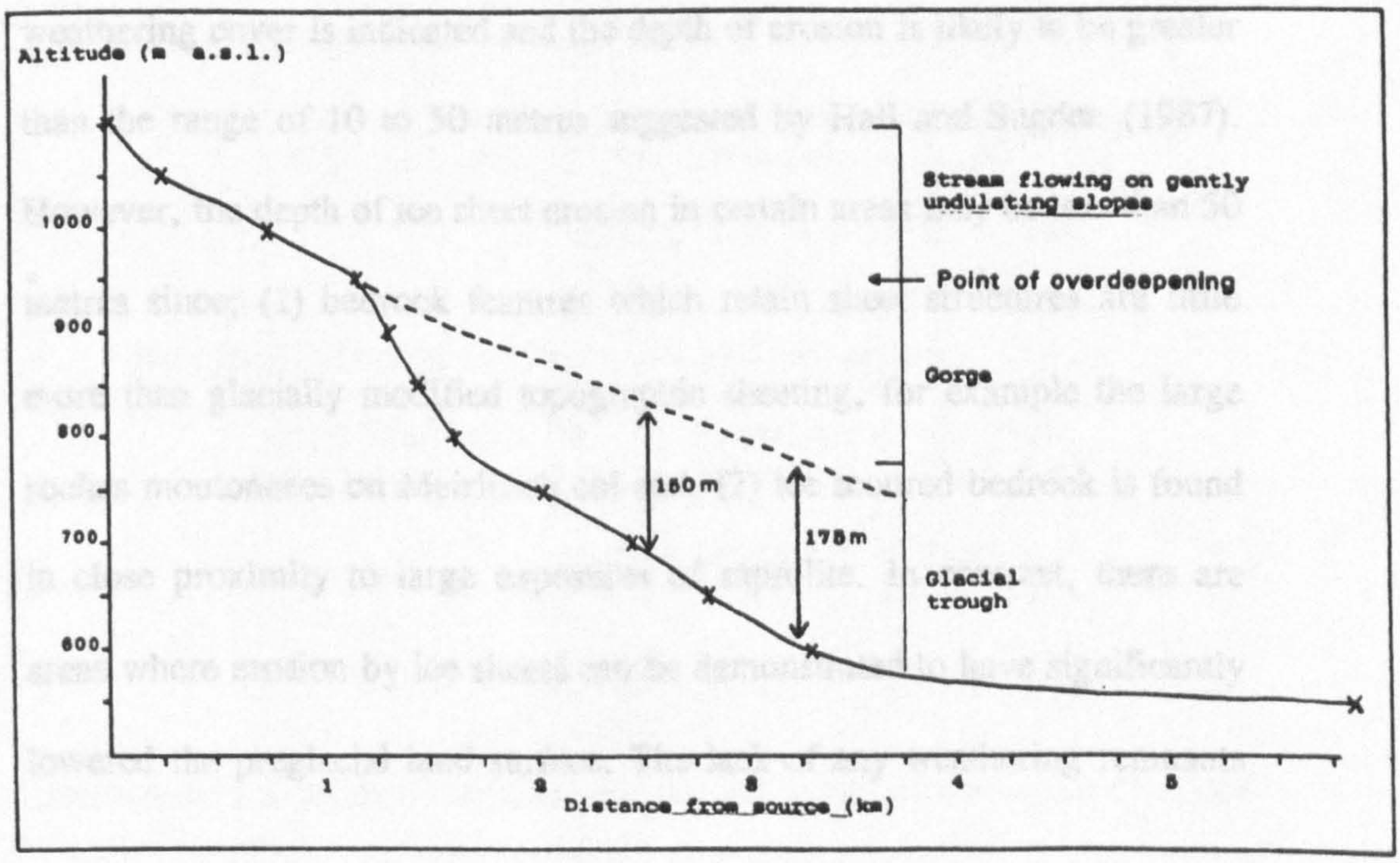

Figure 5.19 Long profile of Allt Clais an t-Sabhail, Cairngorm Mountains. Preglacial profile is indicated by broken line.

topography to be reconstructed (Figure 5.17). The reconstruction shows the minimum height of the preglacial land surface, because the estimates of the depth of the preglacial valleys are minimum values. The landscape is one of gentle rolling slopes, with open and mature river valleys. The land surface is covered by a thick mantle of deeply weathered rock into which the river valleys of the Geusachan, Dee and Allt Garbh are etched. The plateau areas, with their shallow pockets of deep weathering and isolated tors, probably looked much as they do now although some of their former weathering mantle may have been removed by ice sheet erosion.

5.4.3.5 The depth of ice sheet erosion

The distribution of ice sheet erosion is given by comparison between the present day contour map and the reconstruction of the preglacial relief. Wherever fresh glaciated bedrock is found, the removal of any former weathering cover is indicated and the depth of erosion is likely to be greater than the range of 10 to 50 metres suggested by Hall and Sugden (1987). However, the depth of ice sheet erosion in certain areas may be less than 50 metres since; (1) bedrock features which retain sheet structures are little more than glacially modified topographic sheeting, for example the large roches moutonnees on Meirleach col and; (2) ice scoured bedrock is found in close proximity to large exposures of saprolite. In contrast, there are areas where erosion by ice sheets can be demonstrated to have significantly lowered the preglacial land surface. The lack of any weathering remnants

and the absence of sub-horizontal topographic sheeting in the glacial troughs of the Geusachan and Dee Valleys suggest much greater depths of ice sheet erosion. Estimates of the depth of ice sheet erosion are fraught with danger but can be made on the basis of the following assumptions:

(1) Where plateau remnants with saprolite survive, a depth of ice sheet erosion of 10 metres minimum and 40 metres maximum is assumed. A depth of 50 metres is locally possible where no saprolite survives. Plateau surfaces cover an area of approximately 7.5 km^2.

(2) The troughs indicate a depth of erosion of between 150 metres minimum and 200 metres maximum. Glacial troughs occupy approximately 17.5 km^2 of the study area. The total volume of ice sheet erosion is therefore:

Minimum depth of ice sheet erosion:

$$\begin{aligned} 7.5\ km^2 \ @0.01\ km\ erosion &= 0.075\ km^3 \\ 17.5\ km^2 \ @0.15\ km\ erosion &= 2.625\ km^3 \\ \text{TOTAL VOLUME} &= 2.7\ km^3 \end{aligned}$$

Maximum depth of ice sheet erosion:

$$\begin{aligned} 7.5\ km^2 \ @0.04\ km\ erosion &= 0.3\ km^3 \\ 17.5\ km^2 \ @0.2\ km\ erosion &= 3.5\ km^3 \\ \text{TOTAL VOLUME} &= 3.8\ km^3 \end{aligned}$$

Expressed as a depth of erosion per unit area, the minimum depth of ice

sheet erosion is 108 metres and the maximum is 152 metres.

5.4.3 Glen Feshie study area

5.4.3.1 Site location and description

The second field site is located in the upper Glen Feshie, to the south west of the Cairngorm Mountains (Figure 1.1). The River Feshie provides the lowest altitude of 480 metres in the area, whilst the highest point is at 893 metres above sea level at the summit of Cnapan Mor (Figure 5.3). The solid geology of this area is dominated by metamorphic rocks, in this case undifferentiated Moine schists (Geological Survey of Britain (Scotland) Sheet 64).

5.4.3.2 The preglacial landscape

The majority of the terrain comprises a rolling landscape with rounded hill summits and gentle slopes (Figure 5.3). The north to south profile through the area shows the relatively flat nature of the terrain and the gentle curvatures of slope as the land rises slowly away from the floor of the Geldie valley (Figure 5.20). The east to west profile also illustrates these shallow gradients, with a relief amplitude of only 100 metres in 5 kilometres. The valley occupied by the Geldie is flat-floored and open. Dendritic river patterns are found in conjunction with these gentle slopes; a good example being the streams which drain the south facing slopes of

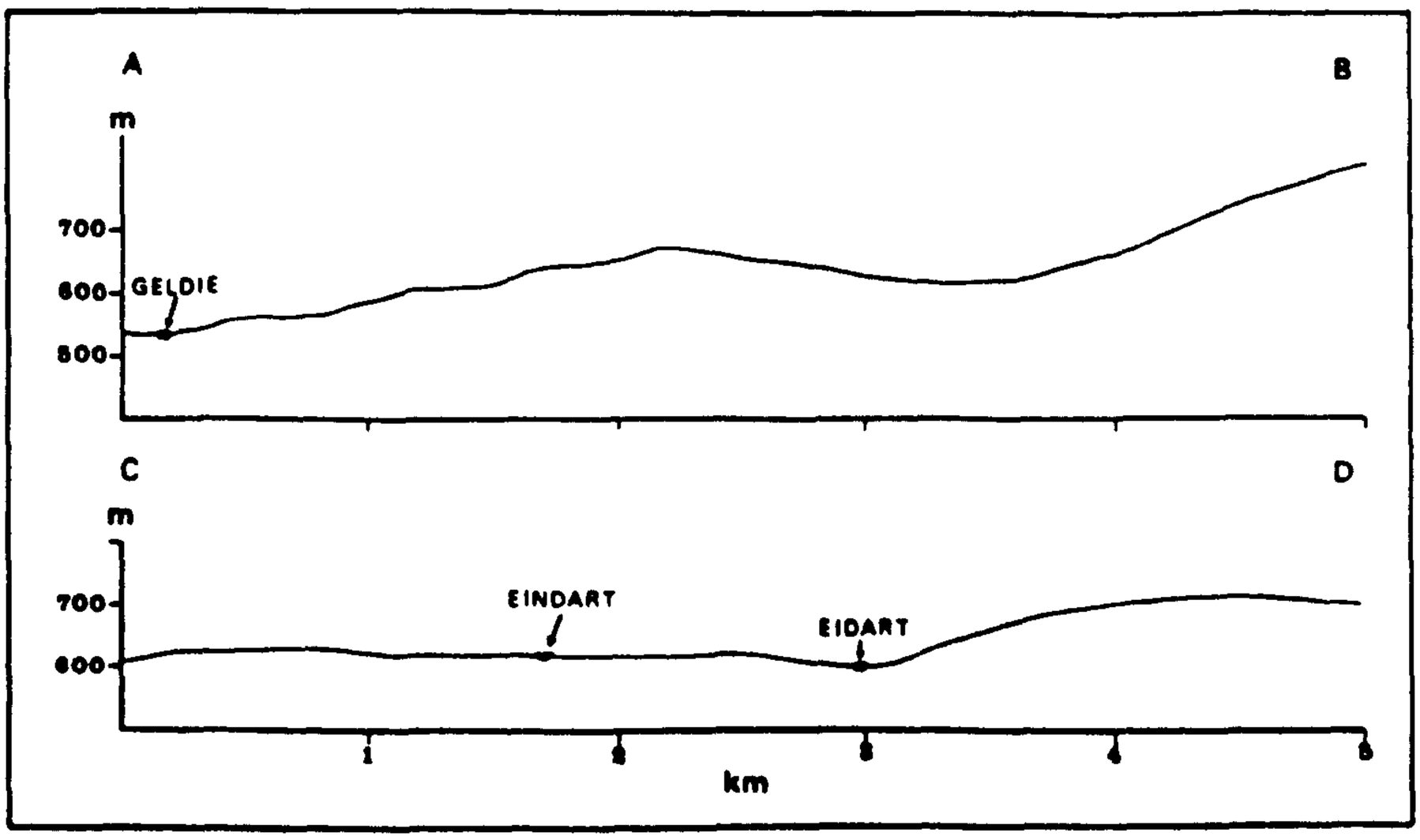

Figure 5.20 Topographic profiles of Glen Feshie field study area. For location of profiles see Figure 5.3.

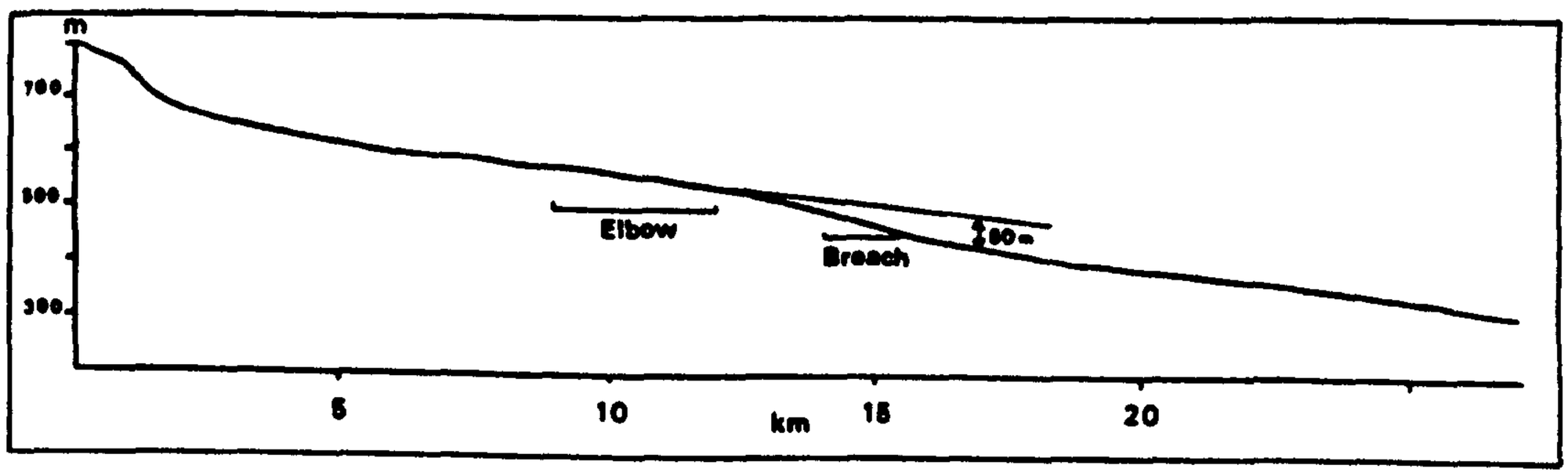

Figure 5.21 Long profile of River Feshie.

the area.

A longitudinal profile of the River Feshie from its source at an altitude of 800 metres shows a typical concave form (Figure 5.21). The flat, open nature of the area is shown by the shallow gradient of the Feshie at the river elbow. The concave profile is interrupted further downstream with a steep section below an altitude of approximately 500 metres. Extrapolation of the concave profile suggests an overdeepening of around 50 metres at this glacial breach (Figure 5.21).

The floor of the Geldie, and much of the land surrounding the Feshie, is mantled by thick deposits of peat and glacial till. The peat and drift support thick heather, obscuring the land surface in most places. The best place to observe the sub-surface structures is in the cuttings made by rivers and streams. Allt Eindart is incised into exposures of saprolite (Figure 5.3). The weathered bedrock is approximately 1 metre thick and retains its original structure (Figure 5.22) with foliations at 1 to 2 centimetre intervals. The weathered rock can be disintegrated manually and specimens crumbled by hand. The close spacing of the foliations and the grey hue suggest that the exposure is weathered schist. The saprolite is overlain by a layer of glacial till 3.65 metres thick containing clasts of unweathered schist. The till is overlain by 1.2 metres of peat.

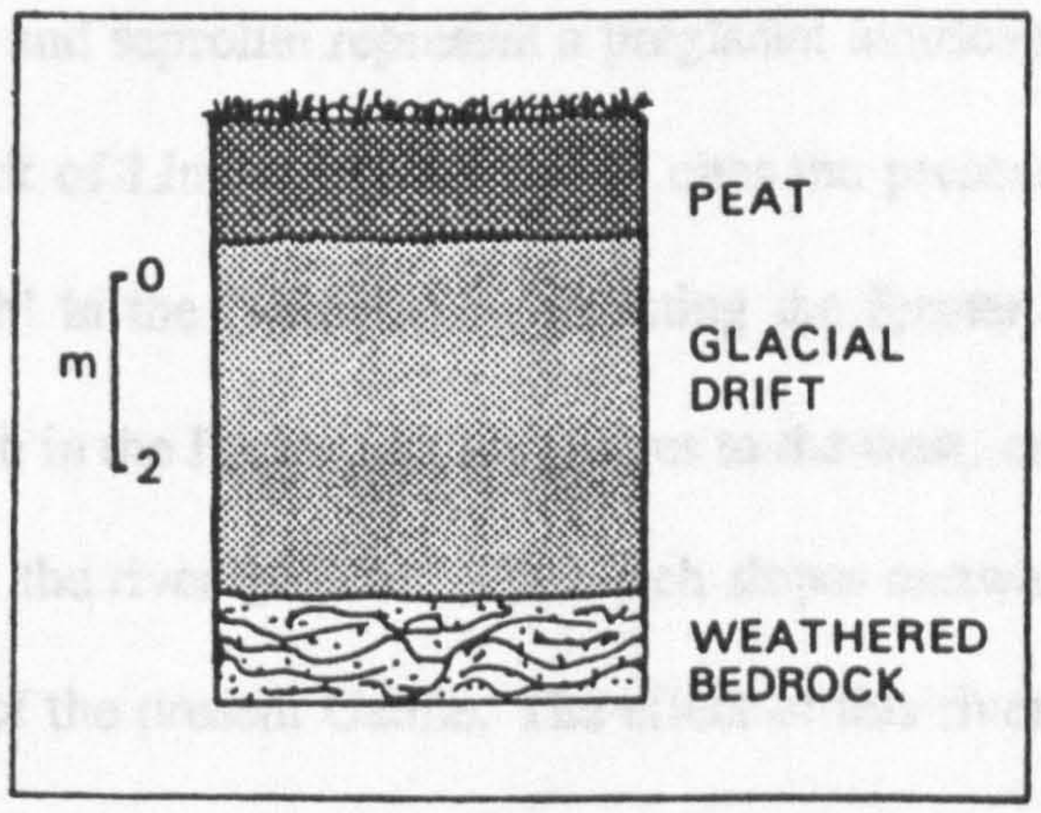

Figure 5.22 Weathering profile through saprolite exposure, Allt Eindart, near Glen Feshie.

Following Allt Eindart downstream the saprolite exposures in the stream banks appear to be less weathered and are more consolidated. In the southern exposure the weathering is confined to the joint planes, although specimens of rock between joints can still be crumbled manually. Near its confluence with the Feshie the stream is flowing on firm bedrock. The depth of weathering decreases with altitude, from 1.5 metres in the northern exposure to 1 metre in the south (Figure 5.3).

The proposal that the gently undulating slopes, dendritic river network, open valleys and saprolite represent a preglacial landscape is in agreement with the work of Linton (1949). Linton cites the presence of a preglacial valley 'bench' in the Geldie as representing the former valley floor. The glacial breach in the Feshie, six kilometres to the west, captured the Geldie and reversed the river gradient. The bench slopes eastward until it reaches the altitude of the present Geldie. The effect of this river capture has been to create the elbow in the River Feshie and change the course of the upper Geldie (Linton 1949). The bench can be picked out on Figure 5.3, forming a ledge at an altitude of between 600 and 650 metres. It can also be seen at an altitude of c. 600 metres on the profile in Figure 5.20. Interestingly, this is the same altitude at which the saprolite exposures occur and it is tempting to suggest the saprolite is also a remnant of the former valley floor.

5.4.3.3 The glacial landscape

Throughout the study area fresh bedrock is absent from the surface, although there are isolated occurrences in some stream beds. There is a widespread cover of glacial till. On the banks of the Eidart the depth of the till is around one metre, while along the River Feshie it is several metres. Further south the depth of the glacial deposits increases, and on the flanks of a large meander in the Feshie a section of till averaging seven metres thick is exposed. The maximum depth of till recorded in the study area is 12 metres.

5.4.3.4 The depth of ice sheet erosion

No landforms of ice sheet erosion occur in the area, and nowhere is there fresh or ice scoured bedrock. The river valleys are flat and open, and the topography is gently undulating and rounded in nature. Although the glacial till and peat may hide glacially polished bedrock beneath, this is considered unlikely as the preservation of preglacial structures such as the saprolite suggest minimal erosion by ice sheets.

The depth of ice sheet erosion in this area is probably relatively uniform. The river profile of the Feshie (Figure 5.21) suggests that the depth of erosion may be up to 50 metres at the glacial breach north of the study area. However, within the study area the scattered pockets of saprolite are evidence of minimal ice sheet erosion. A minimum depth of erosion of 10

metres and a maximum of 40 metres is assumed on the basis of the depth of the remaining saprolite. The total volume of ice sheet erosion is therefore:

Minimum depth of ice sheet erosion:

$25\ km^2$ @0.01 km erosion = $0.25\ km^3$

TOTAL VOLUME = $0.25\ km^3$

Maximum depth of ice sheet erosion:

$25\ km^2$ @0.04 km erosion = $1\ km^3$

TOTAL VOLUME = $1\ km^3$

5.4.4 Balmoral field study area

5.4.4.1 Site location and description

The study area in the central Dee Valley, some 25 kilometres to the east of the Cairngorm Mountains, is dominated by the River Dee at an altitude of c. 300 metres (Figure 5.4). In the south, the land rises away from the river and consists of isolated hills and high valley spurs. These hills rise above the Dee valley; Ripe Hill reaching an altitude of 519 metres, Canup 451 metres and Stob Liath 698 metres. Further south the land is dominated by the Lochnagar massif, with a highest summit of over 1100 metres. The solid geology of the area consists almost entirely of granite, although isolated outcrops of schist occur (Geological Survey of Britain (Scotland) Sheet 62).

5.4.4.2 The preglacial landscape

The land is punctuated by a series of isolated hills and valley spurs (Figure 5.23). Breaks of slope are often sharp, giving the land a jagged and rough appearance. The river pattern displays no regular dendritic network; rather the stream tributaries join the Dee at sharp angles and the drainage appears deranged (Figure 5.4). No saprolite occurs in this area and other deep weathering remnants are also rare. A tor exists on the summit of Canup, and further tors are known to exist on the higher ground to the south of this area (Sugden et al., submitted). The main surviving element of the preglacial land surface is marked by the topographic sheeting found in the granites. The sheeting is most common on the western flanks of the hills and spurs, for example on the western slopes of both Ripe Hill and Canup (Figure 5.4).

The sheeting is consistently parallel to topographic surfaces. Ripe Hill provides a good example of this parallelism, especially on the northern side where topographic sheeting is exposed over a large area. The sheeting is extensive, separated only by small patches of vegetation, and forms a continuous surface over much of the hill. In all cases where topographic sheeting is observed, the dip of the granite sheets is within a few degrees of the hill slope angle.

5.4.4.3 The glacial landscape

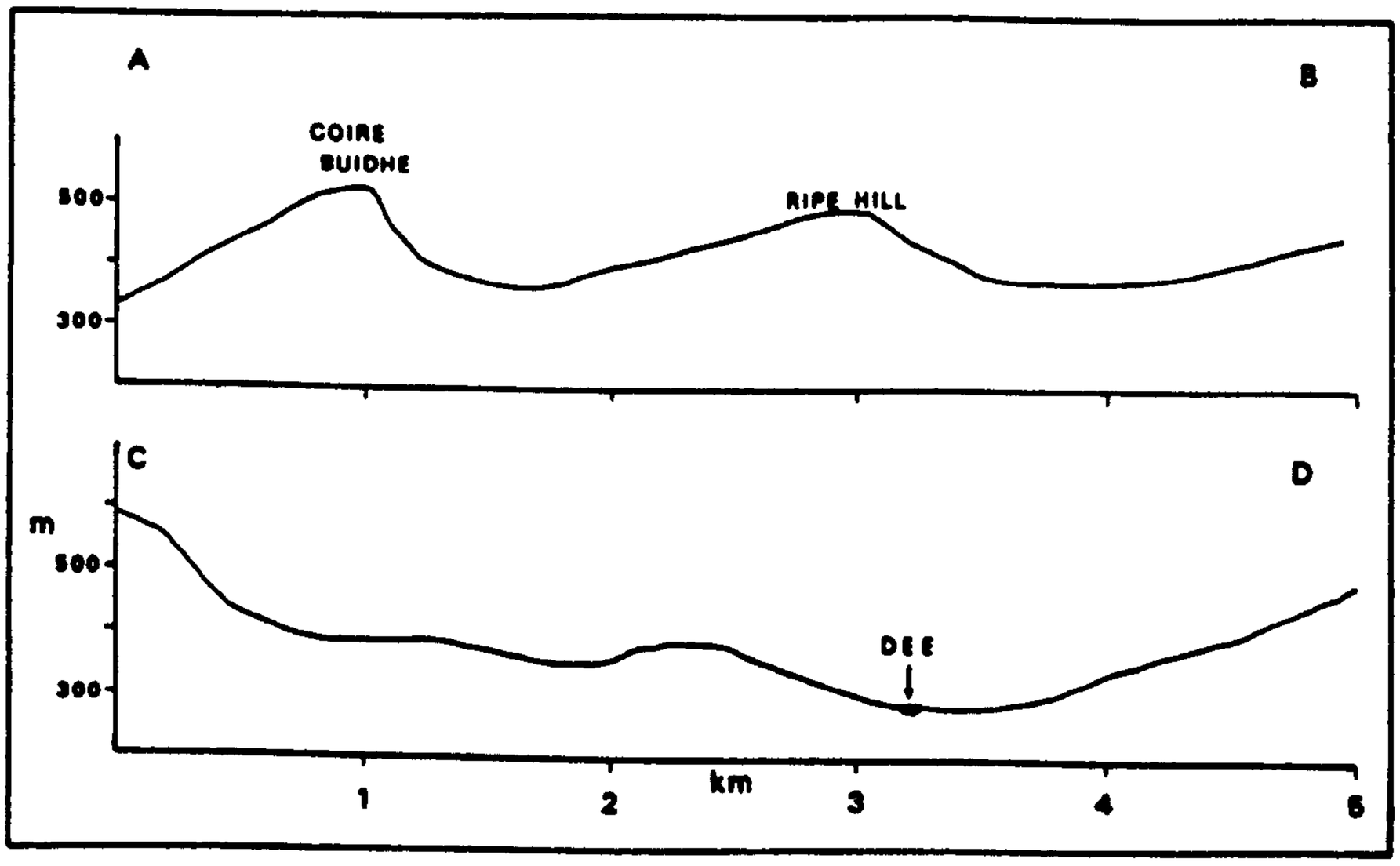

Figure 5.23 Topographic profiles of Balmoral field study area. For location of profiles see Figure 5.4

There are abundant landforms of ice sheet erosion. Fresh bedrock is exposed at many localities and evidence of ice scouring is widespread (Figure 5.4). Of particular importance are the large roches moutonnees, up to 500 metres in length and 150 metres in amplitude. They are classic stoss and lee features, with asymmetric long profiles (Figure 5.24), rock polishing and abrasion on slopes proximal to ice flow directions, and rock plucking and quarrying on distal slopes.

There are two main types of roches moutonnees; (1) those carved from free-standing and isolated hills, for example Ripe Hill and Canup and; (2) those carved from the valley spurs which run transverse to the main Dee Valley, for example Cnap a' Choire Bhuidhe and Craig Doin. Profiles across these features are shown in Figures 5.24 to 5.26. Sugden et al. (submitted) have drawn attention to the importance of fracture mechanics in controlling the development of lee side cliffs on these roches moutonnees, providing an explanation for the operation of processes of glacial erosion at this scale. It is not intended to discuss this process further here, but to concentrate on the use of these features in reconstructing depths of ice sheet erosion.

5.4.4.4 The depth of ice sheet erosion

A decreasing intensity of ice sheet erosion from the centre of the Dee Valley to the spurs is suggested by the profiles across three roche moutonnee forms

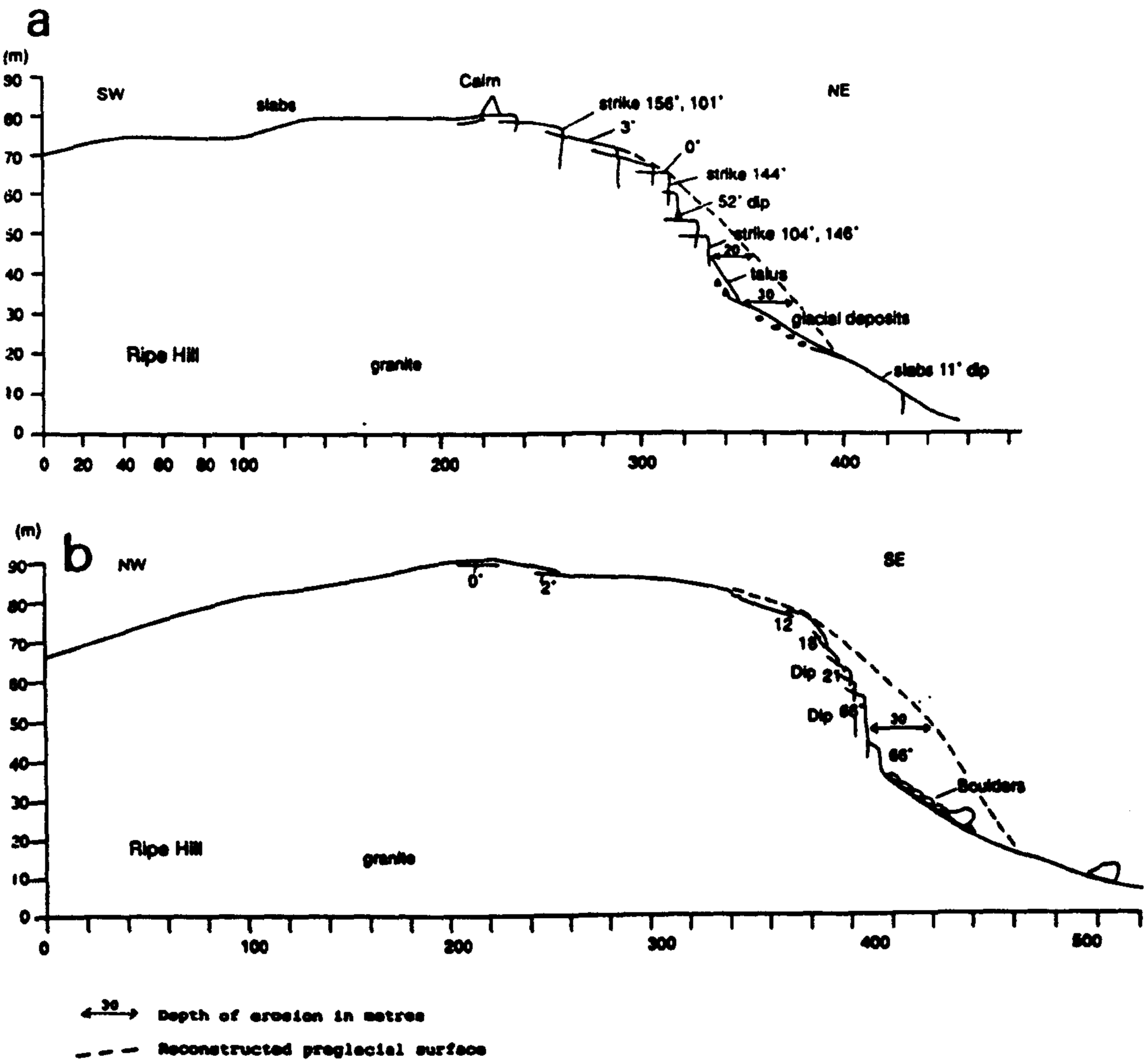

Figure 5.24 Topographic profiles across Ripe Hill. Reconstructed preglacial surface is indicated by broken line.

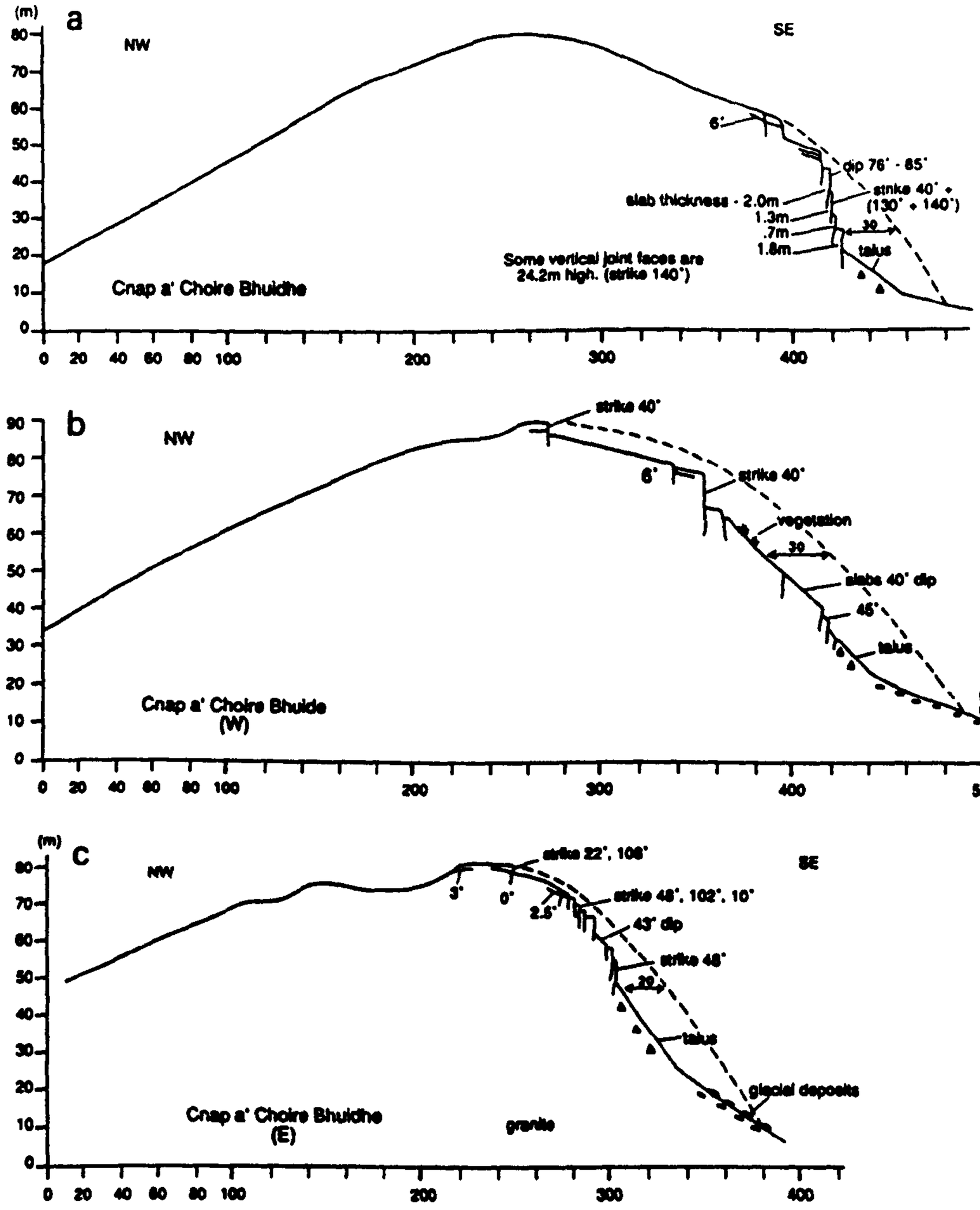

Figure 5.25 Topographic profiles across Cnap a' Choire Bhuidhe. Reconstructed preglacial surface is indicated by broken line.

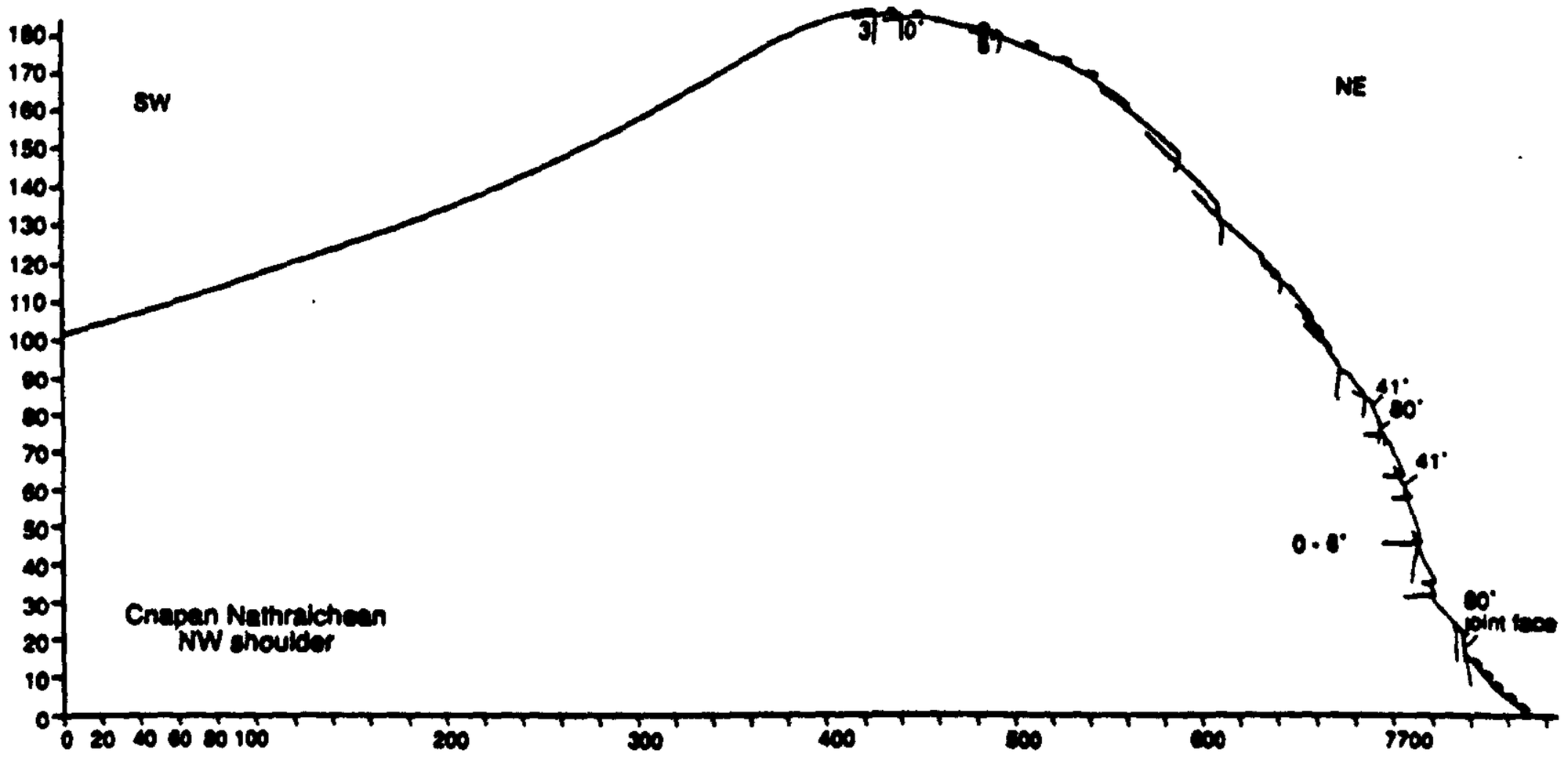

Figure 5.26 Topographic profile across Cnapan Nathraichean. Reconstructed preglacial surface is indicated by broken line.

(Figures 5.24 to 5.26). There is a gradual decrease in the degree of modification from the highly altered forms in the Dee Valley, such as Canup and Ripe Hill with lee side cliffs of up to 60 metres in height, to the almost intact preglacial hills on the higher ground, such as Cnapan Nathraichean. The large bedrock hills in the Dee Valley are plucked on their eastern lee sides, while those further away from the valley are not. In the case of Cnapan Nathraichean, the preservation of the topographic sheeting can be used to demonstrate that glacial erosion has only removed a single bedrock slab from the base of the lee side (Figure 5.26). This continuum of glacial forms can be traced even further south, with the existence of a tor and more areas of topographic sheeting on the slopes leading up to Lochnagar (Sugden et al., submitted).

The depth of ice sheet erosion is calculated using the method outlined by Jahns (1943). The topographic sheeting can be used to calculate the differential in erosion between stoss and lee slopes of roches moutonnees. This is because the sheeting is assumed to be parallel to the preglacial surface and truncated by glacial erosion on lee sides. Figures 5.24 and 5.25 are profiles across Ripe Hill and Cnap a' Choire Bhuidhe. In both cases topographic sheeting occurs parallel to the hill slope and is confined to proximal and lateral hill sides. The contrast between the topographic sheeting on stoss sides and summits, and the cliffed forms of glacial erosion where sheeting is absent is shown in the profiles. The Ripe Hill profile

(Figure 5.24) shows sheeting parallel to the hill slope angle, outcropping in patches up to five metres across. On the summit of the hill dip angles are low and often horizontal, whilst these angles increase away from the summit as the surface slope increases. The sheeting on the summit also exhibits fretting parallel to the surface slope.

To the north east and south east of the summit the rock jointing becomes more complex. The rock jointing differs from the topographic sheeting in that the joints are not parallel to the hill surface. Instead, cliff faces are dominated by vertical and near vertical joints striking between 140° and 146° (Figure 5.24). A second set of joints dip out of the cliff face at angles of 21° near the hill summit, increasing to 66° near the base of the cliff. The topographic sheeting is truncated by glacial plucking on the upper part of the cliffed side of Ripe Hill.

The topographic sheeting continues to the east of Ripe Hill below the cliff, and it is not difficult to envisage it comprising a coherent convex hill entirely composed of sheeting in preglacial times. If this is the case, the preglacial form of the hill can be reconstructed by extrapolating the form of the granite sheets (Figure 5.24). The total depth of ice sheet erosion is the depth of lee side plucking plus any glacial abrasion which has taken place on the stoss side. Using this method, the depth of lee side plucking on Ripe Hill is between 20 and 30 metres (Figure 5.24). Reconstructions of the

preglacial topographic sheeting at two locations on Ripe Hill and at three locations on Cnap a' Choire Bhuidhe suggest an average depth of lee side plucking of between 20 and 30 metres.

A depth of erosion of 25 metres is therefore assumed in the lee of the roches moutonnees. Elsewhere, a depth of ice sheet erosion of 10 metres minimum and 50 metres maximum is assumed because of the convex slopes and topographic sheeting, and absence of saprolite. The two estimates are combined in the lee of the roches moutonnees to allow for the additional glacial plucking.

Minimum depth of ice sheet erosion:

$25\ km^2$ @ 0.01 km erosion = $0.25\ km^3$
$2\ km^2$ @ 0.025 km erosion = $0.05\ km^3$

TOTAL VOLUME = $0.3\ km^3$

Maximum depth of ice sheet erosion:

$25\ km^2$ @ 0.05 km erosion = $1.25\ km^3$
$2\ km^2$ @ 0.025 km erosion = $0.05\ km^3$

TOTAL VOLUME = $1.3\ km^3$

Expressed as a depth of erosion per unit area, the minimum depth of ice

sheet erosion is 12 metres and the maximum is 52 metres.

5.4.5 Speyside study area

5.4.5.1 Site location and description

The site in the upper reaches of the Spey Valley is on the eastern flanks of the Monadliath Mountains (Figure 5.5). The terrain is generally low-lying with the highest point in the area at 574 metres above sea level at Creag na Doire Duibhe. The River Spey flows from west to east through the area, and its wide floodplain divides the study area at an altitude of 250 metres above sea level. The solid geology of this area is dominated by metamorphic rocks, in this case undifferentiated schists (Geological Survey of Britain (Scotland) Sheet 63).

5.4.5.2 The preglacial landscape

The most important preglacial features in this area are the saprolite exposures which are found in several stream tributaries of the Spey (Figure 5.5). A good example of this is Allt Granda, where a 20 metre deep, steep-walled channel runs almost due south into the Spey. The channel has cut mainly into solid bedrock but exposes sections of deeply weathered rock in its walls. The saprolite can be traced upstream for a considerable distance, persisting up to an altitude of 500 metres above sea level. Near the mouth of the stream the weathered material is schistose, while further up and on the eastern side of the channel the saprolite is granite (Plate 5.9).

The Allt Granda exposure displays a marked vertical variation in the degree of weathering. Only the bottom layer of the weathering profile remains as fresh bedrock, the upper 11 metres of the section being decomposed into a gravel matrix. Figure 5.27 shows a representative section through the weathering profile. Weathered rock 8.7 metres thick is exposed immediately above the stream. Here the weathering is incomplete and the patches of fresh bedrock are supported in a saprolite matrix. Above this a small rock ledge marks the transition from the more cohesive weathered rock to the sandy saprolite above which has undergone greater disintegration. This is overlain by a thin cover of glacial till containing unweathered material, in this case around 10 centimetres in depth. The saprolite is brick red in colour and is probably derived from granite.

Similar weathering profiles are found throughout the north of the study area, for example in the extreme north east corner of the area an outcrop of saprolite, 2 metres by 3.5 metres in size and 2 metres in depth, is found in a stream rock wall. The original structures are still visible, but the rock is easily fractured by hand, especially along the major joints and the numerous foliation planes. The degree of weathering is relatively slight, as a decomposition to granular particles is not evident. Unlike the red granite exposure at Allt Granda, the saprolite here is a light grey colour and weathering has been controlled more by the jointing in the schist parent

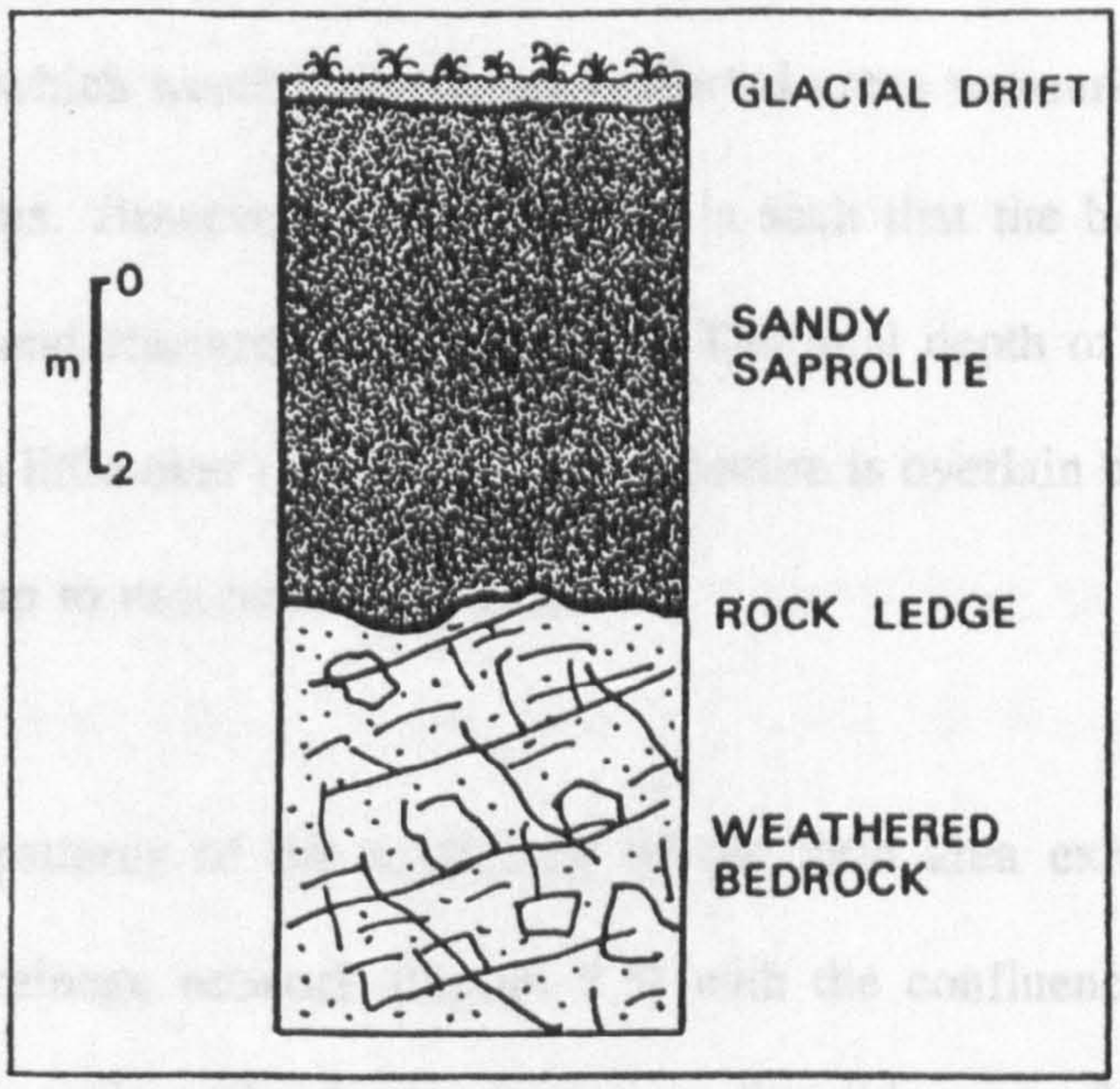

Figure 5.27 Weathering profile through saprolite exposure, Allt Granda, Speyside.

rock.

Another outcrop of weathered rock appears in a cutting made by Allt na Cubhaige near its confluence with the Spey. A thin layer of saprolite, up to 20 centimetres in depth, overlies more coherent schist bedrock in the stream bed. The saprolite is fine grained and grey in colour. Below the saprolite is bedrock in which weathering has only affected areas surrounding the joints and foliations. However, the weathering is such that the bedrock can be dismantled and fractured easily by hand. The total depth of weathering at this site is a little over one metre. This exposure is overlain by a blanket of glacial till up to two metres in depth.

The river patterns of the south east of the field area exhibit a regular dendritic drainage network (Figure 5.5) with the confluences marked by acute angles and gentle slopes. It appears that this part of the field area retains much of its preglacial river valley pattern. However, because the solid geology of the area is largely metamorphics, sheeting parallel to topographic surfaces is not developed. No tors or similar weathering remnants are found in association with the saprolite.

5.4.5.3 The glacial landscape

About 50 per cent of the study area is ice scoured, with fresh bedrock at the surface (Figure 5.5). Ice scoured bedrock is absent from the east of area

where there is a thick cover of peat and till, and from the alluvial floodplain occupied by the River Spey. Although these surficial deposits may hide ice scoured bedrock, the dendritic river valley pattern and gentle slopes suggest the eastern section retains much of its preglacial character.

On the valley floors, the ice scouring takes the form of individual roches moutonnees with an amplitude of one to three metres. The strike of the lee sides suggests an ice flow direction to the north east down the Spey Valley. The land between individual rock knolls and roches moutonnees is infilled with glacial till, and the knolls are separated by cliff faces (Plate 5.10). These may be large, up to 40 metres in the case of Creag na Doire Duibhe, or smaller where the relief amplitude is less severe, for example in the Spey Valley. The majority of these cliff faces are orientated in a down-valley direction in relation to the Spey.

Close to the valley floor of the Spey, cliff faces on spurs are parallel to the valley. A good example is the cliff face at An Dun (Figure 5.5). Similar truncated spurs occur at various points along the opposite valley wall, generally of the order of 10 to 15 metres in height. The Spey is the only glacial trough in this area. The valley walls are steep-sided and mostly cut in bedrock, although in some locations the valley is more open and shallow (Figure 5.28). The trough has a gentle parabolic profile, with a centre line depth of 210 metres and valley top width of 2500 metres. This yields a form

↑

Plate 5.10 Areal scouring, Spey Valley.

Plate 5.9 Saprolite exposure at Allt Granda, Speyside. Fragments of the rock can be removed and crumbled manually. The chemical weathering is most advanced along joints in the rock. →

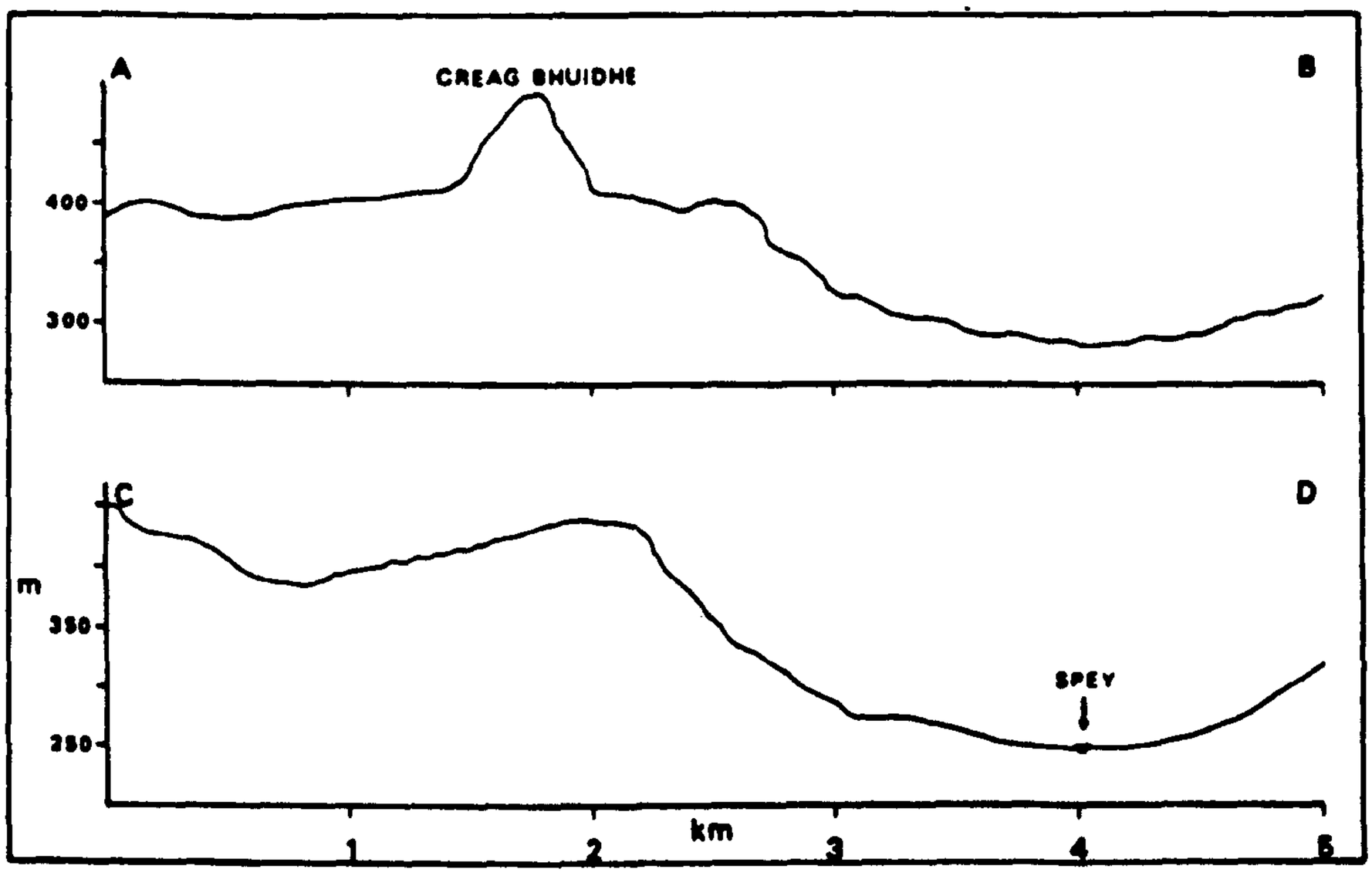

Figure 5.28 Topographic profiles of Speyside field study area. For location of profiles see Figure 5.5.

ratio (depth divided by width) of 0.084, slightly lower than the form ratios of between 0.242 and 0.445 suggested for alpine troughs (Graf 1970). However, the morphology of the trough represents a degree of erosion under ice sheet conditions, even if it is not particularly deep.

5.4.5.4 The depth of ice sheet erosion

Overall, erosion by ice sheets has been both widespread and effective. Over 50 per cent of the area is comprised of scoured bedrock. Scouring is not limited to the main trough of the Spey, but also occurs on the surrounding land at a distance from the valley itself. The largest zone of ice scouring occurs in the south west of the study area in a band jutting out into the Spey Valley (Figure 5.5). The remnants of the preglacial landscape are represented by isolated exposures of saprolite which occur only in the V shaped valleys south of the Spey and are absent from the floor of the main valley. The saprolite in the north of the area lies in incised valleys aligned at right angles to the Spey Valley. The saprolite in the centre of the area occupies a lee side location relative to ice movement.

Assigning a value to the depth of ice sheet erosion in this area is difficult, given the lack of evidence with which to reconstruct the preglacial landscape. The absence of sheeting in the granites does not allow preglacial valley cross-sections to be reconstructed with any conviction. Neither are there many preglacial fluvial valleys from which depths of overdeepening

may be calculated. The best available evidence is that provided by the remnants of the deep weathering mantle.

The survival of saprolite suggests that ice sheet erosion has not been sufficiently deep to remove all traces of the preglacial landsurface. In addition, the close proximity of saprolite to ice scoured bedrock demonstrates that erosion has not removed all of the weathered material, especially in topographically protected sites. Assuming a depth of 10 to 50 metres of preglacial weathering, it is possible to make tentative estimates of the depth of ice sheet erosion based on the following three erosional zones:

(1) The Spey Valley, approximately 6.25 km^2 or 25 per cent of the total area, is a glacial trough where no former weathering mantle survives. The mimimum depth of erosion in this area is assumed to be 50 metres. Extrapolation of the valley cross-profile suggests a maximum depth of 100 metres (Figure 5.28).

(2) An ice scoured zone occupies approximately 12.5 km^2 or 50 per cent of the total area. In this zone, ice sheet erosion has lowered the land surface to bedrock but scattered patches of the former weathering cover survive. The depth of erosion in this area is therefore assumed to be 40 metres.

(3) A zone of thick peat and drift cover occupies approximately 6.25 km^2 or

25 per cent of the total area. Although the land surface is obscured, minimal ice sheet erosion is suggested by the survival of the preglacial river valley forms associated with the existence of saprolite. The depth of erosion in this zone is assumed to be 10 metres.

Minimum depth of ice sheet erosion:

6.25 km^2 @0.05 km erosion = 0.3125 km^3
12.5 km^2 @0.04 km erosion = 0.5 km^3
6.25 km^2 @0.01 km erosion = 0.0625 km^3

TOTAL VOLUME = 0.875 km^3

Maximum depth of ice sheet erosion:

6.25 km^2 @0.1 km erosion = 0.625 km^3
2.5 km^2 @0.04 km erosion = 0.5 km^3
6.25 km^2 @0.01 km erosion = 0.0625 km^3

TOTAL VOLUME = 1.1875 km^3

Expressed as a depth of erosion per unit area, the average glacial lowering in this 25 km^2 grid is a minimum of 35 metres and a maximum of 47.5 metres.

5.4.6 Aberdeen study area

5.4.6.1 Site location and description

The easternmost study area is closest to the proposed margin of the former ice sheet. The southern edge of the area is four kilometres north of the Dee

Valley (Figure 1.1), and the terrain is generally low lying. The highest summit is Brimmond Hill at 265 metres (Figure 5.6), which rises above the general surface of the area at 100 to 150 metres above sea level. The undulating nature of the land is demonstrated in the two topographic profiles across the area. Relative relief of around only 50 metres is common (Figure 5.29). The solid geology of the area consists of Dalradian metamorphics, in this case of the Aberdeen Formation. More specifically, these rocks are mainly of pelitic, semi-pelitic, and psammitic metasediments that are interbanded on a small scale (1-10 metres) (Geological Survey of Britain (Scotland) Sheet 77).

5.4.6.2 The preglacial landscape

Specific evidence of the preglacial landscape in this area is provided by an exposure of saprolite near the centre of the study area (Figure 5.6). This exposure was found in temporary excavations at a building site and is overlain by a layer of glacial till up to eight metres thick. The saprolite is a highly weathered grey metamorphic rock with a foliated structure. Weathering is advanced along these foliation planes; the rock is friable and easily disintegrated by hand. Occurrences of weathered bedrock are common in this region, and have been indicated previously by Fitzpatrick (1963) and Hall (1985). The existence of a layer of chemically weathered bedrock throughout this region is noted by Munro (1986), although surface exposures are uncommon due to the thick till cover. Most of the data concerning these

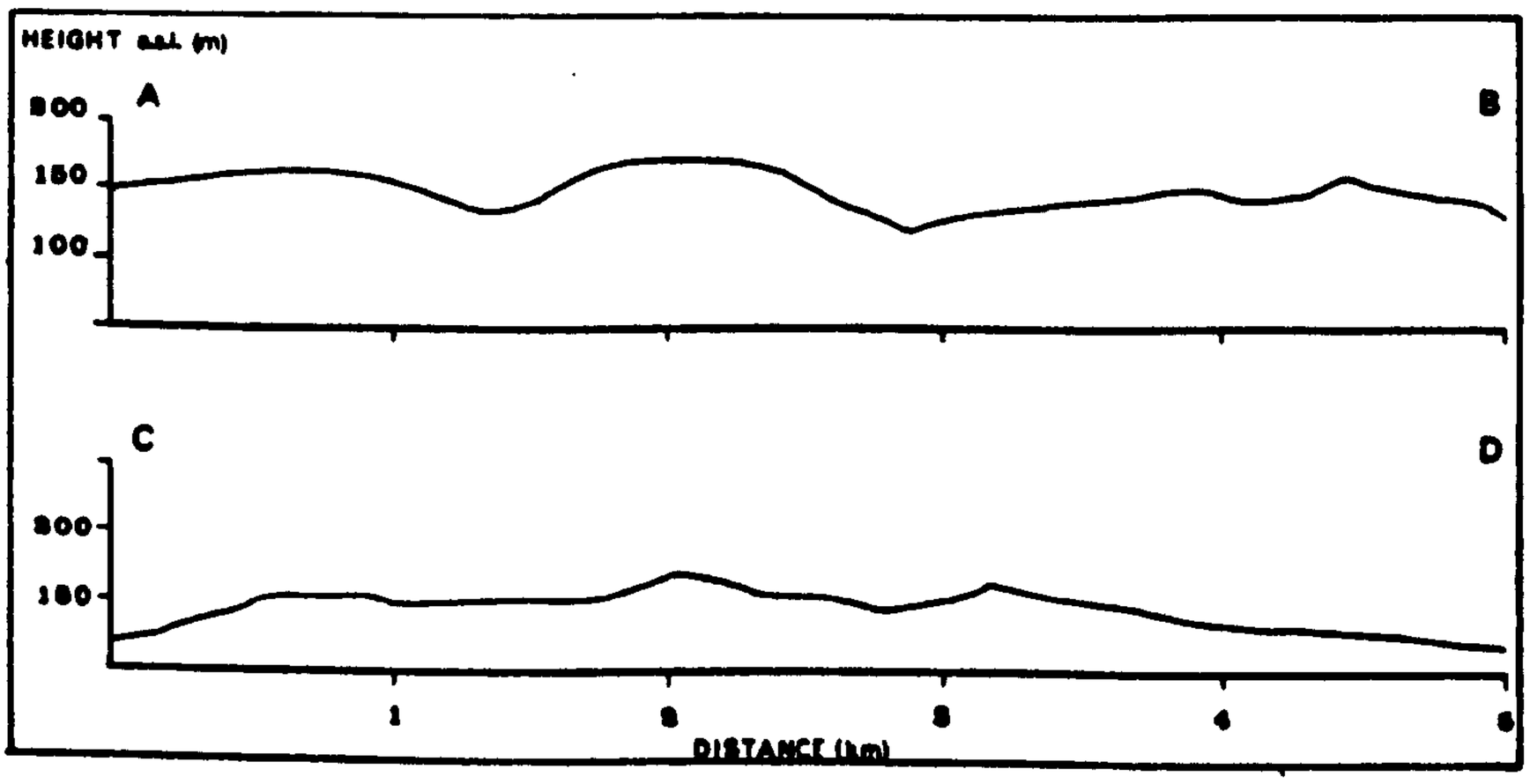

Figure 5.29 Topographic profiles of Aberdeen field study area. For location of profiles see Figure 5.6

exposures originate from trenches and drill holes which suggest that the till is underlain by a zone of saprolite over 2.5 metres thick (Munro 1986).

Small tors on the summits of low lying hills, for example Brimmond Hill, are further evidence of the preglacial land surface (Figure 5.6). It has also been argued that the undulating topography and the basins in this area are essentially preglacial features (Hall and Sugden 1987). Although there is little new independent evidence, the main features are thought to be a preglacial landscape (Clapperton and Sugden 1977; Hall and Sugden 1987). The thickness of the glacial till masks much of the landscape and the entire region is known to be covered by between 1.5 and 4 metres of till (Munro 1986).

5.4.6.3 The glacial landscape

The effects of erosion by ice sheets are indicated by the presence of ice scoured bedrock on the summits of the gently undulating hills. Good examples of hills where the summits display ice scouring are Brimmond Hill, Cloghill and Kingshill. Striations also occur on the hill summits in this region (Hall and Sugden 1987). For example, the summit of Brimmond Hill comprises three distinct rock knolls, the largest of which is situated on the eastern summit of the hill and measures c. 20 metres across. On the western flank of the hill smaller and flatter ice smoothed bedrock outcrops in patches of 1 to 2 metres in diameter.

In addition to the bedrock exposures, large scale steamlining of rock and drift can be used as evidence of erosion by former ice sheets. Many of the large hills in this area show a marked elongate form, with their long axes aligned approximately west to east (Figure 5.5). Typically they are drumlinoid in form, with steep western slopes and a long gentle tail to the east (Figure 5.30). Relief amplitude is generally small, with an average amplitude of around 30 metres and overall length of up to 500 metres. Two of the largest streamlined hills, Cloghill and Kingshill, are ice scoured on their summits with fresh bedrock to the west of the hill crests. The elongate form of the hills extends eastward from these bedrock knolls (Figure 5.30).

The majority of the streamlined hills, however, do not display fresh bedrock at the surface. The lower lying undulations in the south and centre of the study area appear to be streamlined entirely in drift (Figure 5.6). These hills tend to have a lower relief amplitude than those carved in bedrock (Figure 5.30), and appear as more rounded undulations in the terrain. However, they are similarly aligned in a west to east direction. Large scale streamlining of the topography has also been noted by Hall and Sugden (1987) and it is known from trench exposures that bedrock profiles are often smooth and gently rounded over horizontal distances of several hundred metres (Munro 1986).

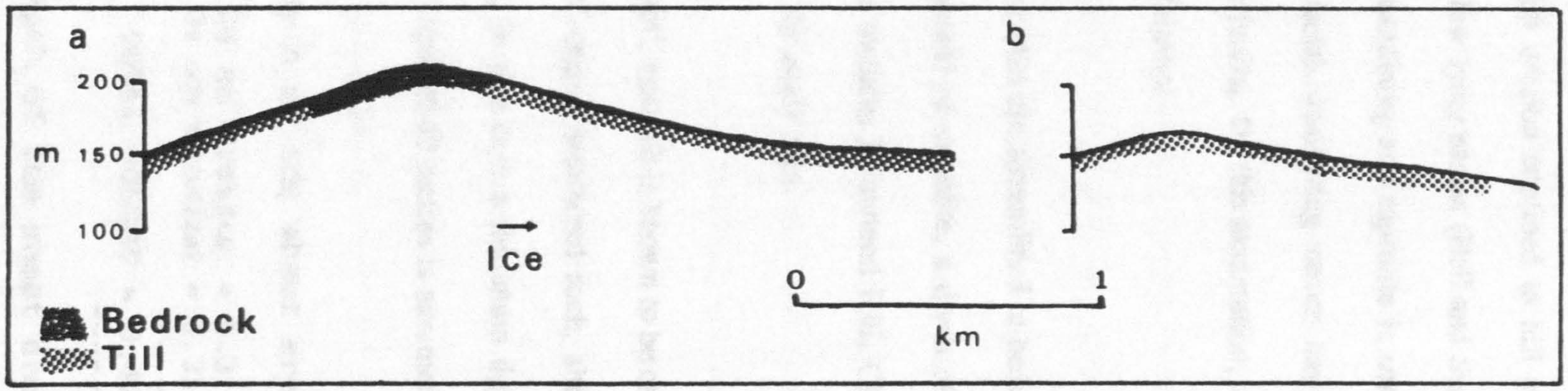

Figure 5.30 Long profiles of streamlined hills:
(a) Streamlined in till with bedrock knob
(b) Streamlined entirely in till.

5.4.6.4 The depth of ice sheet erosion

There is thought to be a relationship between topography and ice sheet erosion in this area, with erosion confined to hill summits and saprolite confined to intervening low lying basins (Hall and Sugden 1987). Since all hills are affected by streamlining and saprolite is confined to basins, it is probable that the preglacial weathering cover has been stripped from everywhere except these basins. On this assumption, the depth of ice sheet erosion is estimated as follows:

(1) In the locations where hills are streamlined in bedrock with evidence of ice scouring and the removal of saprolite, a depth of erosion of up to 50 metres is assumed. This includes Brimmond Hill, Cloghill and Kingshill, approximately 4 km^2 of the study area.

(2) In the remaining 21 km^2, bedrock is known to be close to the surface yet co-exists with patches of deeply weathered rock, although both are often obscured by glacial till. In this case a minimum depth of erosion of 10 metres and a maximum depth of 40 metres is assumed.

Minimum depth of ice sheet erosion:

4 km^2	@0.05 km erosion	= 0.2 km^3
21 km^2	@0.01 km erosion	= 0.21 km^3
	TOTAL VOLUME	= 0.41 km^3

Maximum depth of ice sheet erosion:

4 km^2	@0.05 km erosion	= 0.2 km^3
21 km^2	@0.04 km erosion	= 0.84 km^3
	TOTAL VOLUME	= 1.04 km^3

Expressed as a depth of erosion per unit area, the minimum depth of erosion is 16.4 metres and the maximum depth of erosion is 41.6 metres.

5.5 The depth of ice sheet erosion in the regional transect

A calculation of the volume and depth of ice sheet erosion in the entire regional study area can now be made, based on the landscape classification and the depth of erosion estimates made in the five field study areas (Table 5.1). This calculation rests on the assumptions that each of the five field study areas is representative of its overall landscape class, and that the estimates of the minimum and maximum depths of erosion reflect the degree of ice sheet modification. The estimates of the minimum and maximum depth of glacial erosion in the study areas are then used to calculate the minimum and maximum depths of erosion in the regional transect. The estimates of minimum and maximum depths of ice sheet erosion in the landscape types are as follows:

Study area	Minimum estimate	Maximum estimate
Cairngorms	108 metres	152 metres
Balmoral	12 metres	52 metres
Speyside	35 metres	47.5 metres
Aberdeen	16.4 metres	41.6 metres
Glen Feshie	10 metres	40 metres

Table 5.1 Depths of erosion in the field study areas expressed in metres per unit area.

Areal scouring

minimum depth of erosion per unit area = 35 m

maximum depth of erosion per unit area = 47.5 m

Upland selective linear erosion

minimum depth of erosion per unit area = 108 m

maximum depth of erosion per unit area = 152 m

Unmodified preglacial landscape

minimum depth of erosion per unit area = 10 m

maximum depth of erosion per unit area = 40 m

Selective linear erosion

minimum depth of erosion per unit area = 12 m

maximum depth of erosion per unit area = 52 m

Restricted glacial erosion and/or glacial deposition

minimum depth of erosion per unit area = 16.4 m

maximum depth of erosion per unit area = 41.6 m

The transect has a total area of approximately 2775 km^2, and is comprised of the following landscape classes; areal scouring approximately 525 km^2, upland selective linear erosion approximately 475 km^2, unmodified preglacial landscape approximately 250 km^2, selective linear erosion approximately 500 km^2, and restricted glacial erosion and/or glacial

deposition approximately 1025 km^2. The location of these landscape types and the range in depth of ice sheet erosion which they represent are shown in Figure 5.31. Multiplying the total area of each landscape class by the minimum and maximum estimates of the depth of erosion, expressed per unit area, gives the following volumes of erosion:

Areal scouring

525 km^2 x35 m = 18.375 km^3 (minimum volume)

525 km^2 x47.5 m = 24.9375 km^3 (maximum volume)

Upland Selective linear erosion

475 km^2 x108 m = 51.3 km^3 (minimum volume)

475 km^2 x152 m = 72.2 km^3 (maximum volume)

Unmodified preglacial landscape

250 km^2 x10 m = 2.5 km^3 (minimum volume)

250 km^2 x40 m = 10 km^3 (maximum volume)

Selective linear erosion

500 km^2 x12 m = 6 km^3 (minimum volume)

500 km^2 x42 m = 21 km^3 (maximum volume)

Restricted glacial erosion and/or glacial deposition

1025 km^2 x16.4 m = 16.81 km^3 (minimum volume)

1025 km^2 x41.6 m = 42.64 km^3 (maximum volume)

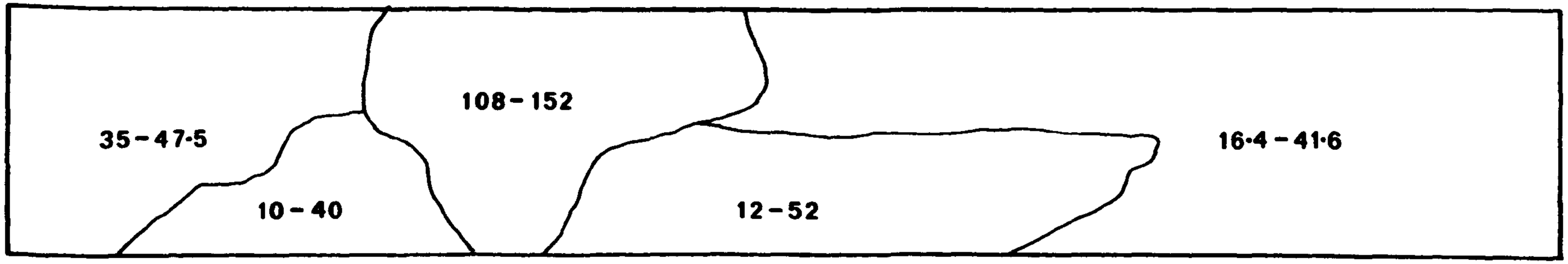

Figure 5.31 Minimum and maximum depths of ice sheet erosion (in metres per unit area) represented by the landscape classes within the regional transect study area.

Summing the estimates of minimum volumes of erosion, the total minimum volume of erosion in the transect is 94.985 km^3. Expressed as a depth of erosion per unit area, this equals an average of 34 metres of erosion over the transect. Summing the estimates of maximum volumes of erosion, the total maximum volume of erosion is 170.7775 km^3. Expressed as a depth of erosion per unit area this equals an average 61.54 metres of erosion over the transect. These minimum and maximum depths of glacial erosion differ only by a factor of 2, and average depths of erosion in the range of 34 to 61 metres over the entire transect appear reasonable. It is interesting to note that in both the minimum and maximum estimates there is a large regional variation in the depth of erosion. For example, landscapes of selective linear erosion account for over 50 per cent of the total volume of erosion in the minimum estimate, largely because of the significance of glacial erosion in mountain troughs.

5.6 Conclusions

The main conclusions of this chapter are as follows:

(1) The intensity of ice sheet erosion in Scotland declines from west to east from the proposed former ice divide to the eastern margin.

(2) A relationship exists between topography and ice sheet erosion, with areal scouring most intense in areas of moderate relief and valley areas.

(3) At a local scale it is possible for glacial landscapes to co-exist with preglacial landscapes in close proximity. This is most apparent in the Cairngorm Mountains, where the existence of saprolite, tors and topographic sheeting on the Cairngorm plateau co-exists with deep glacial troughs.

(4) The implication is that ice sheet erosion is highly selective. In four of the five study areas examined remnants of a former weathering cover survive, suggesting erosion has been locally ineffective.

(5) The total volume of erosion in the transect is calculated to be a minimum of 94.985 km^3 and a maximum of 170.7775 km^3. Expressed as a depth of erosion per unit area this is equivalent to a minimum depth of erosion of 34 metres and a maximum depth of erosion of 61.54 metres over the entire transect.

(6) In the study areas where there is a high or moderate relief amplitude (e.g. Cairngorms, Balmoral, Speyside) erosion by ice sheets has been quantitatively more important than in those areas where relief amplitude is low (e.g. Aberdeen, Glen Feshie).

CHAPTER SIX

THE CORRELATION BETWEEN BASAL THERMAL REGIME AND ICE SHEET EROSION

6.1 Aim

The original hypothesis stated at the outset of the thesis was that basal thermal regime is a crucial control on glacial erosion. Zones of basal melting are associated with areas of intense erosion under former ice sheets and zones of basal freezing associated with areas of less intense or no ice sheet erosion. The aim of this chapter is to test this hypothesis by making a comparison between the predicted pattern of basal thermal regime and pattern and depth of ice sheet erosion.

The comparison is important because it provides a test of the relationship between basal thermal regime and ice sheet erosion. If the relationship is strong then it may be suggested that either:

(1) basal ice temperature is crucial in determining the location of erosional zones under ice sheets and the majority of this erosion occurred at the ice sheet maximum or that;

(2) the relationship is coincidental, through an incorrect or insufficiently sensitive choice of input parameters, or through hidden assumptions in the method used to calculate basal ice temperatures.

Conversely, if the pattern of basal thermal regime at the ice sheet maximum shows no relationship with the zones of erosion then it may be suggested that either:

(1) No relationship exists between basal thermal regime and ice sheet erosion, and other factors need to be considered in order to explain the observed pattern of ice sheet erosion.

(2) The pattern of erosion is not related to the basal ice temperatures at ice sheet maximum, but is a product of other time periods such as ice sheet initiation and decay.

(3) The pattern of erosion cannot be explained by a model of ice sheet temperatures because it is a complex system in time and space which cannot be simplified to a series of mathematical equations. The model may contain too many assumptions or simplifications to realistically predict the pattern of erosion.

(4) There are errors in the field mapping of the pattern of ice sheet erosion.

6.2 The comparison between basal thermal regime and ice sheet erosion

The comparison between the modelled pattern of basal thermal regime and the pattern of ice sheet erosion is made at two spatial scales; for the flowband as a whole and for the field study areas within the flowband. The first part of the chapter is concerned with comparisons at the regional scale of the flowband; the second with comparisons at the local scale.

6.3 Comparisons at the regional scale

Modelled basal thermal regime is shown for the regional flowband assuming uniform ice flow (Figure 6.1a), and for the regional flowband including convergence and divergence of ice flow (Figure 6.1b). Three temperature zones are distinguished: (1) basal melting; (2) basal freezing where the basal ice temperature is between 0°C and -8°C and; (3) basal freezing where the basal ice temperature is below -8°C. The zone of basal melting is distinctive because ice is everywhere warm based; in the zone of basal freezing between 0°C and -8°C the ice is cold based but pressure melting is possible in certain locations; and in the zone below -8°C basal melting does not occur. Figure 6.1 also shows the pattern of ice sheet erosion in the regional transect.

6.3.1 Standard model run

In the standard model run, which does not allow for convergence and

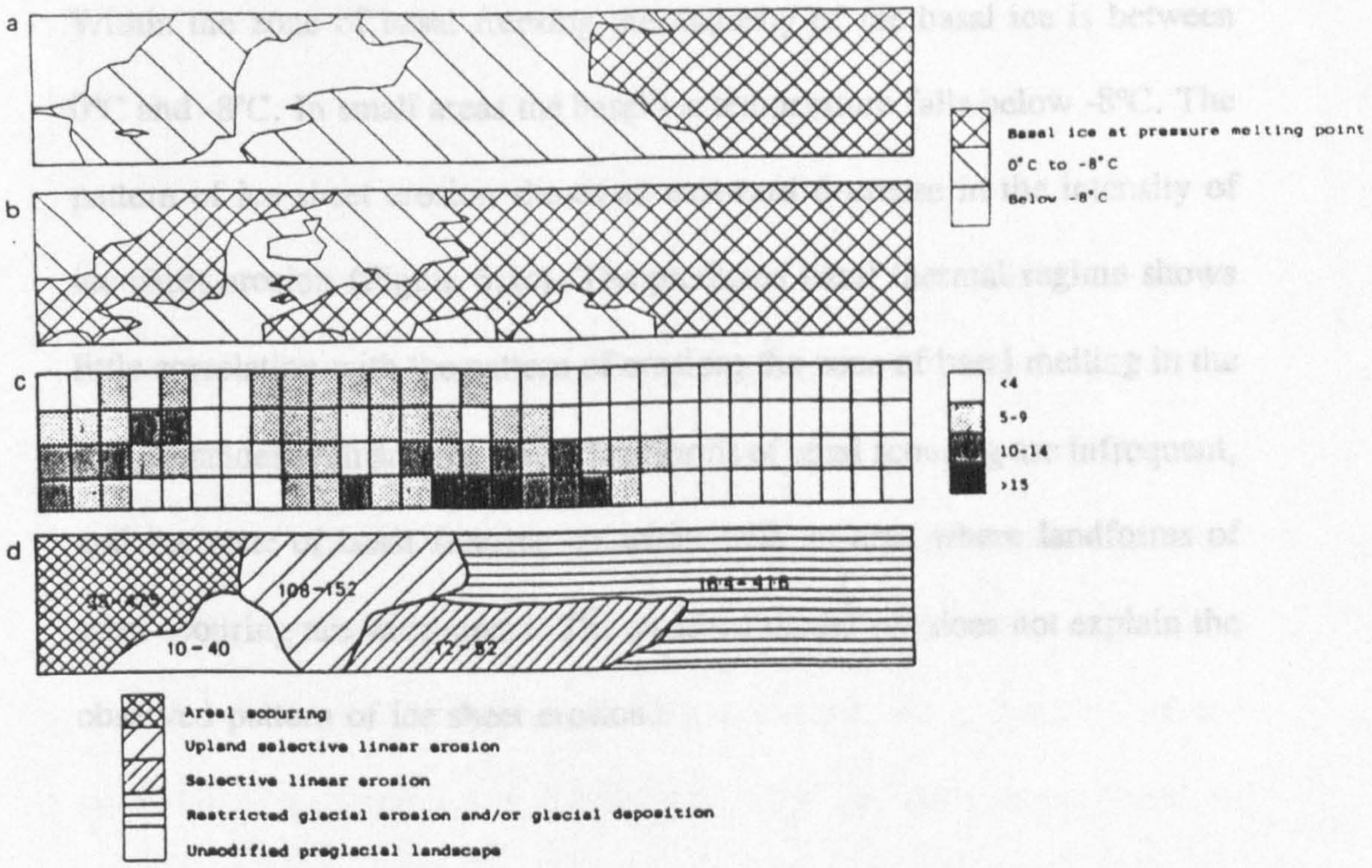

Figure 6.1 Modelled basal thermal regime and the pattern of ice sheet erosion in the regional transect:
(a) Basal thermal regime, standard model run
(b) Basal thermal regime, including convergence and divergence of ice flow.
(c) Frequency of landforms of areal scouring in 5 x 5 km grid squares
(d) Landscape classification and depths of ice sheet erosion.

divergence of flow, basal freezing extends over most of the flowband, with ice at the pressure melting point only in the extreme east (Figure 6.1a). Within the zone of basal freezing the majority of the basal ice is between 0°C and -8°C. In small areas the basal ice temperature falls below -8°C. The pattern of ice sheet erosion shows an eastward decrease in the intensity of ice sheet erosion (Figure 6.1c). The predicted basal thermal regime shows little correlation with the pattern of erosion; the zone of basal melting in the east coincides with an area where landforms of areal scouring are infrequent, and the zone of basal freezing coincides with an area where landforms of areal scouring are widespread. The standard model run does not explain the observed pattern of ice sheet erosion.

A comparison between the modelled basal thermal regime and landscape classification derived from aerial photograph interpretation (Figure 6.1d) also shows little correlation; the areas of scouring, upland selective linear erosion and selective linear erosion coincide with a zone of basal freezing, and the area of restricted glacial erosion and/or glacial deposition coincides with a zone of basal melting. In one area of agreement, the model predicts basal freezing over the unmodified preglacial landscape. Overall, there is little agreement between the modelled basal thermal regime and the location of the landscape types, although the pattern of basal thermal regime does help to explain the preservation of the unmodified preglacial landscape. It could also be argued that there is a relationship between the location of

restricted glacial erosion and/or deposition and the zone of basal melting because a thawed bed condition is required for glacial deposition (Boulton 1974; Mooers 1990).

6.3.2 Convergence and divergence of flow

When convergence and divergence of ice flow are included in the calculations of basal thermal regime, the pattern becomes more complex (Figure 6.1b). The eastern half of the flowband is still a zone of basal melting, and warm based ice occurs at several other locations in the flowband, most notably in two ice streams following the routes of the Spey and Dee Valleys. These zones of basal melting are a function of the relatively high basal ice velocities and high ice thicknesses found in topographic depressions. The two areas of basal melting are separated by a zone of cold based ice, predominantly between 0°C and -8°C but where temperatures fall below -8°C in isolated spots. Two small patches of basal melting also occur within this cold based zone (Figure 6.1b).

The pattern of basal thermal regime at the ice sheet maximum, including convergence and divergence of flow, shows a strong relationship with the pattern of areal scouring, as zones of intense ice sheet erosion are associated with basal melting and zones of minimal ice sheet erosion are associated with basal freezing. The area dominated by areal scouring in the west of the transect coincides with a zone of basal melting centred over the Spey valley

(Figure 6.1c). The area immediately to the east where areal scouring is uncommon coincides with a zone of basal freezing and a zone of areal scouring follows a tongue of warm based ice extending along the Dee Valley. Finally, an area of infrequent areal scouring in the extreme east of the flowband coincides with a zone of basal melting.

The good fit is confirmed by comparison between Figure 6.1b and the landscape classification (Figure 6.1d). Landscapes of areal scouring in the west coincide with basal melting. The area of upland selective linear erosion coincides with a zone of predominantly cold based ice within which small patches of basal melting occur, and the area characterised by selective linear erosion coincides with a zone of basal ice which is warm based in topographic depressions but flanked by cold based ice. These are precisely the thermal conditions under which these landscapes of selective linear erosion might be expected to form, with a transition from warm based ice in depressions to cold based ice on interfluves. A zone of basal freezing coincides with the area where the preglacial landscape survives unmodified in the west. This prediction is in good agreement with the original hypothesis in that the preservation of the preglacial landscape is likely where basal freezing is the dominant thermal regime.

Overall there is a strong relationship between the modelled basal thermal regime and the distribution of the landscape types. The pattern of basal

temperatures explains the location of four of the five landscape classes. Areal scouring is closely correlated with warm based ice, areas of upland selective linear erosion and selective linear erosion are associated with zones where there is a transition from warm based to cold based ice, and the unmodified preglacial landscape is associated with a zone of basal freezing. The exception is in the east where there is a relationship between warm based ice and limited glacial erosion. However, here there is a partial agreement in that the field evidence of scouring on hill summits and glacial tills is a product of warm based ice.

The pattern of basal temperatures at the ice sheet maximum including convergence and divergence of ice flow also explains the variations in the depth of ice sheet erosion (Figure 6.1d). For example, the depth of erosion indicated in the unmodified preglacial landscape class is low, at the lower end of a range of 10 to 40 metres and this is an area associated with basal freezing. The depth of erosion indicated in the zone of areal scouring is high, at the upper end of a range of 35 to 47.5 metres and this is an area associated with basal melting. The greatest average depths of erosion are associated with upland selective linear erosion (108 to 152 metres), an area where basal melting in valleys is predicted.

In summary, zones of basal melting and freezing only coincide with areas of intense and minimal ice sheet erosion if convergence and divergence of

flow are taken into account in the calculation of basal thermal regime. With this effect included, the basal thermal regime shows a strong correlation with the regional pattern of ice sheet erosion.

6.4 Comparisons at the local scale

The tests at the local scale involve the comparison between the calculated basal thermal regime at the ice sheet maximum and the distribution of glacial and preglacial landforms in the field study areas. The five topographic cross sections used in the calculations of basal thermal regime are shown in Figures 6.2 to 6.6. The basal topography, the calculated basal thermal regime and the intensity of modification by ice sheet erosion are indicated. In each case the upper limit of the box represents the ice surface, determined by a 50 kPa parabolic profile. The calculated basal thermal regime is shown for the models assuming uniform ice flow and including convergence and divergence of flow. Direction of ice sheet movement in all cases is into the plane of the paper.

Two basal thermal conditions are distinguished; basal freezing and basal melting. The extent of these thermal regimes is indicated immediately below the line representing the basal topography. In order to simplify representation of the field evidence, two categories of ice sheet modification are distinguished; areas of glacial erosion and areas of limited glacial modification (Figures 6.2 to 6.6). The superimposition of the intensity of

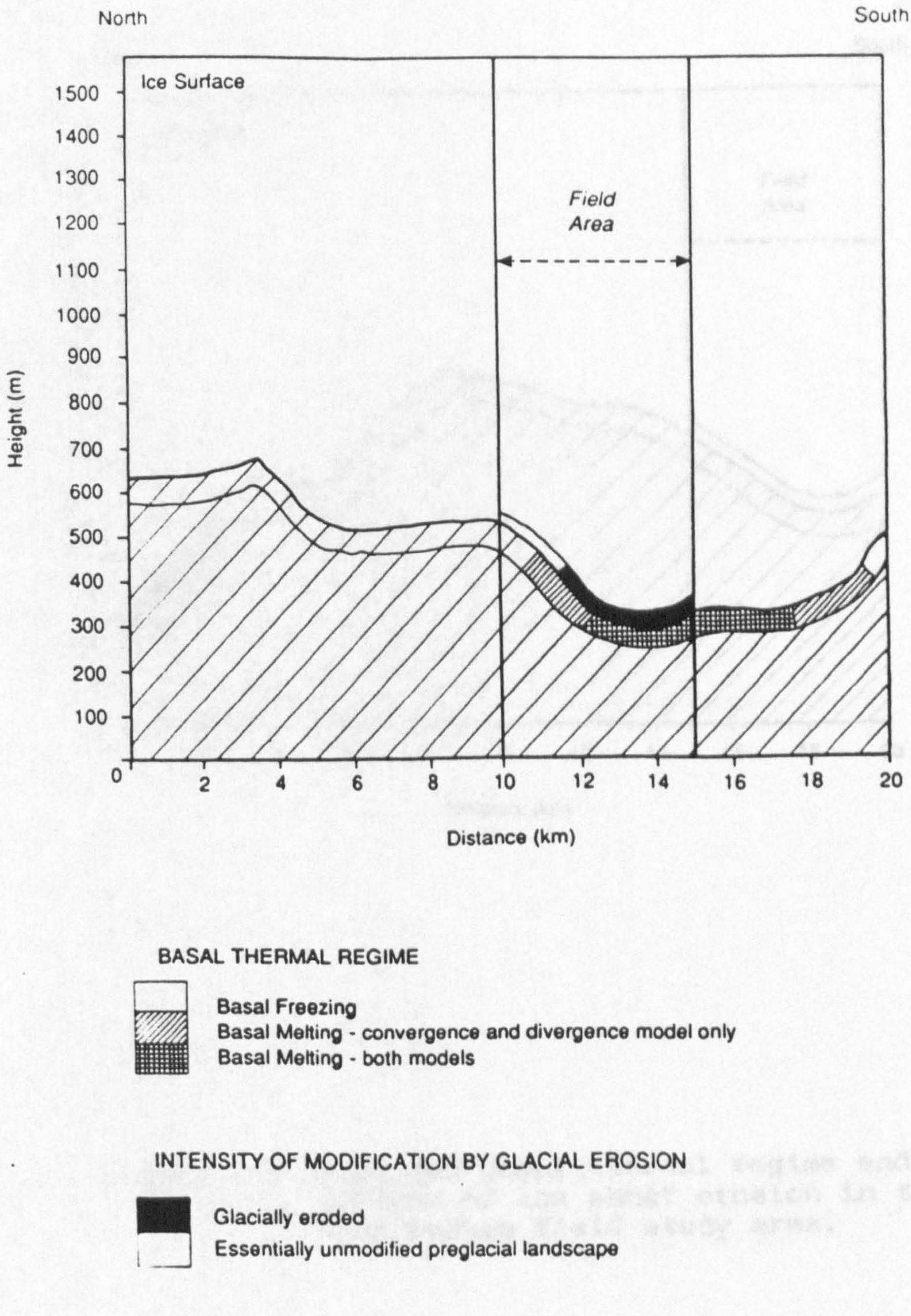

Figure 6.2 Modelled basal thermal regime and pattern of ice sheet erosion in the Speyside field study area.

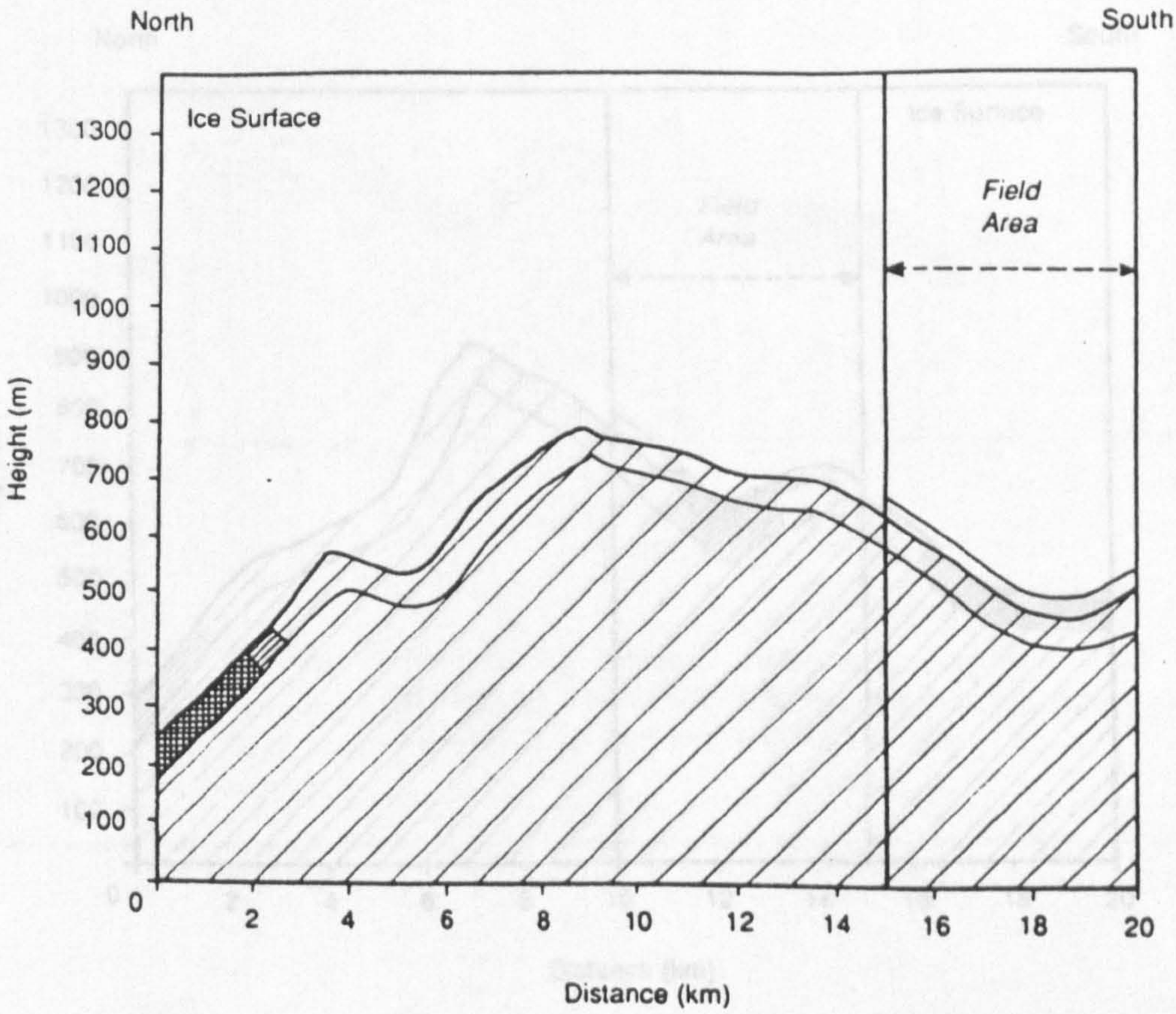

Figure 6.3 Modelled basal thermal regime and pattern of ice sheet erosion in the Glen Feshie field study area.

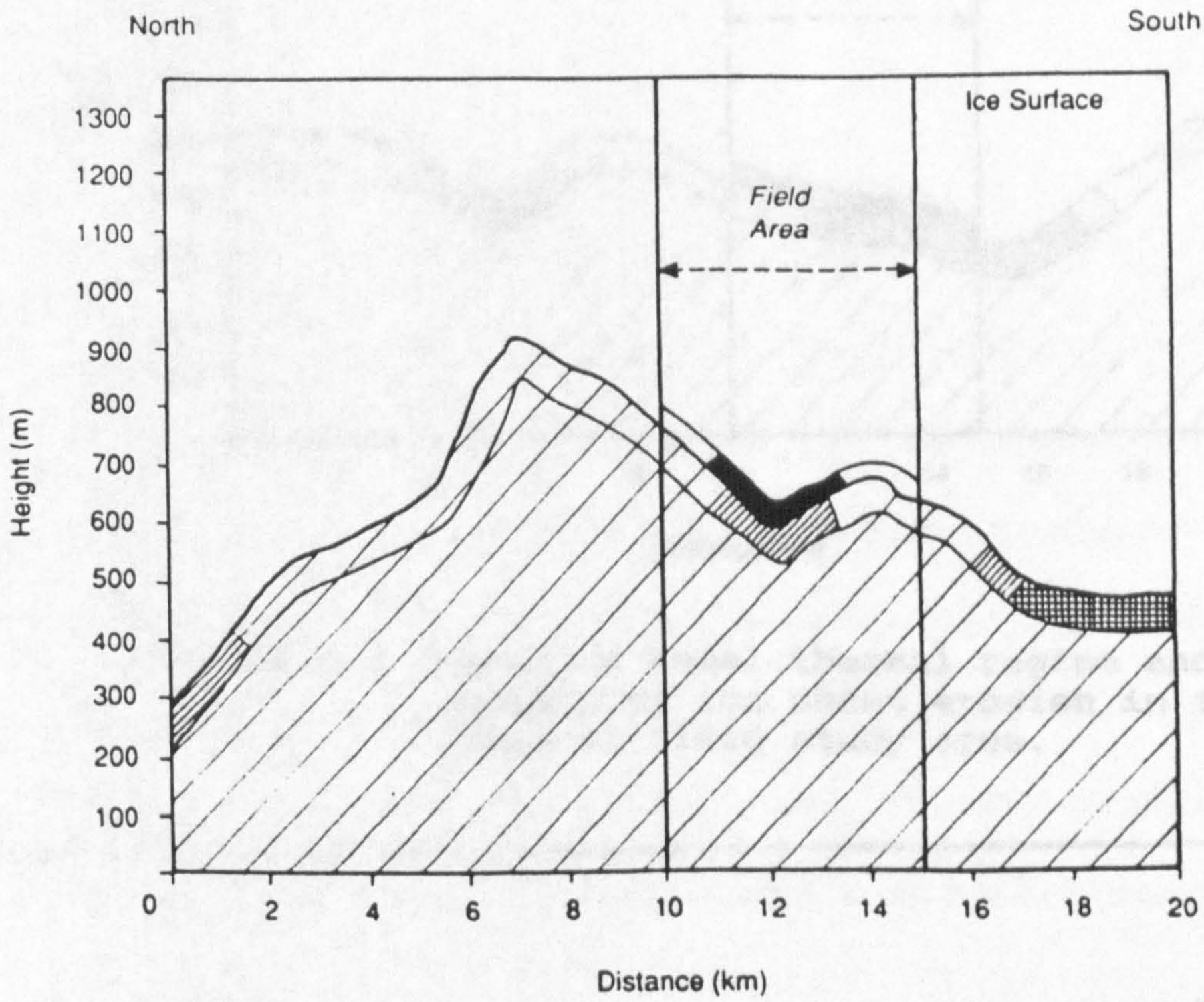

Figure 6.4 Modelled basal thermal regime and pattern of ice sheet erosion in the Cairngorms field study area.

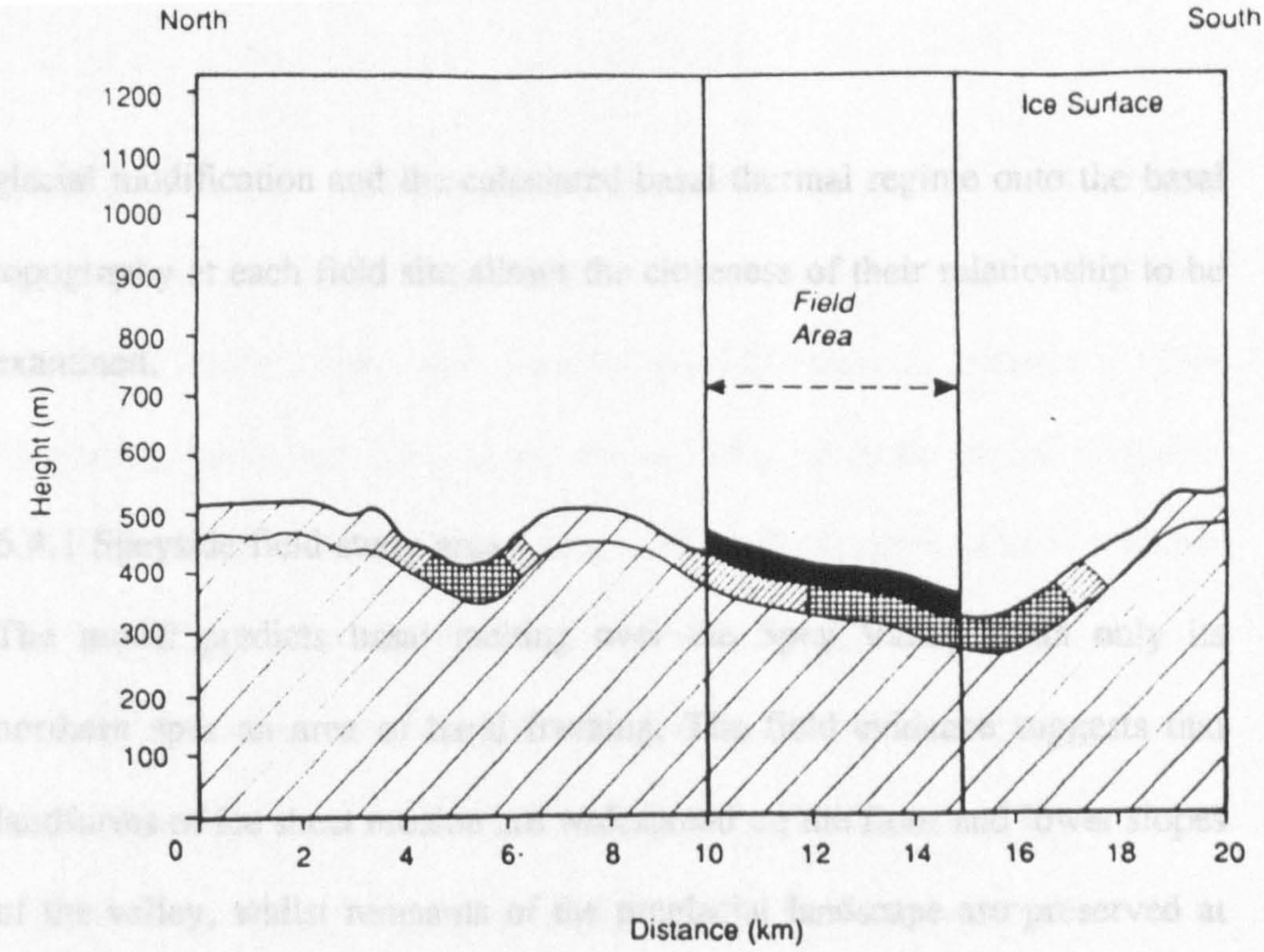

Figure 6.5 Modelled basal thermal regime and pattern of ice sheet erosion in the Balmoral field study area.

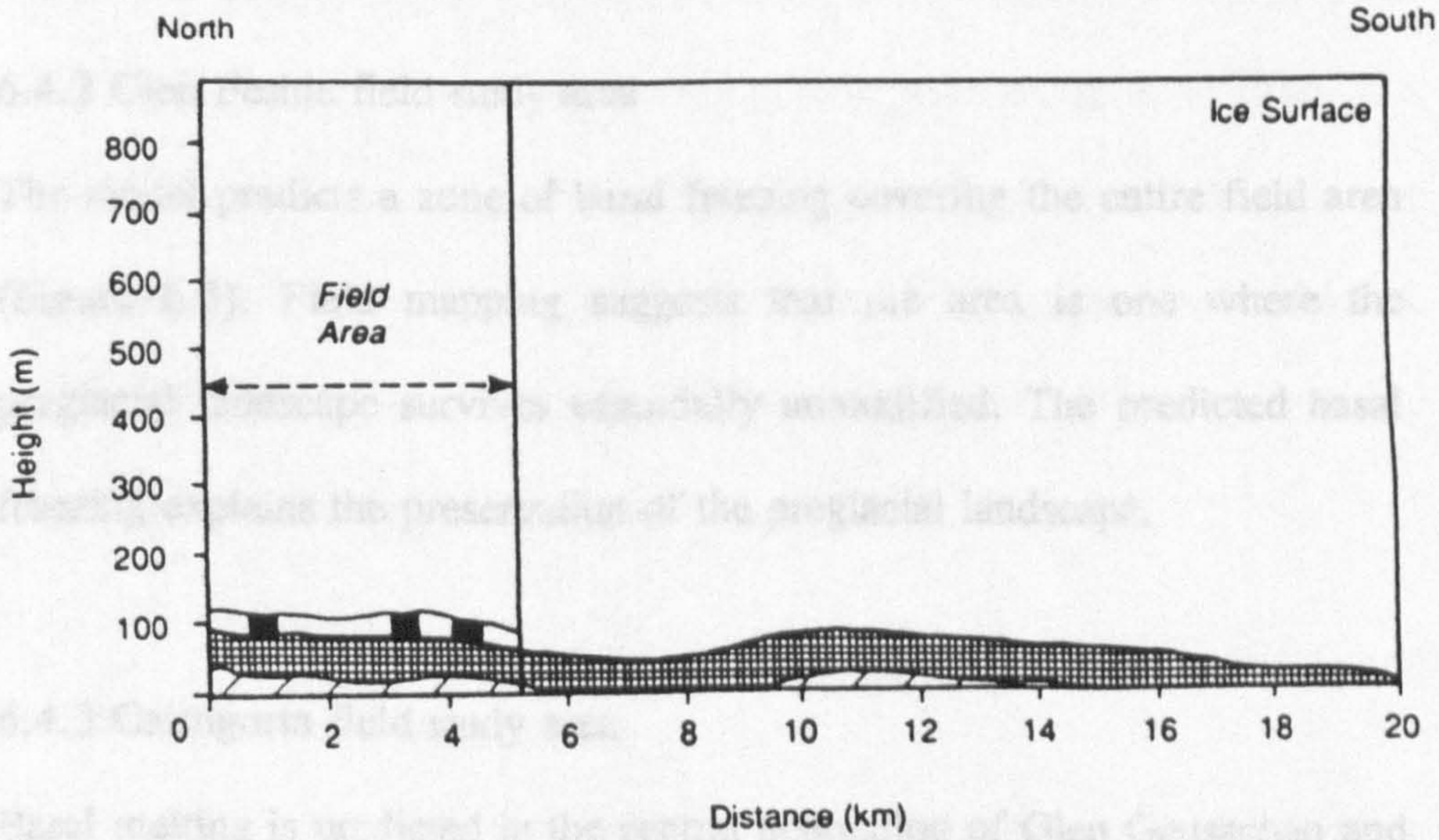

Figure 6.6 Modelled basal thermal regime and pattern of ice sheet erosion in the Aberdeen field study area.

glacial modification and the calculated basal thermal regime onto the basal topography at each field site allows the closeness of their relationship to be examined.

6.4.1 Speyside field study area

The model predicts basal melting over the Spey Valley, with only its northern spur an area of basal freezing. The field evidence suggests that landforms of ice sheet erosion are widespread on the floor and lower slopes of the valley, whilst remnants of the preglacial landscape are preserved at a distance from the valley. The upper field limit of the intense areal scouring is 400 metres and this coincides with a calculated upper limit of basal melting of 420 metres (Figure 6.2). There is therefore a good correlation between the area of intense erosion and the predicted zone of basal melting.

6.4.2 Glen Feshie field study area

The model predicts a zone of basal freezing covering the entire field area (Figure 6.3). Field mapping suggests that the area is one where the preglacial landscape survives essentially unmodified. The predicted basal freezing explains the preservation of the preglacial landscape.

6.4.3 Cairngorm field study area

Basal melting is predicted in the central depression of Glen Geusachan and basal freezing on the surrounding interfluves (Figure 6.4). The predicted

upper limit of the zone of basal melting is 640 metres. The field evidence suggests that landforms of glacial erosion are restricted to the valley floor and lower slopes; the upper limit of glacial erosional features in Glen Geusachan is around 800 metres. Above this, remnants of the preglacial landscape survive on both valley sides. Although the upper limit of erosional features is higher than the upper limit of basal melting, there is nevertheless a good correlation since the zone of basal melting in the valley coincides with an area of ice sheet erosion, and the zone of basal freezing coincides with an area where the preglacial landscape survives unmodified.

6.4.4 Balmoral field study area

The model run predicts that the entire field area is a zone of basal melting (Figure 6.5). The field evidence in this area suggests that it is predominantly an area of intense ice sheet erosion, with the development of large scale roches moutonnees in the Dee Valley and slopes leading away from the valley floor. The maximum altitude of glacial erosional features in this area is around 470 metres. This conforms with a calculated upper limit of basal melting of 500 metres. Thus there is remarkably good agreement between the model and the field evidence.

6.4.5 Aberdeen field study area

The model predicts that the entire field area is a zone of basal melting (Figure 6.6). This is an area of restricted glacial erosion and /or glacial

deposition with ice sheet erosion restricted to isolated hill summits and saprolite surviving in low-lying basins. In this case the predicted basal melting does not show a strong correlation with field evidence of restricted glacial erosion. However, the predicted zone of basal melting helps explain the presence of the glacial tills in the study area, as well as the scouring on hill summits.

6.4.6 Synthesis of comparisons at the local scale

The predicted basal thermal regime matches the field evidence in four of the five field areas. In the Glen Feshie and Balmoral areas there is a strong correlation, with zones of basal freezing and melting coinciding with the preglacial landscape and glacial erosion respectively. In the Speyside field study area a zone of basal melting explains the development of the glacial landforms on the floor of the valley, and in the Cairngorm field area basal melting in valleys and basal freezing on the higher slopes explains the selectivity of ice sheet erosion. In the Aberdeen field study area there is little correlation between the calculated basal ice temperatures and intense glacial erosion. With the latter exception, the predicted basal thermal regime explains the location, and in some cases the precise boundaries, of the areas of ice sheet erosion and protection.

6.5 Confidence level of results

Before the results of the comparisons can be assessed it is necessary to

scrutinize further the method of comparison and the reliability of the data used in the comparisons. Visually the match between the zones of thermal regime and intensity of ice sheet erosion is good (Figure 6.1). Unfortunately, it is not possible to test the strength of the relationship between the calculated basal ice temperatures and the observed pattern of erosion statistically. However, it is useful to assess the potential errors which may cause the relationship to exist by coincidence as an alternative means of assessing the value of the comparison. There are potential errors linked to both the model and the field evidence.

6.5.1 Model reliability

A potential error is that the model incorrectly calculates basal ice temperatures. This possibility can be dismissed as serious since the model has been shown to predict basal ice temperatures under the Antarctic ice sheet to within 0.1°C of measured ice core temperatures (Budd et al. 1971b).

Other errors may arise because of the values chosen to represent the input parameters. The sensitivity of the model to changes in input parameter values was examined using sensitivity tests, summarised in Table 6.1. The biggest changes are due to changes in the ice surface profile and the mean annual air temperature at the ice sheet margin.

The adoption of a 100 kPa ice sheet profile increases the ice thickness and

MODEL PARAMETER	NATURE OF CHANGE	EFFECT ON BASAL ICE TEMPERATURE	MODEL SENSITIVE?
Ice sheet profile	Increasing ice thickness	Warmer	YES, esp. near margin
Velocity	Increasing velocity	Warmer	YES, esp. near margin
Mean annual air temperature	Increasing surface temperature	Warmer	YES
Basal Topography	Increasing resolution	Warmer in valleys Colder on interfluves	YES
Altitudinal lapse rate	Increasing lapse rate	Colder	NO
Geothermal heat flux	Increasing heat flux	Warmer	NO
Accumulat-ion rate	Reducing accumulation	Warmer at divide Colder at margin	NO

Table 6.1 Sensitivity of basal ice temperatures to changes in model parameters.

thus results in warmer basal ice temperatures. The effects are most important near the ice sheet margin since the relative increase in ice thickness is greatest in this area. Values of basal shear stress under ice sheets lie in the range of 50 to 100 kPa (Paterson 1981). A 100 kPa parabola produces a steep ice sheet profile and therefore great ice thicknesses. Since recent research stresses the importance of local topography in influencing ice flow and implies that former ice sheets were relatively thin (Ballantyne 1990; Murray and Locke 1989; Thorp 1991), a 50 kPa parabola is more likely to describe correctly the former ice surface. If the ice sheet were thinner than predicted by the 50 kPa parabola, then an increase in the extent of basal freezing is likely.

A direct relationship exists between the mean annual air temperature imposed at the ice sheet margin and basal ice temperatures; the warmer the imposed marginal temperature the warmer the basal temperature and vice versa. Increasing the mean annual air temperature from -9°C to -3°C is sufficient to produce basal melting over the majority of the ice sheet bed. However, mean annual air temperatures above -9°C are considered unlikely on the basis of the palaeoecological literature (Table 2.1). If mean annual air temperatures were below -9°C, an increase in basal freezing would result.

Other factors which are important in the model are the representation of the ice sheet bed and changes in ice sheet velocity due to convergence and

divergence of flow (Table 6.1). An accurate representation of the basal topography is used, with a high spatial resolution used in calculations of basal thermal regime. Sensitivity tests of the method used to assign convergence and divergence of flow in the topographic cross-sections suggest that the calculated basal temperatures are minimum values. Changes in the method are especially important near the ice sheet margin where balance velocities are greatest. Decreasing the increment attached to convergence and divergence of flow results in a cooling of basal ice temperatures, although the overall pattern of basal thermal regime remains stable.

The predicted basal thermal regime in the Aberdeen field study area is one of basal melting, but the erosional evidence could reflect basal freezing with only localised pressure melting. The mismatch in this area may be a result of the high basal ice velocities calculated by the balance velocity term near the equilibrium line, which lead to artificially high basal temperatures.

Another issue which must be addressed is the assumption that the ice sheet reached a steady-state. Although true steady-state may not have occurred, recent work by Hindmarsh et al. (1989) suggests that the characteristic temperature distribution in a thermo-mechanically coupled ice sheet of a warm based zone inside the margin and a cold based interior emerges early in the evolution of an ice sheet. High dissipation from internal deformation

and basal friction causes temperatures just inside the margin to rise quickly. This pattern persists through the ice sheet's evolution until it reaches a near steady-state. A true equilibrium is not reached even after a long time period, because cold ice introduced at high altitudes eventually reaches the margin and has a slight cooling effect (Hindmarsh et al. 1989). Thus, although true steady-state is never reached, a relatively constant temperature field is possible. If the Scottish ice sheet remained relatively stable at its maximum position, then such a near steady-state could exist (Boulton et al. 1991). Even if the Scottish ice sheet did not attain a true steady-state maximum, its basal temperature distribution may not have been far-removed from such a steady-state solution.

6.5.2 Field evidence

Another potential source of error lies in the fieldwork. Detailed fieldwork at study sites in each of the landscape classes suggests the aerial photograph interpretation provides a reasonable picture of the regional pattern of ice sheet erosion. It should be noted that a slight discrepancy occurs in the east of the transect, where aerial photograph interpretation suggests restricted glacial erosion, but detailed fieldwork reveals many isolated hill summits to be ice scoured (Hall and Sugden 1987). The small scale of these features and the depth of drift cover renders them obscure on aerial photographs. The regional map is likely to be a minimum estimate of the intensity of ice sheet erosion as small scale features may be under-represented.

A second factor which must be considered is the extent of preglacial weathering, since this is crucial in the estimates of the depth and location of ice sheet erosion. This is especially important in the context of this area of Scotland, since it is known to have been greatly affected by deep chemical weathering in preglacial times (Hall 1985). One of the assumptions used in estimating depths of erosion is that preglacial weathering depths were relatively uniform, constituting a mantle 10 to 50 metres deep. Whilst these depths seems reasonable, chemical weathering in favourable locations such as basins and valleys may have exceeded this amount. In the Aberdeen field study area, saprolite survives in basins but does not occur on hill summits. In all other field areas the reverse is the case, with saprolites preserved on high ground and stripped from valleys and basins.

The survival of saprolite in the basins of North East Scotland may be because the depth of preglacial weathering was much greater than on surrounding hills. Relatively uniform depths of ice sheet erosion have since left pockets of saprolite intact only where the weathering was sufficiently deep to survive modification. If this is the case the ice sheet may indeed have been warm based over this area.

Although there are therefore limitations in both the model and the field evidence, the errors are not sufficiently large to detract from the main

conclusion that there is a good fit between the modelled basal thermal regime and the pattern of ice sheet erosion in the study area. The main problem appears to be in the marginal area of the ice sheet, where the model predictions are most sensitive to changes in the input parameters and the field evidence is most difficult to interpret.

CHAPTER SEVEN

DISCUSSION AND CONCLUSIONS

7.1 Alternative explanations

Before developing the implications of the correlations between the model predictions and the field evidence made in Chapter 6 it is necessary to consider alternative explanations for the observed pattern of ice sheet erosion. The significance of the apparent relationship between basal thermal regime and ice sheet erosion is increased if alternative factors are unable to explain the observed pattern of erosion. Other factors which are important in this context are glaciological and geological.

7.1.1 Glaciological factors

Andrews (1972) suggests velocity is a key variable determining patterns of erosion under ice sheets as it is a measure of the amount of work done by the glacier system, or 'the energy of glacierization'. The amount of work done is a function of the mass loss at the equilibrium line, which is related to the ice sheet velocity. High velocities also increase frictional heating and are therefore important in producing areas of basal melting. From a theoretical point of view, the higher the velocity, the more basal ice which passes a given point on the bedrock and therefore the greater the erosion

potential. For these reasons, the calculated pattern of velocity might be expected to reflect the pattern of ice sheet erosion. Comparing the pattern of ice sheet erosion (Figure 6.1) with the pattern of ice sheet velocity (Figure 3.11a) shows this is not the case. Lowest velocities are found near the ice divide where areal scouring is the dominant landform type and depths of erosion are high; high velocities are found near the equilibrium line in an area of restricted ice sheet erosion and/or deposition where depths of erosion are low. The calculated pattern of velocity at ice sheet maximum is insufficient on its own to explain the observed pattern of erosion. However, this does not preclude the possibility that the pattern of ice sheet erosion is related to patterns of velocity at time periods other than glacial maximum.

Hallet (1979) and Boulton (1979) have suggested that patterns of ice sheet erosion will be related to areas of low effective pressure, as the high basal water pressure in these locations reduces overburden pressure and facilitates sliding over bedrock. High basal water pressures and therefore low effective pressures are predicted over valley areas where basal meltwater collects in subglacial conduits (Hooke 1989). The work presented in this thesis supports this theory since both basal meltwater production and intensity of ice sheet erosion are greatest along valleys. However, the location of areas of low effective pressure alone cannot explain the pattern of ice sheet erosion because the rate of basal meltwater production is a function of basal ice temperature and therefore ultimately governed by the requirement for basal

melting. The reduction in effective pressure due to basal melting and the associated rise in sliding velocity coupled with fluctuations in basal water pressure could, however, be a process enhancing glacial erosion in valley areas (Iverson 1990; Sugden et al., submitted).

7.1.2 Geological factors

Geological factors such as lithology (Zumberge 1955), rock structure (Addison 1981), and relative particle hardness (Boulton 1979) are known to influence the processes of glacial erosion at the local scale. Without a detailed project to map the joint structures, orientations and fault patterns for the whole transect, it is difficult to isolate the role of bedrock geology. However, a simple geological map of the area shows the bedrock to consist entirely of metamorphics, predominantly schist, and igneous rocks (Figure 7.1). The granites are known to be relatively uniform throughout this area of Scotland (Barrow et al. 1912) and, in addition, do not differ greatly from metamorphic rocks in compressive strength. Values for the unconfined compressive strength of these rock types vary from 55.2 MPa in the case of schist to 141.1 MPa in the case of granite (Goodman 1980). Both these values lie in a range well above the cryostatic stresses quoted by Drewry (1986), suggesting their susceptibility to glacial erosion may not be radically different. The geological map shows little correlation with the calculated depths of ice sheet erosion, and although rock type may be an important control on glacial erosion at a local scale, it does not explain the variation

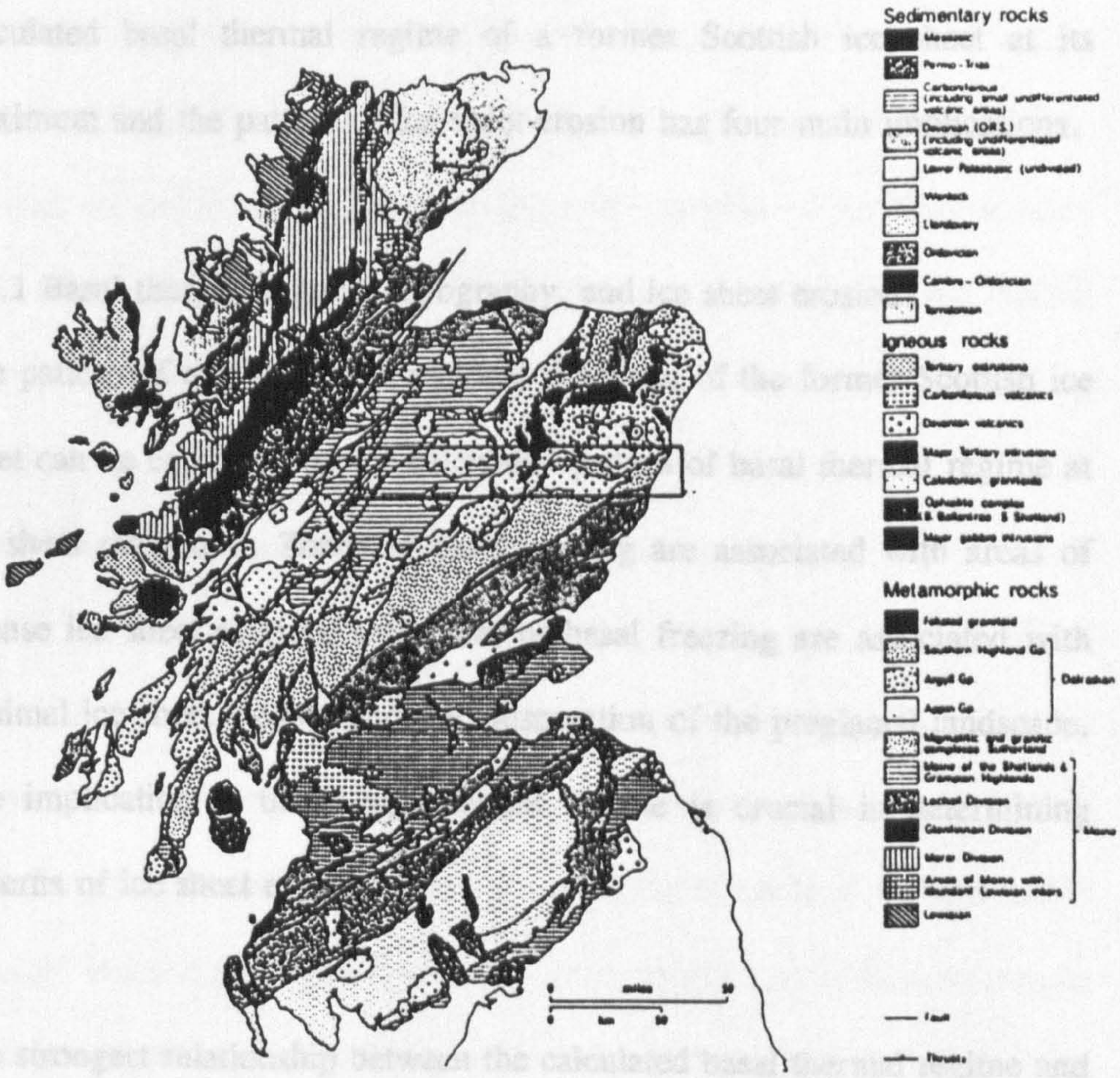

Figure 7.1 Bedrock geology of the regional transect study area.

Adapted from Craig (1983).

in intensity of erosion over wider zones of the ice sheet.

7.2 Implications of results

In the absence of alternative explanations, the agreement between the calculated basal thermal regime of a former Scottish ice sheet at its maximum and the pattern of ice sheet erosion has four main implications.

7.2.1 Basal thermal regime, topography, and ice sheet erosion

The pattern of erosion in the regional flowband of the former Scottish ice sheet can be explained by the calculated pattern of basal thermal regime at ice sheet maximum. Zones of basal melting are associated with areas of intense ice sheet erosion, and zones of basal freezing are associated with minimal ice sheet erosion and the preservation of the preglacial landscape. The implication is that basal thermal regime is crucial in determining patterns of ice sheet erosion.

The strongest relationship between the calculated basal thermal regime and pattern of erosion occurs when the effects of topography are included in the calculations. This produces zones of convergent and divergent ice flow, which are associated with zones of basal melting and freezing respectively. Zones of intense ice sheet erosion are concentrated in areas where the basal topography favours convergence of flow. The important role of topography is highlighted by comparison of the model calculations which calculate basal

ice temperatures with and without including the effect of convergent and divergent ice flow (Figure 6.1 a and b).

The implication of this finding is that without a detailed consideration of subglacial topography the predicted pattern of basal ice temperatures will be a gross oversimplification. Previous attempts to compare models of basal thermal regime at ice sheet maximum with patterns of ice sheet erosion (e.g. Gordon 1979) have resulted in a mismatch partly because the models lack a sufficiently detailed representation of the subglacial topography.

The relationship between basal thermal regime, topography, and ice sheet erosion has important implications for studies of landscape evolution under ice sheets. It means that landscape evolution is governed to a great extent by the preglacial topography; large preglacial valleys will capture and maintain flow during ice sheet initiation and are exploited to become the sites of ice streams. Positive feedback through erosion ensures these ice streams remain important in determining the location of areas of relatively high basal temperatures, and thus continued erosion.

7.2.2 The importance of the ice sheet maximum

Since the pattern of ice sheet erosion shows a strong relationship with the pattern of basal thermal regime modelled at the ice sheet maximum, including convergence and divergence of flow, the implication is that much

of the erosion under this part of the former ice sheet occurred during maximum conditions.

The apparent importance of the pattern of basal thermal regime at the ice sheet maximum is surprising since other patterns of erosion would be expected to occur during build-up and decay (Boulton and Clark 1990; Boulton 1991). The influence of basal thermal regime at time periods other than the glacial maximum is difficult to assess because very little is known about the evolution of ice sheet thermal regime over time.

During growth, the evolution of an ice sheet's thermal regime is complex since it depends on overall climate, mass balance, rate of growth, the long term vertical and horizontal advection of accumulating ice, and the interaction between all these variables. The complexity allows very little certainty to be placed in possible thermal regimes at time periods other than a steady-state maximum condition. Hindmarsh et al. (1989), however, suggest that a pattern of warm based margin and cold based interior emerges early in ice sheet evolution. A. Payne (Pers. Comm.) has modelled the growth of the Fennoscandian ice sheet using a thermodynamic model. The model predicts that certain zones of thermal regime remain stable during ice sheet growth since the ice sheet is cold based at the divide and warm based at the margin. As the ice sheet expands, these thermal zones move outwards so that a zone of basal melting near the ice sheet margin advances across the

landscape. This result is compatible with the predicted basal thermal regime for this part of the Scottish ice sheet at its maximum, where basal ice temperatures increase with distance from the ice divide.

The match between calculated basal ice temperatures at ice sheet maximum and the pattern of ice sheet erosion implies that the period of glacial maximum may have been a protracted event, since the ice sheet would require a relatively long period of time to establish an erosional pattern. Although the time of the maximum thickness and extent of the ice sheet over Scotland is not known, the ice sheet may have been stable at its maximum position for some considerable length of time. The mismatch between the modelled basal thermal regime and the pattern of erosion in the Aberdeen area may be due to the influence of thermal regime at time periods other than maximum, such as during growth and decay.

The suggestion that many of the glacial erosional features in Scotland were formed at ice sheet maximum deserves further attention since there is evidence from mountain massifs such as the Cairngorms and Lochnagar that the formation of radial troughs represents a period of local ice cap glaciation. Numerous high level corries and radial troughs such as Glens Dee, Derry, Muick and Shee suggest that many glacial erosional features are not related to ice sheet maximum conditions. However, the orientation of Glens Geusachan, Avon and Einich which are incised into the Cairngorm

massif, are related to full ice sheet flow across the mountains (Sugden 1968). In addition, all the evidence in the regional transect studied here points to erosion under an ice sheet flowing eastward over the area. The large scale glacial troughs of the Spey and Dee, and the large cliffed roches moutonnees developed along the Dee all suggest the erosion is related to a period of relatively stable eastward ice flow at right angles to flow from the adjacent mountain massifs.

7.2.3 Depth and rate of ice sheet erosion

The calculated depths of erosion are important because of the recent debate over depths of erosion under former ice sheets. Gravenor (1975), Sugden (1976) and Kaszycki and Shilts (1987) have argued that depths of erosion under the Laurentide ice sheet amount to the removal of no more than a few tens of metres, whereas White (1972, 1988) and Bell and Laine (1985) argue for erosion of several hundreds of metres. Volume estimates of glacially-derived sediment in the offshore record have not resolved the debate because of the problems in relating the volume of glacial sediment in an offshore region to an assumed glacial source area, and because of the problem of estimating the contribution of glacial debris to marine sediments (Summerfield 1991). Thus the disparity in the estimates of depth of glacial erosion under the Laurentide ice sheet has not been resolved by examination of the oceanic record. The same offshore record leads Bell and Laine (1985) to estimate the total amount of rock eroded by ice sheets to range between

100 and 200 metres, and Kaszycki and Shilts (1987) to conclude the total glacial denudation to be less than 20 metres.

Given this disparity, it is difficult to assess the significance of the depths of erosion calculated for this area of Scotland. A minimum depth of ice sheet erosion of 34 metres and a maximum of 61.5 metres is closer to the minimal estimates of Gravenor (1975), Sugden (1976) and Kaszycki and Shilts (1987) than to those of White (1972, 1988) and Bell and Laine (1985). In addition, the preservation of remnants of a preglacial weathering cover are strong evidence that although ice sheet erosion in Scotland may have been locally very important, overall depths of erosion are relatively low.

However, these estimates do not account for erosion of the preglacial landsurface prior to the onset of glaciation. The review in Chapter 5 of the hypothetical erosional processes acting upon the Scottish landscape immediately prior to glaciation suggests a probable ranking of these processes in order of importance as follows. Fluvial erosion is likely to have been the most quantitatively important process, followed by periglacial, aeolian and coastal erosion. Bearing this in mind, it is possible to recalculate the volume of glacial erosion in the transect with the depth of preglacial weathering mantle adjusted to take into account a wider range of possible preglacial topographic considerations. These recalculations were made in the same manner as those presented in Chapter 5 except that the

assumed depth of regolith varies to allow for higher amounts of preglacial erosion. This gives the following estimates:

Assumed depth of regolith	Total volume of glacial erosion in study area	Depth of erosion per unit area	Rate a	Rate b
5 m	68.991 km^3	24.9 m	0.249 mma^{-1}	0.049 mma^{-1}
10	80.55	29	0.29	0.058
20	103.67	37	0.37	0.074
30	126.775	45.6	0.456	0.091
40	149.88	53.6	0.536	0.1
50	173	62	0.62	0.124

Rate a applies to a glacial occupancy of 100,000 years and Rate b applies to a glacial occupancy of 500,000 years.

The calculated depths of erosion can be used to calculate rates of ice sheet erosion and are equivalent to the removal of a layer of regolith averaging a minimum of 34 metres and a maximum of 61.5 metres in depth. Taking the mean of these two values, 47.77 metres, yields an average erosion rate over the whole Quaternary (~2 million years) of 0.025 mma^{-1}. Since it is unlikely that full glacial conditions existed throughout the Quaternary, this

calculation underestimates the rate of erosion. Oxygen isotope studies of deep ocean cores can be used to derive estimates of the volume of glacier ice on land, and these suggest a minimum length of glaciation of 100,000 years and a maximum of 500,000 years in the Quaternary (Shackleton 1990). A glacial occupancy of 100,000 years yields an average erosion rate of 0.477 mma^{-1}, and a glacial occupancy of 500,000 years yields an average erosion rate of 0.1 mma^{-1}. These erosion rates of between 0.1 mma^{-1} and 0.5 mma^{-1} are consistent with the estimates of Andrews (1972), and with the observed erosion rates of between 0.5 mm^{-1} and 1 mma^{-1} under present day glaciers in Iceland (Boulton 1974).

The calculations of the depth of ice sheet erosion assuming preglacial erosion of any weathering mantle fall mostly within the brackets given above. However, assuming a depth for this regolith of only 5 metres the calculated glacial erosion rates through the Quaternary are low (0.049 to 0.249 mma^{-1}) and of the same order of magnitude as those suggested by Summerfield (1991) for rates of fluvial denudation in temperate regions (0.03 to 0.07 mma^{-1}). With higher assumed depths of regolith, the calculated rates of glacial erosion exceed the fluvial rate given above only if glacial occupancy was around 100,000 years. With a longer glacial occupancy (500,000 years) rates of glacial erosion only exceed the fluvial rates if the assumed depth of regolith were around 30 metres. The conclusion is that if length of glacial occupancy were nearer the upper figure and the depth of the preglacial

weathering mantle was reduced to under 30 metres by preglacial erosion, then rates of glacial erosion are comparable to those of fluvial erosion. However, the rates are still faster than those of other erosional processes such as aeolian, periglacial and coastal.

7.2.4 Meltwater production under the former ice sheet

The map of calculated melt rates under this part of the former ice sheet suggests that high melt rates of up to 10 mma^{-1} are found along the route of the present Dee Valley (Figure 3.15). The annual discharge of subglacial meltwater along a proto-Dee would help to explain the number of large subglacial channels reflecting eastward meltwater flow in this area. Numerous large channels up to 60 metres deep, such as Clais Fhearnaig (NJ 075 934), cut eastward across valley spurs in the eastern Cairngorms, whilst much of the north east of Scotland is covered by a network of subglacial meltwater channels (Clapperton and Sugden 1977). The suggestion that large quantities of meltwater followed the Dee Valley is supported by Munro (1986), who notes the occurrence of no less than 21 major channels or channel systems in the area covered by the lower Dee near Aberdeen. The channel systems trend approximately west to east and are associated with large quantities of meltwater sediments (Munro 1986). Thus the geomorphological evidence supports the predicted location of high rates of meltwater production.

7.2.5 The problem of the mismatch in the Aberdeen field study area

The mismatch between the predicted basal melting and the field evidence of restricted glacial erosion in the Aberdeen field study area deserves further discussion. There are several possible explanations for this mismatch. First, the field area is located close to the former ice margin, an area where the model calculations are most sensitive to changes in the ice sheet profile, ice velocities and the imposed marginal cooling. Thus the mismatch may be a result of the model sensitivity near the ice margin. Second, the preglacial weathering cover may have been thicker in this lowland area. A great depth and intensity of ice sheet erosion is therefore required to explain the removal of the greater thickness of weathered rock, a result compatible with a predicted zone of basal melting. Third, it is possible that the permeability of the weathered rock reduced sliding at the ice/rock interface because subglacial meltwater drained through the permeable material (Hall and Sugden 1987). Thus erosion was supressed even in this zone of basal melting. Finally, the area occupies a zone of deposition because it is near an ice margin. Evidence of areal scouring is therefore obliterated by the depth of glacial sediments (Sugden 1978). This suggestion is supported by the widespread till cover in the area (Munro 1986). Thus the mismatch in the Aberdeen area can be explained in several ways, and does not undermine the conclusion that there is a strong correlation between basal thermal regime and ice sheet erosion.

7.3 Further work

The model is a starting point in investigating the variation in basal thermal regime under the ice sheet, and could be refined by the addition of, for example, more detailed input parameter values. This might include a more complex accumulation or ice surface temperature pattern, or higher grid resolution. Calculations could also be made of basal ice temperatures in a true three dimensional topography where the effects of convergent flow are transmitted to subsequent cross sections along a flow line. These improvements were not made to the model presented in the thesis because the increase in accuracy which they represent in a regional context is probably low. In addition, the mathematics of three dimensional ice flow have yet to be solved (Hooke 1989).

Another obvious refinement to the model of basal ice temperatures would be to relax the assumption of ice sheet maximum and extend the calculations of temperatures to periods of ice sheet build-up and decay. The evolution of the basal temperature field could then be traced over a glacial cycle, and its relationship to topography during these crucial initiation and decay periods could be examined. This would inevitably lead to a higher level of explanation since some of the ice sheet erosion must be the product of events at the start and close of glacial cycles.

An overall aim must be to consider the role of topography and the effects

7.3 Further work

The model is a starting point in investigating the variation in basal thermal regime under the ice sheet, and could be refined by the addition of, for example, more detailed input parameter values. This might include a more complex accumulation or ice surface temperature pattern, or higher grid resolution. Calculations could also be made of basal ice temperatures in a true three dimensional topography where the effects of convergent flow are transmitted to subsequent cross sections along a flow line. These improvements were not made to the model presented in the thesis because the increase in accuracy which they represent in a regional context is probably low. In addition, the mathematics of three dimensional ice flow have yet to be solved (Hooke 1989).

Another obvious refinement to the model of basal ice temperatures would be to relax the assumption of ice sheet maximum and extend the calculations of temperatures to periods of ice sheet build-up and decay. The evolution of the basal temperature field could then be traced over a glacial cycle, and its relationship to topography during these crucial initiation and decay periods could be examined. This would inevitably lead to a higher level of explanation since some of the ice sheet erosion must be the product of events at the start and close of glacial cycles.

An overall aim must be to consider the role of topography and the effects

of convergence and divergence of ice flow in future ice sheet models. Consideration of the ice sheet bed and its interaction with ice sheet dynamics will lead to more realistic and testable models of ice sheets, both past and present.

7.4 Conclusions

The conclusions of the thesis can be summarised as follows:

(1) There is a strong correlation between the pattern of basal thermal regime at the ice sheet maximum and the pattern of ice sheet erosion if the effects of topography on ice flow are taken into account.

(2) The implication is that much of the erosion under this part of the former ice sheet occurred at the ice sheet maximum.

(3) Estimates of the depth of ice sheet erosion in the flowband of the former ice sheet suggest depths of glacial denudation of between 34 metres and 61.5 metres. These depths of erosion are equal to rates of glacial denudation between 0.1 and 0.5 mma^{-1}. This is the first time such calculations have been made at this level of detail.

(4) A map of the location and calculated quantity of meltwater production under the former ice sheet suggests melt rates of up to 10 mma^{-1} are found in valley areas where the topography favours convergence of ice flow.

Mathematical Nomenclature

K - constant dependent on basal shear stress (-)
h - ice surface elevation (m)
s - ice sheet half width (m)
x - distance from ice divide (m)
H - ice surface elevation at ice divide (m)
Ob - basal ice temperature (°C)
Os - ice surface temperature (°C)
Z - ice thickness (m)
Yb - basal temperature gradient (°C/100m)
Ys - ice surface temperature gradient (°C/100m)
y - dimensionless thermal parameter (-)
Yg - geothermal heat flux (W/m/sec)
τ_b - basal shear stress (kPa)
V - ice velocity (m/s)
J - mechanical equivalent of heat (J)
K - thermal conductivity of ice (W/m/sec)
ρ - density of ice ($kgcm^{-2}$)
g - gravitational constant ($cmsec^{-2}$)
α - ice surface slope (radians)
A - accumulation rate (m/a)
Ax - mean accumulation rate (m/a)
λ - altitudinal lapse rate (°C/100m)
k - temperature dependent thermal diffusivity of ice (W/m/sec)
erf y - error function (-)
F(x) - Dawson integral (-)
M - basal melt rate (ma^{-1})
Yc - calculated base gradient (°C/100m)
l - latent heat of fusion of ice ($kJkg^{-1}$)
A - flow law parameter (Pa^{-3}/s)
n - flow law multiplier (-)
U - average velocity (m/a)
q - ice discharge (m/a)

LIST OF REFERENCES

Abramowitz M. and Stegun I.A. (1965)
Handbook of mathematical functions with formulas, graphs, and mathematical tables. Dover Publications, New York.

Addison K. (1981)
The contribution of discontinuous rock-mass failure to glacier erosion. Ann. Glaciol. 2; 3-10.

Alley R.B. (1989)
Ice sheets and climate. Earth and Mineral Sciences 58; 41-45.

Alley R.B., Blankenship D.D., Rooney S.T. and Bentley C.R. (1989)
Water-pressure coupling of sliding and bed deformation: III. Application to Ice Stream B, Antarctica. J. Glaciol. 35; 130-39.

Andrews J.T. (1972)
Glacier power, mass balance, velocities and erosion potential. Z.Geomorph.13; 1-17.

Andrews J.T. (1982)
On the reconstruction of Pleistocene ice sheets: a review. Quat. Sci. Rev. 1; 1-30

Andrews J.T., Clark P., and Stravers J.A., (1985)
The patterns of glacial erosion across the eastern Canadian Arctic in Andrews J.T. (ed) Quaternary Environments - Eastern Canadian Arctic, Baffin Bay and Western Greenland; 69-92. Allen and Unwin, London.

Andrews J.T. and Miller G.H. (1979)
Glacial erosion and ice sheet divides, northeastern Laurentide ice sheet, on the basis of the distribution of limestone erratics. Geology 7; 592-6.

Aseyen A.A. and Makkaveyen A.N. (1977)
Glaciomorphological criteria for erosion by former continental ice caps on Europe. Materialy Glyatsiologicheskikh Issledovaniy. Khronika Obsuzhdeniya 29; 240-7 (English Summary p. 247).

Bakker J.P. (1965)
A forgotten factor in the interpretation of glacial stairways. Z. Geomorph. N.F. Suppl. Bd. 9; 18-34.

Ballantyne C.D. (1990)
The Late Quaternary glacial history of the Trotternish Escarpment, Isle of Skye, Scotland, and its implications for ice-sheet reconstruction. Proc. Geol. Ass. 101; 171-86.

Barrow G., Cunningham Craig E.H., and Hinxman L.W. (1912)
The geology of the districts of Braemar, Ballater and Glen Clova (explanation of sheet 65). Mem. Geol. Surv. Scot. London, H.M.S.O.

Barrow G., Hinxman L.W., and Cunningham Craig E.H. (1913)
The geology of Upper Strathspey, Gaick and the Forest of Atholl (explanation of sheet 64). Mem. Geol. Surv. Scot. London, H.M.S.O.

Battey M.H. (1960)
Geological factors in the development of Veslgjuvbotn and Vesl-Skautbotn. Royal Geographical Society Research Series No. 7; 5-11.

Bell M. and Laine E.P. (1980)
More evidence from the deep sea on the depth of glacial erosion in North America. EOS 61; 276.

Bell M. and Laine E.P. (1985)
Erosion of the Laurentide Region of North America by glacial and glacio-fluvial processes. Quat. Res. 23; 154-174.

Bouchard M. (1985)
Weathering and weathering residuals on the Canadian Shield. Fennia 163; 327-32.

Bouchard M. and Godard A. (1984)
Les alterites du bouchlier Canadien: Premier bilan d'une campagne de reconnaissance. Geographie physique et quaternaire 38; 149-163.

Boulton G.S. (1972)
The role of thermal regime in glacial sedimentation. Institute of British Geographers Spec. Pub. No. 4; 1-19.

Boulton G.S. (1974)
Processes and patterns of glacial erosion. In Coates D.R. (ed) Glacial Geomorphology: Proceedings of 5th Geomorphological Symposium, Binghampton, N.Y. 1974; 41-87. State Univ. New York, Binghampton.

Boulton G.S. (1979)
Processes of glacial erosion on different substrata. J. Glaciol. 23; 15-37.

Boulton G.S. (1991)
Glacier erosion, deposition and sediment dispersal through glacial cycles. INQUA Abstracts, XIII International Congress, Beijing, China; p.33.

Boulton G.S., Jones A.S., Clayton K.M., and Kenning M.J. (1978)
A British ice sheet model and patterns of glacial erosion and deposition in Britain. In Shotton F.W., (ed) British Quaternary Studies: Recent advances; 231-246. Oxford University Press, Oxford.

Boulton G.S., Smith G.D., Jones A.S., and Newsome J., (1985)
Glacial geology and glaciology of the last mid-latitude ice sheets. J.Geol.Soc.London 142; 447-474.

Boulton G.S. and Clark C.D. (1990)
A highly mobile Laurentide ice sheet revealed by satellite imagery of glacial lineations. Nature 346; 813-817.

Boulton G.S., Peacock J.D. and Sutherland D.G (1991)
Quaternary. In Craig G.Y. (ed) Geology of Scotland 3rd Edition; 503-543. The Geological Society, London.

Boyé M. (1968)
Défense et illustration de l'hypothèse du "defonçage périglaciaire". Biuletyn Peryglacjalyn 17; 5-56.

Braun D.D. (1989)
Glacial and periglacial erosion of the Appalachians. In Gardner T.W. and Sevon W.D. (Eds) Appalachian Geomorphology. Geomorphology 2; 233-256.

Brepson R. (1979)
Simulated glacier sliding over an obstacle. J. Glaciol. 23; 143-56.

Brotchie J.F. and Silvester R. (1969)
On crustal flexure. J. Geophysical Research 74; 5240-52.

Buchardt B. (1978)
Oxygen isotope palaeotemperatures from the Tertiary period in the North Sea. Nature 275; 121-3.

Budd W.F. (1969)
The dynamics of ice masses. ANARE Scientific Reports, Ser. A(IV). Glaciology. Publication No. 108.

Budd W.F. and Young N.W. (1979)
Results from the I.A.G.P. flow-line study inland of Casey, Wilkes Land, Antarctica. J. Glaciol. 24; 89-101.

Budd W.F., Jenssen D., and Radok U. (1971a)
Derived physical characteristics of the Antarctic ice sheet. ANARE Interim Reports, Ser. A. Glaciology. Publication No. 120.

Budd W.F., Jenssen D., and Radok U. (1971b)
Reinterpretation of deep ice temperatures. Nature 232; 84-85.

Budd W.F., Keage P.L., and Blundy N.A. (1979)
Empirical studies of ice sliding. J. Glaciol. 23; 157-70.

Caine N. (1967)
The tors of Ben Lomond, Tasmania. Z. Geomorph 11; 418-429.

Carol H. (1947)
The formation of roches moutonnées. J. Glaciol. 1; 57-59.

Chapman C.A. and Rioux R.L. (1958)
Statistical study of topography, sheeting and jointing in granite, Acadia National Park, Maine. Am. J. Sci. 256; 111-127.

Clapperton C.M. and Sugden D.E. (1977)
The Late Devensian glaciation of North-East Scotland. In Gray J.M. and Lowe J.J. (eds) Studies in the Scottish Lateglacial Environment; 1-13. Pergamon, Oxford.

Clowes A. and Comfort P. (1982)
Process and Landform: An outline of contemporary geomorphology. Oliver and Boyd, Edinburgh.

Coope G.R. (1975)
Climatic fluctuations in northwest Europe since the last interglacial, indicated by fossil assemblages of Coleoptera. In Wright A.E. and Moseley F. (eds) Ice Ages: Ancient and Modern; 153-168. Seel House Press, Liverpool.

Coope G.R. (1977)
Quaternary Coleoptera as aids in the interpretation of environmental history. In Shotton F.W. (ed) British Quaternary Studies: Recent Advances; 55-68. Oxford University Press, Oxford.

Craig G.Y. (1983)
Geology of Scotland. Scottish Academic Press, Edinburgh.

Dansgaard W., White J.W.C., and Johnsen S.J. (1989)
The abrupt termination of the Younger Dryas climate event. Nature 339; 532-534.

Devoy R.J.N. (1987)
Sea Surface Studies: A global view. Croom Helm, London.

Diamond M. (1960)
Air temperature and precipitation on the Greenland ice sheet. J. Glaciol. 3; 558-67.

Dowdeswell J.A. (1986)
Drainage-basin characteristics of Nordaustlandet ice caps, Svalbard. J. Glaciol. 32; 31-38.

Drewry D. (1986)
Glacial Geologic Processes. Edward Arnold, London.

Duval P. (1979)
Creep and recrystallization of polycrystalline ice. Bull. de Mineralogie 102; 80-5.

Embleton C. and King C.A.M. (1975)
Glacial Geomorphology. Edward Arnold, London.

Eyles N (1985)
Glacial Geology: An introduction for engineers and earth scientists. Pergamon, Oxford.

Faniran A. and Jeje L.K. (1983)
Humid tropical geomorphology. Longman, London.

Feininger T. (1971)
Chemical weathering and glacial erosion of crystalline rocks and the origin of till. U.S. Geological Survey Professional Paper 750-C; 65-81.

Fitzpatrick E.A. (1963)
Deeply weathered rock in Scotland, its occurrence, age, and contribution to soils. J. Soil Science 14; 33-43.

Frenzel B. (1967)
Die Klimaschwankungen des Eiszeitalters. Braunschweig, Vieweg.

Geological Survey of Britain (Scotland) Sheet 62. London, H.M.S.O.

Geological Survey of Britain (Scotland) Sheet 63. London, H.M.S.O.

Geological Survey of Britain (Scotland) Sheet 64. London, H.M.S.O.

Geological Survey of Britain (Scotland) Sheet 77. London, H.M.S.O.

Gerrard A.J. (1988)
Rocks and landforms. Unwin Hyman, London.

Glasser N.F. and Warren C.R. (1990)
Medium scale landforms of glacial erosion in South Greenland; Process and form. Geogr. Ann. 72A; 211-215.

Godard A. (1962)
L'efficacitė de l'erosion glaciaire en Ecosse du nord. Revue de Geomorphologie Dynamique 12; 33-42.

Goodman R.E (1980)
Introduction to rock mechanics. Wiley and Sons, New York.

Gordon J.E. (1979)
Reconstructed Pleistocene ice-sheet temperatures and glacial erosion in Northern Scotland. J. Glaciol 22; 331-44.

Graf W.L. (1970)
The geomorphology of the glacial valley cross-section. Arctic and Alpine Research 2; 303-12.

Gravenor C.P. (1975)
Erosion by continental ice sheets. Am. J. Sci. 275; 594-604.

Gray J.M. and Lowe J.J. (1977)
Studies in the Scottish lateglacial environment. Pergamon, Oxford.

Grosswald M.G. and Glazovsky A.F. (1984)
Glacial erosion of continental margins. Polar Geogr. Geol. 8; 113-27.

Hall A.M. (1983)
Weathering and landform evolution in north-east Scotland. Unpublished PhD thesis, Univ. of St. Andrews.

Hall A.M. (1985)
Cenozoic weathering covers in Buchan, Scotland and their significance. Nature 315; 392-95.

Hall A.M. (1986)
Deep weathering patterns in north-east Scotland and their geomorphological significance. Z. Geomorph N.F. 30; 407-22.

Hall A.M. (1990)
Pre-Quaternary landscape evolution in the Scottish Highlands. Transactions of the Royal Society of Edinburgh: Earth Sciences 82; 1-26.

Hall A.M. and Sugden D.E. (1987)
Limited modification of mid-latitude landscapes by ice sheets: the case of north-east Scotland. Earth Surface Processes and Landforms 12; 531-42.

Hall A.M. and Mellor A. (1988)
The characteristics and significance of deep weathering in the Gaick area, Grampian Highlands, Scotland. Geogr. Ann. 70A; 309-14.

Hall A.M., Mellor A., and Wilson M.J. (1989)
The clay mineralogy and age of deeply weathered rocks in north-east Scotland. Z. Geomorph. Suppl. Bd. 72; 97-108.

Hallet B. (1979)
A theoretical model of glacial abrasion. J. Glaciol. 23; 39-50.

Harbor J.M., Hallet B., and Raymond C.F. (1988)
A numerical model of landform development by glacial erosion. Nature 333; 347-9.

Harland W.B. (1957)
Exfoliation joints and ice action. J. Glaciol. 3; 8-10.

Harry W.T. (1965)
The form of the Cairngorm granite pluton. Scot. J. Geol. 1; 1-8.

Hillefors A., (1985)
Deep-weathered rock in western Sweden. Fennia 163; 293-301.

Hindmarsh R.C.A., Boulton G.S., and Hutter K. (1989)
Modes of operation of thermo-mechanically coupled ice sheets. Ann. Glaciol. 12; 57-69.

Holmes R. (1977)
Quaternary deposits of the central North sea, 5. The Quaternary geology of the UK sector of the North Sea between 56° and 58° N. Report of the Institute of Geological Sciences 77/14.

Hooke R.L. (1977)
Basal temperatures in polar ice sheets: A qualitative review. Quat. Res. 7; 1-13.

Hooke R.L. (1989)
Englacial and subglacial hydrology: A qualitative review. Arctic and Alpine Research 21; 221-33.

Hooke R.L., Laumann, T. and Kohler, J. (1990)
Sublacial water pressures and the shape of subglacial conduits. J. Glaciol. 36; 67-71.

Hughes T.J. (1981)
Numerical reconstruction of paleo-ice sheets. In Denton G.H. and Hughes T.J. (eds) The Last Great Ice Sheets; 222-74. John Wiley and Sons, New York.

Iverson N.R. (1990)
Laboratory simulations of glacial abrasion: comparison with theory. J. Glaciol. 36; 304-14.

Iverson N.R. (1991)
Potential effects of subglacial water-pressure fluctuations on quarrying. J. Glaciol. 37; 27-36.

Jahns R.H. (1943)
Sheet structure in granite; its origin and use as a measure of glacial erosion in New England. J. Geol. 51; 71-98.

Jenssen D. (1977)
A three-dimensional polar ice sheet model. J. Glaciol. 18; 373-90.

Jonsson S. (1983)
On the geomorphology and past glaciation of Storöya, Svalbard. Geogr. Ann. 65A; 1-17.

Kaitanen V. (1985)
Problems concerning the origin of inselbergs in Finnish Lapland. Fennia 163; 359-64.

Kaszycki C.A. and Shilts W.W. (1979)
Average depth of glacial erosion, Canadian Shield. Geol. Surv. Can. Pap. 79- 1B; 395-6.

Kaszycki C.A. and Shilts W.W. (1980)
Glacial erosion of the Canadian Shield: Calculation of average depths. At. Eng. Can. Ltd., Tech. Rep., TR-106, 37 pp.

Kaszycki C.A. and Shilts W.W. (1987)
Glacial erosion of the Canadian Shield. In Shilts W.W., Aylsworth C.A., Kaszycki C.A., and Klassen R.A. (eds) in Graf W.L. (ed) Geomorphic systems of North America, Geol. Soc. Am. Cent. Vol.2; 155-61.

Kejonen A. (1985)
Weathering in the Wyborg rapakivi area, southeastern Finland. Fennia 163; 309-13.

Kerr A.R. (Submitted)
The initiation of maritime ice sheets. Z. Gletscherk. Glazialgeol.

Kleman J. (1988)
Linear till ridges in the southern Norwegian-Swedish mountains - evidence for a subglacial origin. Geogr. Ann. 70A; 35-45.

Kleman J. and Borgström I. (1990)
The boulder fields of Mt. Fulufjället, west-central Sweden. Geogr. Ann. 72A; 63-78.

Kleman J., Borgström I., Robertsson A-M. and Lilliesköld M. (1991)
Pre-Late Weichselian morphology and stratigraphy at Transtrandsfjällen and Fulufjället, south-central Sweden. Submitted to Journal of Quaternary Science.

Klimaszewski M. (1964)
On the effect of the preglacial relief on the course and magnitude of glacial erosion in the Tatra mountains. Geographia Polonica 2; 11-21.

Lagerbäck R. (1988a)
Periglacial phenomena in the wooded areas of Northern Sweden - relicts from the Tärendö Interstadial. Boreas 17; 487-99.

Lagerbäck R. (1988b)
The Veicki moraines in northern Sweden - widespread evidence of an Early Weichselian deglaciation. Boreas 17; 469-86.

Lagerbäck R. and Robertsson A-M. (1988)
Kettle holes - stratigraphical archives for Weichselian geology and palaeoenvironment in northernmost Sweden. Boreas 17; 439-68.

Lahti S.I. (1985)
Porphyritic pyroxene bearing granitoids - a strongly weathered rock group in central Finland. Fennia 163; 315-21.

Laine E.P. (1980)
New evidence from beneath the western North Atlantic for the depth of glacial erosion in Greenland and North America. Quat. Res. 14; 188-98.

Laine E.P. and Bell M. (1982)
Reply to Andrew's comment. Quat. Res. 17; 125-27.

Lamb H.H (1977)
Climate: Present, Past and Future - Volume 2: Climatic History and the Future. Methuen, London.

Lee W.H.K. and Uyeda S. (1965)
Review of heat flow data. In Lee, W.H.K. (ed) Terrestrial Heat Flow; 87-190. American Geophysical Union, Washington.

Leopold L.B., Wolman M.G., and Miller J.P. (1964)
Fluvial process in geomorphology. W.H. Freeman and Company, San Francisco.

Lewis W.V. (1954)
Pressure release and glacial erosion. J. Glaciol. 2; 417-22.

Lidmar-Bergström K. (1982)
Pre-Quaternary geomorphological evolution in southern Fennoscandia. Sveriges geologiska undersøkning, Ser. C. 785, Uppsala. 202 pp.

Lidmar-Bergström K. (1988a)
Preglacial weathering and landform evolution in Fennoscandia. Geogr. Ann. 70A; 273-6.

Lidmar-Bergström K. (1988b)
Exhumed Cretaceous landforms in south Sweden. Z. Geomorph. N.F. Suppl. Bd. 72; 21-40.

Lindström E. (1988)
Are roches moutonnées mainly preglacial forms? Geogr. Ann. 70A; 323-31.

Linton D.L. (1949)
Some Scottish river captures re-examined. Scott. Geogr. Mag. 65; 123-32.

Linton D.L. (1952)
The significance of tors in glaciated lands. Proc. 8th Gen. Assembly Int. Geogr. Congr. (Washington 1947); 354-57.

Linton D.L. (1955)
The problem of tors. Geogr. Journal 121; 470-87.

Linton D.L. (1959)
Morphological contrasts between eastern and western Scotland. In Miller R. and Watson J.W. (eds) Geographical Essays in Honour of Alan Ogilvie; 16-45. Nelson, Edinburgh.

Lliboutry L.A. (1968)
General theory of subglacial cavitation and sliding of temperate glaciers. J. Glaciol. 7; 21-58.

Lorius C., Jouzel J., Raynaud D., Hansen J., and Le Treut H. (1990)
The ice-core record: climate sensitivity and future greenhouse warming. Nature 347; 139-45.

Lowe J.J. and Walker M.J.C. (1984)
Reconstructing Quaternary Environments. Longman, New York.

Lundqvist J. (1985)
Deep-weathering in Sweden. Fennia 163; 287-92.

Lundqvist J. (1988)
The Revsund Area, Central Jämtland - an example of preglacial weathering and landscape formation. Geogr. Ann. 70A; 291-298.

Mabbutt J.A. (1961)
'Basal surface' or 'weathering front'. Proc. Geol. Assn. 72; 357-8.

Marchant D.R. (1990)
Surficial geology and stratigraphy in Arena Valley, Quartermain Mountains, Antarctica: Implications for Late Tertiary glacial history. Unpublished Masters thesis, Univ. of Maine, 312pp.

Marchant D.R. and Denton G.H. (1990 in press)
Late Tertiary ice-sheet overriding: Evidence from Neibelungen Valley, Western Asgard Range, Antarctica. Ant.J. of U.S.

Marchant D.R., Denton G.H., Wilson S.C., and Swisher C. (1991)
Paleoclimatic significance of Taylor Glacier fluctuations in Arena Valley, Antarctica. Submitted to Geogr. Ann.

Matthes F.E. (1930)
Geologic history of the Yosemite Valley. U.S. Geological Survey, Professional Paper No. 160.

Matthes F.E. (1937)
Exfoliation of massive granite in the Sierra Nevada of California. Proc. Geol Soc. Am. for 1936; 342-3.

Mazo V.L. (1987)
Effects of glacial erosion on the flow of ice sheets and the morphology of their beds. I.A.H.S. Publ. No. 70; The Physical basis of ice sheet modelling; 145-52.

Mazo V.L. (1989)
Waves on glacier beds. J. Glaciol. 35; 179-82.

McCraw J.D. (1965)
Landscapes of central Otago. N.Z. Geog. Misc. Ser. No. 5; 30-45.

McIntyre N.F. (1985)
The dynamics of ice-sheet outlets. J. Glaciol. 31; 99-107.

Mooers H.D. (1990)
A glacial-process model: the role of spatial and temporal variations in glacial thermal regime. Geological Society of America Bulletin 102; 243-51.

Morisawa M. (1985)
Rivers. Longman, London, 222pp.

Munro M. (1986)
Geology of the country around Aberdeen. Mem. Br. Geol. Surv. Sheet 77. H.M.S.O. London.

Murray D.R. and Locke W.W. III (1989)
Dynamics of the late Pleistocene Big Timber Glacier, Crazy Mountains, Montana, USA. J. Glaciol 35; 183-92.

Nesje A. and Sejrup H.P. (1988)
Late Weichselian/Devensian ice sheets in the North Sea and adjacent land areas. Boreas 17; 371-84.

Nichols T.C. Jnr. (1980)
Rebound, its nature and effect on engineering works. Q. J. Engng. Geol. 13; 133-52.

Nye J.F. (1952)
A method of calculating the thicknesses of the ice sheets. Nature 169; 529-30.

Nye J.F. (1965)
The flow of a glacier in a channel of rectangular, elliptical or parabolic cross-section. J. Glaciol. 5; 661-90.

Nye J.F. and Martin P.C.S. (1968)
Glacial erosion. Association Internationale d'Hydrologie Scientifique Publ. No. 79; 78-86.

Oerlemans J. (1984)
Numerical experiments on large-scale glacial erosion. Zeit. Gletscherk. Glazialgeol. 20; 107-26.

Ollier C.D. (1965)
Some features of granite weathering in Australia. Z. Geomorph. 9; 285-304.

Ollier C.D. (1984)
Weathering. Longman, London.

Palmer J. (1956)
Tor formation at the Bridestones in North-east Yorkshire, and its significance in relation to problems of valley-side development and regional glaciation. Trans. Int. Brit. Geog. 22; 55-71.

Paterson W.S.B. (1981)
The Physics of Glaciers. Pergamon, Oxford.

Payne A.J. (1988)
Modelling former ice sheets. Unpublished PhD thesis, University of Edinburgh.

Payne A.J. and Sugden D.E. (1990)
Topography and ice sheet growth. Earth Surface Processes and Landforms 15; 625-40.

Payne A.J., Sugden D.E., and Clapperton C.M. (1989)
Modeling the growth and decay of the Antarctic Peninsula ice sheet. Quat. Res. 31; 119-34.

Phemister T.C. and Simpson S. (1949)
Pleistocene deep weathering in North-east Scotland. Nature 164; 318-9.

Philberth K. and Federer B. (1971)
On the temperature profile and the age profile in the central part of cold ice sheets. J. Glaciol. 10; 3-14.

Porter S.C. (1989)
Some geological implications of average Quaternary glacial conditions. Quat. Res. 32; 245-261.

Rainbird R.H., Nesbitt H.W., and Donaldson J.A. (1990)
Formation and diagenesis of a sub-Huronian saprolith: comparison with a modern weathering profile. J. Geol. 98; 801-22.

Rastas J. and Seppälä M. (1981)
Rock jointing and abrasion forms on roches moutonnées, S.W. Finland. Ann. Glaciol. 2; 159-63.

Reed W.J. (1988)
The vertical dimensions of the last ice-sheet and late Quaternary glacial event in Northern Ross-shire, Scotland. Unpublished PhD thesis, University of St. Andrews.

Reeh N. (1982)
A plasticity theory approach to the steady-state shape of a three-dimensional ice sheet. J. Glaciol. 28; 431-55.

Reeh N. (1988)
A flow-line model for calculating the surface profile and the velocity, strain-rate, and stress fields in an ice sheet. J. Glaciol. 34; 46-54.

Richards K. (1982)
Rivers: Form and process in alluvial channels. Methuen, London.

Richey J.E. (1964)
Granite. Mine Quarry Engng. 30; 20-5.

Robin G. de Q. (1976)
Is the basal ice of a temperate glacier at the pressure melting point? J. Glaciol. 16; 183-96.

Rodhe L. (1988)
Glaciofluvial channels formed prior to the last deglaciation: examples from Swedish Lapland. Boreas 17; 511-6.

Röthlisberger H. (1968)
Erosive processes which are likely to accentuate or reduce the bottom relief of valley glaciers. Int. Assoc. Sci. Hydrol. Publ. 79; 87-97.

Röthlisberger H. and Iken A. (1981)
Plucking as an effect of water-pressure variations at the glacier bed. Ann. Glaciol. 2; 57-62.

Rudberg S. (1973)
Glacial erosion forms of medium size - a discussion based on four Swedish case studies. Z. Geomorph. N.F. Suppl. Bd. 17; 33-48.

Selby M.J. (1977)
On the origin of sheeting and laminae in granitic rocks: evidence from Antarctica, The Namib Desert and the Central Sahara. Madoqua 10; 171-9.

Shackleton N.J., Berger A., and Peltier W.R. (1990)
An alternative astronomical calibration of the lower Pleistocene timescale based on ODP Site 677. Transactions of the Royal Society of Edinburgh: Earth Sciences 81; 251-61.

Sharp M., Dowdswell J.A., and Gemmell J.C. (1989a)
Reconstructing past glacier dynamics and erosion from glacial geomorphic evidence: Snowdon, North Wales. J. Quat. Sci. 4; 115-30.

Sharp M., Gemmell J.C. and Tison J-L. (1989b)
Structure and stability of the former subglacial drainage system of the Glacier De Tsanfleuron, Switzerland. Earth Surface Processes and Landforms 14; 119-134.

Shreve R.L. (1984)
Glacier sliding at subfreezing temperatures. J. Glaciol. 30; 341-47.

Sissons J.B. (1981)
The last Scottish ice-sheet; facts and speculative discussion. Boreas 10; 1-17.

Sissons J.B. (1983)
Quaternary. In Craig G.Y. (ed) Geology of Scotland 2nd Edition; 399-424. Scottish Academic Press, Edinburgh.

Sørensen R. (1988)
In-situ rock weathering in Vestfold, southeastern Norway. Geogr. Ann. 70A; 299-308.

Sparks B.W. (1971)
Rocks and relief. Longman, London 404pp.

Spencer E.W. (1977)
Introduction to the structure of the earth. McGraw-Hill, New York 640pp.

Stewart F.S. (1991)
A reconstruction of the Eastern margin of the late Weichselian ice sheet in Northern Britain. Unpublished PhD Thesis, University of Edinburgh.

Stoker M.S. and Bent A.J.A. (1985)
Middle Pleistocene glacial and glaciomarine sedimentation and in the west central North Sea. Boreas 14; 325-332.

Stoker M.S., Long D., and Fyfe J.A. (1985)
A revised Quaternary stratigraphy for the central North Sea. Report British Geological Survey 17; 2.

Sugden D.E. (1965)
Aspects of the glaciation of the Cairngorm Mountains. Unpublished D.Phil. Thesis, University of Oxford.

Sugden D.E. (1968)
The selectivity of glacial erosion in the Cairngorm Mountains, Scotland. Trans. Inst. Brit. Geogr. 45; 79-92.

Sugden D.E. (1974)
Landscapes of glacial erosion in Greenland and their relationship to ice, topographic and bedrock conditions. In Waters R.S. and Brown E.H. (eds) Progress in Geomorphology; 177-95. London, Institute of British Geographers (Institute of British Geographers Special Publication No. 7).

Sugden D.E. (1976)
A case against deep erosion of shields by ice sheets. Geology 4; 580-82.

Sugden D.E. (1977)
Reconstruction of the morphology, dynamics, and thermal characteristics of the Laurentide Ice Sheet at its maximum. Arctic and Alpine Research 9; 21-47.

Sugden D.E. (1978)
Glacial erosion by the Laurentide Ice Sheet. J. Glaciol. 20; 367-91.

Sugden D.E. (1987)
The Landscape. In Omand D. (ed) The Grampian Book; 48-68. Northern Times, Golspie.

Sugden D.E. (1989)
Modification of old land surfaces by ice sheets. Z. Geomorph. 72; 163-72.

Sugden D.E. and John B.S. (1976)
Glaciers and landscape. Edward Arnold, London. 376pp.

Sugden D.E. and Watts S.H. (1977)
Tors, felsenmeer, and glaciation in Northern Cumberland Peninsula, Baffin Island. Canadian J. Earth Sci. 14 (12); 2817-23.

Sugden D.F., Glasser N.F., and Clapperton C.M. (Submitted)
Evolution of large roches moutonnées, Deeside, Scotland. Geogr. Ann.

Summerfield M.A. (1991)
Global Geomorphology. Longman, London.

Sutherland D.G. (1984)
The Quaternary deposits and landforms of Scotland and the neighbouring shelves. Quat. Sci. Rev. 3; 157-254.

Thomas M.F. (1965)
Some aspects of the geomorphology of tors and domes in Nigeria. Z. Geomorph. 9; 63-81.

Thomas M.F. (1974)
Tropical geomorphology: A study of weathering and landform development in warm climates. Macmillan, London.

Thomson M.E. and Eden R.A. (1977)
Quaternary deposits of the central North Sea. 3. The Quaternary sequence in the west-central North Sea. Rep. Inst. Geol. Sci. London 77/12.

Thornbury W.D. (1969)
Principles of geomorphology. John Wiley and sons, New York. 594pp.

Thorp P.W. (1987)
Late Devensian ice sheet in the western Grampians, Scotland. J. Quat. Sci. 2; 103-12.

Thorp P.W. (1991)
Surface profiles and basal shear stresses of outlet glaciers from a Late-glacial mountain ice field in western Scotland. J. Glaciol. 37; 77-88.

Twidale C.R. (1982)
Granite Landforms. Elsevier, Amsterdam. 372pp.

Vialov S.S. (1958)
Regularities of ice deformation. International Union of Geodesy and Geophysics. International Association of Scientific Hydrology, Symposium of Chamonix 1958 Physics of the Movement of Ice. I.A.S.H. Publ. 47; 383-91.

Vivian R. (1970)
Hydrologie et érosion sous-glaciaires. Revue. Géogr. alp. 58; 241-64.

Waters R.S. (1954)
Pseudobedding in the Dartmoor granite. Trans. R. Geol. Soc. Cornwall 18; 456-62.

Watson E. (1977)
The periglacial environment of Britain during the Devensian. Phil. Trans. R. Soc. Lond. B 230; 183-98.

Watson J.V. (1985)
Scotland as an Atlantic-North Sea divide. J. Geol Soc. London 142; 221-43.

Watts S. (1981)
Bedrock weathering features in a portion of eastern high Arctic Canada: Their nature and significance. Ann. Glaciol. 2; 170-5.

Weertman J. (1957)
On the sliding of glaciers. J. Glaciol. 3; 33-8.

Whillans I.M. (1981)
Reaction of the accumulation zone portions of glaciers to climatic change. J. of Geophys. Res. 86; 4274-4282.

White W.A. (1972)
Deep erosion by continental ice sheets. Geol. Soc. Am. Bull. 83; 1037-56.

White W.A. (1988)
More on deep glacial erosion by continental ice sheets and their tongues of distributary ice. Quat. Res. 30; 137-50.

Wheeler D.A. (1979)
The overall shape of longitudinal profiles of streams in Pitty A.F. (ed) Geographical Approaches to Fluvial Processes; 241-60. Geobooks, Norwich.

Williams, R.B.G. (1975)
The British climate during the last glaciation; An interpretation based on periglacial phenomena. In Wright A.E. and Moseley F. (eds) Ice Ages: Ancient and Modern; 95-110. Seel House Press, Liverpool.

Zotikov I.A. (1986)
The Thermophysics of Glaciers. Reidel, Dordrecht.

Zumberge J.H. (1955)
Glacial erosion in tilted rock layers. J. Geol. 63; 149-58.